Preclinical Evaluation of a Novel Drug Delivery System for Cisplatin

Balaji Venugopal
MBBS, MRCP

The thesis submitted to University of Glasgow in partial fulfilment of the requirement for the award of

Doctor of Medicine

Cancer Research UK Beatson Laboratories
Institute of Cancer Sciences
University of Glasgow

September 2012

Abstract

The aim of this body of work was to characterise a novel cisplatin drug delivery system and to develop new tools based on biophotonic imaging that could be used to enhance studies of drug delivery *in vivo*.

Cucurbiturils (CB) are macrocycles which are formed by acid catalysed condensation of glycoluril and formaldehyde. The internal cavity of CB[7] encapsulates a single molecule of cisplatin and the hypothesis was that encapsulation would reduce thiol degradation of the drug. Drug sensitivity studies *in vitro* with the cisplatin-sensitive human ovarian cancer cell line, A2780, and a cisplatin-resistant derivative, A2780/cp70, showed that the CB[7] encapsulated cisplatin retained activity but that this encapsulation drug delivery system was not able to overcome resistance to platinum. However, when these cell lines were grown as subcutaneous xenografts in nu/nu mice, the encapsulated cisplatin was able to reduce the growth of A2780/cp70 tumours which are resistant to the maximum tolerated dose of cisplatin *in vivo*. One possible explanation of this observation is that encapsulation might alter the pharmacokinetics of cisplatin and a method for the detection of platinum in biological samples by ICP-MS was established and validated. This assay was sufficiently sensitive to detect the low levels of platinum present in mouse plasma 24 hours after administration of either free or encapsulated cisplatin. Plasma and tissue pharmacokinetics show that encapsulation had no effect on the peak plasma concentration of cisplatin but did reduce the rate at which cisplatin was cleared from the plasma. The increased plasma AUC of cisplatin resulted in a non-selective increase in the delivery of cisplatin to both tumour and normal tissues. However, there was no apparent increase in toxicity which could be explained by the fact that encapsulation, unlike an increase in the dose of free cisplatin, had no effect on the peak plasma concentration.

Subcutaneous xenografts lack critical features of human tumours. The development of more complex models for use in drug development has been limited due to lack of a method for monitoring tumour growth. Biophotonic imaging was, therefore, investigated to determine whether it is sufficiently sensitive and reproducible to be able to evaluate growth of disseminated

tumours in mice. The bioluminescent signal is dependent on the metabolism of luciferin by luciferase. Subcutaneous injection of luciferin was shown to produce a consistent signal in all injected mice. The bioluminescent signal was transient but reached a maximum intensity 6 minutes after injection and remained stable for about 4 minutes which defined the window during which measurements were taken. Sensitivity was shown to be dependent on the level of expression of luciferase by the cells. Injection of commercially available HCT116Luc cells, where the luciferase gene was inserted by a lentiviral system, was shown to allow detection of 10,000 cells in the lungs of mice. This sensitivity was about 10 fold greater than was obtained by lipofectamine based gene transfection. When HCT116Luc cells were grown as subcutaneous xenografts in mice, an exponential growth pattern was easily detected by bioluminescence imaging and the reproducibility between mice was comparable to that routinely obtained by calliper measurements.

Activity of encapsulated cisplatin was determined in a model of disseminated ovarian cancer. Rab25, a member of the RAS oncoprotein superfamily, is up-regulated in around 80% of ovarian cancer samples compared to normal ovarian epithelium. Rab25 contributes to tumour progression by enabling the tumour cells to invade the extracellular matrix by altering the trafficking of integrin. Transfection of Rab25 into A2780 cells results in cells that can grow in the peritoneal cavity of mice. A2780-Rab25 cells were 4 fold resistant to cisplatin *in vitro* which confirms a previous observation that Rab25 expression in A2780 makes them less sensitive to the induction of apoptosis in response to stress. A2780-Rab25 cells that express the luciferase gene (A2780-Rab25Luc) were injected into the peritoneal cavity of mice and growth was measured by biophotonic imaging. Exponential growth was clearly apparent at a stage at which no obvious abdominal distension was apparent. The disseminated A2780-Rab25Luc tumour xenografts were less sensitive to cisplatin than are subcutaneous xenografts of A2780. This is the first study that suggests that Rab25 over-expression results in reduced drug sensitivity *in vivo*. In contrast, a very significant growth inhibition was observed when mice were treated with an equivalent dose of encapsulated cisplatin regardless of whether it was administered by the intraperitoneal or subcutaneous route. These results are very encouraging since they confirm the enhanced activity of encapsulated

cisplatin and also demonstrate the value of biophotonic imaging for measurement of tumour growth *in vivo*.

Pharmacodynamic measures of drug activity *in vivo* in animal models are often based either on measures of surrogate tissue response or on single measures on tumour tissue removed at the end of the experiment. Biophotonic imaging *in vivo* allows the translation of reporter assays used in cell lines *in vitro* to studies of tumour response *in vivo*. A plasmid was prepared that links the p53 transcriptional response element to the luciferase gene and it was then transfected in to A2780 cells which express wild type p53. Stable transfectants of A2780p53Luc were treated with cisplatin, doxorubicin and paclitaxel and induction of p53 determined by bioluminescence and confirmed by Western blotting. A very low bioluminescent signal was present in untreated cells and a clear dose dependent increase in bioluminescence was seen in response to all three drugs. When A2780p53Luc cells were grown as subcutaneous xenografts the bioluminescent signal was significant in untreated tumours but was markedly increased 24 hours after treatment of the mice with cisplatin. Induction of p53 in the tumours was confirmed by immunohistochemistry and this also confirmed significant expression of p53 in untreated tumours.

The possible implications of these findings for the improved delivery of cisplatin are discussed.

Table of Contents

List of Tables

List of Figures

Acknowledgement

I would like to thank my supervisors Prof Jim Cassidy and Dr Jane Plumb for their support and guidance throughout my project and even after moving on to other jobs. I appreciate the assistance provided by all the members of O3 group; Fiona McGregor, Natividad-Roman Gomez and Alyson Sim in teaching me various laboratory techniques and for the useful discussions. I also thank Colin Nixon for guiding me with immunohistochemistry and all the members of central and biological services at Beatson Institute.

I specially thank my research adviser and clinical mentor Prof Jeff Evans whose steadfast support has motivated me to complete my research and continued to help in my professional development. I extend my gratitude to our collaborators David Stirling and Prof Andrew Hursthouse at University of West of Scotland who were helpful in ICP-MS and Dr Nial Wheate at University of Strathclyde for providing us the novel drug.

I thank my parents for giving their best for me without whom I would not be where I am. I am gifted to have Preethy as my wife who always stands by me in particular on occasions when I have doubted myself. I specially thank her for her patience and understanding when I spent long evenings and weekends in the labs away from my lovely daughter and son.

I dedicate this thesis to my brother, Dr V Aravinth and my father-in-law, Dr G Subash whose untimely demises have left a huge vacuum in my life but remain a key driving force in all my endeavours.

This work was funded by Cancer Research UK.

Author's declaration

I hereby declare that I am the sole author of this thesis. The body of work discussed in chapter 5 is partly that of my colleague Dr Gomez-Roman and partly done in collaboration. Unless otherwise stated all the other work presented in this thesis was performed by me.

Definitions/Abbreviations

µL	Microlitre
µg	Microgram
µM	Micromole
AUC	Area under concentration
BLI	Bioluminescence imaging
C	Celsius
CB[7]	Cucurbit[7]uril
Cmax	Maximum concentration
CO_2	Carbon dioxide
DLT	Dose limiting toxicity
DNA	Deoxyribo nucleic acid
DMSO	Dimethylsuphoxide
DTT	Dithiothreitol
EDTA	Ethylenediaminetetracaetic acid
FCS	Foetal calf serum
HCl	Hydrochloric acid
Hrs	Hours
HNO_3	Nitric acid
ICP-MS	Inductively coupled plasma mass spectrometry
ICPS	Integrated counts per second
In	Indium
i.p	Intraperitoneal
i.v	Intravenous
kDa	Kilo Dalton
Kg	Kilogram
LLOQ	Lower limit of Quantitation

mg	Milligram
mL	Millilitre
mRNA	messenger RNA
MTD	Maximum tolerated dose
MTT	3-(4, 5-dimethylthiazol-2-yl)-2, 5-diphenyl-tetrazolium bromide
ng	Nanograms
OS	Overall survival
PARP	Poyl-ADP ribose polymerase
PCR	Polymerase chain reaction
PD	Pharmacodynamics
Ph	Photons
PK	Pharmacokinetics
pmol	Picomoles
PPB	Parts per billion
PPM	Parts per million
PPT	Parts per trillion
Pt	Platinum
PVDF	Polyvinylidine difluoride
PR	Partial response
pUF	Plasma ultra-filtrate
QC	Quality control
RD	Recommended dose
RNA	Ribonucleic acid
RT-PCR	Reverse transcriptase polymerase chain reaction
Sec	Seconds
SEM	Standard error of mean
s.c	Subcutaneous

$T_{1/2}$	Half-time
Tmax	Time to reach maximum concentration
UV	Ultraviolet
V	Volts

1 General Introduction

1.1 Cancer: A global problem

Cancer remains the leading cause of mortality both in economically developed and developing countries with incidence of 12.7 million cancer cases worldwide and an associated mortality of 7.6 million lives in 2008. Overall the incidence of cancer continues to rise globally (Coleman, Quaresma et al. 2008; Ferlay, Shin et al. 2010). In the United Kingdom, the age standardised incidence rate for all cancers has increased by 20% in males (from 354/100,000 in 1975-77 to 426/100,000 in 2007-09) and by 40% in females (from 265/100,000 in 1975-77 to 370/100,000 in 2007-09) (www.cancerresearchuk.org/cancerstats).

Significant improvements in the awareness and healthy life style, better screening programmes, novel surgical techniques, radiotherapy and modern cytotoxic and targeted agents have all resulted in improvement in cancer related survival rate. For example, population based screening programmes for breast cancer have clearly demonstrated a significant improvement in cancer related mortality (Broeders, Moss et al. 2012). The use of adjuvant chemotherapy and hormone therapy has resulted in 57% reduction in the risk of death in women with oestrogen receptor (ER) positive, early stage breast cancer (EBCTCG 2005). Similarly downsizing of tumour with chemotherapy and better oncosurgical approaches in patients with colorectal liver metastases have raised the hope of cure and long term disease eradication in patients deemed to have unresectable metastatic disease (Adam, Wicherts et al. 2009). Cumulatively this has led to fall in cancer related mortality in the UK, which has decreased by 11% from 219 to 189 deaths per 100,000 of population in 2007. Despite these advances cancer remains a major health burden and was attributed in 28% of deaths in the U.K. In 2010, there were 157,275 deaths in the U.K due to cancer indicating that cancer is a major health problem (CancerResearchUK 2012) (www.cancerresearchuk.org/cancerstats).

1.2 Overview of chemotherapy

Chemotherapy plays a vital role in the reduction of cancer related mortality although prevention and early detection of cancer along with combined modality treatments have all contributed to the reduction in deaths. The origin of cytotoxic chemotherapy dates back to 1942 when Goodman and Gilman observed that exposure to nitrogen mustard in the soldiers of First World War, resulted in lymphoid hypoplasia and myelosuppression. These pharmacologists injected the active component of nitrogen mustard into a patient with non–Hodgkin lymphoma and observed the regression of mediastinal and lymphatic mass (Gilman and Philips 1946; DeVita and Chu 2008). Despite the initial promising response this patient had progression of the disease after a few weeks. Nevertheless this observation had established that drugs could be used to treat cancer. In parallel, Sydney Farber and colleagues discovered that folic acid was required for DNA synthesis and depletion of folates in the body resulted in tumour regression. This discovery led to the development of aminopterin and methotrexate which was successfully used to treated acute leukaemia (Farber, Diamond et al. 1948). National drug screening programmes then resulted in screening a variety of natural compounds yielding an array of cytotoxics including camptothecins, actinomycin D, mercapto-purines and paclitaxel which were approved for clinical use once the issues with mass production were overcome (Chabner and Roberts 2005).

The concept of curing cancer with combination chemotherapy was established by De Vita and colleagues, who used the combination of nitrogen mustard, vincristine, procarbazine and prednisolone (MOPP) to treat advanced Hodgkin's disease and demonstrated complete remission in 81% of treated patients (Devita, Serpick et al. 1970). During the same period Skipper's cell kill hypothesis that drugs achieve better cell-kill when the tumour burden is small and, eradicating micro-metastatic disease translates into better survival outcomes led to the concept of adjuvant chemotherapy (Bonadonna, Brusamolino et al. 1976). Although Li and colleagues reported curing gestational trophoblastic cancer with methotrexate (Li, Hertz et al. 1958), the concept of curing cancer with primary chemotherapy in solid malignancies was established by Lawrence Einhorn and his team who used the combination of cisplatin bleomycin and vinblastine and were able to cure 70% of patients with metastatic germ cell

cancer. To date, this cisplatin based chemotherapy remains a model of cure for treating solid malignancies (Einhorn 2002; Calabro, Albers et al. 2012).

1.2.1 Treatment failure

Conventional chemotherapeutics and drug discovery programs have been based on the principle that rapidly proliferating cancer cells are more susceptible to chemotherapy than normal cells. Whilst this principle still holds good, it is now apparent that cytotoxics kill all proliferating cells in a non-selective manner and this non-selective cell kill results in intolerable toxicities to normal tissues. Though the newer generation targeted agents are thought to selectively target the aberrant cancer pathway they also result in significant toxicities, e.g. hypertension, thromboembolic disease and delayed wound healing noted with anti-angiogenic agents (Stone, Sood et al. 2010). These toxicities preclude the safe and effective delivery of many active cytotoxic drugs due to their narrow therapeutic index. In addition, cancer is a genetically and phenotypically heterogeneous disease which is not reliant of single oncogenic pathway and is characterised by genomic instability with associated redundancies and crosstalk between the cell signalling pathways (Hanahan and Weinberg 2011). Cumulatively these properties result in tumour drug resistance and failure of treatment.

1.2.2 New drugs

Advances in the understanding of molecular biology of cancer and better drug screening process have resulted in the approval of number of novel chemotherapeutic agents. At least 68 drugs have been approved by the US FDA from 1990 till 2005 for the treatment of cancer (DiMasi and Grabowski 2007). In addition to the targeted therapies, most of the recently approved new drugs have been utilising drug delivery systems. Nano-particle albumin bound (nab-paclitaxel) has proven to improve the tolerance and also the overall survival in patients with metastatic breast cancer. The clinical development of na-pacltaxel is discussed in detail in following sections. Besides drug delivery, antibody-cytotoxic drug conjugates have also been successfully developed for the treatment of cancer. Trastuzumab emtansine (T-DM1) is an antibody-drug conjugate composed of emtansine, a derivative of anti-microtubule agent

maytansine and trastuzumab (Lewis Phillips, Li et al. 2008). T-DM1 combined the cytotoxic properties of the emtansine with the Her2 receptor targeted delivery of trastuzumab in patients with metastatic breast cancer and has resulted in improved progression free survival of these patients both in first line setting and in previously treated patients (Hammond, Hayes et al. 2010; Krop, LoRusso et al. 2012; Hurvitz, Dirix et al. 2013). Clearly these new drugs have resulted in an improvement of median survival of patients with cancer. In early 1990s, 5-fluoro uracil (5-FU) was the only therapeutic option for patients with metastatic colorectal cancer with median overall survival was only 12 months. With the addition of oxaliplatin, irinotecan and biologicals namely bevacizumab and cetuximab, there have been incremental improvements in overall survival and the median survival has nearly doubled to 24 months (Venugopal and Cassidy 2009).

1.2.3 Need to improve current drugs

Despite the advances in the understanding of cancer biology and the advent of molecularly targeted agents, cancer associated mortality is still high and there remains an unmet need to design better drugs to treat cancer. The inability to accurately recapitulate the tumour microenvironment in preclinical cancer models, lack of specificity of the drug and absence of suitable pharmacodynamic marker are some of the frequently implicated causes for the failure of a novel drug (Sharpless and DePinho 2006). There is clearly a need to improve the processes involved in the preclinical evaluation of drug. In addition to evaluating the aberrant molecular pathways in cancer and developing novel targeted therapy, targeted drug delivery to tumour is a strategy that can improve cancer treatment outcomes. Trastuzumab emtansine is a drug conjugate of trastuzumab and vinca alkaloid emtansine which has shown to be effective in breast cancer (Krop, LoRusso et al. 2012; Hurvitz, Dirix et al. 2013). Even before the advent of new era of cytotoxics Paul Ehrlich, the eminent German physician who coined the word chemotherapy, conceptualised the idea of “magic bullet” that would selectively target and destroy microbial organisms or tumour cells (Strebhardt and Ullrich 2008). Hence the focus is on finding novel ways to improve the currently available chemotherapeutics using drug delivery systems.

1.3 Cisplatin

Cisplatin was discovered serendipitously by Barrett Rosenberg and colleagues from Michigan State University who, when investigating the growth effect of electromagnetic field on bacteria, observed that Escherichia coli ceased dividing and began to elongate when grown in an electrical chamber with platinum electrodes. This inhibition of cell division without an apparent reduction in the growth was attributed to the elution of platinum compounds from the platinum electrodes used in the chamber (Rosenberg, Van Camp et al. 1965). Further experiments and analysis of platinum compounds led to the identification of cis-diammine dichloroplatinum(II) (cisplatin) as the compound that exerted the anti-proliferative actions. Cisplatin, subsequently was demonstrated to have significant preclinical anti-tumour activity in mice with transplantable sarcoma (S180) and leukaemia L1210 (Rosenberg, Vancamp et al. 1969). Cisplatin was approved by the US Food and Drug Administration (FDA) for use as anti-cancer treatment in 1978 (Kelland 2007).

Cisplatin is now a widely used chemotherapeutic agent in the treatment of a variety of malignancies including testicular, ovarian, lung, gastric and bladder cancers and also in paediatric malignancies (von der Maase, Hansen et al. 2000; Einhorn 2002; Schiller, Harrington et al. 2002; Cunningham, Allum et al. 2006; Hennessy, Coleman et al. 2009). Treatment with cisplatin based chemotherapy regimen results in cure in 70% of patients with testicular cancer and, in early stage testicular cancer nearly 100% of patients can be cured (Jones and Vasey 2003). In addition, cisplatin is used in palliative treatment of various other cancers with varying response rates.

1.3.1 Mechanism of action of cisplatin

Despite the extensive clinical experience with cisplatin, the precise mechanism of action of cisplatin is not clearly understood and it is widely accepted that the main target of cisplatin is DNA (Jamieson and Lippard 1999; Wang and Lippard 2005; Kelland 2007). Cisplatin is a neutral charged moiety which needs to be activated in order to react with DNA, the key intracellular target. Cisplatin enters the cells by passive diffusion where it undergoes aquation. The extracellular compartment or serum has a high concentration of chloride ions

(90-100mM) compared to intracellular compartment (3-20mM). The high chloride concentration in serum stabilises the cisplatin which, following entry into cells, undergoes aquation reaction resulting in the loss of one or both of the chloride moiety of cisplatin. The mono-hydrated and di-hydrated cisplatin reacts readily with DNA and forms platinum adducts (Figure 1.1). The platinum atom of cisplatin binds covalently to the N^7 position of the purine bases, primarily with guanine but also with adenine, to form intra-strand and inter-strand crosslinks. 60-65% of the DNA-platinum adducts occurs at the same strand of the DNA (intra-strand) and 20-25% of crosslinks are between the purine bases at opposite strands (inter-strand). Eventually the DNA-platinum adducts distort the helical structure of the DNA by unwinding and bending of the helix and evoke a variety of cellular responses resulting in transcription inhibition, replication inhibition, cell cycle arrest, DNA damage all of which eventually culminates in cellular apoptosis (Jamieson and Lippard 1999; Wang and Lippard 2005; Kelland 2007).

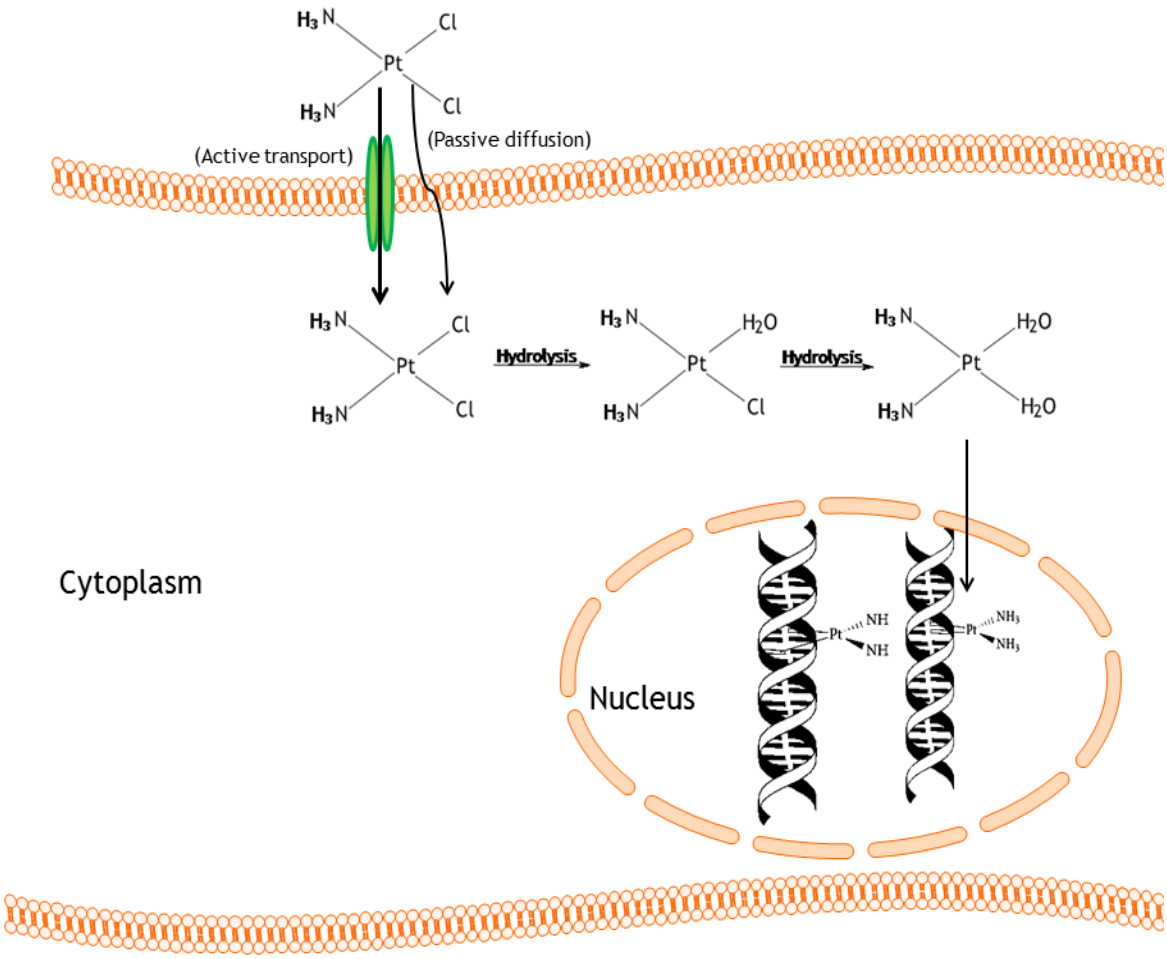

Figure 1.1: Mechanism of action of cisplatin

1.3.2 Limitations of cisplatin chemotherapy

The key limitations of cisplatin, as with most other cytotoxic chemotherapy, are toxicity and resistance both inherent and acquired. The cytotoxic action of cisplatin is not specifically targeted against tumour cells and all proliferating cells are targeted. This non-selective cytotoxic action results in significant clinical toxicities. The dose-limiting toxicity of cisplatin is nephrotoxicity as cisplatin is primarily excreted by kidneys. In addition to nephrotoxicity, other toxicities include ototoxicity resulting in sensori-neural deafness, emetogenicity, and neurotoxicity (Hartmann and Lipp 2003). Aggressive hydration with 0.9% saline before and after the infusion of cisplatin has significantly reduced the nephrotoxicity of cisplatin (Cornelison and Reed 1993). The use of effective anti-emetics has attenuated the emetogenic side effects of cisplatin respectively (Marty, Pouillart et al. 1990; Hesketh, Grunberg et al. 2003). Cancer cells either

are inherently resistant to cisplatin or acquire resistance after a few cycles of treatment with cisplatin. Ovarian cancer has a good overall response rate to treatment with cisplatin, both in early stage and advanced stage disease, but the response is not sustained as the tumour eventually becomes resistant to cisplatin (Hennessy, Coleman et al. 2009). Resistance to cisplatin can be multifactorial and includes decreased cellular uptake, increased inactivation and degradation, increased DNA damage repair, decreased ability to induce apoptosis and increased cellular efflux of cisplatin (Siddik 2003; Galluzzi, Senovilla et al. 2012).

Cisplatin enters cells through a non-saturable process of passive diffusion, and current evidence also suggests that the influx of cisplatin is mediated by high affinity copper transporter which is encoded by copper transporter (CTR1) gene. Deletion of CTR1 gene decreases the intracellular accumulation of cisplatin and results in increased resistance to cisplatin (Ishida, Lee et al. 2002; Wang and Lippard 2005; Kelland 2007). In addition to drug influx, efflux of platinum mediated by ATP binding cassette subfamily C2 (ABCC2) which is also known as multi-drug resistance protein 1 (MRP1) or canalicular multi-specific organic anion transporters (cMOAT) also appears to play a role in intracellular accumulation of cisplatin by promoting its efflux from the cells (Galluzzi, Senovilla et al. 2012).

Inactivation of cisplatin even before their interaction with DNA by intracellular thiol-containing molecules has emerged as a key determinant of drug resistance to cisplatin (Siddik 2003; Galluzzi, Senovilla et al. 2012). Cisplatin, once inside the cells, does not primarily react with DNA but also with other nucleophiles including cysteine rich metallothionein and glutathione. Glutathione (L- γ-glutamyl-L-cysteinyl-glycine; GSH), a non-protein thiol which is abundant in mammalian cells, acts as a reducing agent by scavenging free radicals and defends the cells from variety of xenobiotics. Cisplatin interacts with these sulphur containing molecules through conjugation and forms cisplatin-thiol conjugate which eventually deplete the levels of intracellular cisplatin (Siddik 2003; Galluzzi, Senovilla et al. 2012). Even in early 1990s, cells with high levels of glutathione were shown to be resistant to cisplatin (Godwin, Meister et al. 1992). Glutathione also protects the cells from cisplatin induced cytotoxicity by interaction with reactive oxygen species and anti-apoptotic proteins like Bcl2 (Brozovic, Ambriović-Ristov et al. 2010). Despite the absence of understanding

of the precise mechanism of glutathione-cisplatin interaction, it is evident that glutathione does play a significant role in cisplatin resistance.

Mismatch repair proteins (MMR) are DNA damage repair proteins which recognise and repair mismatched or damaged DNA. hMLH1, the human homologues of bacterial protein MutS, plays a vital role in cisplatin resistance and cells deficient of hMLH1 lose their ability to undergo apoptosis due to cisplatin induced DNA damage. This resistance to cisplatin could be acquired by epigenetic modification, primarily by demethylation (Brown, Hirst et al. 1997; Strathdee, MacKean et al. 1999; Plumb, Strathdee et al. 2000). Clinical studies have shown that such methylation of hMLH1 confers resistance to patients who are treated with cisplatin (Gifford, Paul et al. 2004).

Malignant cells can also develop resistance to cisplatin through the increased repair of DNA damage. The key effector of the cytotoxic action of cisplatin is the platinum-DNA adduct and cells which repair or remove the platinum adducts from the DNA could remain free from the cytotoxic effects of cisplatin. Nucleotide Excision Repair (NER) pathway is the key pathway through which the platinum-DNA adduct, that alters the helical structure of DNA, is excised and the integrity of genome is maintained. Excision repair cross-complementation group 1 (ERCC1), a NER protein dimerises with Xeroderma pigmentosa complex which eventually results in the excision of damaged DNA containing the platinum adduct (Martin, Hamilton et al. 2008). This NER pathway plays a significant role in mediation of cisplatin resistance and patients with lung cancer who have high expression of XRCC1 do not appear to derive clinical benefit when treated with cisplatin based chemotherapy (Olaussen, Dunant et al. 2006). The mechanisms of resistance to cisplatin discussed thus far is not exhaustive but gives an understanding of the reasons for treatment failure and allows us to evaluate the novel ways to improve the efficacy of cisplatin.

1.4 Platinum analogues

To overcome the toxicities of cisplatin and to circumvent chemo-resistance to cisplatin numerous analogues of platinum have been studied. However, to date,

carboplatin and oxaliplatin are the only other platinum compounds that have been approved in clinical practice (Figure 1.2). As discussed in earlier sections, cisplatin undergoes aquation reaction and loses one or both of the chloride groups, which are called the “leaving groups”. The two ammine groups are called the “carrier ligands” which remain attached to the platinum, the warhead which forms adducts with DNA. Numerous strategies have been employed to modify the leaving group and carrier ligand of cisplatin with the hope of improving the stability and efficacy of cisplatin.

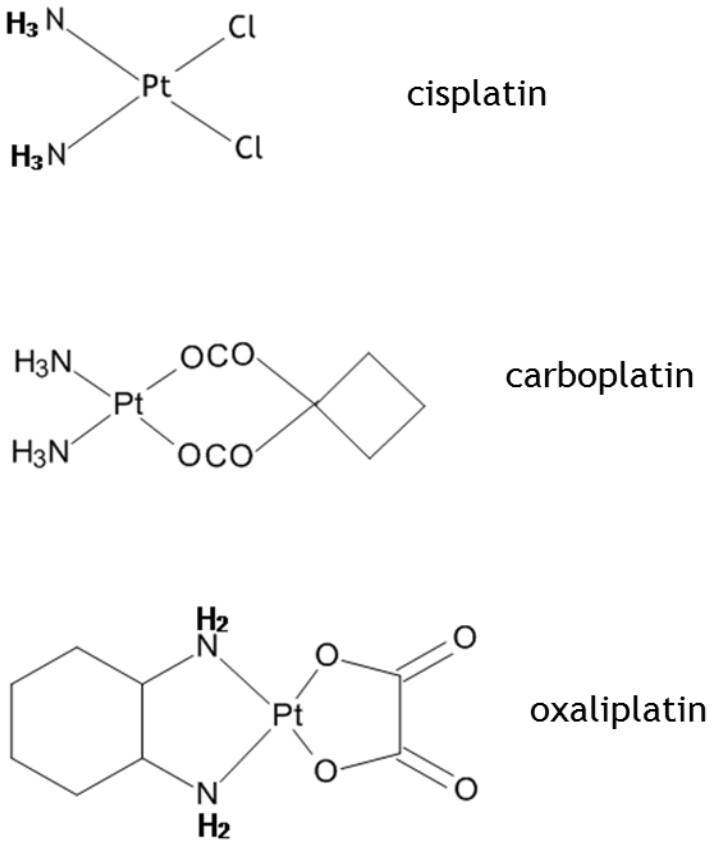

Figure 1.2: Chemical structure of platinum compounds used in cancer chemotherapy.

On the basis of the hypothesis that cisplatin toxicity is related to the speed of aquation reaction, it was thought that stabilising the leaving groups could decrease the toxicity of cisplatin. Hence the chloride groups were substituted by cyclobutane dicarboxylate ligands which are more stable than chloride

groups of cisplatin which resulted in the genesis of the new platinum compound, carboplatin (Diammine[1,1-cyclobutanedicarboxylato(2-)-*O,O'*]platinum(II) (Figure 1.2). Carboplatin forms similar platinum-DNA adducts but at a slower rate and requires higher concentration of the drug to achieve cell kill (Harrap 1985). However it differs from cisplatin in that the dose limiting toxicity is thrombocytopaenia with sparing of nephrotoxicity when administered according to patient's renal function (Calvert, Newell et al. 1989). Carboplatin maintains a similar spectrum of anti-cancer activity as compared to cisplatin. Carboplatin is the mainstay in the treatment of ovarian cancer where it has replaced cisplatin as the platinum drug of choice (Konstantinopoulos Pa 2012). Carboplatin also demonstrates comparable clinical efficacy to cisplatin in non-small cell lung cancer (Schiller, Harrington et al. 2002; Hotta, Matsuo et al. 2004; Ardizzoni, Boni et al. 2007).

Other researchers have modified the structure of cisplatin by amending the binding ligands in addition to replacing the leaving groups. Oxaliplatin (1R, 2R-diaminocyclohexane oxalatoplatinum [II]) is one such compound with a bulky carrier ligand (1,2,diaminocyclohexane-DACH) which exhibits improved and divergent anti-cancer activity in comparison with cisplatin (Figure 1.2). Oxaliplatin entry into the cells is relatively less dependent upon copper transporters (Holzer, Manorek et al. 2006) and the platinum-DNA adducts are not recognised by MMR proteins (Kelland 2007). In addition, oxaliplatin also exhibits cytotoxic actions against cells lines like L1210 and HT29 cells (which are resistant to cisplatin) indicating the divergent mechanistic action of oxaliplatin (Rixe, Ortuzar et al. 1996; Raymond, Chaney et al. 1998). Based on the convincing pre-clinical and robust clinical data, oxaliplatin is now standard chemotherapy in combination with fluoropyrimidines for the treatment of colorectal cancer (Engstrom, Arnoletti et al. 2009). Besides modifying the carrier ligands and leaving groups, attempts to improve platinum drugs were made by using platinum (IV) complexes and the most notable was satraplatin which has largely been unsuccessful in clinical practice (Choy, Park et al. 2008).

1.5 Drug delivery

A variety of other platinum based drugs namely nedaplatin, lipoplatin and picoplatin have been tested in clinical trials. However none of the newer

platinum analogues have gained wide spread clinical acceptance (Wheate, Walker et al. 2010). In order to augment the clinical efficacy of cisplatin advances have been achieved through modifying the chemotherapy partner of cisplatin. In ovarian cancer, the combination of cisplatin and paclitaxel resulted in a significant survival advantage compared to the combination of cisplatin and cyclophosphamide (Piccart, Bertelsen et al. 2000).

Another approach to improve the efficacy of established chemotherapeutics is through improved drug delivery. The clinical efficacy and toxicity profile of doxorubicin has been significantly modified using drug delivery with pegylated liposomes. Pegylated liposomal doxorubicin (caelyx) is a licenced indication for the treatment of ovarian cancer and unlike doxorubicin, cardiac toxicity is not a major concern (Gordon, Fleagle et al. 2001). In addition to altered drug pharmacology, drug delivery systems can also increase the selective delivery of drugs to the tumour either by passive or active targeting (Danhier, Feron et al. 2010). Passively targeted drug delivery systems exploit the inherent deficiencies in tumour vasculature and microenvironment. Active targeting relies on the knowledge of tumour biology and could also be termed ligand targeted therapeutics.

Maeda and Matsumura reported that tumour vasculature has widespread fenestrations resulting in increased permeability through which macromolecules can extravasate from the blood vessel (Matsumura and Maeda 1986). In addition, due to poorly formed lymphatic drainage the macromolecular drug gets trapped in the interstitium. This unique patho-physiological phenomenon was termed as “enhanced permeability and retention” (EPR) effect and could be exploited for drug delivery. The macromolecular drug delivery system along with its drug permeates into the tumour where they are trapped due to poorly formed lymphatics and the drug dissociates preferentially into the tumour (Matsumura and Maeda 1986). The defective angiogenesis in the tumours results in wide gaps between the endothelial cells ranging from 400-600nm (Yuan, Dellian et al. 1995). Matsumura and Meada observed that polymer-drug conjugate, SMANCS, which is a co-polymer of styrene and maleic acid (SMA) conjugated to cytotoxic drug, neocarzinostatin (NCS), exhibited tumoritrophic properties when compared to free drug (NCS) and the $T_{1/2}$ of SMANCS was almost 20 times that of free NCS. They were then able to demonstrate that Evans blue dye tagged to albumin, due

to the large molecular size of albumin (68kDa), was preferentially deposited in these tumours than in normal skin or tissues (Matsumura and Maeda 1986).

Conventional nanoparticles ranging from 5-15nm, due to their small size, are rapidly excreted from the body through renal clearance (Choi, Liu et al. 2007; Petros and DeSimone 2010). Conversely, if the drug carrier size increases towards micro-molar range they get deposited in the reticulo-endothelial systems primarily in the liver, spleen and bone marrow where they undergo sequestration. The average size of the sinusoids in the liver and spleen is 150-200nm and the drug carriers should not be over this size in order to avoid sequestration (Wisse, Braet et al. 1996). The defective angiogenesis in the tumours results in wide gaps between the endothelial cells ranging from 400-600nm (Yuan, Dellian et al. 1995). In order to exploit the defective tumour vasculature and EPR phenomenon, the size of the drug carrier should be within a specific range of 5-100nm (Cho, Wang et al. 2008). However this is a reductionist view of drug delivery and various other factors like the surface charge, shape and immunogenicity of the drug-carriers and unique characterises of the tumour micro-environment, pH and interstitial pressure play a significant role in the effective drug delivery (Petros and DeSimone 2010). Drug penetration in solid tumours is not uniform and is dependent on the distance from the blood vessel and while EPR phenomenon could increase the passive targeting of drugs the defective vasculature can also result in increased interstitial pressure which could also hamper drug delivery (Minchinton and Tannock 2006).

Active targeting involves tagging a ligand to the drug delivery system which could then target the cancer cells that overexpress the receptors for the ligands. To date, the commonly used ligands are folic acid and transferrin. Rapidly dividing malignant cells express folic acid receptors which help in the proliferation and drug carriers attached to folic acid or folic acid receptor antibodies which then gets internalised through folate receptor mediated endocytosis. Overexpression of folic acid receptor is demonstrated in breast and ovarian cancer. This principle could also be used for conjugating chemotherapeutics as well as imaging agents (Hartmann, Keeney et al. 2007; Low, Henne et al. 2007; Salazar and Ratnam 2007). Promising *in vivo* studies have demonstrated increased tumour delivery of doxorubicin when administered

as folate targeted liposomal derivative and clinical studies are awaited (Yamada, Taniguchi et al. 2008).

Drug delivery systems are broadly divided into polymer based and lipids based systems and are briefly discussed in the following sections. However recently protein bound drug delivery systems have also been successful.

1.5.1 Polymer based drug delivery systems

The concept of polymer based drug delivery was established by Helmut Ringsdorf in 1975 wherein he elegantly explained that polymer backbone bound to "pharamacon" (the compounds which elicit the therapeutic response) or drug could be used to develop a pharmacologically active compound. Typically the drug delivery system consists of a water soluble polymer linked to the drug via a biodegradable linker and the strength of the linker influences the rate of release of the drug from the polymer chain (Ringsdorf 1975).

Polymer-drug conjugates increase the circulatory half-life of the compounds and exploit the EPR effect in tumours (Maeda, Bharate et al. 2009). Cassidy and colleagues have demonstrated that polymer conjugated duanorubicin was preferentially deposited in tumour through EPR effect (Cassidy, Duncan et al. 1989). In addition to decreasing the renal clearance and increasing the bio-distribution of the payload, polymer-drug conjugates also increase the protein solubility, decrease the immunogenicity and reduce the receptor mediated clearance in the reticulo-endothelial system. Polymer-drug conjugates involve covalent bonding of the polymer to the active drug through a linker which is commonly a peptide sequence which could be broken in an acid pH, which is called lysosomotropic delivery. Currently the term polymer therapeutics encompasses polymer-drug conjugates, polymeric micelles and polymer–protein/enzyme conjugates (Duncan 2006). Polyethyleneglycol (PEG), N-(2-hydroxypropyl) methacrylamide (HPMA) and polyglutamic acid (PGA) are the commonly used polymers for drug delivery (Duncan 2006).

1.5.2 Lipids based drug delivery systems

Liposomes are microscopic vesicles that are made of phospholipid bilayer comprising a central aqueous core which can carry hydrophobic drugs. Liposomes

were discovered in 1965 by Bangham and colleagues and were initially termed as phospholipid spherules (Bangham, Standish et al. 1965). Liposomes, due to their physico-chemical properties, have been extensively researched as drug delivery systems. Liposomes have a size range of 50-250nm and have been used in the delivery of number of chemotherapeutics of which doxorubicin needs special mention. Consistent with other nanoparticle based drug delivery systems, liposomes also target the tumour passively through EPR effect. Liposome encapsulated doxorubicin was demonstrated to be non-inferior to free doxorubicin but with the advantages of reduced cardiotoxicity. However the pharmacokinetic profile was not superior to free doxorubicin and this was due to rapid clearance of the drug from circulation (Batist, Ramakrishnan et al. 2001). Liposomes could be rapidly cleared from circulation by the reticulo-endothelial system (RES) by a process called opsonisation. Adsorption of specific protein to the particles surface owing to their surface characteristics results in targeting the liposomes to the reticulo-endothelial system where they get sequestered. Covalent bonding or simple attachment of PEG moiety to the liposomes or other nano-carrier, termed pegylation, alters the physico-chemical property of the nano-carriers, which escape opsonisation and eventual sequestration by the reticulo-endothelial system (Howard, Jay et al. 2008). The pegylated liposomes are also called “stealth” liposomes due to evasion of immunological detection by reticulo-endothelial system. Unlike polymer based drug delivery systems, liposomes based drug delivery systems have been reasonably successful in clinical practice (Hofheinz, Gnad-Vogt et al. 2005).

1.5.3 Nanoparticle albumin based drug delivery system

In addition to conventional polymer based and lipid based DDS, novel DDS based on nanoparticle bound albumin (nab) have been shown to be clinically effective. Once such compound is ABI-007, nanoparticle albumin bound paclitaxel (Abraxane) with a mean diameter of 130nm. ABI-007 is produced by high pressure homogenisation of paclitaxel along with human serum albumin which results in nanoparticle colloidal suspension which is free of Cremophor, the solvent implicated in the hypersensitivity reactions associated with paclitaxel (Ibrahim, Desai et al. 2002).

Taxanes which include paclitaxel and docetaxel are commonly used chemotherapy in management of breast and lung cancers. In addition to the myelosuppression typically seen with cytotoxic chemotherapy, paclitaxel also causes hypersensitivity reactions which is due to the non-ionic surfactant, polyoxyethylated castor oil (Cremophor EL)(Weiss, Donehower et al. 1990). Despite pre-medication with steroids and better management of hypersensitivity reactions, safe and effective administration of paclitaxel is still restricted due to hypersensitivity reactions (Markman, Kennedy et al. 2000). In addition to hypersensitivity reactions, neurotoxicity is a recognised toxicity of cremophor, and these adverse events related to the solvent are not unique to paclitaxel. Various other non-ionic solvents used in the formulation of hydrophobic drugs namely polysorbate and Teewn20 have also been implicated to cause adverse events (ten Tije, Verweij et al. 2003). Research efforts to find a paclitaxel formulation which is free of cremophor led to the development of ABI-007.

1.5.3.1 Clinical experience with nanoparticle albumin bound paclitaxel

Phase I clinical trials with ABI-007 established the maximum tolerated dose (MTD) as 300mg/m^2 for 3 weekly regimes and 150mg/m^2 for weekly regimes which is 70-80% higher than the reported MTD for standard paclitaxel (Ibrahim, Desai et al. 2002; Sparreboom, Scripture et al. 2005). Comparative preclinical and clinical pharmacokinetic analysis of ABI-007 and paclitaxel revealed that paclitaxel clearance and volume of distribution was significantly higher for ABI-007 than standard paclitaxel, underpinning a distinct pharmacokinetic profile for ABI-007 (Sparreboom, Scripture et al. 2005). Phase III clinical trial comparing ABI-007 with paclitaxel in metastatic breast cancer has been conducted where the dose of ABI was 270mg/m^2. The overall response rate was significantly higher in patients treated with ABI-007 than standard paclitaxel; 33% versus 19% respectively, p=0.001. Median time to progression was significantly longer for ABI-007 treated patients (23.0 versus 16.9 weeks, HR: 0.75; P=0.006) when compared to paclitaxel treated patients (Gradishar, Tjulandin et al. 2005). Notably, significantly lower incidence of grade IV neutropaenia was seen with ABI-007 than paclitaxel (9% versus 22%, p<0.001) and none of the ABI-007 treated patients experienced severe (grade3/4) hypersensitivity reactions. ABI-007 has

been approved in metastatic breast cancer patients who have progressed after anthracycline based chemotherapy (Yamamoto, Kawano et al. 2011). On the basis of these promising results, ABI-007 is being evaluated in other tumour sites where taxanes chemotherapy has shown efficacy.

1.6 Cisplatin based drug delivery systems

A number of research groups have attempted to improve the delivery of cisplatin. These studies include a wide range of drug delivery systems which include both the polymer based and lipid based drug delivery systems.

1.6.1 Polymer–cisplatin conjugates

AP5280 is a polymer–platinum conjugate which was produced by the reaction between HPMA-containing peptidyl side chain and cisplatin in a multistep process. The molecular weight of AP5280 is 28kDa and the platinum loading is approximately 8%. As with other polymer-drug conjugates, the pharmacokinetic analysis indicated prolonged systemic exposure of the drug (platinum) and this was associated with reduced toxicity (Gianasi, Wasil et al. 1999; Lin, Zhang et al. 2004). The release of platinum from the polymer was facilitated by acidic milieu found in hypoxic regions of tumours and intracellularly in lysosomes. Phase I study of AP5280 in patients with refractory cancers was conducted in two centres in Netherlands and France, and patients were treated with three weekly infusion of AP5280 in 1 litre of 5% dextrose over 1 hour. Doses ranging from 90 mg Pt/m^2 to 4500 mg Pt/m^2 were evaluated in 29 patients. Nausea and vomiting was noted at dose of 4500 mg Pt/m^2 which was deemed as the maximum tolerated dose (MTD) and 3300 mg Pt/m^2 was the recommended dose (RD) for phase II trials. There was a dose proportional increase in AUC and T_{max} of platinum but this correlation was not pronounced in Pt-DNA adduct formation. Despite the favourable pharmacokinetic profile, the Pt-DNA adduct formation was significantly lower compared to standard cisplatin thereby raising questions about its clinical efficacy. It has to noted that although the doses appear to be high, the actual platinum content in these polymer conjugates was less than 10% (Rademaker-Lakhai, Terret et al. 2004).

AP5346 (ProLindac) is a pro-drug comprising a linear polymer and DACH platinum (the active component of oxaliplatin) attached together by a peptidyl linker. Preclinical studies of AP5346 in mice bearing melanoma and ovarian cancers revealed substantially higher platinum delivery both to tumour and DNA when compared with oxaliplatin. *In vitro,* there was a conclusive evidence of platinum release at pH 5.4 when suspended in dextrose (Rice, Gerberich et al. 2006). In the phase I study of AP5346, doses from 40 mg/m^2 to 1280mg/m^2 administered in 3 out of 4 weeks were explored and the commonly noted adverse events were nausea, vomiting and hypersensitivity reactions. Patients who did not get pre/post hydration also experienced nephrotoxicity and one patient died of renal failure which was related to AP5346. Even in this group of heavily pre-treated patients, two of 15 evaluable patients achieved partial response. The MTD of AP5346 was established as 900 mg/m^2 (Campone, Rademaker-Lakhai et al. 2007). A subsequent phase II exploring different schedules of AP5236 in patients with platinum resistant ovarian cancer was reported to show CA125 marker response in more than 10% of the 23 patients. However the final results of this trial is yet to be published (Nowotnik and Cvitkovic 2009).

1.6.2 Polymeric micelles based drug delivery system for cisplatin

Polymeric micelles incorporating cisplatin has been shown to have effective anti-tumour activity. Polymeric micelles containing cisplatin was formulated through polymer-metal complex formation between cisplatin and block polymers (polyethylene glycol and polyglutamic acid) with a size of 23nm. Nishiyama and colleagues published the results of their experiments in nude mice bearing Lewis lung carcinoma and C26 (murine colon carcinoma cell line) which were treated with cisplatin-incorporated polymeric micelles. Mice treated with cisplatin-incorporated polymeric micelles demonstrated significant anti-tumour activity and increased tumour platinum accumulation through EPR effect. The platinum circulation time in the plasma was also prolonged (Nishiyama, Okazaki et al. 2003). Subsequent studies of cisplatin incorporated polymeric micelles in mice also demonstrated that there was decreased incidence of nephrotoxicity and neurotoxicity and increased anti-tumour activity in comparison with standard cisplatin (Uchino, Matsumura et al. 2005).

A phase I clinical study of cisplatin–incorporated polymeric micelles (NC-6004) has been recently published. Patients with advanced malignancies who had failed standard therapy with adequate haematological, renal and hepatic functions were administered NC-6004 as an one hour infusion, every three weeks starting at a dose of 10mg/m^2. Unexpectedly, higher proportion of patients developed hypersensitivity reactions from dose level 90mg/m^2 onwards and patients also experienced nephrotoxicity at 40mg/m^2 which warranted post-infusion hydration (1.0 to 1.5 litres of fluid over 2 hours). In view of the nephrotoxicity and hypersensitivity reactions, although dose level beyond 120mg/m^2 was not explored, the MTD was established as 120mg/m^2 and recommended dose for phase II studies was estimated to be 90mg/m^2 (Plummer, Wilson et al. 2011). Hypersensitivity reactions occurred in six out of 17 patients and one patient treated at 120mg/m^2 suffered hypersensitivity despite prophylaxis with dexamethasone, chlorphenamine and ranitidine, which was hypothesised to be secondary to plasma protein-bound cisplatin.

The plasma levels of ultra-filterable free platinum species including cisplatin and micellar platinum were measured. The pharmacokinetic parameters, however, were notable. In total plasma platinum, the AUC_{inf} was 11 fold higher for NC-6004 in comparison with published data for cisplatin. The $T_{1/2}$ was longer and clearance (Cl) was shorter indicating prolonged systemic circulation of platinum in plasma. Notably, both the $T_{1/2}$ and AUC_{inf} of ultra-filterable platinum was longer with NC-6004. The value of micellar platinum mirrored the value of total platinum. The author conclude that the reduced Cmax has resulted in attenuated nephrotoxicity whereas the prolonged circulation of free platinum has resulted in enhanced anti-tumour activity(Plummer, Wilson et al. 2011). These data indicate the sustained and controlled release of cisplatin from the drug delivery system. Clearly the hypersensitivity reactions and nephrotoxicity have reduced the therapeutic index of this drug although preclinical studies did not show significant nephrotoxicity in mice. Better ways to reduce the hypersensitivity reactions and nephrotoxicity are required to optimise this compound in light of the favourable pharmacokinetic profile.

1.6.3 Liposome based drug delivery system for cisplatin

1.6.3.1 Liposomal cisplatin

Liposomal cisplatin, lipoplatin was formed from cisplatin and liposomes based on methoxypolyethylene glycol-disteaoryl phophatidylethanolamine (mPEG2000-DSPE), dipalmitoyl phosphatidyl glycerol (DPPG) and soy phosphatidyl choline (SPC-3) (Boulikas 2009; Stathopoulos 2010). *In vivo* experiments in rats which were administered lipoplatin (30mg/kg) intraperitoneally, demonstrated the absence of nephrotoxicity in comparison with cisplatin. In immunodeficient mice with human breast and prostate cancer xenografts, the anti-tumour activity was maintained (Boulikas 2004). Initial phase I studies established the MTD as 125mg/m^2 and combination studies were done with 5FU at this dose level (Stathopoulos, Boulikas et al. 2005). Preliminary comparative pharmacokinetic analysis between lipoplatin and cisplatin when administered in combination with 5-Fluorouracil revealed an interesting pharmacokinetic profile whereby lipoplatin had significantly shorter $T_{1/2}$ and increased clearance(CL) than cisplatin (Jehn, Boulikas et al. 2007). However, the dose of lipoplatin was only 100mg/m^2 in this study which was far lesser than the updated MTD either as monotherapy or a as combination. The result of the dose escalating phase I trial of liposomal cisplatin in patients with advanced cancer was recently reported. The starting dose of lipoplatin was 125mg/m^2 and the final MTD was derived as 300mg/m^2 when administered intravenously every two weeks as monotherapy and 200mg/m^2 when administered in combination with paclitaxel (Stathopoulos, Rigatos et al. 2010). Lipoplatin in combination with gemcitabine has shown comparable activity to gemcitabine and cisplatin in patients with advanced non-small cell lung cancer (Mylonakis, Athanasiou et al. 2010). A randomised phase III trial was conducted in patients with advanced non-small cell lung cancer where patients were randomised to the combination of lipoplatin (200mg/m^2) plus paclitaxel (135mg/m^2) [Arm A] or cisplatin (75mg/m^2) plus paclitaxel (135mg/m^2) [Arm B] administered intravenously every two weeks (Stathopoulos, Antoniou et al. 2010). The primary endpoint was toxicity analysis and there was a significant reduction in cisplatin associated toxicity namely nephrotoxicity (6.1% in Arm A versus 40% in Arm B, $P<0.001$), neutropaenia (33.3% in Arm A versus 45.2% in Arm B, $P=0.017$) and nausea/vomiting (32.5% in Arm A versus 45.2% in Arm B, $P=0.042$). Although the overall response rate was numerically

higher in lipoplatin compared with cisplatin (58.8% versus 47.0%, P=0.073), the median overall survival was similar in both groups of patients (9 versus 10 months, P=0.57). Pre-hydration was not required but lipoplatin had to be administered over an 8-hour infusion period (Stathopoulos, Antoniou et al. 2010). Lipoplatin has been tested in combination with gemcitabine and 5FU in non-small cell lung cancers and squamous cell cancers of the head and neck but the results of these trials have not been published yet. Lipoplatin has demonstrated that the nephrotoxicity associated with cisplatin could be offset by the liposomal formulation without the loss of anti-tumour activity. However, robust clinical data to support optimum dosing and clinical efficacy is warranted.

1.6.3.2 SPI-777

Stealth liposomal cisplatin (SPI-077) is formulation of cisplatin encapsulated in liposomes containing methoxy-polyethyleneglycol (mPEG). SPI-077 exhibited remarkable *in vivo* anti-tumour activity in colon and lung cancer models with prolonged circulation time and increased tumour deposition of platinum (Newman, Colbern et al. 1999). A phase I clinical trial of pegylated liposomal cisplatin with dose up to 420mg/m^2 administered intravenously every four weeks was conducted in patients with advanced stage cancer. Significant gastro-intestinal and renal toxicities were not seen. Consistent with *in vivo* data, the pharmacokinetic profile in patients indicated that liposomal delivery of cisplatin resulted in increased circulation time and decreased clearance of platinum (Meerum Terwogt, Groenewegen et al. 2002). Phase II trial of SPI-077 in non-small cell lung cancer did not demonstrate meaningful clinical response although no significant neurotoxicity or ototoxicity was noted. Similar results were also noted in a phase I/II trial in patents with inoperable head and neck cancer (Kim, Lu et al. 2001; White, Lorigan et al. 2006). Clinical development of this drug was abandoned due to these disappointing results and preclinical experiments were repeated to ascertain the reasons for failure. In tumour models of melanoma treated with SPI-077 (with a dose of 10mg/kg) or cisplatin (with a dose of 10mg/kg), there was evidence of increased accumulation of platinum in tumour with total platinum in tumour homogenates (3.12 ± 1.2 μg/g for cisplatin compared with 11.9 ± 3.0μg/g for SPI-077) but unbound platinum was not detected with SPI-077. This indicates that although the liposomal drug delivery

system for cisplatin was effective in tumour platinum delivery, it was not released from its liposomal formulation, as was also shown by Plummer and colleagues (Zamboni, Gervais et al. 2004; Plummer, Wilson et al. 2011). These data again illustrate the complexities faced with drug delivery and demonstrate that the drug-release from the drug delivery system is vital for anti-tumour activity of the drug.

1.7 Aims of the thesis

None of the drug delivery systems described for cisplatin is ideal and there is a clear need for new drug delivery systems. The aims of the thesis can be summarised as follows:

1) To characterise the activity of a novel drug delivery system for cisplatin in a well characterised human ovarian cancer cell line both *in vitro* and *in vivo*.

2) To compare the pharmacokinetics of free cisplatin with that of the drug delivery system.

3) To evaluate the use of bioluminescence imaging *in vivo* to monitor growth and drug sensitivity of a novel model of disseminated ovarian cancer.

4) To exploit bioluminescence imaging to develop a pharmacodynamic measure of cytotoxic drug activity in human tumour xenograft model *in vivo*.

1.8 Cucurbiturils: The drug delivery system

Cucurbiturils are macrocycles which are formed by acid catalysed condensation reaction between glycoluril and formaldehyde. Behrend and colleagues, in 1905, reported that condensation of glycoluril and formaldehyde in the presence of concentrated hydrochloric acid resulted in a polymeric substance which was named Behrend's polymer (Freeman, Mock et al. 1981). Though it was shown to form inclusion complexes with various dyes including Congo red and methylene blue, it was not until 1981 when Mock and colleagues characterised the compound and discovered the hexagonal macrocyclic structure with a hollow

core containing 6 glycoluril rings and 12 methylene bridges. This compound was subsequently called cucurbit[6]uril (CB[6]) with molecular formula of $C_{36}H_{36}N_{24}O_{12}$ (Mock and Shih 2002). It is a pumpkin shaped molecule with a wider cavity and a narrow portal on both sides. Hence it derived its name from cucurbitaceae, the taxonomical name for the family of pumpkins or gourds. In simple terms, it could be described as a "Halloween pumpkin" which has been hollowed out in the centre with holes drilled at the top and bottom. Cucurbiturils are characterised by hydrophobic cavity which is capable of hosting a variety of guest molecules and hydrophilic carbonyl lined portals which serve as entry and exit points for the cavity (Jason, Pritam et al. 2005).

Kim and colleagues and other researchers (Kim, Jung et al. 2000; Day, Arnold et al. 2001), characterised cucurbit[6]uril and developed other homologues namely cucurbit[n]urils (n=5,7,8) with "n" denoting the number of glycoluril rings (Figure 1.3). In brief, in variation with the initial synthesis of cucurbit[6]uril where higher temperature was used, reaction between glycoluril and formaldehyde catalysed by sulphuric acid at 75-90^{o}C for 24 hours resulted in a mixture of cucurbit[n]uril family. The resultant cucurbituril homologues (CB[5], CB[7] and CB[8]) were then separated by fractional crystallisation and characterised by X-ray crystallography. The ratio of the different cucurbit[n]urils could be altered by varying the concentration of the acid and temperature of reaction.

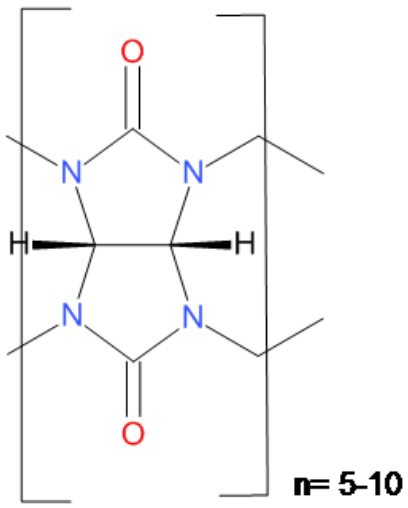

Figure 1.3: Chemical structure of cucurbit[n]uril, where "n" denotes number of glycoluril rings.

The size of internal cavity and portal of the CB homologues increases with the number of glycoluril rings and a variety of organic compounds including but not restricted to ranitidine, proflavine, curcumin and platinum based agents could be encapsulated within the cavity of CB homologues. Similarly the solubility also varies between the cucurbit[n]uril homologues (Lee, Samal et al. 2003; Jason, Pritam et al. 2005; Kim, Selvapalam et al. 2007). The X-ray crystallography of cucurbituril homologues (CB[5], CB[7] and CB[8]) and their physical properties are shown in figure 1.4 and table 1.1.

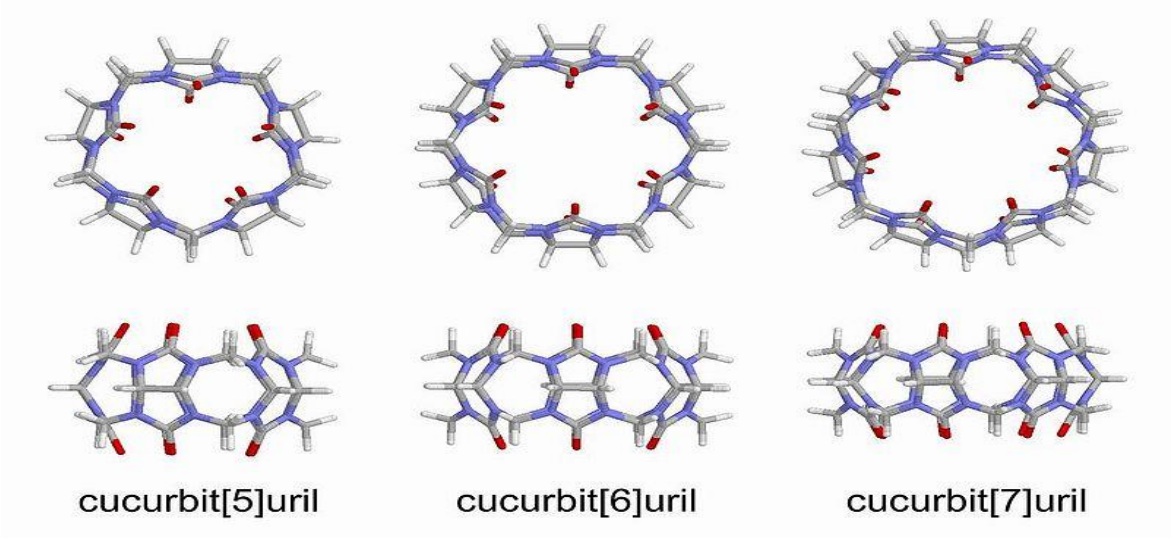

Figure 1.4: Top and side views of X-ray crystallography images of cucurbit[n]uril homologues. The red colour indicates carbonyl oxygen atoms lined portals (adapted from Jason, Pritam et al. 2005).

CB homologue	Portal width(Å)	Cavity width(Å)	Mass	Solubility in water (mM)
CB[6]	3.9	5.8	996.3	<0.05
CB[7]	5.4	7.3	1162.4	3.5
CB[8]	6.9	8.8	1328.4	<0.05

Table 1.1: Physical and structural characteristics of CB[n] homologues (Å=angstrom).

Cucurbit[7]uril exhibits many properties of an ideal drug delivery system. Cucurbit[7]uril is thermally stable and study of host guest chemistry reveals that a complex of di-platinum and CB[7] is stable at temperatures up to 290^{o}C (Kennedy, Florence et al. 2009). Homologues of cucurbit[7]urils are also capable of slow release of carrier drugs like ruthenium complexes (Pisani, Zhao et al. 2010). CB[7] is a biologically inert compound without inherent cytotoxic activity (Hettiarachchi, Nguyen et al. 2010) and maximum tolerated dose upon intravenous administration in mice was 250mg/kg (Uzunova, Cullinane et al. 2010).

Besides encapsulating various organic compounds, CB homologues in particular, CB[7] can encapsulate platinum compounds including cisplatin and oxaliplatin (Wheate 2008; Walker, Oun et al. 2011). Of note, the cavity of cucurbit[7]uril is adequate enough to encapsulate cisplatin to form inclusion complex in 1:1 ratio, and is relatively most soluble of all the CB homologues. Cisplatin upon encapsulation within CB[7] is completely within the cavity and when hydrolysed appears to be bound to the portals (Wheate 2008). These properties make CB[7] a suitable drug delivery system for cisplatin. A schematic representation of molecular modelling of CB[7]cisplatin with cisplatin encapsulated within the cavity of CB[7] is illustrated in figure 1.5.

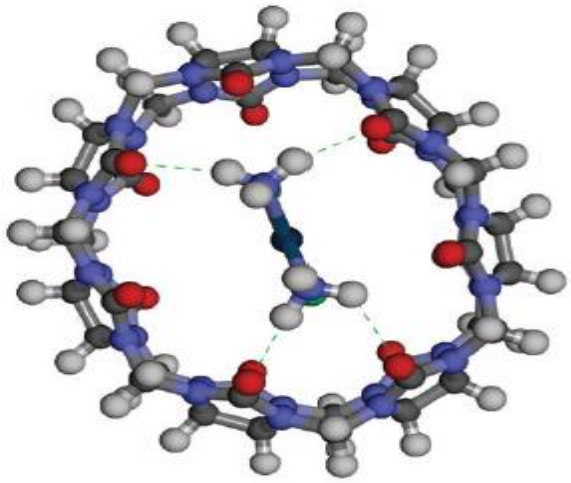

Figure 1.5: A schematic representation of CB[7]cisplatin. Cisplatin (central insert) is bound to the carbonyl lined portal of CB[7] (red bulb) through four hydrogen bonds (green dotted line) from the ammine group of cisplatin. (Figure reproduced with permission from Plumb, Venugopal et al. 2012).

1.9 Layout of the thesis

Chapter 2 describes the general methods used throughout these studies.

Chapter 3 describes the activity of CB[7] encapsulated cisplatin. This study was carried out in collaboration with Dr Nial Wheate (Strathclyde Institute of Pharmacy and Biological Sciences, Glasgow), a chemist with expertise in platinum delivery systems. Very little was known about activity of cucurbituril encapsulated cisplatin but it was known that cucurbiturils were well tolerated by mice at doses well above those required for drug delivery (250mg/kg, Wheate personal communication). The cell line model chosen for this study was, the well characterised human ovarian cancer cell line A2780, and the cisplatin-resistant derivative, A2780/cp70 (Plumb, Strathdee et al. 2000). This model was established in the department and the mechanism of resistance to cisplatin, loss of DNA mismatch repair through loss of MLH1 expression had already been shown to be clinically relevant (Plumb, Strathdee et al. 2000). Furthermore A2780 cell line is very sensitive to cisplatin and shows a clear dose response to treatment when grown as a xenograft in nude mice and small changes in cisplatin activity resulting from encapsulation should be detectable.

Chapter 4 describes the pharmacokinetics of cucurbituril encapsulated cisplatin in tumour bearing mice. Although the department had extensive experience of pharmacology associated with clinical trials there was no assay available for the estimation of cisplatin in biological samples. Cisplatin is a small molecule and is not suitable for the more traditional approaches to drug detection such as high-performance liquid chromatography (HPLC). Measurement of free platinum metal by mass spectroscopy has been widely used to establish the pharmacokinetic properties of platinum compounds (Graham, Lockwood et al. 2000). In order to detect the very low concentrations of platinum present in plasma and tumour samples the more sensitive Inductively Coupled Plasma Mass Spectroscopy (ICP-MS) has been used. This specialised equipment was not available in the department and the work was, therefore, carried out in collaboration with Professor Andrew Hursthouse (Professor of Environmental Geochemistry, School of Science, University of the West of Scotland, Paisley). He had extensive experience of elemental analysis but had no experience of elemental analysis of biological samples. This chapter, therefore, describes both

the development and validation of a method for the analysis of platinum and the application of the assay in a study of the pharmacokinetics of free and encapsulated cisplatin.

Human tumour xenografts are widely used in drug development studies. They are attractive since they are based on cell lines derived from human tumours and are thus thought to represent the characteristics of these tumours when grown *in vivo*. Studies with cell lines *in vitro* can give valuable information about the mechanism of action of drugs but do not take account of the pharmacology of the drug or of the effects on normal tissues and physiological processes. Xenografts are not ideal models of human cancers. They lack the appropriate tumour vasculature and microenvironment. Alternative models including orthotopic tumour implantation and those that display disseminated tumour growth are attractive but have lacked a suitable method for estimation of tumour growth. Even for subcutaneous xenografts, calliper measurements of tumour size do not give a true representation of the viable tumour mass and may underestimate growth inhibition. The development of technology that allows biophotonic imaging *in vivo* provides a mechanism for monitoring tumour cell burden in these more complex models. This technology was available in the department and the application and optimisation of bioluminescence imaging to monitor tumour cell growth *in vivo* in mice is described in chapter 5. This work enabled the assessment of drug sensitivity in a disseminated model of ovarian cancer. The disseminated ovarian cancer model was developed by a colleague, Dr Natividad Gomez-Roman, who also carried out the drug sensitivity study *in vivo*. The results are included in this thesis since the drug sensitivity study was a collaboration designed to evaluate the activity of both free and encapsulated cisplatin and the results clearly demonstrate the value of the more complex model.

Development of pharmacodynamic markers of drug activity is now an integral part of preclinical drug development. Whilst these assays are relatively easily applied to studies *in vitro* they do not readily translate to studies in animal models *in vivo* due to limited access to tumour tissue. In addition to measurement of tumour growth biophotonic imaging *in vivo* should allow the development of dynamic real-time markers of drug activity. Chapter 6 describes the development and evaluation of a luciferase based reporter of p53 activity

both *in vitro* and *in vivo*. The results are compared with those obtained by Western blotting and immunohistochemistry.

The final conclusions of the body of work are presented in chapter 7

2 Materials and Methods

Please refer appendix 1 for buffer and tissue culture media recipes, appendix 2 for contact details of manufacturers and suppliers and appendix 3 for antibodies and drugs.

2.1 Tissue culture techniques

2.1.1 Materials

Iwaki T75 sterile tissue culture flasks	Becton Dickinson
Iwaki T25 sterile tissue culture flasks	Becton Dickinson
Iwaki 6 well tissue culture plates	Becton Dickinson
Iwaki 24 well tissue culture plates	Becton Dickinson
Iwaki 96 well microtitre plates	Becton Dickinson
Petri dishes (5cm, 10cm)	Bibby Sterlin
Bijous (5mL)	Bibby Sterlin
Pippette aid pippetor	Drummond scientific
Costar pipettes (1mL, 5mL, 10mL, 25mL)	Corning, USA
Disposable tips	Central services, Beatson
Casy-1 cell counter	Scharfe system
Nunc Cryotubes	Thermo scientific
Growth medium (DMEM, RPMI)	Invitrogen
Fetal calf serum	Invitrogen
L-Glutamine	Invitrogen
Trypsin 2.5%	Invitrogen
Penicillin-Streptomycin	Invitrogen
Blasticidin	Invitrogen
Genetecin (G418)	Invitrogen
Phosphate buffered saline (PBS)	Refer appendix 1
Dimethylsulphoxide (DMSO)	Fisher
Large centrifuge 4K15	Sigma

2.1.2 Methods

Tissue culture was done under aseptic conditions in a microbiological safety cabinet with vertical laminar flow hood. Adherent human cancer cell lines were used for routine tissue culture. Cells were propagated by suspending them in growth medium supplemented with foetal calf serum (10%) and glutamine (2mM) in 75 cm^2 Iwaki flasks which were equilibrated with 5-10% CO_2. The cells were allowed to attach and grow by incubating in a humidified incubator at 37ºC. The culture medium was changed after 3-4 days and cells were sub-cultured once a subconfluent monolayer was formed.

Subconfluent monolayer culture was trypsinised by aspirating off the old medium, rinsing the cell monolayer with PBS to wash off the serum and adding trypsin solution (10mL of 2.5% trypsin [10 x] in 90mL PBS containing 1mM EDTA) to the cells. The volume of trypsin solution was dependant on the area of the flask and approximately 0.05mL of trypsin per cm^2 of flask was used. Subsequently the flask was left at 37ºC in humidified incubator for 2-3 minutes. The cells were examined under a microscope to confirm the detachment and then resuspended in growth medium to neutralise the trypsin. The cells were counted and aliquots of the cell suspension were added to flasks with fresh growth medium for further propagation. Cells were regularly monitored for mycoplasma contamination.

The source, origin and growth conditions of the cells are given in table 2.1

Cell line	Tumour type	Source	Growth conditions
A2780	Ovarian adenocarcinoma	Dr R F Ozols, Fox Chase Cancer center, Philadelphia, USA	RPMI 1640+10% FCS, 5% CO_2
A2780/cp70	Ovarian adenocarcinoma	Dr R F Ozols, Fox Chase Cancer center, Philadelphia, USA	RPMI 1640+10% FCS, 5% CO_2
MCP1	Ovary	Established "in house" (Strathdee, MacKean et al. 1999)	RPMI 1640+10% FCS, 5% CO_2
HCT116	Colon	American Type Culture Collection (ATCC), Maryland, USA	DMEM+10% FCS, 10% CO_2

Table 2.1: Origin, source and growth conditions of cell lines

2.1.3 Cryopreservation of cells

2.1.3.1 Materials

Routine tissue culture materials Refer section 2.1.1

-70ºC freezer	NuAire, U.K
Liquid nitrogen freezer	Sanyo, U.K

2.1.3.2 Method

Adherent cells in exponential growth phase were trypsinised and resuspended in growth medium. The cells were centrifuged at 300g for 5 minutes at room temperature. The supernatant was aspirated and discarded and the cell pellet was resuspended at a density of at least 10^6/mL in growth medium containing DMSO (10%). 1mL aliquots of the cell suspension were transferred to labelled cryotube™ vials. Cells were cryofrozen in a two-step process. Cryotubes were placed in a polystyrene foam box which was wrapped in cotton wool and frozen overnight to -70ºC in a freezer. Once the cells were frozen at -70ºC, the vials were transferred to isothermal dry storage liquid nitrogen freezer to be stored at -190ºC.

Thawing of cryopreserved cells was done by placing the cryotube vial in a waterbath at 37ºC. The contents of the cryotube vial were transferred to an universal container, resuspended in warm growth media and then centrifuged at 300g for 5 minutes at room temperature. The supernatant media containing DMSO was aspirated after which the cell pellet was resuspended in fresh growth media and seeded in a culture flask. After 24 hours, the cells were re-fed or sub-cultured depending on their confluency.

2.1.4 Quantitation of cells

2.1.4.1Materials

Routine tissue culture materials	Refer section 2.1.1.1

2.1.4.2 Method

Subconfluent monolayer cultures were trypsinised and collected in growth medium. Cells were then centrifuged at 300g for 5 minutes and the cell pellet was resuspended in growth medium. 400µL of the cell suspension was added to a counting cup and 19.6mL of Casyton solution added. They were counted in a CASY™ electronic cell counter.

2.1.5 Extraction of protein from cultured cells

2.1.5.1 Materials

PBS	Refer appendix 1
Trypsin 0.25% solution	Refer appendix 1
Protein lysis buffer	Refer appendix 1
Complete protease inhibitor cocktail tablets	Roche diagnostics, U.K
Large centrifuge 4K15	Sigma
Refrigerated centrifuge 5415R	Eppendorf
Soniprep 150	Thermo life sciences

2.1.5.2 Method

Growth medium from flasks containing a subconfluent monolayer culture was aspirated and the cells were washed twice with ice-cold PBS. Remnants of the PBS were aspirated and appropriate volume of protein lysis buffer was added to the cells and the cells incubated on ice for 20 minutes. Typically 100µL of protein lysis buffer was added to a $25cm^2$ volume flask. The lysed cells were then scrapped from the flasks and transferred to 1.5mL microfuge (Eppendorf ™) tubes which were placed on ice. Cells were sonicated with Soniprep 150 Sonifier® (ultrasonic cell disintegrator). The cell lysate was centrifuged in a bench top centrifuge at 12,000g for 30 minutes at 4ºC to remove cell debris. The supernatant, containing the protein, was collected and stored at -20ºC until further analysis.

2.1.6 Estimation of protein concentration

2.1.6.1 Materials

Bovine serum albumin	Sigma Aldrich, U.K
Bio-rad protein dye	Bio Rad laboratories
UV/Vis spectrophotometer	Perkin Elmer
Plastic cuvettes	Elkay Laboratory, U.K
Deionised water	Millipore

2.1.6.2 Method

Estimation of protein concentration was carried out by a calorimetric assay based on Bradford dye binding procedure (Bradford 1976). Protein standards, at concentrations ranging from 0.2mg/mL to 1 mg/mL, were prepared with bovine

serum albumin to generate a standard curve. Protein samples, to be analysed, were diluted ten-fold with distilled water. 800µL of distilled water was added to plastic cuvettes to which 10µL of diluted protein samples was added. Finally, 200µL of Bio-Rad protein assay dye reagent was added to all the cuvettes and the solution was thoroughly mixed by inversion. The absorbance was measured at a wavelength of 595nm with Parkin Elmer Lambda 25 UV/Vis spectrophotometer. UV Winlab™ software was used to determine the protein concentration.

2.2 Chemosensitivity assay

The drug sensitivity of cells was assessed using a tetrazolium dye-based microtitration assay (Plumb, Milroy et al. 1989). MTT (3-(4, 5-dimethylthiazol-2-yl)-2, 5-diphenyltetrazolium bromide), a yellow water soluble tetrazolium dye, is reduced by viable cells to a purple MTT-formazan dye which is insoluble in aqueous solution. The amount of MTT-formazan produced corresponds to the surviving cell number. Upon solubilisation with DMSO, the amount of MTT-formazan produced can be determined spectrophotometrically, which provides an estimate of the surviving cell fraction.

2.2.1.1 Materials

Costar multichannel pipette	Corning International
96-well microtitre plates, flat bottomed	Iwaki
3-(4, 5-dimethylthiazol-2-yl)-2, 5-diphenyltetrazolium bromide (MTT)	Sigma
Sorensen's glycine buffer	Refer appendix 1
Labsystems multidrop 384 dispenser	Thermo Electron
Plate reader	Molecular devices
Routine tissue culture materials	Refer section 2.1.1

2.2.1.2 Method

A subconfluent monolayer culture was trypsinised, resuspended in growth medium. Cells were counted and diluted to the appropriate plating density (ranging from 1.5 to 10 x 10^3 cells/mL) in fresh growth medium. A multi-channel pipette was used to dispense 200µL of cell solution in to microtitre plates from columns 2 to column 11. 200µL of growth medium alone was added to columns 1 and 12. Cells were allowed to attach and grow in a humidified incubator at 37ºC

for 2-3 days. Drug solutions with 8 different concentrations of drug in growth medium were freshly prepared by serial dilution with a starting concentration, which typically was 100μM. The concentrations of the drug were chosen such that the highest concentration would achieve 100% cell-kill and the lowest concentration would not result in cell-kill. The growth medium was removed and the cells in columns 2 and 11 were fed with drug free growth medium. The drug containing growth medium was added to the cells in columns 3 to 10 (4 wells/concentration). The plates were then incubated in a humidified atmosphere at 37ºC for 24 hours. The medium was removed and replaced with 200μL of fresh drug-free growth medium. After 2-3 days the cells were fed with 200μL of fresh growth medium and 50μL of MTT was added to wells from column 1 to column 11. The plates were wrapped in aluminium foil to protect from light exposure and incubated in a humidified atmosphere at 37ºC. After 4-6 hours of incubation with MTT, both medium and MTT were removed from all the wells. The purple MTT-formazan crystals were dissolved by the addition of 200μL of DMSO, which was dispensed with microplate dispenser. 25μL of Sorensen's glycine buffer was added to all the wells in columns 1 to column 11 to shift the pH of the wells to 10.5 and the absorbance was recorded at 570nm in a microtitre plate reader. The absorbance was plotted in Y axis against drug concentration plotted in X axis and a graph was generated using software programme, Softmax PRO™. The mean absorbance from the wells in columns 2 and 11 was used as a control and the IC_{50} was determined as the drug concentration that results in 50% reduction of the absorbance of the control. Each experiment was carried out in triplicate and repeated at least once. The results are presented as mean ± S.E.M of a representative experiment.

2.3 Western Blotting

Western blotting is an effective technique for immunodetection of proteins based on their molecular weight. Proteins, under denatured and reducing conditions (by addition of DTT and heating), are separated using sodium dodecyl sulphate polyacrylamide gel electrophoresis (SDS-PAGE). The addition of negatively charged SDS to the denatured proteins imparts a net negative charge to the proteins which when loaded on to a polyacrylamide gel are separated according to their molecular weight on applying electric current through the gel. A molecular weight marker dye is also loaded on to one of the lanes of the gel as

a guide to indicate the molecular weight of the separated proteins. The separated proteins are then transferred to nitrocellulose or polyvinylidene fluoride (PVDF) membrane and specific proteins can be identified by adding primary antibodies directed against them. This protein-antibody binding reaction can be amplified by addition of horse radish peroxidase (HRP) conjugated secondary antibody directed against the primary antibody, followed by addition of chemiluminescent substrate which emits a light signal that is captured with autoradiography.

2.3.1 Materials

NuPage MOPS running buffer	Invitrogen
NuPage transfer buffer	Invitrogen
NuPage SDS sample buffer	Invitrogen
NuPage antioxidant	Invitrogen
Ultrapure water	Millipore
Dithiothreitol (DTT)	Sigma
Novex X-Cell Sure-Lock minicell	Invitrogen
Dri-Block heating block	Techne
Whirlmixer vortex	Fisher
Novex pre-cast polyacrylamide gels (4-12%, 10%)	Invitrogen
See-blue Plus 2 protein Standard	Invitrogen
Running buffer	Refer appendix 1
Transfer buffer	Refer appendix 1
Blocking solution	Refer appendix 1
Marvel milk powder	Premier foods, U.K
Immobilin-P transfer membrane	Millipore
3MM filter paper	Whatman International
Antibodies – primary and secondary	Refer appendix 2
Hulme Martin heat bag sealer	Jencons
Rocking 4RT table	Luckham
Rotatest R100 shaker	Luckham
ECL Western detection reagent	Amersham Biosciences
Fuji Super RX Medical X-ray Film	Fuji
Hypercassette 18 x 24 cm	Amersham Biosciences
X-OMAT 480 RA processor	Kodak

2.3.2 SDS-PAGE

The Novex mini-gel system was used for Western blotting. Proteins were separated according to their molecular weight using sodium dodecyl sulphate polyacrylamide gel electrophoresis (SDS-PAGE) and analysed further by Western blotting. 100µg of protein extract, made up to volume of 65µL distilled water, was denatured and reduced by adding 25µL of NuPAGE (4X) SDS sample buffer

and 10µL of DTT followed by heating at 70ºC for 10 minutes. Molecular weight marker (SeeBlue plus2 ™ pre-stained standard) and 20µg of denatured protein sample were loaded to separates wells in NuPAGE polyacrylamide gel which was immersed in X-Cell Sure lock ™ minicell tank filled with NuPAGE MOPS running buffer. The gradient of polyacrylamide gel was dependent on the molecular weight of proteins analysed and the commonly used gradients were 4-12% or 12% acrylamide gel. The gel tank was connected to a power pack and run at 200V for 50 minutes at room temperature.

2.3.3 Immunoblotting

The proteins were transferred from the acrylamide gel to polyvinylidene fluoride (PVDF) microporous membrane (Immobilin-P ™ transfer membrane) using semi-dry electroblotting transfer method according to the manufacturer's instructions. The transfer membrane was pre-wet in 100% methanol for 1-2 minutes and then equilibrated with transfer buffer together with blotting paper and sponge pad. The gel and transfer membrane was sandwiched between the pre-wet blotting paper and sponge pads soaked in transfer buffer and, placed in a transfer unit. The transfer unit was then held vertically in a gel tank, with platinum electrodes, that was filled with transfer buffer and run at 30V for 1 hour. This resulted in the transfer of negatively charged SDS-loaded protein from the gel to the transfer membrane. The efficiency of the transfer was assessed by complete visualisation of the coloured bands of the molecular weight marker in the transfer membrane.

2.3.4 Immunodetection of proteins

Following transfer of proteins to transfer membrane, the unoccupied protein binding sites in the transfer membrane were blocked by gently agitating the transfer membrane in blocking buffer (Marvel plus Tween 20 in Tris buffered saline) at room temperature for 1 hour. The transfer membrane was then incubated overnight at 4ºC with primary antibody (with dilution as per appendix 3), in sealed airtight plastic sleeve which was placed in an orbital shaker. The next day, the transfer membrane was rinsed and washed three times with washing buffer by gentle agitation in an orbital shaker for 10 minutes each. The transfer membrane was then incubated at room temperature for I hour, with

appropriate horse radish peroxidase conjugated secondary antibody which was diluted in blocking solution. Following this process, the membrane was rinsed and washed three times as before with washing buffer. The visualisation of secondary antibody was enhanced by incubating the washed transfer membrane with Amersham ECL western blotting reagents for 1 minute and the light emission was detected by short exposure to blue light sensitive autoradiography film. The film was developed using Kodak X-OMAT 480 RA processor.

2.4 Animal experiments

2.4.1 Materials

CD-1® athymic nude mice	Charles River
25G needles	Becton Dickinson
Syringes 1mL, 3mL	Becton Dickinson
Balance	Mettler
Vacutainer (EDTA bottles)	Becton Dickinson
Small CO2 chamber	Vet Tech solution
Calliper	

CD-1® athymic nude mice were obtained from Charles River laboratories. Mice were housed in a sterile environment in the biological services unit, Beatson Institute of Cancer Research. All the procedures were carried out under a UK Home office project licence.

2.4.2 Development of subcutaneous xenografts

2.4.2.1 Materials

Routine tissue culture materials	Refer section 2.1.1
Animal experiment materials	Refer section 2.4.1

2.4.2.2 Method

Cells were trypsinised, collected and centrifuged at 300g for 5 minutes. The supernatant was discarded the cell pellet was resuspended in sterile PBS to achieve a concentration of 5-10 x 10^6 cells per 100µL. 100-200µL of the cell suspension was injected subcutaneously into the flank of immunodeficient nude mice using a 1mL syringe with 23G needle. Mice were inspected once every 2-3

days for general welfare and tumour growth. Once the mean diameter of the tumours had reached 5mm mice were used for experiments. Mice were randomised into groups of six and treated as specified in specific experiments. All handling and injections were carried out in a laminar flow hood under aseptic conditions. Mice were weight daily and tumour volumes determined by calliper measurements. The volume of the tumour was calculated using the formula ($\pi/6$ X d^2), where "d" is the mean of the two perpendicular diameters.

2.5 Molecular Biology Techniques

2.5.1 Reverse Transcriptase-Polymerase Chain Reaction (RT-PCR)

Polymerase chain reaction is a useful tool to amplify specific DNA sequence. DNA of interest is denatured and annealed by subjecting to thermal cycles of heating and cooling. This denatured and annealed DNA when subjected to a reaction between appropriate combination of oligonucleotides, thermo stable Taq or DNA polymerase and Magnesium salts results in the exponential amplification of the DNA sequence of interest. The final product of PCR can be checked by agarose gel electrophoresis using ethidium bromide as DNA marker, which can be visualised by illumination under ultraviolet light.

2.5.1.1 Materials

Sterile water for injection	Braun
Agarose	Bio-Rad
TAE buffer	Refer appendix 1
Ethidium bromide (0.625mg/mL)	NBS Biologicals
Electrophoresis unit	Pharmacia, Biotech
DNA ladder	Invitrogen
Oligonucleotides	Promega
Peltier Thermal Cycler DNA engine	Bio-Rad
Agarose	Melford

2.5.1.2 Method

Reverse Transcriptase-Polymerase Chain Reaction (RT-PCR) was used to obtain the plasmids for recombination reaction by BIO-RAD tetrad peltier thermal cycle. Taq polymerase (0.5µL), primers (10µM), dNTP (10µM), $MgCl_2$ (50µM) and

DNA (100nGµL) were mixed in a PCR tube and the machine was run at the following setting: 94ºC for 3 minutes, 94ºC for 45 seconds, 55ºC for 30 seconds, 72ºC for 90 seconds, 72ºC for 10 minutes and finally cooled to 4ºC overnight.

The final product from PCR was analysed with agarose gel electrophoresis (1.5% agarose gel with ethidium bromide, run at 50 volts for 45 minutes) and the DNA bands were visualised with UV transilluminator.

2.5.2 Restriction digest

2.5.2.1 Materials

Restriction enzymes and buffers	Invitrogen
RT-PCR materials	Refer section 2.5.1.1

2.5.2.2 Method

DNA was digested by mixing 1µL each of appropriate restriction digest enzyme and buffer along with 8µL of DNA in a vortex mixer and incubating at room temperature for 1 hour. The digested fragments were analysed by agarose gel electrophoresis (1.0% agarose gel with ethidium bromide, run at 100V for 45 minutes). Electrophoresis gels were prepared by dissolving electrophoresis grade agarose in TAE buffer and boiling in microwave at full power for 1-2 minutes. Once the solution was cooled to 50ºC, 5µg/mL of ethidium bromide was added and gel was allowed to solidify in a gel former.

The bands were assessed for the appropriate fragment size by correlating against the bands from the DNA ladder and were subsequently imaged with SYNGENE gel visualisation system.

2.5.3 Bacterial Transformation

2.5.3.1 Materials

Transformation competent E.coli cells	Invitrogen
SOC medium	Invitrogen
LB broth	Central services, Beatson
Rocking incubator	Innova
Ampicillin	Sigma
Kanamycin	Sigma

2.5.3.2 Method

Bacterial transformation was performed using One Shot® Stbl3 ™ chemically competent E.coli cells or other cells as specified by manufacturer. One vial of E.coli cells was thawed on ice and the DNA (prepared from recombination reaction) was added to the vial and mixed gently. The mixture was placed on ice for 30 minutes and the cells were then heat-shocked for 45 seconds at 42ºC. The vial was removed from the water bath and placed on ice for 2 minutes. 250µL of pre-warmed SOC medium was added to the vial. The vial was closed tightly and placed in a shaking incubator to be shaken horizontally at 225rpm for 1 hour at 37ºC. The contents of the vial were streaked on pre-warmed selective agar plate with appropriate antibiotics (chosen according to the resistance cassette in the plasmid) and incubated overnight at 37ºC. The volume used for streaking varied from 25µL to 250µL according to the density of colony formed. The next day, colonies were picked and cultured overnight in LB medium, containing appropriate antibiotics, by agitating the medium in a shaking incubator at 37ºC. The broth was centrifuged at 1200g for 15 minutes at room temperature to obtain a bacterial pellet, which was used for DNA extraction as per manufacturer's instruction (e.g. Qiagen).

2.5.4 Extraction of DNA

2.5.4.1 Materials

DNA extraction kit	Qiagen
Micro centrifuge tubes	Eppendorf
Refrigerated centrifuge	Eppendorf

2.5.4.2 Method

Extraction of genomic DNA from cultured cancer cell lines was done accordance with the protocol from Qiagen. Briefly, cultured cells in exponential growth phase were trypsinised, resuspended in growth medium and centrifuged at 300g for 5 minutes. The supernatant was discarded and the pellet was resuspended in 200µL of PBS to which 20µL of Proteinase K was added. 200µL of buffer AL was

then added, mixed thoroughly, and incubated at 56ºC for 10 minutes. 200µL of ethanol was added to the sample and mixed by vortexing to obtain a homogenous solution. The contents were pipetted into a DNeasy mini spin column placed in a 2mL collection tube and centrifuged at ≥6000g for 1 minute. The mini spin column was placed in a new collection tube and 500µL of buffer AW1 was added and centrifuged at ≥6000g for 1 minute. Subsequently 500µL of buffer AW2 was added to the mini spin column which was now placed in another fresh collection tube and centrifuged at ≥20,000g for 3 minutes, to dry the membrane. The mini spin column was placed in a clean 1.5mL micro centrifuge tube and 200µL of buffer AE was added. DNA was eluted by incubating the membrane for 1 minute at room temperature and then centrifuging for ≥6000g for 1 minute. The DNA was quantified as described below (section 2.5.5).

2.5.5 Quantification of DNA

2.5.5.1 Materials

Spectrophotometer	Nanodrop
Deionised water	Millipore

2.5.5.2 Method

DNA was quantified using Nanodrop™ ND1000 spectrophotometer based on its absorbance of UV light. 1-2µL of sample was placed on a fibre optic pedestal (sample arm) which forms a liquid column when in contact with another fibre optic pedestal (receiving arm). Light shone through the sample liquid column using a pulsed xenon flash lamp was analysed using a spectrophotometer, measures the DNA concentration of the sample using Beer's law. The ratio of absorbance at 260nm and 280nm was calculated and A_{260}/A_{280} ratio of 1.8 was the accepted standard for purity of DNA. Distilled water (1µL), used as a blank, was pipetted on to the sample pedestal which was wiped clean with tissue paper. The sampling arm was closed and the absorbance was measured. Once the measurement is complete, the surfaces were wiped clean and 1µL of samples were sequentially analysed.

2.5.6 Transfection with DNA

2.5.6.1 Materials

Routine tissue culture materials	Refer section 2.1.1
Lipofectamine™ 2000	Invitrogen
Opti-MEM	Invitrogen

2.5.6.2 Method

Transfection of cells was done in accordance with Lipofectamine 2000™ protocol. Briefly, 7.5 - 10 x 10^5 cells were seeded in 6 well plates in growth medium without antibiotics aiming for 90-95% confluence after 24 hours of incubation in humidified incubator at 37ºC. On the day of transfection, the cells were fed with 2mL of fresh growth medium per well. The volume of the transfection reagent and the amount of the DNA per well could be scaled up or down according to the Lipofectamine 2000™ protocol. In the case of 6 well plates, 4µg of DNA per well was used to transfect the cells, which was diluted in 240µL of serum free Opti-MEM. Similarly, 10µL of Lipofectamine transfection reagent was diluted with 240µL of serum free Opti-MEM. The diluted DNA and transfection reagent were mixed together and incubated at room temperature for 20 minutes, following which the DNA-transfection reagent complexes were added to the cells. The plates were left in humidified incubator with 95% atmospheric air and 5% CO_2 at 37ºC. The medium in all the wells was changed after 6 hours and the incubation was allowed to continue for 24 hours, before checking for transgene expression. Stably transfection cell lines were then produced by propagating the cells in growth medium containing appropriate selection antibiotics.

3 Activity of cucurbituril encapsulated cisplatin in ovarian cancer

3.1 Introduction

Cisplatin is widely used in the treatment of variety of malignancies including testicular, lung, ovarian and gastric cancers both with curative and palliative intent. Ovarian cancer has a good overall response rate to treatment with cisplatin both in early and advanced stage. Unfortunately the response is not sustained and the tumour eventually becomes resistant to cisplatin (Ozols 2002; Hennessy, Coleman et al. 2009; Ledermann and Raja 2011). In contrast, treatment with a cisplatin based chemotherapy regimen is curative in 70% of patients with testicular cancer and in early stage testicular cancer nearly 100% of patients can be cured (Einhorn 2002; Jones and Vasey 2003). However, in the majority of tumour types the clinical activity of cisplatin is restricted by toxicity and drug resistance, both inherent and acquired. Cisplatin kills rapidly dividing cells. It is a low molecular weight molecule and once administered is distributed non-specifically to both malignant and normal tissues. The proliferating compartments of normal tissues such as the bone marrow and gut are damaged, resulting in intolerable toxicities which limit the clinical efficacy of cisplatin. The dose limiting toxicity of cisplatin is nephrotoxicity and other toxicities include nausea, vomiting, ototoxicity and neurotoxicity (Hartmann and Lipp 2003; Kelland 2007). Aggressive hydration with 0.9% saline before and after the infusion of cisplatin has significantly reduced the nephrotoxicity of cisplatin (Cornelison and Reed 1993). Similarly the use of effective anti-emetics has attenuated the emetogenic side effects of cisplatin (Marty, Pouillart et al. 1990; Hesketh, Grunberg et al. 2003). However, the other toxicities like neurotoxicity still continue to hamper the clinical use of cisplatin and there is evidence that these toxicities persist even decades after treatment (Sprauten, Darrah et al. 2012). Attempts to circumvent toxicity through the development of less toxic analogues have had limited success. To date, only carboplatin and oxaliplatin have been approved globally. The introduction of carboplatin resulted in a significant reduction in the nephrotoxicity associated with platinum based chemotherapy. By contrast, oxaliplatin has a different clinical profile compared to cisplatin in that it is active in colorectal cancer, a tumour type otherwise

resistant to platinum based chemotherapy (Sugasawa, Ng et al. 1998; Raymond, Faivre et al. 2002; Ibrahim, Hirschfeld et al. 2004).

An alternative approach to the toxicity problem is to deliver the drug preferentially to the tumour. Drug delivery systems can protect the drug from degradation or alter the pharmacokinetics of the drug resulting in prolonged plasma/tissue half-life, reduced toxicities and enhanced anti-tumour efficacy. Drug delivery systems include polymer based drug carriers, lipid based carriers such as liposomes and micelles, dendrimers and gold nanoparticles. To date, no one system has been shown to be ideal. Liposomal drug delivery is hampered by lack of controlled release, rapid clearance by reticuloendothelial system and instability of the carrier resulting in opsonisation, a process by which liposomes are cleared from circulation by the Kupffer cells in the liver (Yan, Scherphof et al. 2005). Polymer-drug conjugates suffer from polymer-induced immunogenicity and toxicity, tight binding of polymer to the drug with resultant suboptimal release of drug and loose binding leading to premature drug release has limited the widespread use of these agents. Attempts to improve the delivery of cisplatin using drug delivery systems have involved conjugation with polymers or encapsulation within liposomes as discussed in chapter 1. The conjugation of platinum compound with HPMA co-polymer (AP5280) resulted in increased tumour delivery of platinum but did not translate to increased platinum-DNA adduct formation and there was no reduction in the nephrotoxic side effects of platinum (Lin, Zhang et al. 2004; Rademaker-Lakhai, Terret et al. 2004). Liposomal formulation of cisplatin, lipoplatin, demonstrated limited or absence of nephrotoxicity in mice bearing prostate cancer and although this drug has been evaluated in early phase clinical trials, significant questions remain about its pharmacokinetic profile and clinical efficacy (Jehn, Boulikas et al. 2007). Polymeric micelles incorporating cisplatin (NC-6004) have shown promising pre-clinical activity with increased anti-tumour activity and decreased nephrotoxicity in mice (Nishiyama, Okazaki et al. 2003). However in the phase I trial NC-6004 in patients with advanced cancer, there were increased incidence of nephrotoxicity and hypersensitivity reactions (Plummer, Wilson et al. 2011). These data indicate that drug delivery systems using cisplatin confer advantages namely increased plasma circulation time and increased platinum delivery to tumour but are limited by toxicities and/or absence of anti-tumour activity in

clinical trials. There is an unmet need to evaluate novel drug delivery systems to enhance the activity of cisplatin.

3.1.1 Cucurbit[7]uril encapsulated cisplatin

Many delivery systems are toxic and some show anti-tumour activity (Gabizon, Shmeeda et al. 2003). There are few if any studies that compare delivery systems in the same experimental model and it is, thus, difficult to select a drug delivery system that will suit the drug of interest. Cucurbiturils offered a novel drug delivery system that is commercially available but has not been exploited extensively. Cucurbiturils are not cytotoxic to cells in culture and are well tolerated *in vivo* (Wheate, personal communication). Besides encapsulating various organic compounds CB[7] and CB[8] can encapsulate platinum compounds including cisplatin and oxaliplatin (Wheate 2008; Walker, Oun et al. 2011). The cavity of cucurbit[7]uril is large enough to encapsulate cisplatin to form an inclusion complex in a 1:1 ratio, and is the most soluble of all the CB homologues (Figure 1.5, chapter 1). These properties make CB[7] a suitable drug delivery carrier for cisplatin. Cisplatin upon encapsulation within CB[7] is completely within the cavity and when hydrolysed appears to be bound to the portals (Wheate 2008) . The complex is too small to exploit the EPR effect but could protect cisplatin from thiol degradation once in the circulation. The aim of this study was to determine whether cisplatin when incorporated within cucurbit[7]uril retained cytotoxicity *in vitro* in cancer cell lines and *in vivo* in a human tumour xenograft model. The human ovarian cancer cell line A2780 and two independently derived cisplatin resistant variants (A2780/cp70 and MCP1) were used since these are established in the department and have been well characterised for cisplatin sensitivity. Both A2780/cp70 and MCP1 lack a functional DNA mismatch repair mechanism due to methylation of the *MLH1* gene promoter and cisplatin resistance can be reversed by re-expression of MLH1 (Plumb, Strathdee et al. 2000). The human colon cancer cell line HCT116 was included as a second tumour type since this cell line is resistant to cisplatin due the lack of a functional DNA mismatch repair system (Wheeler, Beck et al. 1999). Cucurbit[7]uril cisplatin, herein after, will be referred to as CB[7]cisplatin.

3.2 Methods

3.2.1 Synthesis of CB[7]cisplatin

CB[7] was either obtained commercially or synthesised by Dr Nial Wheate (Strathclyde Institute of Pharmacy and Biomedical Sciences-SIBPS, University of Strathclyde). CB[7]cisplatin was synthesised by Dr Nial Wheate at SIBPS, University of Strathclyde by the addition of equimolar quantities of CB[7] and cisplatin in distilled water. The resultant solution was then freeze dried or rotary evaporated to dryness for 3 hours. Binding of cisplatin to CB[7] was confirmed by nuclear magnetic resonance (NMR) spectroscopy. CB[7] dissolved on its own in distilled water has a spike in the resonance at 5.6 ppm (parts per million), whereas, upon addition of cisplatin, there is a division of the peak resonance. The representative NMR spectrum of CB[7] alone and CB[7]cisplatin (which has been provided by Dr Nial Wheate's group) is illustrated in figure 3.1 whereby the splitting of the resonances indicate that cisplatin is encapsulated within the cavity of CB[7] (Wheate 2008) .

The molecular weight of the final product was analysed by mass spectrometry, from which the amount of water molecules was calculated. The molecular weight of the resultant CB[7]cisplatin was dependent on the number of water molecules which could be controlled to be between 5 and 13 per batch. The molecular mass of CB[7] is 1162.4. Dependent on the method of preparation, the water content of CB[7] cisplatin can vary and the formula weight of CB[7]cisplatin was calculated according to each individual formulation to account for the number of water molecules. For *in vitro* and *in vivo* experiments in this thesis, the molecular mass of CB[7]cisplatin was calculated as 1697.2g since there were six water molecules in the formulation of CB[7]cisplatin.

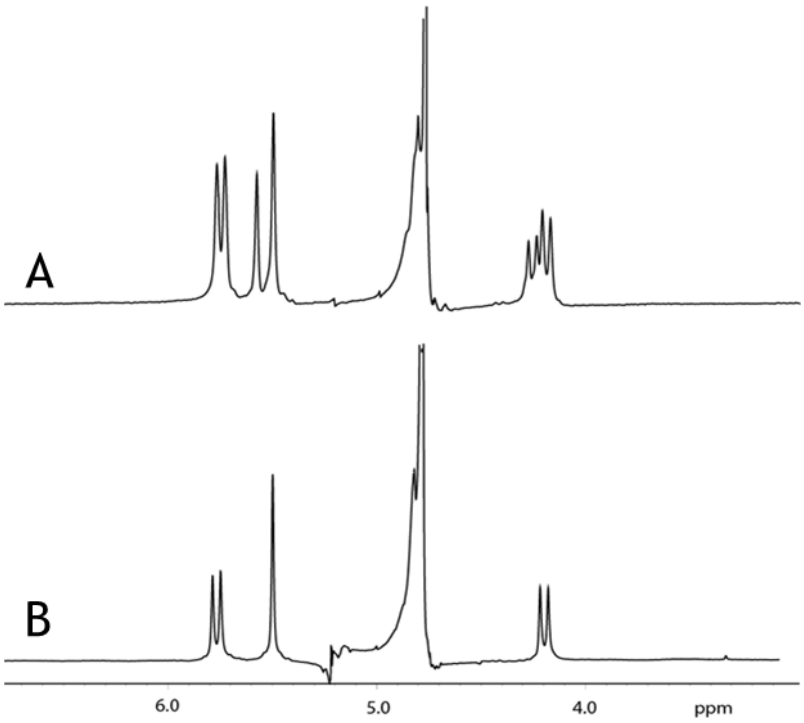

Figure 3.1: Representative NMR spectra of CB[7] cisplatin (A) and CB[7] in distilled water(B). The spike in the resonance at 5.6 ppm corresponds to CB[7] (B) which is split in to two upon addition of cisplatin to CB[7](A).

3.2.2 Cytotoxicity of CB[7]cisplatin in vitro

The cytotoxicity of CB[7]cisplatin was determined by the MTT based growth inhibition assay as described in section 2.2, chapter 2. CB[7]cisplatin was dissolved in PBS at a concentration of 10mM immediately before further dilution in culture medium and addition to the cells. Cells were exposed to drug for 24 hours. CB[7]cisplatin when dissolved in PBS was shown to be stable based on the NMR studies done by our collaborators at University of Strathclyde. However in order to avoid any potential interactions due to the stability of CB[7]cisplatin was freshly constituted in PBS just before using for *in vitro* or *in vivo* experiments.

3.2.3 Induction of p53 and PARP inhibition

A2780 cells were grown in T25 flasks to reach 70-80% confluence and were incubated with a range of concentrations of cisplatin and CB[7]cisplatin (0.04 to 5μM) for 24 hours. Cells were washed with ice cold PBS and lysed with protein lysis buffer and protein was extracted as described in section 2.2.2, chapter 2.

Samples (20μg protein) were analysed by Western blotting as described in section 2.1.5, chapter 2. The primary antibody was anti-p53, clone DO-1 or anti-PARP.

3.2.4 Activity of CB[7]cisplatin in vivo

3.2.4.1 Drugs

The clinical formulation of cisplatin at 1mg/ml was obtained from the pharmacy Beatson West of Scotland Cancer Centre (BWoSCC) for use in the animal experiments. It was diluted to 0.6mg/ml with sterile PBS such that injection of 10μL/g body weight gave a dose of 6mg/kg which was selected as the maximum tolerated dose from previous experience (Plumb, personal communication). CB[7]cisplatin was administered at a dose of 34mg/kg which was equivalent to 6mg/kg cisplatin. It was dissolved in sterile PBS at a concentration of 3.4mg/ml and administered at a rate of 10μL /g body weight. CB[7] was administered at a dose of 250mg/kg which was known to be non-toxic (Wheate, personal communication). This dose of CB[7] is also consistent with published literature indicating that the MTD of CB[7] is 250mg/kg when administered intravenously (Uzunova, Cullinane et al. 2010).

3.2.4.2 Human ovarian cancer xenografts

Xenograft experiments were conducted in collaboration with Dr Jane Plumb. Subcutaneous human tumour xenografts were developed as described in section 2.4.2, chapter 2. Briefly, 10^7 cells which were suspended in PBS were injected subcutaneously into the right flank of athymic nude mice and were monitored for tumour growth. Once the tumours reached a mean diameter of 5mm (day 0), mice were randomly divided into four groups of 5. They were treated by subcutaneous injection of either PBS (control), cucurbit[7]uril (250mg/kg), cisplatin (6mg/kg body weight of mouse) or CB[7]cisplatin (34mg/kg, equivalent to cisplatin at 6mg/kg). Tumour volumes and body weight were measured daily for one week. Tumour volume and body weight on day 0 was equated to unity and change in tumour volume and body weight relative to day 0 was calculated to obtain relative tumour volume and body weight.

3.3 Results

3.3.1 Cytotoxicity of CB[7]cisplatin in vitro

The cytotoxicity of cisplatin and CB[7]cisplatin determined *in vitro* is shown in Table 3.1. All the experiments were performed in triplicates and were repeated at least three times. CB[7] alone at doses up to 1mM did not result in any growth inhibition for all the tested ovarian cancer cell lines. The cytotoxicity of cisplatin and CB[7]cisplatin was comparable for all four cell lines studied (Table 3.1) and is clearly seen from the survival curves for A2780 and A2780/cp70 shown in figure 3.2 and 3.3 respectively. Resistance factors (fold resistance) which is derived by dividing the IC_{50} of resistant cell lines (A2780/cp70 or MCP1) by the IC_{50} of sensitive cell line (A2780) were comparable for both cisplatin and CB[7]cisplatin. As shown in table 3.2, A2780/cp70 and MCP1 are 21 and 5.6-fold resistant to cisplatin and exhibit comparable resistance factors for CB[7]cisplatin which has a resistance factor of 23-fold and 4.6-fold for A2780/cp70 and MCP1 respectively. The cytotoxicity of cisplatin and CB[7]cisplatin was different for human colon cancer cell line HCT116 but this data still demonstrate that encapsulation of cisplatin within CB[7] has not resulted in any loss of cytotoxicity in these colon cancer cell lines.

Cell line	IC_{50} (μM)	
	Cisplatin	CB[7]cisplatin
A2780	0.10 ± 0.004	0.11 ± 0.006
MCP1	0.56 ± 0.007	0.51 ± 0.16
A2780/cp70	2.06 ± 0.07	2.13 ± 0.08
HCT116	5.63 ± 0.58	2.52 ± 0.70

Table 3.1: Cytotoxicity of cisplatin and CB[7]cisplatin in cell lines *in vitro* as determined by an MTT based growth inhibiton assay. Cells were exposed to drug for 24 hours and sensitivity is expressed as the concentration required to reduce cell survival by 50% (IC_{50}). The results are mean ± S.E.M of three replicates.

Cell line	Resistance factors	
	Cisplatin	CB[7]cisplatin
A2780/cp70	21	23
MCP 1	5.6	4.6

Table 3.2: Resistance factors of A2780/cp70 and MCP1 to cisplatin and CB[7]cisplatin relative to A2780 cells as calculated from MTT based growth inhibition assays.

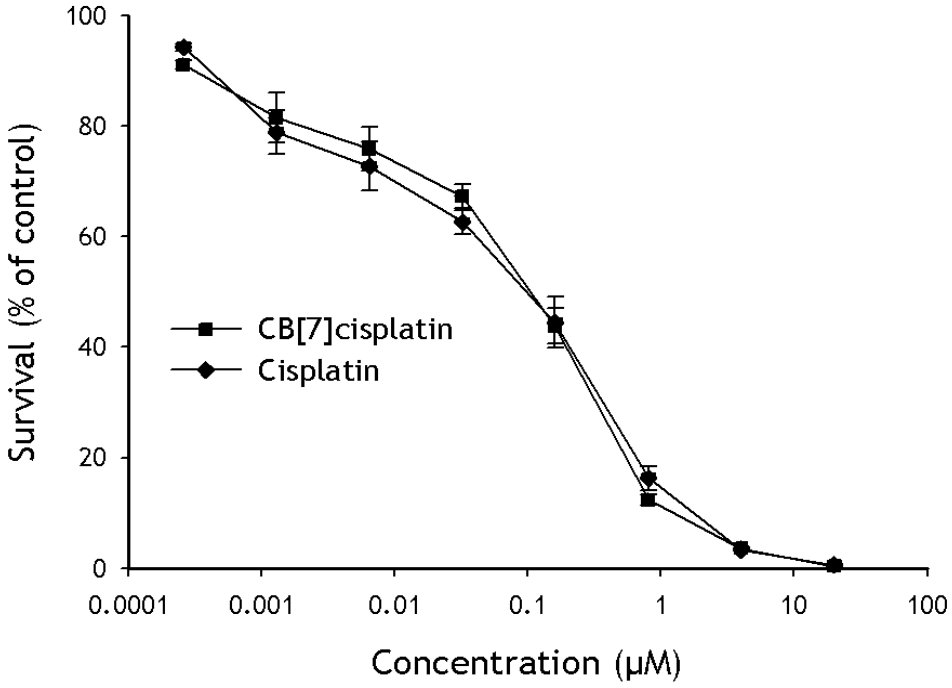

Figure 3.2: MTT based growth inhibition assay for A2780 cells treated with cisplatin or CB[7]cisplatin. The results are mean of three replicates with the error bars representing S.E.M

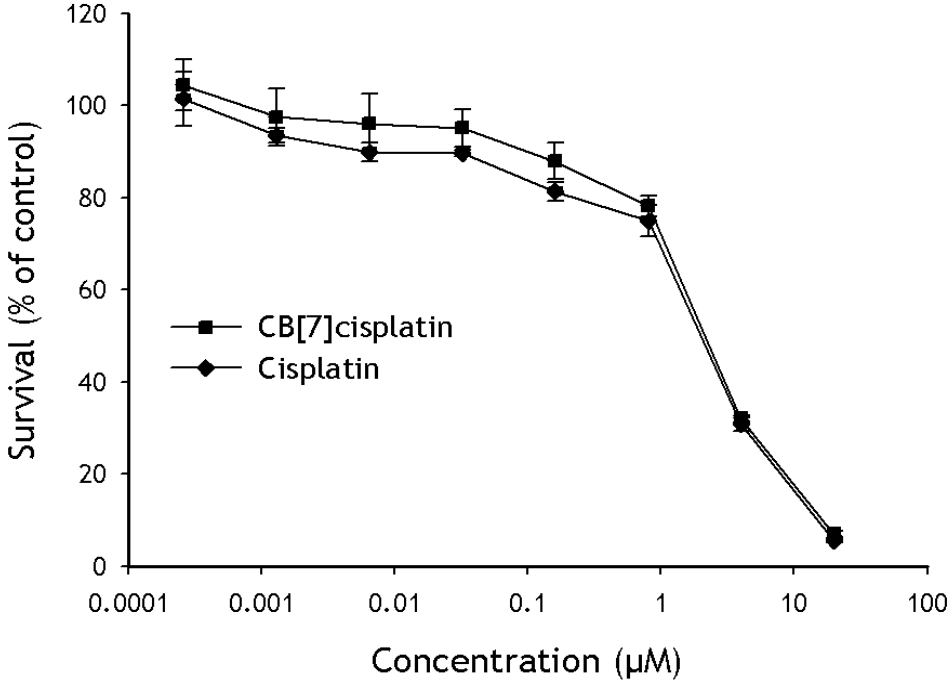

Figure 3.3: MTT based growth inhibition assay for A2780/cp70 cells treated with cisplatin or CB[7]cisplatin. The results are mean of three replicates with the error bars representing S.E.M.

3.3.2 Induction of p53

Expression of p53 in cell line A2780 determined by Western blotting following treatment of cells with either cisplatin or CB[7]cisplatin for 24 hours is shown in figure 3.4. A2780 has low levels of expression of p53 and expression increases with increasing concentrations of cisplatin. A similar increase is observed after exposure to CB[7]cisplatin.

3.3.3 PARP Expression

Expression of PARP in cell line A2780 determined by Western blotting following treatment of cells with either cisplatin or CB[7]cisplatin for 24 hours is shown in figure 3.5. Intact PARP is observed as a band at 116kd in untreated A2780 cells. Treatment of cells with either cisplatin or CB[7]cisplatin results in cleavage of PARP as shown by the appearance of a cleavage product of 89kd. Cleavage is detected at a concentration of 1μM for both treatments and is much more marked at 5μM.

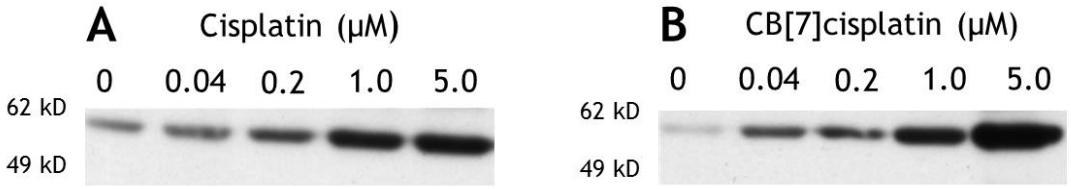

Figure 3.4: Induction of p53 expression by cisplatin (A) and CB[7]cisplatin (B) in A2780. Cells were incubated with a range of concentrations of cisplatin or CB[7]cisplatin for 24 hours and induction of p53 was detected by Western blotting. The position of molecular weight markers is shown. The results of one of two replicate experiments are shown.

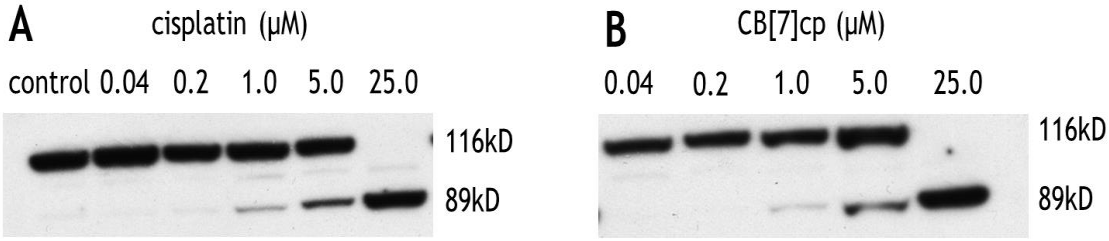

Figure 3.5: Induction of PARP cleavage by cisplatin (A) and CB[7]cisplatin(B) in A2780 cells. Cells were incubated with a range of concentrations of cisplatin or CB[7]cisplatin for 24 hours and PARP cleavage was detected by Western blotting. The results of one of two replicate experiments are shown.

3.3.4 Activity of CB[7]cisplatin in A2780 xenografts

The growth of xenografts of A2780 following treatment with cisplatin or CB[7]cisplatin is shown in figure 3.6 and table 3.3. The tumour doubling time of A2780 xenografts (controls) is 3.1 ± 0.1 days and CB[7] alone had no effect on the growth of the tumours (doubling time 2.9 ± 0.2 days, table 3.3). A2780 xenografts are sensitive to cisplatin and tumour doubling time was increased significantly to 4.9 ± 0.2 days (P=0.0036) following a single intraperitoneal injection of cisplatin (6mg/kg). Treatment with CB[7]cisplatin (34mg/kg, dose equivalent of 6mg/kg cisplatin) also showed a significant growth delay compared to the control group (6.3 ± 0.5 days vs. 3.1 ± 0.1 days, P=0.0042). The tumour growth delay following CB[7]cisplatin treatment (6.3 days) was slightly greater than that seen following cisplatin treatment (4.9 days) but this increase did not reach statistical significance (P = 0.19). All treatments were well tolerated and the mice did not show significant loss of body weight as shown in figure 3.7.

3.3.5 Activity of CB[7]cisplatin in A2780/cp70 xenografts

The growth of xenografts of A2780/cp70 following treatment with cisplatin or CB[7]cisplatin is shown in figure 3.8 and table 3.3. A2780/cp70 xenografts are resistant to the MTD of cisplatin (6mg/kg). The mean tumour doubling time for control untreated mice was 3.2 ± 0.1 days and was not significantly different for the cisplatin treated group (3.8 ± 0.6 days, P = 0.2). By contrast, treatment with CB[7]cisplatin (34mg/kg) resulted in a significant reduction in tumour growth as illustrated by the increase in tumour doubling time to 5.3 ± 0.2 days (P=0.0015; Figure 3.8). Treatment with CB[7] alone had no effect on tumour growth and mice tolerated all treatment with no significant weight loss (Figure 3.9).

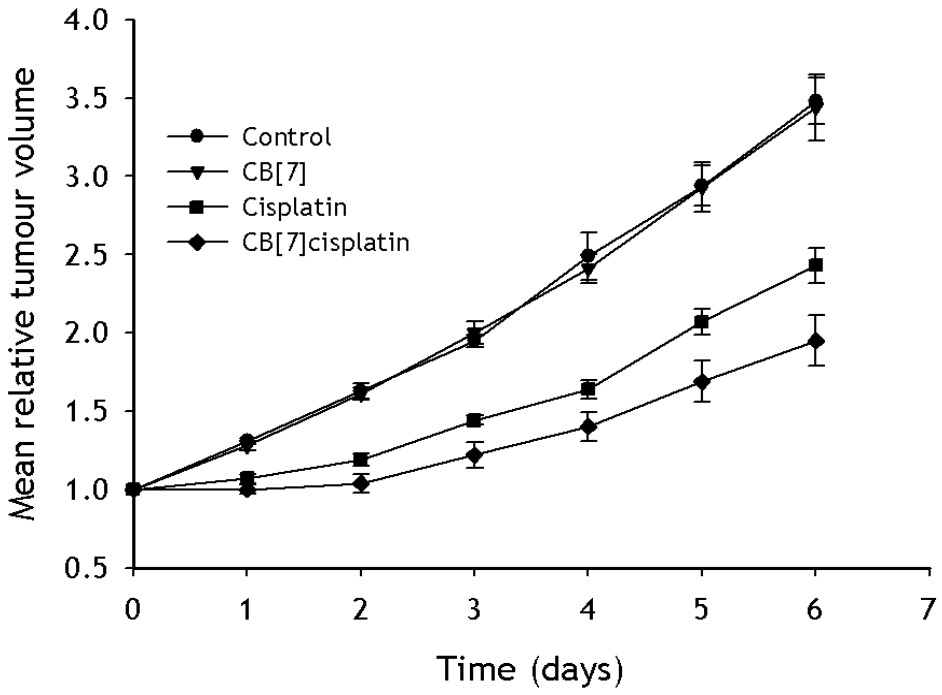

Figure 3.6: Growth of A2780 xenografts following single intraperitoneal injection of saline (●), CB[7] at 250mg/kg(▼), cisplatin at 6mg/kg (■) and CB[7]cisplatin at 34mg/kg (◆). Results shown are mean ± SEM of 5 mice.

.

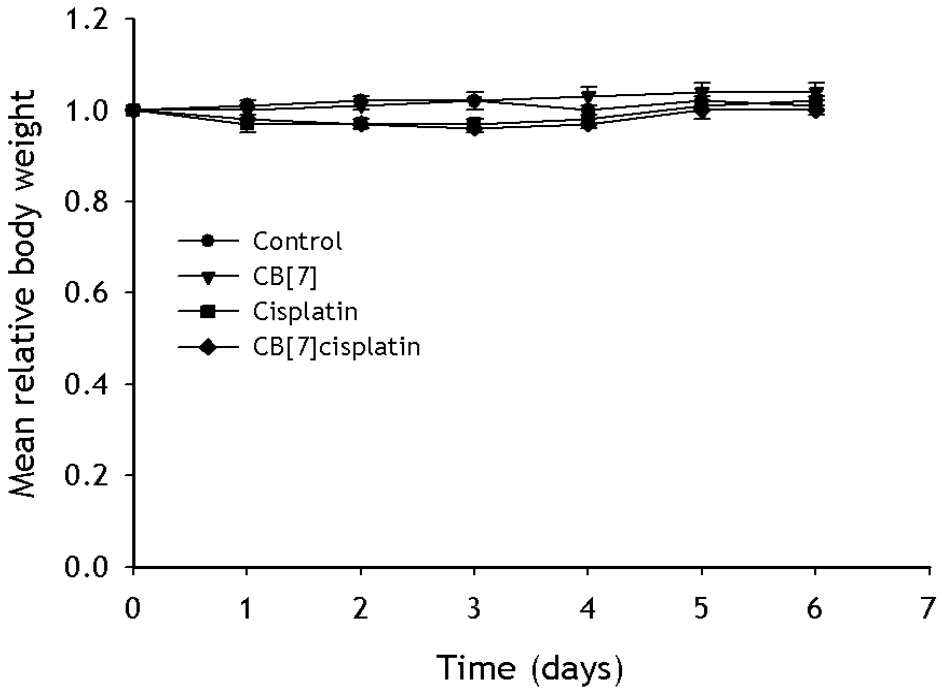

Figure 3.7: Relative body weight of mice following single intraperitoneal injection of saline (●), CB[7] at 250mg/kg(▼), cisplatin at 6mg/kg (■) and CB[7]cisplatin at 34mg/kg (◆). Results shown are mean ± SEM of 5 mice.

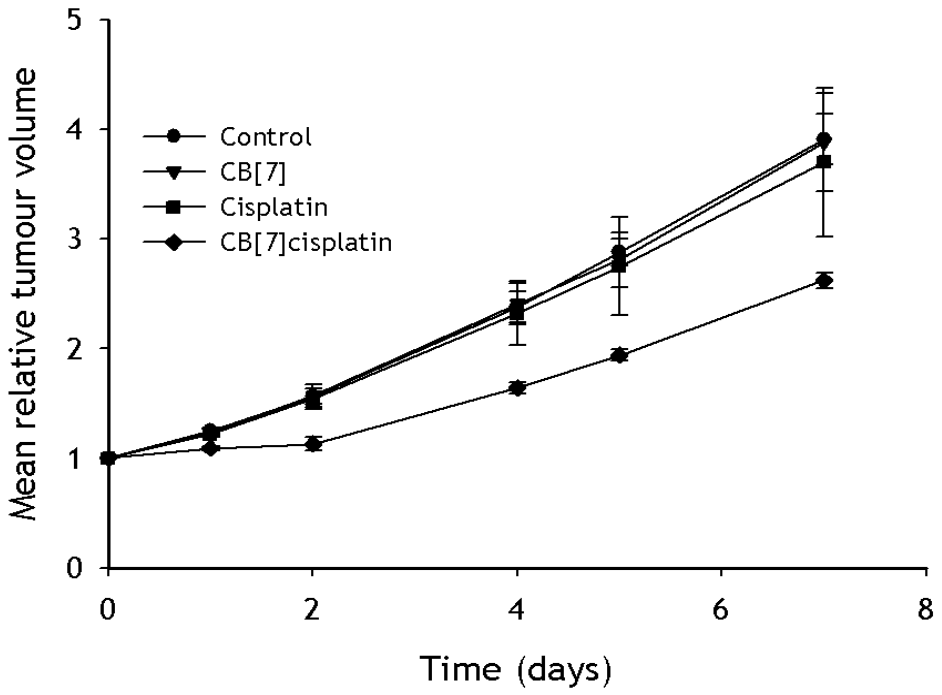

Figure 3.8: Growth of A2780/cp70 xenografts following single intraperitoneal injection of saline (●), CB[7] at 250mg/kg(▼), cisplatin at 6mg/kg (■) and CB[7]cisplatin at 34mg/kg (◆). Results shown are mean ± SEM of 5 mice.

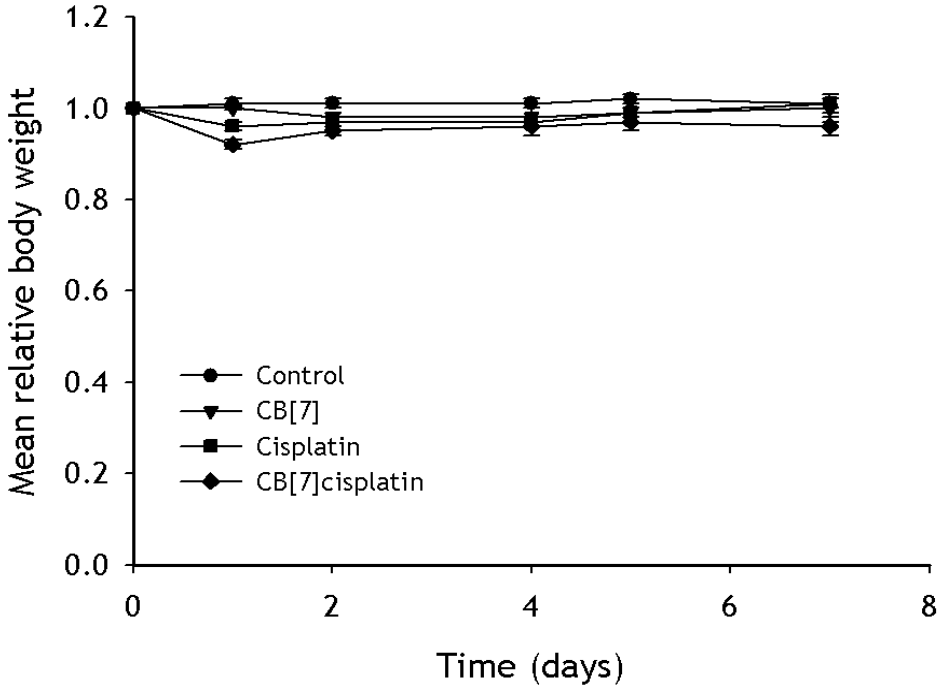

Figure 3.9: Relative body weight of mice with A2780/cp70 xenografts following single intraperitoneal injection of saline (●), CB[7] at 250mg/kg (▼), cisplatin at 6mg/kg(■) and CB[7]cisplatin at 34mg/kg (◆). Results shown are mean ± SEM of 5 mice.

Treatment	Tumour volume doubling time (days)	
	A2780	A2780/cp70
Control	3.1 ± 0.1	3.2 ± 0.1
CB[7]	2.9 ± 0.2	3.4 ± 0.4
Cisplatin (6mg/kg)	4.9 ± 0.2 P=0.0036	3.8 ± 0.6 P=0.19
CB[7]cisplatin (34mg/kg)	6.3 ± 0.5 P=0.0042	5.3 ± 0.2 P=0.0015

Table 3.3: Tumour doubling times for A2780 and A2780/cp70 xenografts following treatment with either saline (control), CB[7], cisplatin or CB[7]cisplatin. The results are mean ± S.E.M of 5 mice. P values indicate statistically significant differences compared to the control group. NS = not significant

3.3.6 Activity of CB[7]cisplatin in HCT116 *xenografts*

The growth of xenografts of HCT116 following treatment with cisplatin or CB[7]cisplatin is shown in figure 3.10. Xenografts of HCT116 are slow growing tumours with a doubling time of approximately 6 days. HCT116 xenografts are resistant to the MTD of cisplatin (6mg/kg). There is a clear tumour growth delay following treatment with CB[7]cisplatin but the duration of this experiment was too short to calculate tumour doubling times. As noted in mice with ovarian tumour xenografts, there was no significant loss of body weight (Figure 3.11).

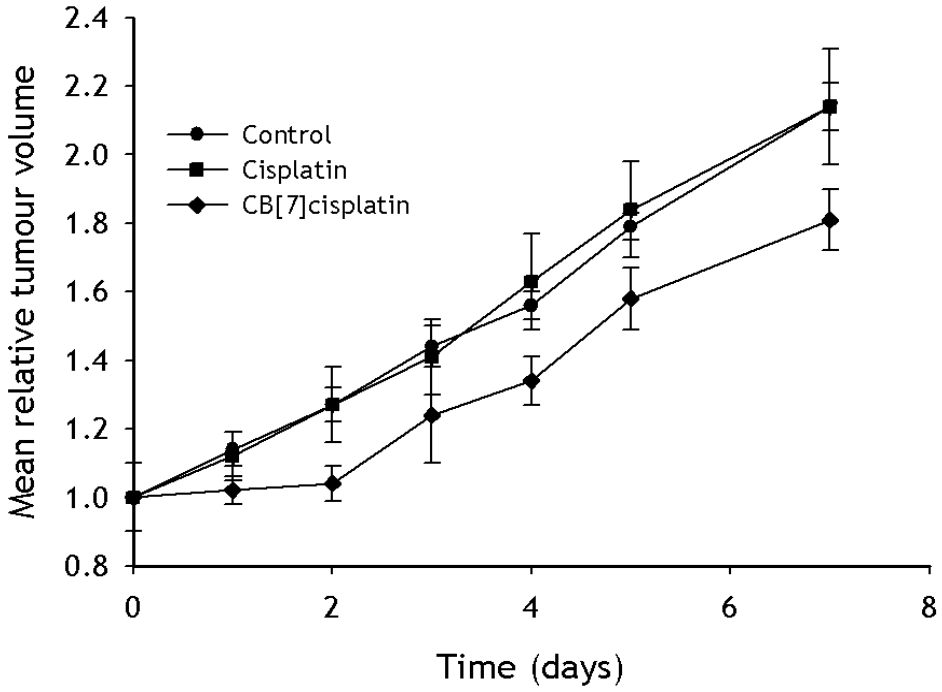

Figure 3.10: Growth of HCT116 xenografts following single intraperitoneal injection of saline (●), cisplatin at 6mg/kg (■) or CB[7]cisplatin at 34mg/ kg (◆). Results shown are mean ± SEM of 5 mice.

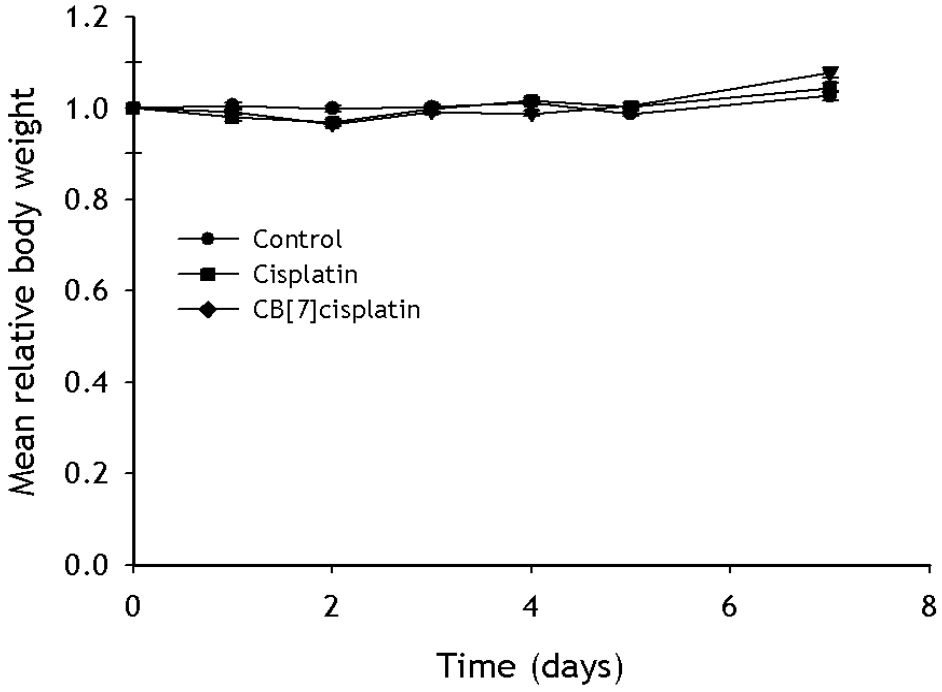

Figure 3.11: Relative body weight of mice with HCT116 xenografts following single intraperitoneal injection of saline (●), cisplatin at 6mg/kg (■) or CB[7]cisplatin at 34mg/ kg (◆). Results shown are mean ± SEM of 5 mice.

3.4 Discussion

Encapsulation of cisplatin within CB[7] has no effect on the cytotoxicity of the drug in cell lines. The IC_{50} values for cisplatin and CB[7]cisplatin in the ovarian cell lines are comparable and encapsulation has no effect on the cellular resistance to cisplatin. In addition, encapsulation has no effect on the ability of cisplatin to induce p53 expression or cleavage of PARP. By contrast, encapsulation of cisplatin results in enhanced anti-tumour activity such that significant growth inhibition is observed in xenografts of A2780/cp70 which are resistant to the maximum tolerated dose of free cisplatin.

3.4.1 Activity of CB[7]cisplatin in vitro

The growth inhibition assays demonstrate that the cytotoxic activity of CB[7]cisplatin is comparable to cisplatin and that the encapsulation of cisplatin within CB[7] does not reduce the cytotoxicity of cisplatin (Figures 3.2 and 3.3, Table 3.2). These results are promising given that encapsulation of platinum compounds, in general, has been shown to result in loss of the cytotoxic activity. Jeon and colleagues reported a 4-10 fold reduction in the *in vitro* cytotoxicity of oxaliplatin encapsulated within CB[7] in a variety of cell lines (Jin Jeon, Kim et al. 2005). Similarly, binding of cisplatin to PAMAM [poly(amidoamine)] dendrimers, resulted in 2-11 fold reduction in the *in vitro* cytotoxicity of cisplatin in both cisplatin sensitive and resistant ovarian cancer cell lines. Of note, it was also demonstrated that the PAMAM bound cisplatin has enhanced *in vivo* efficacy in mice bearing A2780 tumour xenograft (Kirkpatrick, Plumb et al. 2011).

A2780/cp70 cells are resistant to cisplatin and the cellular sensitivities determined in this study are comparable to published results (Plumb, Strathdee et al. 2000). However, CB[7]cisplatin is not able to circumvent drug resistance. Cell lines, A2780/cp70 and MCP1 are independently selected cisplatin resistant derivatives of A2780. Both have lost expression of MLH1 due to gene promoter methylation and A2780/cp70 has also lost functional regulation of p53 (Strathdee, MacKean et al. 1999). These cell lines A2780/cp70 and MCP1 are 21 and 5.6 fold resistant to cisplatin respectively, and the resistance is not reduced

by treatment with encapsulated cisplatin (Figure 3.3). In addition, these results also confirm that cucurbit[7]uril alone does not exhibit any cytotoxicity *in vitro*.

Cisplatin induced DNA damage results in stabilisation and activation of p53 and induction of apoptosis (Wang and Lippard 2005). The ovarian cancer cell line A2780 is relatively sensitive to cisplatin. It has functional wild type p53 and expresses the MLH1 component of DNA mismatch repair pathway. This pathway has been shown to be involved in the recognition of cisplatin DNA adducts and induction of apoptosis (Anthoney, McIlwrath et al. 1996; Strathdee, MacKean et al. 1999). Induction of p53 expression and apoptosis as measured by PARP cleavage were determined by Western blotting. The degree of p53 induction and PARP cleavage was similar in cells treated with cisplatin and cells treated with CB[7]cisplatin (Figures 3.4 and 3.5). These results suggest that the encapsulation of cisplatin within CB[7] does not prevent the interaction between cisplatin and DNA, resulting in apoptosis, which is consistent with the observed similarity in cytotoxicity.

The results from the cell based assays suggest that CB[7]cisplatin is as effective as free cisplatin. This result is promising given that in some instances encapsulation of platinum drugs within different sized cucurbit[*n*]urils (*n* = 6, 7, 8 or 10) led to large or complete loss of cytotoxicity *in vitro* (Jin Jeon, Kim et al. 2005; Kirkpatrick, Plumb et al. 2011). Previously it has been speculated that the decrease in cytotoxicity *in vitro* of some platinum drugs upon encapsulation with cucurbit[*n*]urils was due to either decreased cell uptake or because the drugs were too strongly bound by the cucurbit[*n*]uril and could not go on to bind DNA at a sufficiently fast rate (Wheate 2008). In only a few instances has encapsulation by cucurbit[6]uril increased the cytotoxicity of platinum(II)-based DNA intercalator drugs (Kemp, Wheate et al. 2007; Wheate, Taleb et al. 2007).

However, these results do not exclude the possibility that cisplatin dissociates from the CB[7] cavity whilst in the culture medium and that the activity that is noted is due to the free drug. A cucurbit[7]uril-acridine orange dye complex has been used to demonstrate that cucurbit[7]urils can cross the cell membrane (Montes-Navajas, Gonzalez-Bejar et al. 2009). It has been reported that the fluorescent properties of proflavine change when bound within CB[7] (Kemp, Wheate et al. 2007) and it was thought that this property, whereby the spectral

shift could be used to determine whether CB[7] can penetrate into the ovarian cancer cells. However, no such change in fluorescence was observed when proflavine was encapsulated within CB[7] (data not shown).

3.4.2 Activity of CB[7]cisplatin in vivo

Xenografts of A2780 show a dose-dependent growth delay following treatment with cisplatin (Plumb, Strathdee et al. 2000). The tumour doubling time of A2780 was 3.1 days and this was delayed to 4.9 days when treated with the MTD of cisplatin (6mg/kg) (Figure 3.6). When treated with encapsulated cisplatin at a dose equivalent of 6mg/kg the growth delay for the cisplatin sensitive A2780 xenografts (6.3 days) was equivalent if not greater than when mice were treated with the free drug (Figure 3.6, Table 3.3). Although this increased growth delay did not reach statistical significance, the fact that xenografts of A2780 show a dose dependent growth inhibition indicates that the encapsulation increases the activity of cisplatin. The cisplatin resistant derivative of A2780 (A2780/cp70) has a similar doubling time (3.2 days) to A2780. It is resistant to the maximum tolerated dose of cisplatin but showed a significant growth delay (doubling time delayed to 5.3 days) when mice were treated with CB[7] encapsulated cisplatin at 6mg/kg dose equivalent (Figure 3.8, Table 3.3). The CB[7] control by itself demonstrated no toxic side-effects in these mice, up to a dose of 250 mg/kg, which is consistent with previous studies of this macrocycle that have demonstrated that CB[7] at doses up to 250mg/kg are non-toxic to mice (Wheate 2008; Uzunova, Cullinane et al. 2010). The CB[7] encapsulated cisplatin had no significant effect on the body weight of the mice suggesting that there is no increased toxicity associated with encapsulation (Figures 3.7 and 3.9). That CB[7]cisplatin was active in the drug resistant xenografts of A2780/cp70 suggest that the increased growth delay observed for A2780 xenografts is real.

Since the cucurbiturils have no inherent anti-tumour activity, the observed growth delay for the drug resistant A2780/cp70 xenografts is most likely due to an increased exposure to cisplatin compared to the use of the free drug. This would also explain the slight increase in activity of CB[7]cisplatin in the A2780 xenografts when compared with the free drug. Unfortunately encapsulation did not alter the MTD of cisplatin. The therapeutic index of CB[7]cisplatin could have been widened if the safe delivery of higher dose equivalent of cisplatin is

possible. However the *in vivo* experiments with CB[7]cisplatin at dose of 34mg/kg (equivalent to 6mg/kg of cisplatin) demonstrated that toxicity profile of CB[7] cisplatin was similar to but not better than cisplatin. It could only be speculated that encapsulation of cisplatin within CB[7] did not change the MTD of cisplatin as higher doses of CB[7]cisplatin were not evaluated to avoid suffering to mice.

The encapsulation of cisplatin was thought to protect cisplatin from thiol degradation whilst in the plasma. Partial encapsulation of oxaliplatin within CB[7] resulted in decreased platinum reactivity with methionine and guanosine (Jin Jeon, Kim et al. 2005). NMR spectroscopy studies have also shown that that encapsulation of trans-dinuclear platinum within CB[7] protects the platinum from reacting with sulphur containing thiols, glutathione and methionine (Bali, Buck et al. 2006). It is also possible that degradation occurs within the tumour although increased glutathione levels are not a major mechanism of resistance in A2780/cp70 cells (Plumb, Strathdee et al. 2000). In order to determine whether the activity of CB[7] cisplatin was specific to the ovarian model a human colon tumour xenograft was included in the study. Human colon cancer cell line HCT116 is resistant to cisplatin due to loss of DNA mismatch repair resulting from a mutation in the gene for the MLH1 protein component (Wheeler, Beck et al. 1999). Whilst HCT116 xenografts were resistant to the MTD of cisplatin, a clear growth delay was observed when mice were treated with CB[7]cisplatin (Figure 3.10). This observation indicates that the activity of CB[7]cisplatin is not tumour type specific.

3.5 Conclusion

Encapsulation of cisplatin within CB[7] does not overcome cisplatin resistance at the molecular level but does enhance the anti-tumour activity *in vivo* without an associated increase in toxicity. This is an important observation since a general increase in plasma levels of cisplatin would be expected to increase toxicity as well as anti-tumour activity. Cucurbiturils are too small to exploit the enhanced permeability and retention (EPR) effect and lack a targeting moiety that would selectively deliver the drug to the tumour. It is also possible that the tumour microenvironment could favour CB[7]cisplatin. The most likely explanation for

the enhanced activity in the absence of increased toxicity is that encapsulation alters the plasma and tissue pharmacokinetics. Since toxicity is potentially related to the peak plasma levels of cisplatin it is possible that encapsulation delays the release of cisplatin such that overall exposure is maintained or enhanced without the increase in peak plasma concentration that would be seen with an increased dose of free cisplatin.

4 Pharmacokinetics of cucurbituril encapsulated cisplatin

4.1 Introduction

The xenografts experiments described in chapter 3 demonstrate that CB[7]cisplatin can overcome cisplatin resistance in A2780/cp70 xenografts. However, experiments *in vitro* with CB[7]cisplatin have shown that CB[7]cisplatin does not circumvent the molecular mechanism of resistance in the A2780/cp70 cells. It was concluded that the enhanced activity of CB[7]cisplatin in the xenografts is most likely due to a pharmacokinetic effect. The synthesis of CB[7]cisplatin was based on the hypothesis that the encapsulation would prevent thiol degradation *in vivo* and hence prolong the half-life of cisplatin in the circulation.

The mechanism of action of cisplatin is not tumour-specific since the mechanism of action targets all dividing cells. As a result utility *in vivo* is limited by the therapeutic index of the drug as it is for many conventional chemotherapeutic agents. Provided that the tumour is more sensitive to the drug than is the normal tissue, growth inhibition can be achieved. Cisplatin was used at the maximum tolerated dose *in vivo* in the xenografts and this dose is sufficient to cause a growth delay in the parental A2780 xenografts but not in the A2780/cp70 xenografts (Figure 3.6 and 3.8). Encapsulation of cisplatin has increased the therapeutic index of cisplatin such that activity is observed in the drug resistant xenografts. In order to understand the basis for the enhancement we examined the pharmacokinetics of encapsulated cisplatin in the mice.

Pharmacokinetics is the study of the absorption, distribution, metabolism and excretion of the drug in the body. Each of these factors influences the overall exposure of the body organs and the tumour to the drug. In the mouse studies cisplatin was administered intraperitoneally and has to pass from the peritoneal cavity into the circulation. The amount that reaches the tumour depends on the efficiency of absorption, the volume of distribution and the rate of clearance from the circulation. Encapsulation, in addition to other changes in pharmacokinetics, could affect the rate of absorption, stability of the drug in the circulation and the rate of clearance. For some drugs toxicity is related to

the peak plasma levels (Cmax) achieved while for others it is the overall exposure to the drug that is important. Similarly, anti-tumour activity can be dependent on the peak plasma concentration, overall exposure or a combination of the two (Undevia, Gomez-Abuin et al. 2005). Overall exposure is quantified as the area under the plasma concentration/time plot (AUC). In the mice, cisplatin was administered as a bolus dose. Since cisplatin is readily absorbed into the circulation, the peak plasma concentration is directly related to the dose of cisplatin administered. The pharmacokinetics study was thus designed to measure the peak plasma concentration and the AUC of the free and encapsulated cisplatin.

Evaluation of the pharmacokinetics of a drug ideally requires an assay capable of detecting small amounts of the drug, metabolites and break down products in biological samples. However, there are only few reliable assays for the measurement of cisplatin in biological samples due to lack of a technique for detection of this small molecule. Measurement of free platinum metal has been used to establish the pharmacokinetic properties of platinum compounds (Morrison, White et al. 2000). In particular, in our group there was paucity of a reliable assay to measure the platinum levels in biological samples.

4.2 Platinum analysis with Inductively Coupled Plasma–Mass Spectrometry

4.2.1 Basic principles of ICP-MS

Inductively Coupled Plasma–Mass Spectrometry (ICP-MS) is an elemental analysis technique which is now widely used to quantitatively measure trace amounts of metal based anti-cancer agents like platinum in biological samples (Brouwers, Tibben et al. 2008). Earlier studies utilising atomic absorbance spectrometry (AAS) to estimate the platinum levels were limited by poor sensitivity and were not suitable to demonstrate the lesser magnitude yet pharmacologically significant difference in platinum levels between various newer formulations of platinum compounds (Tothill, Matheson et al. 1990). The use of ICP-MS in evaluating pharmacologically relevant elements has been extensively reviewed (Huang, Hu et al. 2006; Brouwers, Tibben et al. 2008). Briefly, ICP-MS relies on the ability of inductively coupled plasma (ICP) to convert the sample to

distinctly charged ions. These charged ions in turn can be detected by mass spectrometer based on their mass-charge ratio (m/z) which then translates the concentration of the analyte (platinum) in the sample to integrated counts per second.

4.2.1.1 Advantages of ICP-MS

Limited sample availability and low concentration of platinum in the plasma are the limiting factors in performing pharmacokinetics of platinum compounds in human plasma samples and animal models. The high sensitivity and wide linear dynamic range of ICP-MS helps to measure the platinum exposure in cellular samples and in various biological matrices including plasma, plasma ultra-filtrate (pUF) and tissues (tumour and organs).

The signal intensity or the counts per second is not dependent on the chemical structure of the metal compound. This allows the measurement of elemental platinum in both the free and encapsulated cisplatin but does not allow measurement of drug metabolism and degradation. Unlike other bio-analytical assays, such as high-performance liquid chromatography (HPLC), a single validated method and sample preparation protocol can be used to analyse platinum levels in different biological matrices including plasma and tissues. The wide linear dynamic range of detection allows the measurement of platinum levels in plasma at both early and late time points without affecting the sensitivity in a single analytical experiment. The low detection limit aides the evaluation of clinically relevant difference in platinum levels relative to different platinum compounds even at levels as low as ng/L or parts per trillion (ppt).

4.2.1.2 Practical limitations of ICP-MS

The analysis of platinum levels using ICP-MS has some limitations which are inherent to ICP-MS but are not insurmountable. These are spectral interferences from isobaric interference and polyatomic ions. The three abundant isotopes of platinum are ^{194}Pt, ^{195}Pt and ^{196}Pt with abundances of 33.0%, 33.8% and 25.2% respectively (E. E. M. Brouwers 2006). Of these three isotopes, ^{196}Pt alone is subject to interference from mercury (^{196}Hg) and this could be corrected by

monitoring the isotopic ratio of the three platinum isotopes. The interference from polyatomic ions namely Hafnium oxide was not a major concern as the background levels of platinum in our samples were greater than that of Hafnium oxide. There were significant issues from non-spectral interference arising from sample preparation and matrix interference which were dealt by optimising the sample preparation process.

4.2.2 Study design: Validation of ICP-MS

The analysis of platinum by ICP-MS was performed in collaboration with Prof Andrew Hursthouse in the Department of environmental geochemistry, University of the West of Scotland, Paisley. Although skilled in elemental analysis, his expertise did not include analysis of biological materials. A method specific to analysis of platinum in biological samples was developed and validated. The validation of ICP-MS for analysis of platinum was carried out following the principles outlined by the United States FDA Centre for Drug Evaluation and Research (FDA 2001), published literature (Shah, Midha et al. 2000; Miller, Bowsher et al. 2001) and in-house Analytical services unit (ASU) method development and validation protocols.

Briefly, all the vital parameters that were required for validation of bioanalytical methods were tested including specificity, calibration curve and linearity, accuracy, precision, limit of detection and stability. The specificity was analysed by checking the levels of platinum in blank samples containing the biological matrix. Certified reference solution of platinum was purchased from Inorganic ventures, USA. Lower limit of quantitation (LLOQ), the concentration that could be measured with confidence and limit of detection (LLOD), the lowest concentration of the analyte (platinum) that could be reliably differentiated from background levels were defined. The linearity was checked by plotting a calibration curve with minimum of 6 non-zero standards with a correlation co-efficient (r^2) $\geq$ 0.95. Quality control (QC) samples, with a minimum of 5 concentrations, spanning the calibration with the appropriate biological matrix were used for ascertaining the accuracy and precision.

4.2.2.1Accuracy and precision

Accuracy is the closeness of the observed results determined by the assay (ICPMS) to the true value. Accuracy can be determined by analysing the samples with a known quantity of the analyte (quality control samples) and measuring the difference in the observed value. Accuracy (%) = [(expected-observed)/expected] x 100. Accuracy should be tested with a minimum of five concentrations which would be in the range of expected concentrations in the sample and at least five replicates should be tested. Guidelines recommend that the accuracy should be within 15% of the expected concentration, barring the lower limit of quantitation where the accuracy can be within 20%.

Precision could be considered as the reproducibility of the results from the method, when the analyte is measured repeatedly in the same homogenous volume. This is the closeness of the results within the same analytical run for the quality control samples. Similar to accuracy, five determinations per concentration should be performed and the concentrations should cover the expected range of concentration in the sample. Precision values of ≤15% for each concentration (20% for lower limit of quantitation) were acceptable according to the guidelines. For the purposes of platinum analysis using ICPMS, concentrations within range from 250ng/L (ppt) to 100µg/L (ppb) were used for determining precision and accuracy.

4.2.2.2Calibration curve and linearity

Calibration curve and linearity is the relationship between the instrument response and actual known concentration of the analyte. The relation should be linear and a minimum of six standards need to be used. Quantitation was based on linear regression analysis and the correlation coefficient greater than 0.99 ($r > 0.99$) was accepted for each standard curve. In our validation, a minimum of nine calibration standards ranging from 50ng/L to 500µg/L was used.

4.2.2.3Limit of detection

Limit of detection (LOD) is defined as the lowest concentration that can be detected by the method with reasonable confidence that this is not due to contamination from background levels. Lower limit of detection should be more

than at least 5 times the response from the sample compared to blank response. This differs from lowest limits of quantitation (LLOQ) which is the lowest concentration of the analyte which can be determined with acceptable accuracy and precision.

4.2.2.4Stability

The stability of platinum in biological matrices was evaluated both for short term stability (run time: 1-2 days) and also in medium term to deal with the freeze-thaw cycle. The analyte is accepted to be stable when 95%-105% of the original concentration was attained in the stored samples.

The assay was then tested in a small study of drug uptake in cell lines. Once a reliable assay was established the plasma and tissue pharmacokinetics of free and encapsulated cisplatin was determined in tumour bearing mice.

4.2.3 Materials

Platinum(1000 µg/mL) in 10% (v/v) hydrochloric acid and Indium(1000 µg/mL) in 2%(v/v) hydrochloric acid were purchased from Inorganic Ventures, Lakewood, New Jersey, USA. Nitric acid (Fisher Optima™ trace metal grade, product code N/2275) was obtained from Fischer Scientific, U.K. Nalgene® volumetric flasks (Thermo Fisher, U.K) and Polypropylene (transport) tubes (Elkay Laboratories, UK) were used for the volumetric analysis and transport of standards and samples respectively. Cisplatin was a kind donation from pharmacy at the Beatson West of Scotland Cancer Centre (BWoSCC), Glasgow, U.K and CB[7] cisplatin was synthesised as described in chapter 3. Materials required for cellular and animal experiments were sourced from suppliers as mentioned in appendix 2.

Thermo Electron Corporation X-Series II quadrupole ICP-MS was used for the analysis of platinum.

4.2.4 Methods

The Thermo Electron Corporation X-Series II quadrupole ICP-MS uses a concentric nebuliser with a Peltier cooled (to 3^{o}C) conical single-pass spray chamber with

impact bead and has an integral peristaltic pump for sample uptake from a Cetac ASX-520 auto-sampler. The instrument is situated in a temperature and humidity controlled environment to minimise drift. Each run was supervised to ensure quality control, although the instrument could analyse samples through an automated process. Unexpected isobaric interferences were monitored by measuring the ^{194}pt/^{195}pt and the ^{196}pt/^{195}pt isotopic ratios which were consistent throughout. After analysis of each sample, the ICP-MS instrument was flushed with 1% nitric acid to clean the system thoroughly, such that the background analyte (platinum) levels came down to that of blank sample, to avoid carry over effect from previous samples. The Thermo X-Series II provides a monitored sample flush time option. This enabled efficient use of analysis time versus low to zero carry over between standards and between samples. A maximum flush time of 240 seconds was used, while the minimum counts per second allowed before measuring the next sample was set to around the level of the calibration blank. This could be varied depending on the conditions required. The high organic content of the samples by virtue of their biological origin resulted in signal suppression. In addition, there was a risk that these organic particles could block the sample introduction system and interface. Matrix interference was also noted due to high organic content of the sample. This problem was overcome by diluting the samples which resulted in adequate mineralisation without affecting the specificity. In addition, the sampling tubes were regularly changed to avoid cross-over contamination and flow variation due to wear and tear. The sampler and skimmer cones were also regularly inspected and thoroughly cleaned to reduce the non-spectral interferences. Indium (1µg/L) was used as the internal standard which acted as a control for flow variation and matrix interference. The calibration standards were run prior to each analysis and up to 100 samples were analysed as a single batch.

4.2.4.1 Preparation of standards

Chloroplatinic acid containing platinum (1000µg/mL) in 10% hydrochloric acid and Indium (1000µg/mL) in 2% nitric acid was used for the preparation of calibration and internal standards respectively. Initially calibration standards with concentration ranging from 50 ppt (parts per trillion) to 100 ppb (parts per billion) were prepared with 1% nitric acid in ultrahigh pure deionised water. The typical concentrations used for the calibration were 50ppt, 250ppt, 500ppt,

1ppb, 5ppb, 10ppb, 25ppb, 100ppb and 500ppb. A stock solution of 1 µg/mL (part per million-ppm) was prepared from the main stock which was then diluted with 1% nitric acid in ultrahigh pure deionised water (Milli-Q) to obtain the calibration standards. 1% nitric acid in ultrahigh pure deionised water was used as a blank control. The minimum volume of each calibration standard was 50mL which was accurately measured with the volumetric flasks (Nalgene) and then transferred to 50mL polypropylene transport tubes. All the standards were analysed thrice in the ICP-MS and the blank was analysed for 7 times. Similarly serial dilution of the stock of Indium was performed with 1% nitric acid in ultrahigh pure deionised water to obtain the final concentration of 1 µg/mL (1ppb). All the volumetric flasks used for preparation of calibration standards were washed thrice with 1% nitric acid in ultrahigh pure deionised water. The pipette tips and polypropylene transport tubes were discarded after single use.

Quality control samples were prepared by diluting the chloroplatinic acid stock solution with 1% nitric acid in ultrahigh pure deionised water and the concentration of the quality control samples used were 250ppt, 1ppb, 2.5ppb, 10ppb and 100ppb of platinum. In addition, to study the effect of interference from the organic materials in the mouse plasma and tumour tissue, two different solutions were made.

1. Mouse plasma was heat digested at 65^{o}C with concentrated nitric acid (68% Optima grade, from Fisher Scientific) and diluted to 1% plasma and 1% nitric acid with ultrahigh pure deionised water, the biological matrix herein after referred to as “1% plasma in 1% nitric acid”.

2. The quality control samples were prepared by diluting the chloroplatinic acid stock solution with 1% plasma in 1% nitric acid. This biological matrix herein after will be referred to as “quality control samples in 1% plasma”.

Preparing calibration standard solution with 1% plasma in 1% nitric acid would involve sacrificing and collecting blood from large group of mice. However the aim of the ICP-MS was to analyse the platinum levels in the mouse plasma and published guidelines suggest that the matrix used for calibration and test samples need to be similar. To strike a balance, 1% plasma in 1% nitric acid was

used for preparing the quality control samples but the calibration samples were prepared using 1% nitric acid in ultrahigh pure deionised water.

To summarise, the validation of ICP-MS assay was done with three different solutions namely,

a) Both calibration and quality control standards prepared in 1% plasma in 1% nitric acid.

b) Calibration standards prepared in 1% nitric acid in ultrahigh pure deionised water and quality control samples in 1% plasma in 1% nitric acid.

c) Both calibration and quality control standards prepared in 1% nitric acid in ultrahigh pure deionised water.

4.2.4.2 Preparation of cellular samples

The method used to measure platinum uptake in cells was adapted from Samimi and colleagues (Samimi and Howell 2006). Drug uptake was carried out with cell monolayers at 60-80% confluence. Cells (A2780, A2780/cp70) were plated out at a density of 10^5 - 10^6 cells/well in 3mL of medium in 6 well plates and incubated overnight at 37^{o}C in a humidified atmosphere of 5% CO_2 in air. The medium was then replaced with fresh medium alone or with medium containing cisplatin or CB[7]cisplatin at a range of concentrations. Triplicate wells were harvested at various times. The medium was then removed and cells washed with ice cold PBS and the cells lysed by addition of 215μL of nitric acid (68% Optima grade, Fisher Scientific, U.K) to each well. Plates were left at room temperature for 30 minutes. The cells were then collected into microfuge tubes and incubated overnight at 65^{o}C in a heating block. Three further wells were used to estimate the number of cells per well. The cell lysates were diluted in ultrahigh pure deionised water containing Triton-X (0.1%) to give a final nitric acid concentration of 1% (volume /volume).

4.2.4.3Calculation of cellular platinum content

Typically 50μL of nitric acid containing the digested cells was diluted with 4950μL of de-ionised water containing 0.1% Triton-X to achieve a final volume of 5mL. The platinum content of samples was determined by ICP-MS which gives the value of platinum (x) in ppb (ng/μL) which would be equivalent to the platinum content in 50μL of digested cells. The total platinum content of the digested cells in each well was derived by multiplying by a factor 4.3 (i.e. 215μL /50μL). The platinum uptake in each cell was then obtained by dividing the total platinum contents in the 215μL of digested cells by the total cell count. Finally, the cellular platinum uptake was expressed as picomoles (pmol) of drug per 10^6 cells by dividing the final value by 195 (molecular weight of platinum). Results are the mean ± SEM of drug uptake in 3 wells.

For the purpose of comparing the cellular platinum uptake, cells were incubated with cisplatin or CB[7]cisplatin (5μM), which was chosen based on the time course and drug dose finding experiments that were conducted for validating ICP-MS.

4.3 Pharmacokinetics of cucurbit[7]uril cisplatin

Human tumour xenografts were established as described in section 2.4.2, chapter 2. Groups of 3 mice were treated with a single intra-peritoneal injection of cisplatin (6mg/kg body weight) or CB[7]cisplatin (34 mg/kg, dose equivalent to cisplatin 6mg/kg) and sacrificed at specified time points. Blood was collected by cardiac puncture and stored in ethylene diammine tetra acetic acid (EDTA) tubes, which were placed on ice and plasma was separated as soon as possible to minimise the loss of platinum due to binding with erythrocytes. The plasma was separated by centrifuging the blood samples at 1500g for 10 minutes. The supernatant plasma was separated, collected and stored at -20^{o}C until further analysis. Tissues (tumour, kidney and liver) were harvested, snap frozen and stored at -70^{o}C until further analysis.

4.3.1 Preparation of tissue samples

Various methods have been described for the analysis of platinum in biological matrices including plasma (Tothill, Matheson et al. 1990; Morrison, White et al. 2000), plasma ultra-filtrate (E. E. M. Brouwers 2006) and tissues (Jandial, Messer et al. 2009) with their own limitations.

Sample preparation is a vital step in the development of the assay. Inadequate de-mineralisation can lead to contamination and subsequent blockage of the ICP-MS sample introduction system. Conversely use of large quantity of nitric acid to digest the sample could result in higher dilution of the sample and thereby decrease the sensitivity of the assay. Hence it is pertinent to find a balance between adequate demineralisation and dilution of the sample

A variety of methods were evaluated to prepare the tissues for analysis of platinum. Tissues were snap frozen in liquid nitrogen and subsequently ground to fine pieces using a mortar and pestle. Although this process allowed the tissues to be stored in aliquots, there was considerable amount of tissue that was stuck to the pestle which could not be recovered. Other methods of sample preparation were explored. Tissue samples were weighed and then homogenised with PBS using a Dounce homogeniser. The tissue homogenate was nitrolysed by adding nitric acid (68%, Optima grade, Fisher Scientific, U.K) and digested by placing on a heat block at 65^{o}C. The Dounce homogeniser was rinsed thoroughly with 1% nitric acid in ultrahigh pure deionised water between each use. However there was still a possibility of carry over effect from previous sample and hence this method was also abandoned.

Tissue digestion was finally optimised by adding varying volumes of nitric acid and heat digesting for varying time periods to obtain the best results. Addition of nitric acid at ratio of 1:10 (weight:volume) of tissue and heat digestion at 65^{o}C in a water bath for 24 hours achieved the optimum digestion of the tissue. The nitrolysed samples were subsequently diluted 50 to 100 fold (volume/volume) with 0.1% Triton–X in ultrahigh pure deionised water prior to analysis to reduce the matrix effect and contamination of sampler introduction system. Triton-X was used as an emulsifier and to denature proteins. In principle, a combination of acid digestion and dilution method was used to

prepare the samples. Typically 5mL of the solution containing 1% tissue homogenate in 1% nitric acid was prepared for the platinum analysis.

4.3.2 Preparation of plasma samples

Preparation of plasma was adapted from a method published by Jandial and colleagues (Jandial, Messer et al. 2009). Briefly, plasma was nitrolysed by adding equal volumes of plasma and nitric acid (68%, Optima grade, Fisher Scientific, U.K) and digesting overnight at 65^{o}C. Typically 50 µL each of plasma and nitric acid was used. The acid digested plasma was then diluted with 0.1% Triton–X in ultrahigh pure deionised water to obtain a volume of 5mL or 10mL solution containing 1% plasma in 1% nitric acid. Therefore the final dilution was 100 fold when 50µL of digested plasma was added to 4950µL solution containing 1% plasma in 1% nitric acid.

The solution was transported in polypropylene transport tubes and analysed using ICP-MS. The plastic pipette tips and transport tubes were discarded after single use to avoid carry-over of platinum. The values of platinum were given in parts per billion (ppb) which were converted to mg/mL by multiplying by a factor of 100 (to correct for the initial dilution of plasma to 1%) to obtain values of platinum at ng/mL. The resultant values were then divided by 1000 to derive the platinum values in plasma at µg/mL. Since the human pharmacokinetic studies have expressed the platinum levels µg/mL (Plummer, Wilson et al. 2011), the plasma platinum values are expressed as µg/mL and not in molar terms.

4.3.3 Data analysis

Pharmacokinetic parameters were determined by non-compartmental analysis (WinNonLin Version 4.0 software, Pharsight, Mountain View, USA). Statistical analyses were performed with Sigma Plot 8.0 and t-test was used to evaluate statistical significance.

4.4 Results: Method development and validation of ICP-MS

4.4.1 Linearity

Linear relationship was demonstrated between integrated counts per second (ICPS) and platinum concentration of the calibration standards for all the three isotopes of platinum (^{194}pt, ^{195}pt and ^{196}pt) with correlation coefficient, $r>0.999$ when 1% nitric acid in ultrahigh pure deionised water was used to prepare the calibration and quality control standards (Figure 4.1). This linear relationship was also maintained between the platinum levels expressed as ICPS and the concentration of the calibration standards when the calibration standards were prepared with a solution containing 1% plasma in 1% nitric acid (Figure 4.2).

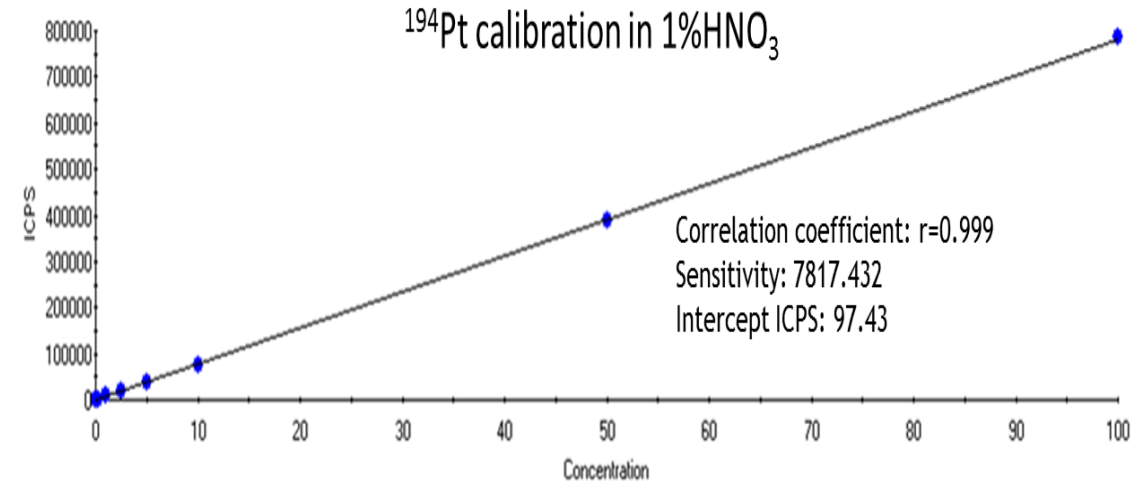

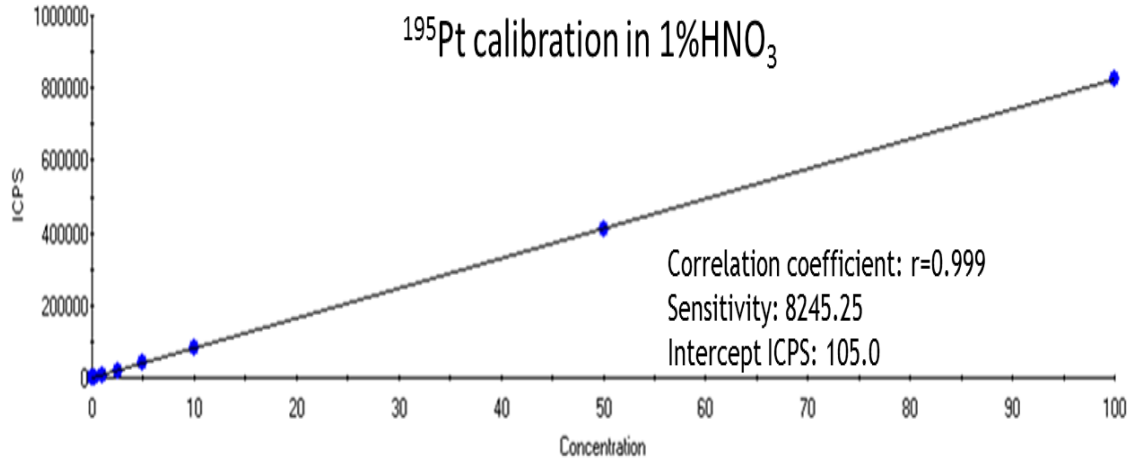

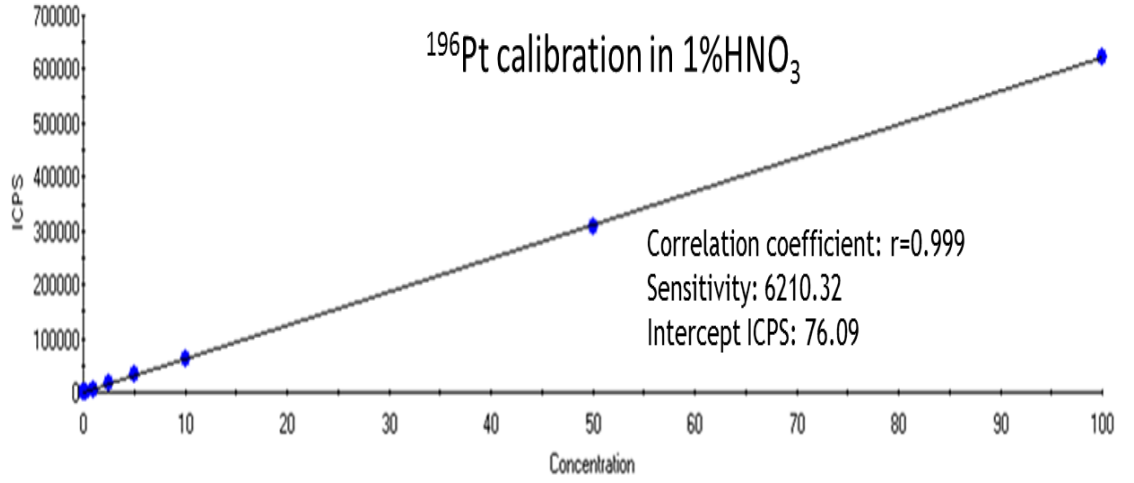

Figure 4.1: Detection of the 3 platinum isotopes when prepared in a matrix of 1% nitric acid in ultrahigh pure deionised water as measured by ICP-MS. Each point represents the mean of three measurements.

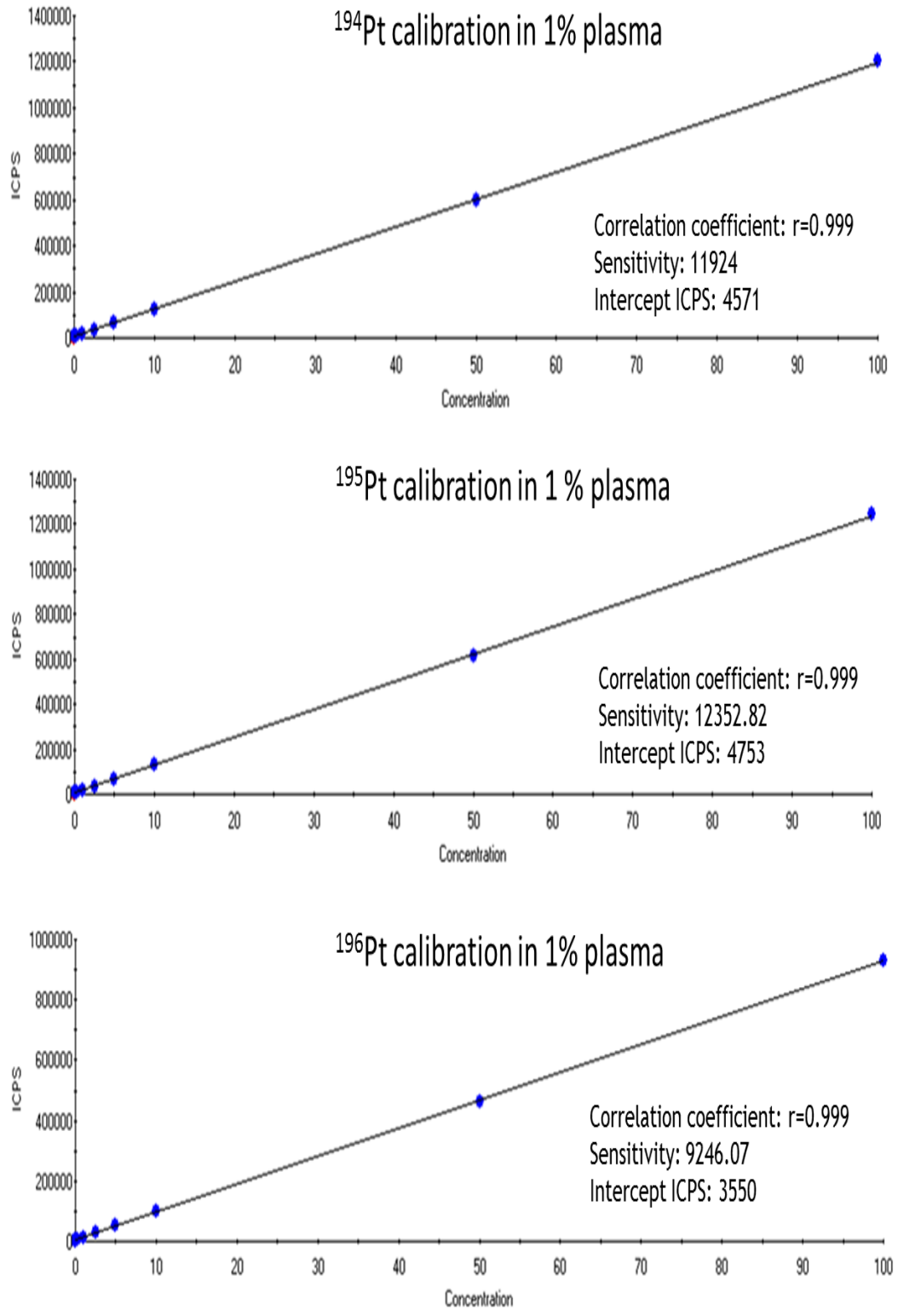

Figure 4.2: Detection of the 3 platinum isotopes when calibration standards and quality control samples were prepared with 1% plasma in 1% nitric acid as measured by ICP-MS. Each point represents the mean of three measurements.

4.4.2 Accuracy and precision

The accuracy and precision were evaluated using five concentrations of quality control samples containing 250ppt, 1ppb, 2.5ppb, 10ppb and 100ppb of platinum. These values were chosen based on pilot runs that demonstrated the possible spread of the platinum concentration in the tissue and plasma samples. The accuracy and precision when 1% plasma in 1% nitric acid was used as the biological matrix to prepare both the calibration and quality control samples is illustrated in table 4.1.

	Analyte value				
	250 ppt	**1 ppb**	**2.5 ppb**	**10ppb**	**100 ppb**
Run 1	0.09	0.85	2.31	10.12	96.27
Run 2	0.08	0.84	2.39	9.97	97.08
Run 3	0.08	0.87	2.37	10.19	97.30
Run 4	0.09	0.84	2.34	9.96	96.43
Run 5	0.08	0.84	2.39	10.02	94.98
Mean	**0.08**	**0.85**	**2.36**	**10.05**	**96.41**
Accuracy	68%	15%	7%	0.5%	3.5%
Precision	**6.3%**	**1.5%**	**1.5%**	**1.0%**	**0.9%**

Table 4.1: Accuracy and precision of ICP-MS with both the calibration standards and quality control samples prepared in 1% plasma in 1% nitric acid solution.

The accuracy and precision of the assay, when calibration standards were prepared with 1% nitric acid in ultrapure deionised water and quality control samples with the biological matrix of 1% plasma in 1% nitric acid is given in table 4.2. The accuracy was within acceptable standards (<15%) in concentration ranging from 1ppb to 100ppb.

	Analyte value				
	250 ppt	**1 ppb**	**2.5 ppb**	**10ppb**	**100 ppb**
Run 1	0.44	1.1487	2.86	10.75	102.20
Run 2	0.44	1.1447	2.89	10.85	101.40
Run 3	0.43	1.1423	2.85	10.80	101.23
Run 4	0.43	1.1413	2.79	10.77	102.53
Run 5	0.41	1.1449	2.84	10.81	102.47
Mean	**0.430**	**1.144**	**2.85**	**10.80**	**101.97**
Accuracy	92%	14%	14%	8%	2%
Precision	**2.30%**	**0.25%**	**1.40%**	**0.37%**	**0.60%**

Table 4.2: Accuracy and precision of ICP-MS with calibration standards made from 1% nitric acid in ultrahigh pure deionised water and quality control samples prepared in 1% plasma in 1% nitric acid solution.

The accuracy and precision when 1% nitric acid in ultrahigh pure deionised water was used as the background matrix for both the calibration and quality control samples is given in table 4.3.

	Analyte value				
	250 ppt	**1 ppb**	**2.5 ppb**	**10ppb**	**100 ppb**
Run 1	0.239	0.926	2.325	9.340	97.123
Run 2	0.237	0.914	2.283	9.385	96.440
Run 3	0.239	0.918	2.294	9.278	95.763
Run 4	0.235	0.879	2.213	9.249	96.097
Run 5	0.238	0.904	2.231	9.353	95.553
Mean	**0.238**	**0.908**	**2.269**	**9.321**	**96.19**
Accuracy	5%	9%	9%	7%	4%
Precision	**0.75%**	**1.99%**	**2.03%**	**0.6%**	**0.64%**

Table 4.3: Accuracy and precision of ICP-MS using 1% nitric acid in ultrahigh pure deionised water based matrix for calibration and quality control samples.

4.4.3 Level of Quantitation

The lower limit of detection of platinum, when 1% plasma in 1% nitric acid was used as the biological matrix, was 1µg/L. However when 1% nitric acid in ultra-high pure, deionised water was used in calibration standard, the limit of detection improved and was in the range of 0.1 – 0.25 µg/L.

4.4.4 Stability

The stability of the platinum in various biological matrices was evaluated by measuring the platinum values in the samples which were maintained at room temperature for short term and at 4°C in refrigerator for longer term. There was no significant deviation from the baseline and it was less than 2% from the baseline in sample analysed within 3 days and 3% in samples analysed after 4 weeks. The stability of platinum (^{195}pt) between days 1 and 4 is illustrated in figure 4.3

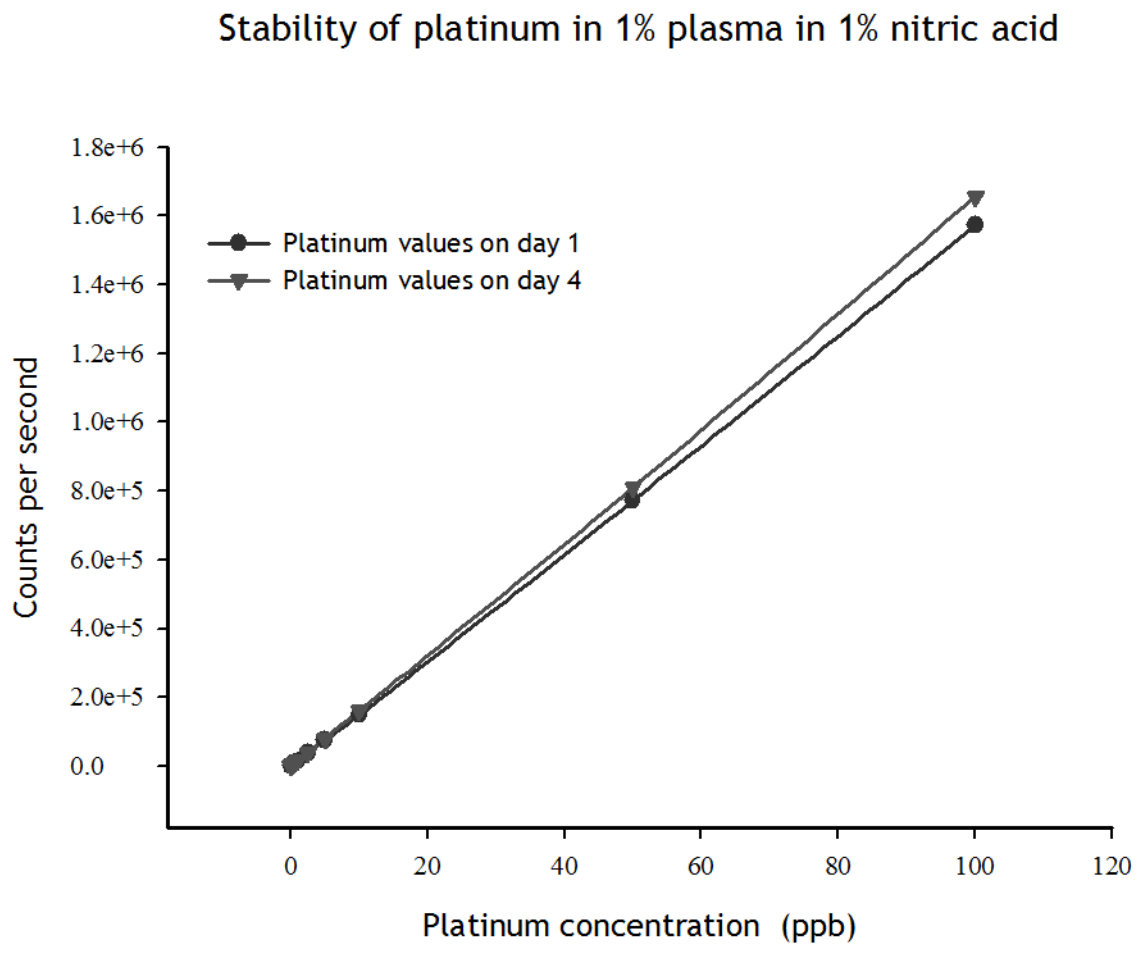

Figure 4.3: Stability of platinum isotope in a matrix containing 1% plasma in 1% nitric acid when measured on days 1 and 4.

4.5 Results: Validation of ICP-MS in cellular samples

The uptake of platinum by A2780 cells incubated for 4 hours with a range of concentrations of cisplatin (0.5μM to 50μM) is shown in figure 4.3. The intracellular accumulation of platinum was proportional to the concentration of cisplatin as illustrated in figure 4.4. The numerical results of uptake of platinum by cells are given in table 4.4.

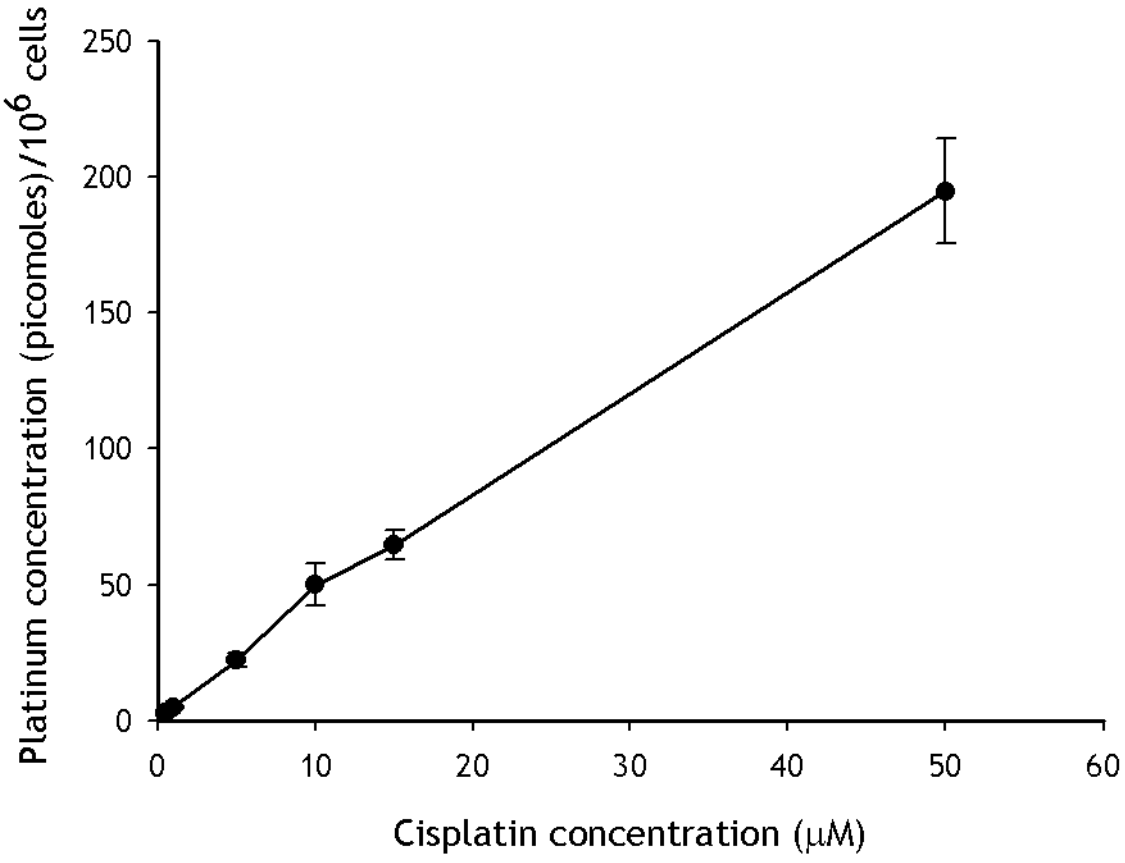

Figure 4.4: Uptake of platinum by A2780 cells with increasing concentrations of cisplatin. Each point represents the platinum content of the cells treated with increasing doses of cisplatin. Values are the mean ± S.E.M of 3 replicates.

Cisplatin (μM)	Pt content (pmol)/10^6 cells
control	1.3 ± 0.4
0.5	2.7 ± 0.1
5	22.2± 2.5
10	77.2 ± 7.6
15	64.6 ± 5.4
50	194.7 ± 19.3

Table 4.4: Platinum accumulation in A2780 cells with increasing doses of cisplatin. Results are the mean ± SEM of three replicates.

4.5.1 Optimum duration of drug exposure

On the basis of the dose finding experiments, the dose of 5μM was chosen for time course experiments and results of the time course experiment with 5μM are illustrated in figure 4.5 which demonstrates that the intracellular accumulation of platinum increases with time of exposure.

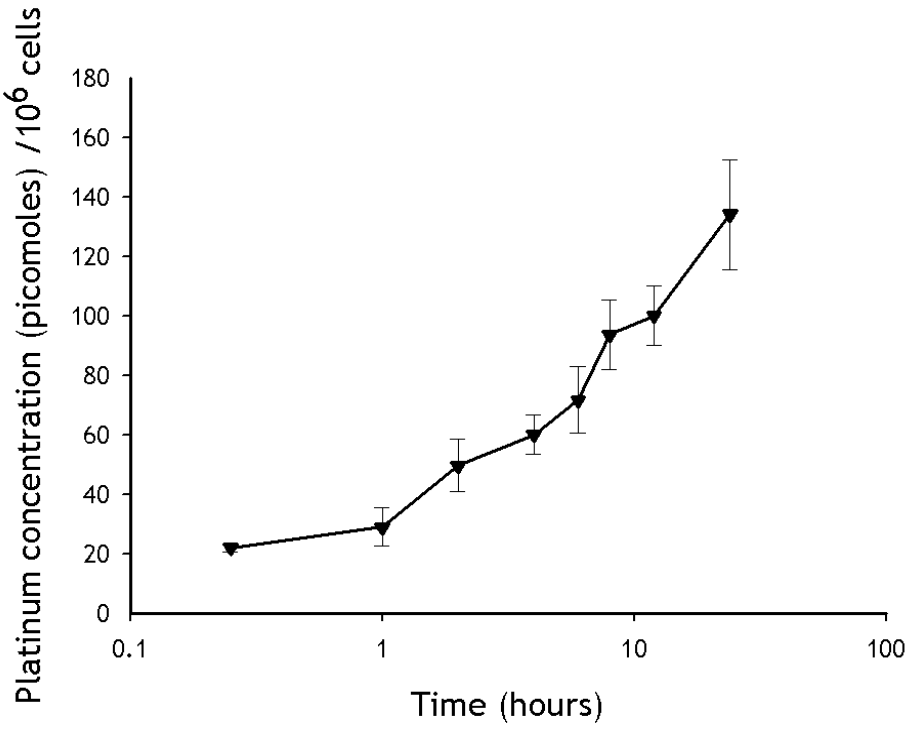

Figure 4.5: Platinum uptake by A2780 cells incubated with 5μM of cisplatin at increasing time. Each point represents the platinum content of the cells measured at corresponding time period. Values are mean ± S.E.M of 3 replicates.

4.5.2 Platinum uptake by A2780 cells with CB[7]cisplatin

The platinum content of A2780 cells when treated with 5μM of either cisplatin or CB[7]cisplatin and incubated for 15 minutes, 1, 4 and 24 hours is as shown in figure 4.6.

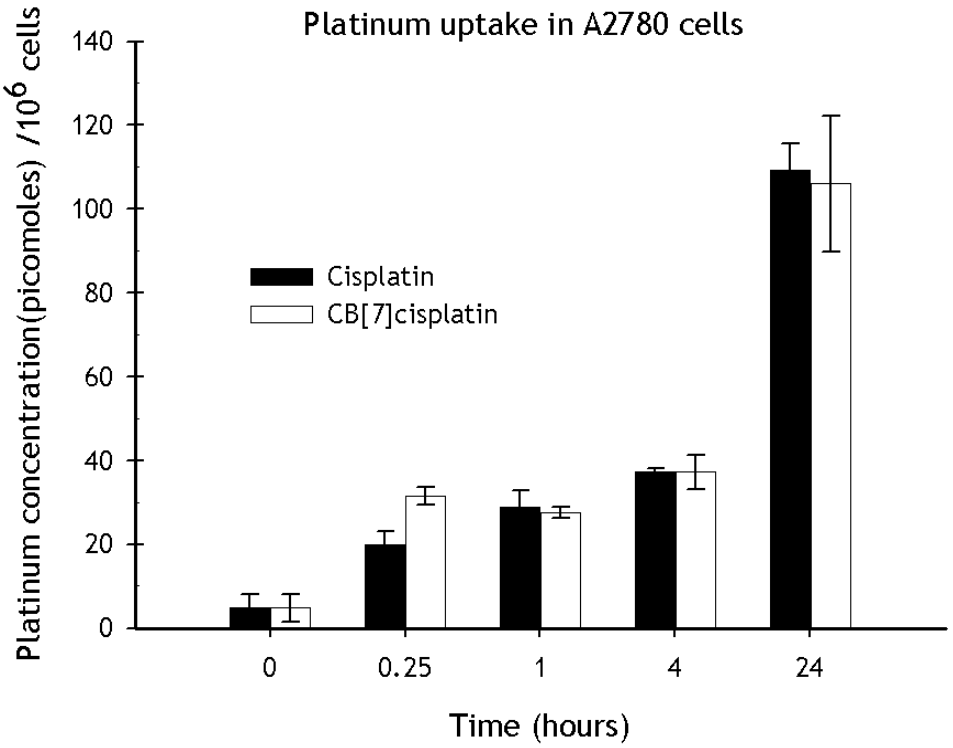

Figure 4.6: Platinum uptake by A2780 cells when incubated with cisplatin (black bars) or CB[7]cisplatin (clear bars) for varying time interval. Values are the mean ± S.E.M of 3 samples.

4.6 Results: Plasma pharmacokinetics of CB[7]cisplatin

Plasma platinum concentrations measured at various times after a single intraperitoneal dose of either cisplatin (6mg/kg) or CB[7]cisplatin (34mg/kg) are shown in table 4.5 and figure 4.6. The pharmacokinetic parameters of cisplatin and CB[7]cisplatin determined by non-compartmental analysis are given in table 4.6. The peak plasma level of platinum was observed 5 minutes after injection and this peak plasma platinum level was higher following injection of free cisplatin than for CB[7]cisplatin (Figure 4.7 and Table 4.6) with Cmax of cisplatin 17.5μg/mL compared with 10.2μg/mL for CB[7]cisplatin. This

difference in Cmax, however, did not reach statistical significance (P=0.09). Plasma platinum levels decreased rapidly but the decline was slower for CB[7]cisplatin such that after 15 minutes, plasma levels of platinum were higher following injection of CB[7]cisplatin. This difference was maintained for up to 48 hours. The AUC for cisplatin and CB[7]cisplatin is similar over the first hour after injection but is higher for the encapsulated cisplatin at all subsequent times (Table 4.6).

Time	Plasma platinum concentration (μg/mL)	
	Cisplatin	CB[7]cisplatin
Control	0.003 ± 0.0001	0.003 ± 0.0001
3 minutes	10.08 ± 1.62	8.48 ± 1.44
5 minutes	17.45 ± 0.85	10.43 ± 2.74
7 minutes	11.78 ± 0.69	8.29 ± 0.38
15 minutes	5.49 ± 0.51	6.92 ± 0.54
30 minutes	2.10 ± 0.12	4.01 ± 0.39
1 hour	0.84 ± 0.07	1.92 ± 0.22
2 hours	0.76 ± 0.06	1.56 ± 0.14
4 hours	0.66 ± 0.05	1.66 ± 0.26
6 hours	0.49 ± 0.03	0.95 ± 0.03
24 hours	0.35 ± 0.03	0.64 ± 0.06
48 hours	0.19 ± 0.02	0.40 ± 0.010

Table 4.5: Plasma platinum levels in mice treated with cisplatin (6mg/kg) or CB[7]cisplatin (34mg/kg, equivalent to cisplatin at 6mg/kg) at various time points. Values are the mean ± S.E.M of at least 3 samples.

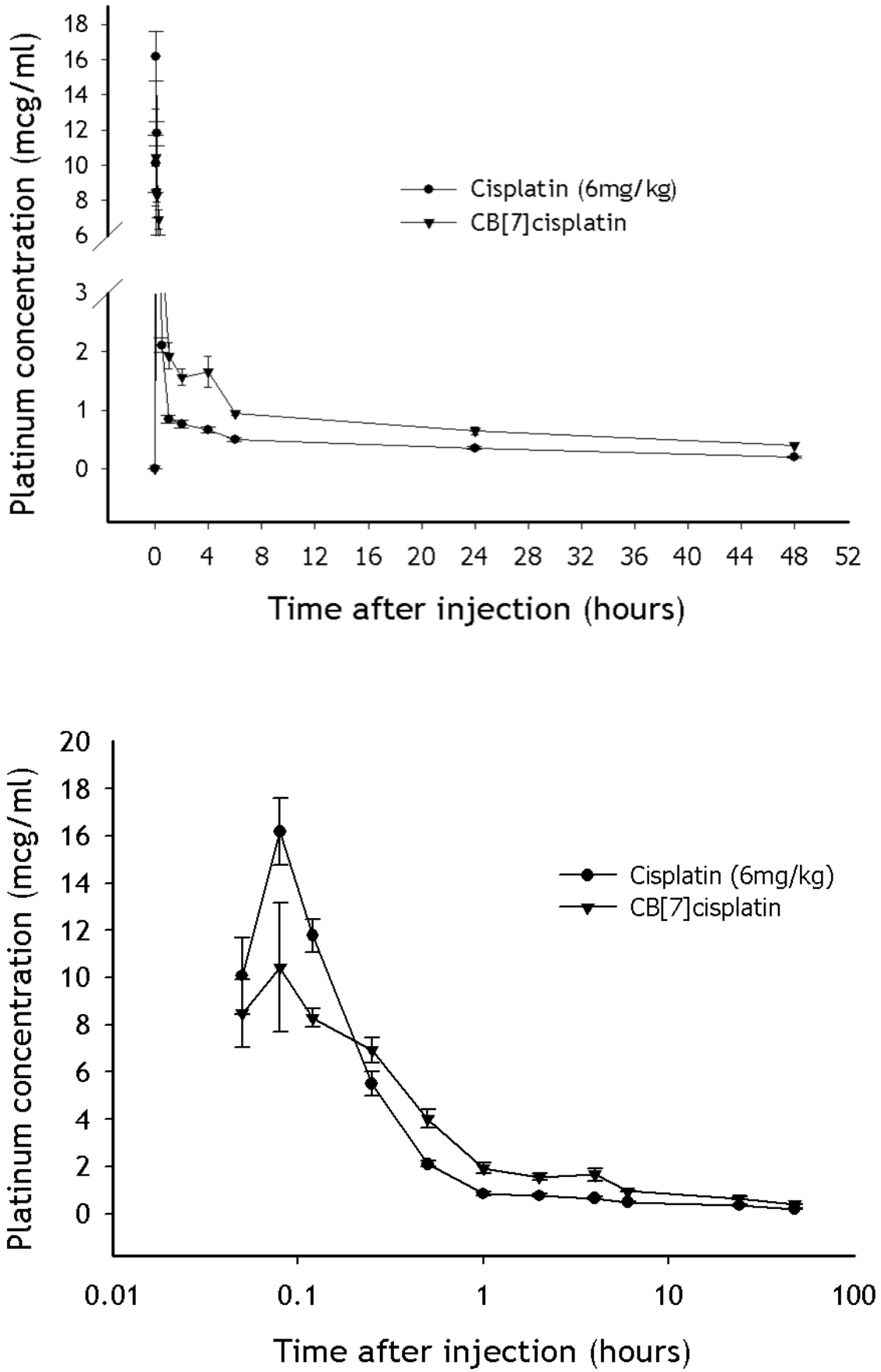

Figure 4.7: Plasma platinum concentration measured at various times after a single intraperitoneal dose of either cisplatin at 6mg/kg (●) or CB[7]cisplatin at 34mg/kg (▼). Results are the mean ± SEM of triplicate measurements and are shown with either a linear (A) or log (B) time scale.

PK Parameter	Cisplatin 6mg/kg	CB[7]cisplatin (34m/kg)
Cmax (μg/mL)	17.5	10.2
Tmax (minutes)	5	5
AUC_{0-1}(hr.μg/mL)	4.0	4.8
AUC_{0-4}(hr.μg/mL)	6.4	10.3
AUC_{0-6}(hr.μg/mL)	7.6	13.2
AUC_{0-24}(hr.μg/mL)	16.3	28.8

Table 4.6: Pharmacokinetic parameters for cisplatin and CB[7]cisplatin when administered as single intraperitoneal injection in nude mice.

It could be argued that the increased plasma platinum concentrations can be achieved by simply increasing the dose of the administered cisplatin. Subsequently, to test the hypothesis that increased platinum exposure could be obtained by simply increasing the dose of cisplatin, the pharmacokinetics of CB[7]cisplatin with a higher dose of cisplatin of 8mg/kg was examined. Previously it has been established that the maximum tolerated doses of cisplatin in mice is 6mg/kg (Dr Jane Plumb, personal communication)(Plumb, Strathdee et al. 2000). Doses beyond 6mg/kg of cisplatin are toxic to mice and hence cannot be tolerated in longer term. However, since the mice were sacrificed after 8 hours these experiments were explored wherein mice were administered single intraperitoneal injection of cisplatin at 2 different doses namely 6mg/kg and 8mg/kg. The time course of platinum in plasma of mice treated with single intraperitoneal injection of cisplatin at two different doses, 6mg/kg and 8mg/kg or CB[7]cisplatin is shown in figure 4.8. Intraperitoneal injection of cisplatin at 8mg/kg resulted in a higher peak plasma level compared to that for cisplatin at 6mg/kg dose (Figure 4.8, Table 4.7). The AUC for the first hour after injection (AUC_{0-1hr}) was 4.2hr.μg/mL for cisplatin at 6mg/kg and increased to 4.9hr.μg/mL for cisplatin at 8mg/kg which was similar to that obtained for CB[7]cisplatin (4.8hr.μg/mL). The AUC over the first 6 hours after injection was higher for CB[7]cisplatin (13.2hr.μg/mL) than for cisplatin at either 6mg/kg (7.6 hr.μg/mL) or 8mg/kg (10.6hr.μg/mL) (Table 4.7).

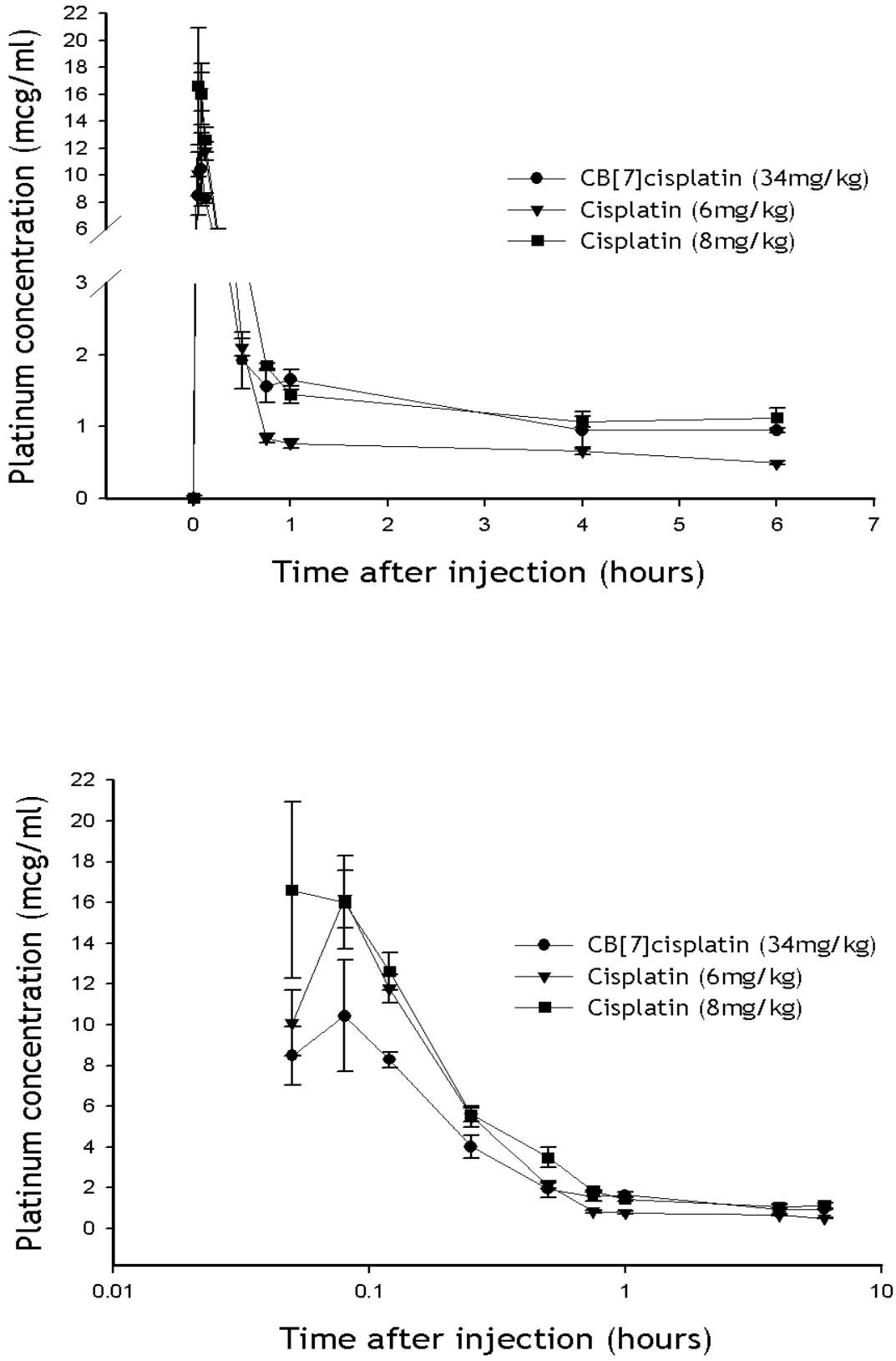

Figure 4.8: Plasma platinum concentration measured at various times after a single intraperitoneal dose of either cisplatin (6mg/kg,▼ or 8mg/kg, ■) or CB[7]cisplatin (34mg/kg, ●). Results are the mean ± SEM of triplicate measurements and are shown with either a linear (A) or log (B) time scale.

PK parameter	Cisplatin 6mg/kg	CB[7]cisplatin (34mg/kg)	Cisplatin 8mg/kg
Cmax (μg/mL)	17.5	10.4	19.3
Tmax (minutes)	5	5	3
AUC_{0-1}(hr.μg/mL)	4.0	4.8	4.9
AUC_{0-4}(hr.μg/mL)	6.4	10.3	8.4
AUC_{0-6}(hr.μg/mL)	7.6	13.2	10.6

Table 4.7: Pharmacokinetic parameters of cisplatin 6mg/kg, 8mg/kg and CB[7]cisplatin when administered as single intraperitoneal injection in nude mouse.

4.7 Results: Tumour and tissue platinum levels

The platinum levels in A2780 and A2780/cp70 xenografts are as shown in figure 4.9, table 4.8 and 4.9. Tumour platinum levels were higher after treatment with CB[7]cisplatin at the dose of 34mg/kg which is equivalent to the dose of cisplatin at 6mg/kg than with free cisplatin in both the cisplatin sensitive (A2780) and cisplatin resistant (A2780/cp70) xenografts. There was a statistically significant difference in tumour platinum levels at 4 hours, favouring CB[7]cisplatin, in both A2780 xenografts (cisplatin 134 ± 13 ng Pt/gm tissue, compared to 187 ± 15ng Pt/gm tissue for CB[7]cisplatin, P=0.03) and A2780/cp70 xenografts (cisplatin 107 ± 16 ng Pt/gm tissue compared with 178 ± 32 ng Pt/gm for CB[7]cisplatin, P=0.04) (Table 4.8 and 4.9). Similar trend favouring CB[7]cisplatin was also noted at 1 hour after drug treatment.

The deposition of platinum in kidney and liver measured at similar time points as the tumours are given in table 4.10 and illustrated in figure 4.9. At 4 hours, the platinum levels in kidney of the mice treated with CB[7]cisplatin was higher compared to cisplatin (1332 ± 39 ng Pt/gm tissue for CB[7]cisplatin versus 878 ± 67 ng Pt/gm tissue for cisplatin, P=0.004.

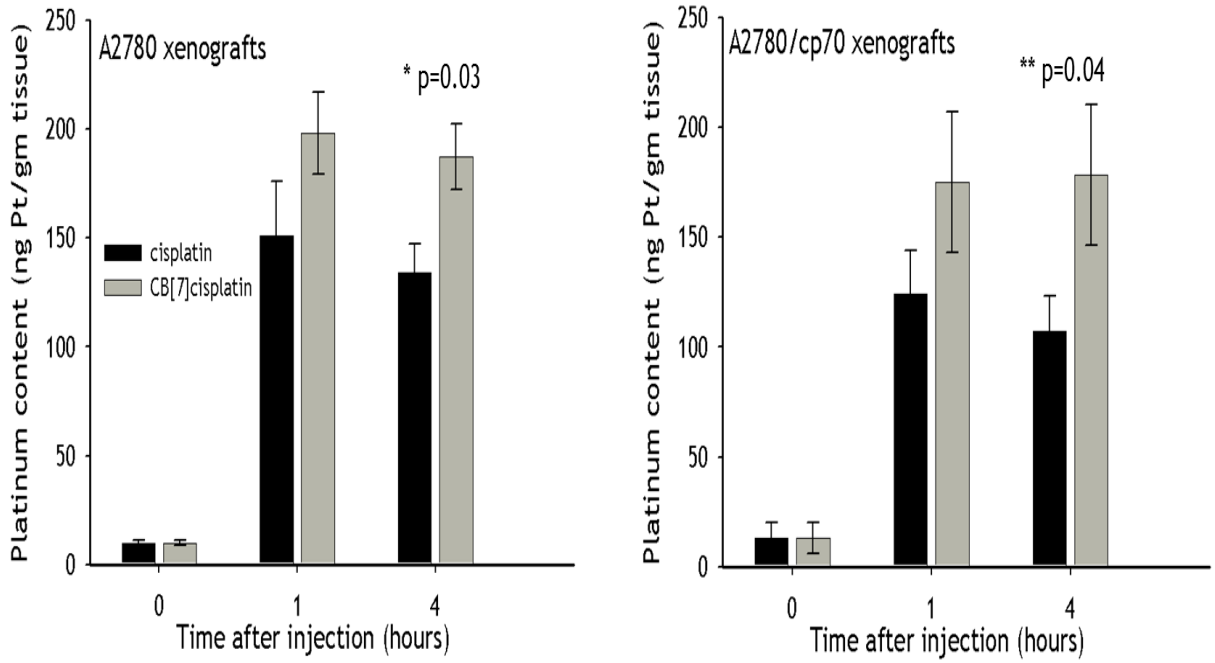

Figure 4.9: Platinum levels in A2780 (left) and A2780/cp70 (right) xenografts measured following single intraperitoneal injection of cisplatin 6mg/kg (black bars) or CB[7]cisplatin 34mg/kg, equivalent dose of cisplatin 6mg/kg (grey bars).Values are mean ± SEM of 6 mice.

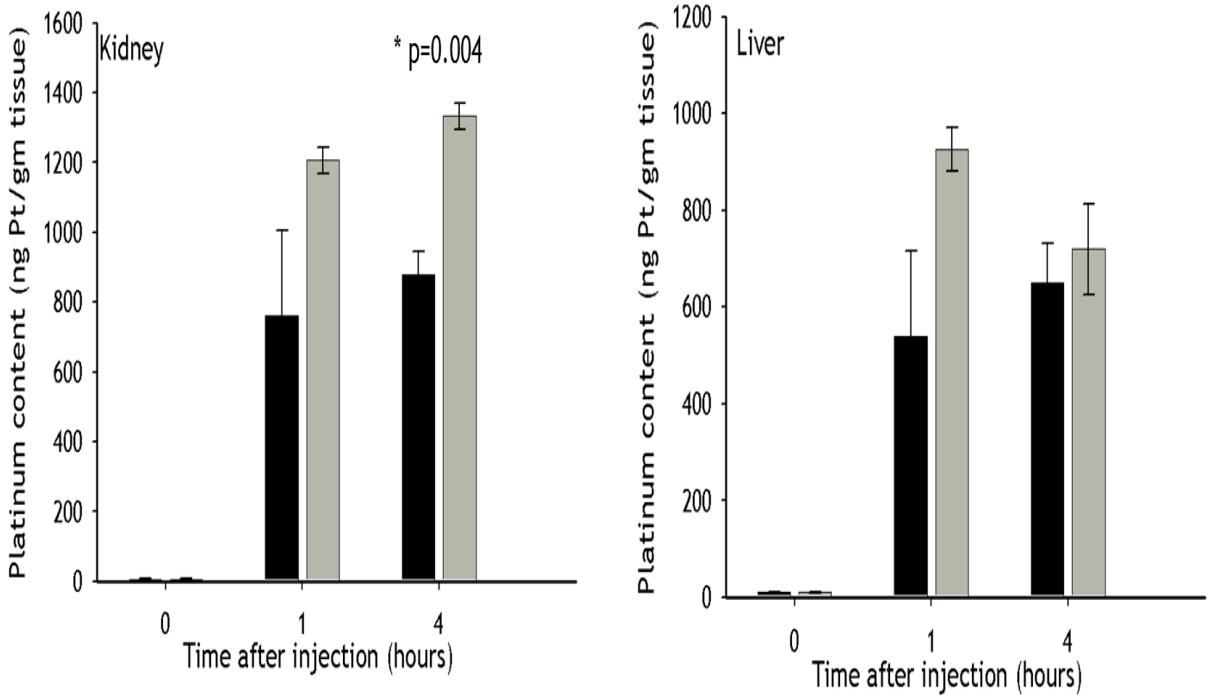

Figure 4.10: Platinum levels in liver (right) and kidney (left) of mice treated with single intraperitoneal injection of cisplatin at 6mg/kg (black bars) or CB[7]cisplatin at 34mg/kg, equivalent dose of cisplatin 6mg/kg (grey bars).Values are mean ± SEM of 6 mice.

Time(hours)	Pt levels in A2780 xenografts (ng of Pt/gm tissue)	
	Cisplatin 6mg/kg	CB[7]cisplatin
0 (control)	13 ± 7	13 ± 7
1	151 ± 25	198 ± 19 (P=0.18)
4	134 ± 13	187 ± 15 (P=0.03)

Table 4.8: Platinum content in A2780 xenografts after single intraperitoneal administration of cisplatin at 6mg/kg or CB[7]cisplatin at 34mg/kg (dose equivalent of cisplatin at 6mg/kg). Results are mean ± S.E.M of 6 samples.

Time(hours)	Platinum levels in A2780/cp70 xenografts (ng of Pt/gm tissue)	
	Cisplatin 6mg/kg	CB[7]cisplatin(34mg/kg)
0 (control)	11 ± 2	11 ± 2
1	124 ± 20	193 ± 33 (P=0.09)
4	107 ± 16	178 ± 32 (P=0.04)

Table 4.9: Platinum content in A2780/cp70 xenografts after single intraperitoneal administration of cisplatin at 6mg/kg or CB[7]cisplatin at 34mg/kg (dose equivalent of cisplatin at 6mg/kg). Results are mean ± S.E.M of 6 samples.

Time (hours)	Kidney (ng of Pt/gm tissue)		Liver (ng of Pt/gm tissue)	
	Cisplatin 6mg/kg	CB[7]cisplatin (34mg/kg)	Cisplatin 6mg/kg	CB[7]cisplatin (34mg/kg)
0 (control)	8 ± 2	8 ± 2	6 ± 2	6 ± 2
1	761 ± 244	1206 ± 37 (P=0.15)	539 ± 177	926 ± 45 (P=0.11)
4	878 ± 67	1332 ± 39 (P=0.004)	649 ± 83	719 ± 94 (P=0.61)

Table 4.10: Values of platinum deposited in kidney and liver of mice treated with single intraperitoneal administration of cisplatin at 6mg/kg or CB[7]cisplatin at 34mg/kg (dose equivalent of cisplatin at 6mg/kg). Results are mean ± S.E.M of 3 samples.

4.8 Discussion

These results demonstrate that the method developed to evaluate platinum levels in biological samples using ICP-MS is reliable and detection limits of ICP-MS are within the acceptable range for bioanalytical assays. This method with ICP-MS was suitable for measuring low levels of platinum obtained in the cellular drug uptake studies. The pharmacokinetic experiments in tumour bearing mice demonstrate that CB[7]cisplatin has a favourable and distinct pharmacokinetic profile compared to cisplatin which results in increased systemic exposure (both plasma and tumour) of platinum.

4.8.1 Validation of ICP-MS

These experiments confirm that ICP-MS can be used as a reliable and reproducible method to analyse platinum compounds in biological matrices. ICP-MS has a wide dynamic linear range and can detect analytes in the range of ng/L or ppt. Clearly, the Thermo Electron Corporation X-Series II quadrupole ICP-MS used in our analyses has a remarkable sensitivity for platinum with a detection limit in the region of 35ng/L. However, this level of sensitivity is difficult to achieve in whole plasma due to inherent high background levels of platinum, interference due to high organic contents of unfiltered plasma and variation between samples. Hence the lower limit of detection according to this assay was established as 1.0µg/L which provides a wide safety net and it is likely that the levels of detection are better than the indicated value of 1.0µg/L. The tests to check the stability of platinum in the biological matrices have confirmed that the deviation of platinum values in the stored samples was less than 5% from the initial value even when samples were stored for more than a month. Nevertheless, potential problems with stability were avoided since both the calibration standards and the test samples were freshly prepared prior to each analysis.

There is a clear linear correlation between the platinum levels expressed as ICPS and the concentration of the calibration standards. The correlation regression coefficient(r) was greater than 0.9999 for all the three isotopes of platinum, irrespective of the matrix used, which conforms to the acceptable levels of $r > 0.95$ for bioanalytical assays. There were high background levels of platinum,

when 1% plasma in 1% nitric acid was used as the biological matrix for calibration and quality control standards as evident by the high intercept value in figure 4.2 (range: 3550-4571). This is notably higher (Intercept value: 76–105) in comparison to the calibration using 1% nitric acid in ultrapure, deionised water as shown in figure 4.1. This could be explained by the matrix interference and signal noise from high organic content in plasma based biological matrix.

The within-day accuracy was in the range of 2%-14% and the precision was 0.9% to 1.5% for platinum concentrations ranging from 2.5µg/L to 100µg/L when 1% plasma in 1% nitric acid was used to prepare the quality control samples (Table 4.1). The deviation of the observed from the expected results was less than 15% for concentration ranging from 1.0µg/L to 100µg/L and the accuracy improved with higher concentrations. The between-day precision and accuracy were also measured and did not vary significantly (results not shown). These results adhere to published criteria for validation of bio-analytical methods (Shah, Midha et al. 2000). It is generally advocated that matrix based calibration should be used for bioanalytical assays. Typically with meticulous care, 1mL of blood could be obtained by cardiac puncture from each mouse from which plasma can be separated by centrifugation. However, preparing calibration standards with plasma derived from mice would involve sacrificing a large number of mice. In keeping with principle of “refine, reduce and recycle” in performing animal experiments, the calibration standards were prepared with 1% nitric acid in ultrahigh pure deionised water but the quality control samples were prepared with plasma based matrix (1% plasma in 1% nitric acid). As shown in table 4.2, both the accuracy and precision were notably better (compared with plasma based calibration) and were within acceptable limits in the concentration ranging from 1.0µg/L to 100µg/L.

The cellular platinum uptake experiment confirms the validity of ICP-MS as tool to analyse platinum at low concentrations. Cisplatin enters the cells primarily by passive diffusion and this process is not saturable when cancer cells are exposed to cisplatin at doses up to at least 100µM (Andrews, Velury et al. 1988). The dose of 5µM was chosen to evaluate the platinum content of cells with increasing time as this was a dose at which the levels of platinum could be reliably detected using ICP-MS and was not toxic to cells within the duration of the experiment. As shown in figures 4.3 and 4.4, the cellular accumulation of

platinum increases proportionally with increasing dose and incubation time. The experiments demonstrate that the uptake of platinum is proportional to dose of cisplatin and time of exposure to cisplatin, in keeping with the published literature (Yoshida, Khokhar et al. 1994; Siddik 2003; Ghezzi, Aceto et al. 2004).

Following the validation of the method described above, ICP-MS was used to evaluate the platinum uptake in cancer cell lines treated with a novel drug delivery system of platinum (gold nanoparticle containing active component of oxaliplatin) that was developed by Dr Nial Wheate and this has been published (Brown, Nativo et al. 2010).

4.8.2 Cellular pharmacokinetics of CB[7]cisplatin

The cellular platinum uptake experiments demonstrate that the encapsulation of cisplatin does not affect the intracellular accumulation of platinum with comparable levels of platinum content in the A2780 cells treated with CB[7]cisplatin or cisplatin (Figure 4.6). The platinum uptake in the cisplatin sensitive ovarian cancer cell line, A2780 is identical for cisplatin compared with CB[7]cisplatin at both early and delayed time points. The cellular platinum uptake experiment is consistent with the observations made in the experiments described in chapter 3 (Figures 3.2 and 3.3) that there is no difference in the *in vitro* cytotoxicity between free and encapsulated cisplatin.

Of note, the uptake and retention of platinum has been suggested as a mechanism of resistance to cisplatin (Siddik 2003). In these experiments, there was no difference in the cellular platinum accumulation between cisplatin or CB[7]cisplatin treated cells which further strengthens the results presented in chapter 3, that CB[7] encapsulation does not play a role in modulating cellular platinum resistance.

4.8.3 Plasma pharmacokinetics of CB[7]cisplatin

The results of the pharmacokinetic experiments in xenografts reliably demonstrate that CB[7]cisplatin has a favourable and distinct pharmacokinetic profile compared to cisplatin which results in increased systemic exposure of platinum. The maximum plasma concentration of the drug is higher for cisplatin than CB[7]cisplatin (Cmax 17.5μg/mL for cisplatin versus 10.4μg/mL for

CB[7]cisplatin, P=0.09). However Tmax, the time taken to attain the Cmax is identical at 5 minutes for both cisplatin and CB[7]cisplatin. These pharmacokinetic parameters for cisplatin are comparable to published data for cisplatin in mice which further validates the method used for platinum analysis (Johnsson, Olsson et al. 1995).

Of note, the platinum values measured in the plasma pharmacokinetics experiments were well within the range of standard curve which covered concentrations ranging from 0 to 50µg/mL.

The xenograft experiments with cisplatin and CB[7]cisplatin have demonstrated that the tumour growth delay by CB[7]cisplatin in comparison with cisplatin was pronounced in the first 48 hours and this tumour growth delay was maintained for the entire duration of the experiment. Early clinical studies with cisplatin have established that the initial half-life of cisplatin is 14-30 minutes and the terminal half-life could vary from 24 hours to 7 days (DeConti, Toftness et al. 1973). Hence the plasma pharmacokinetic analysis in this study was primarily focused towards the initial 48 hours.

The key difference in the pharmacokinetics between the two platinum compounds was noted in AUC. The AUC of CB[7]cisplatin is consistently higher across early time point when compared with cisplatin (AUC_{0-1}: 4.8 hr.µg/mL for cisplatin vs. 4.0 hr.µg/mL for CB[7]cisplatin), mid-time point (AUC_{0-6}: 13.2 hr.µg/mL for cisplatin vs. 7.6 hr.µg/mL for CB[7]cisplatin) and at later time point (AUC_{0-24}: 28.8 hr.µg/mL for cisplatin vs. 16.3 hr.µg/mL for CB[7]cisplatin). This data clearly show that with CB[7]cisplatin, there is prolonged retention of platinum in the plasma which has resulted in increased platinum delivery to tumour with a corresponding increase in anti-tumour activity.

As with any chemotherapeutic agent, it is possible to achieve higher concentrations of platinum in plasma by increasing the dose of cisplatin administered but this would result in unacceptable toxicities. Cisplatin produces dose proportional attenuation of tumour growth at doses ranging from 4 to 8mg/kg but cisplatin at dose of 8mg/kg is poorly tolerated with increased weight loss which is more pronounced after 2-3 days (Dr Jane Plumb, Personal communication)(Plumb, Strathdee et al. 2000). To test the hypothesis that the

higher plasma platinum concentration attained with CB[7]cisplatin could be achieved by merely increasing the dose of cisplatin, the plasma pharmacokinetics of CB[7]cisplatin was compared with cisplatin at dose of 8mg/kg (Figure 4.8). It needs to be emphasised that our group has established that this dose (cisplatin at 8mg/kg) is intolerable to mice. The mice treated at 8mg/kg were monitored for general welfare and distress and were sacrificed within 6 hours in order to avoid any distress which could be caused by the increased dose of cisplatin. Ideally the pharmacokinetic analysis could have been conducted for the entire time spanning 24 hours and this could be considered as a limitation of this pharmacokinetic experiment.

The pharmacokinetic parameters shown in table 4.7 demonstrate that Cmax for cisplatin at 8mg/kg was 19.3 µg/mL which is significantly higher than the Cmax of CB[7]cisplatin which was 10.6 µg/mL, P=0.0005. However the AUC at the mid-time points was not higher for cisplatin at the higher dose of 8mg/kg compared with CB[7]cisplatin. There was a suggestion that the AUC of CB[7]cisplatin is marginally higher than the AUC of cisplatin at 8mg/kg (AUC_{0-4}: 10.3 hr.µg/mL vs. 8.4 hr.µg/mL and AUC_{0-6}: 13.2 hr.µg/mL vs. 10.6 hr.µg/mL for CB[7]cisplatin and cisplatin at 8mg/kg respectively). Together this data suggest that increasing the dose of cisplatin increases the peak plasma platinum concentration resulting in intolerable side effects without an associated significant increase in systemic platinum exposure. There is evidence to indicate that nephrotoxicity of cisplatin is potentially associated with the peak plasma concentration (Nagai, Kinoshita et al. 1996; Erdlenbruch, Nier et al. 2001). CB[7]cisplatin, in contrast, did not result in higher Cmax but resulted in higher AUC even in comparison with cisplatin at 8mg/kg.

Since it is only the elemental platinum that could be measured here with ICP-MS, it is not clear if the platinum in the tissue and plasma is free as cisplatin or still encapsulated within CB[7] cavity. Nevertheless, in the absence of significant toxicity as shown in the xenografts studies and the different pharmacokinetic profiles of these two compounds it could be speculated that cisplatin is still within the CB[7]cavity in plasma. There are ways to measure the free cisplatin in the plasma and one such method could be radionuclide labelling of cisplatin. The difference the radioactive signals emitted by free cisplatin and cisplatin encapsulated within CB[7] cisplatin could be measured by a radioactive camera.

In addition to measuring the free cisplatin, such radionuclide tagging could also help to ascertain the tissue deposition characteristic of CB[7]cisplatin. It could also be hypothesised that the encapsulation of cisplatin within CB[7] protects cisplatin from bio-degradation and metabolism resulting in prolonged circulation of platinum in the plasma.

4.8.4 Choice of biological matrix

Mouse plasma and tissues were chosen as the biological matrix to investigate the pharmacokinetics of CB[7]cisplatin. It is widely accepted that the platinum levels in the plasma ultra-filtrate represent the pharmacologically active component of administered platinum as platinum bound to plasma protein is not thought to be pharmacologically active. The fact that cisplatin and oxaliplatin have shorter initial distribution phase and a long terminal elimination phase (Johnsson, Olsson et al. 1995; Graham, Lockwood et al. 2000) suggests that the platinum bound to plasma protein could be released in later stages and could contribute to the pharmacological actions of these compounds. Studies in patients on renal dialysis who receive cisplatin have demonstrated that the plasma cisplatin levels increase soon after dialysis even in patients where cisplatin was administered prior to dialysis. This indicates that there is degree interplay between free and bound cisplatin (Prestayko, Luft et al. 1978; Watanabe, Takiguchi et al. 2003). Published data indicate a close equilibrium between platinum in plasma and plasma ultra-filtrate and it is possible that the protein binding of platinum is not completely irreversible (Gamelin, Allain et al. 1995). Besides, platinum could be measured in patients even 10 years after their treatment with cisplatin and there is now a growing body of evidence to suggest that long term retention of platinum correlates with the toxicities e.g. neurotoxicity (Gietema, Meinardi et al. 2000; Sprauten, Darrah et al. 2012). It is also plausible that the magnitude of difference in platinum levels in plasma ultra-filtrate between the two platinum compounds (cisplatin and CB[7]cisplatin) could be smaller in comparison with platinum levels in whole plasma and measuring the platinum levels in plasma ultra-filtrate could underestimate a smaller yet clinically meaningful difference in the platinum levels. The plasma protein binding of CB[7]cisplatin is not known and given its atomic mass unit is approximately 1kDa (Dr Nial Wheate, personal communication), any anti-tumour effect that could potentially be attributed to the plasma-protein bound

CB[7]cisplatin could have been overlooked. Preliminary in vitro experiments evaluating the albumin binding of CB[7]cisplatin or cisplatin were inconclusive. For these reasons, levels of platinum in whole plasma were measured.

4.8.5 Tissue pharmacokinetics of CB[7]cisplatin

The tissue pharmacokinetic data indicate that treatment with CB[7]cisplatin results in increased platinum delivery to tumours both in cisplatin sensitive (A2780) and cisplatin-resistant (A2780/cp70) human ovarian cancer xenografts. In A2780 xenografts, the platinum content in tumour, measured 4 hours after administration of the drug, was significantly higher with CB[7]cisplatin in comparison with cisplatin. Platinum levels were 134 ± 13 ng Pt/gm tissue for cisplatin vs. 187 ± 15 ng Pt/gm tissue for CB[7]cisplatin, P=0.03 and there was numerical difference favouring CB[7]cisplatin at 1 hour time point although this difference did not reach statistical significance with P=0.18 (Table 4.8).

A similar difference was also noticed in A2780/cp70 xenografts with higher tumour platinum levels in CB[7]cisplatin treated mice. This observation merits further discussion as A2780/cp70 xenografts are not sensitive to treatment with cisplatin and *in vitro* experiments have shown that the cytotoxicity of CB[7]cisplatin is similar to cisplatin in these ovarian cancer cell lines. At 4 hours' time point, the platinum content in A2780/cp70 tumours was 107 ± 16 ng Pt/gm tissue and 178 ± 32 ng Pt/gm tissue for cisplatin and CB[7]cisplatin respectively, P=0.04 (Table 4.9). Similar to A2780 xenografts, the platinum content in A2780/cp70 tumours measured 1 hour following administration of CB[7]cisplatin was higher than tumours treated with cisplatin (124 ± 20 ng Pt/gm tissue for cisplatin and 193 ± 33 ng Pt/gm tissue for CB[7]cisplatin), although the difference was not statistically significant (P=0.60). It is more than likely that this increased delivery of platinum to A2780/cp70 tumour by CB[7]cisplatin has overcome cisplatin resistance exhibited by these tumours. This enhanced anti-tumour activity does not come at the expense of increased toxicity. This hypothesis could also explain the increased anti-tumour activity demonstrated by CB[7]cisplatin in human colon cancer xenografts, HCT116 (Figure 3.10, Chapter 3).

It could be debated if statistically significance of the tumour platinum levels would result in a meaningful difference. More often a statistically significant result does not always result in clinically meaningful difference. For example in the phase III trial comparing gemcitabine versus the combination of erlotinib and gemcitabine in advance pancreatic cancer resulted in statistically significant improvement in overall survival (6.21 months for the combination group versus 5.9 months for gemcitabine) but a difference of mere 10 days cannot be accepted as clinically meaningful (Moore, Goldstein et al. 2007). However, the in vivo experiments in chapter 3 have demonstrated that there is a significant difference in the tumour doubling time in both the A2780 and A2780/cp70 xenografts. Taken in conjunction with the data from the *in vivo* experiments, these statistically significant differences in tissue platinum values are meaningful and relevant.

Contrary to the hope of tumour targeted drug delivery, the increased delivery of platinum is not specifically targeted towards the tumour tissue alone as the platinum levels were higher in both liver and kidney of mice treated CB[7]cisplatin when compared with cisplatin. This effectively reflects that the increased plasma platinum concentration due to CB[7]cisplatin treatment has resulted in increased, non-specific tissue exposure to platinum. Although the platinum deposition was higher upon CB[7]cisplatin administration particularly in kidneys (878 ± 67ng Pt/gm tissue with cisplatin and 1332 ± 39ng Pt/gm tissue with CB[7]cisplatin at 4 hours, P=0.004) (Table 4.10 and Figure 4.10), this was not associated with increased toxicity as evident by the absence of loss of body weight in these mice. Clearly this increased deposition of platinum in kidneys of mice treated with CB[7]cisplatin is considerably higher when compared to the platinum content in the tumour xenograft. The information about the stability of CB[7]cisplatin would be the key determinant in explaining the absence of significant toxicities despite the increased platinum deposition in these organs.

It is evident from these experiments that the toxicity of cisplatin is influenced by the Cmax than AUC. Cisplatin at 8mg/kg resulted in a Cmax which is significantly higher than the Cmax of CB[7]cisplatin and a similar trend was also noted with cisplatin at 6mg/kg. The AUC of cisplatin at 8mg/kg however, appears to be equal if not lesser when compared with CB[7]cisplatin. Of note, cisplatin at 8mg/kg was not tolerated by the mice whereas all the mice

tolerated CB[7]cisplatin well as evident by absence of loss of body weight. This indicates that Cmax is responsible for the toxicity than AUC. Since CB[7]cisplatin has a lesser Cmax and larger AUC than cisplatin, it was well tolerated by mice and there was enhanced tumour growth attenuation with CB[7]cisplatin. This increased toxicity due to Cmax of platinum is also noted in another platinum analogue, oxaliplatin. Patients treated with oxaliplatin can experience laryngo-pharyngeal dysaesthesia or laryngeal spasm, a significant toxicity of oxaliplatin and this is related to Cmax of oxaliplatin. In patients who experience laryngeal spasm, increasing the duration of infusion to 6 hours reduces the Cmax by approximately 50% when compared to one hour infusion and results in lesser occurrence of such spasm (Graham, Lockwood et al. 2000).

In addition, as hypothesised for the plasma pharmacokinetics, it is plausible that encapsulation of cisplatin within CB[7], besides protecting the platinum from biodegradation, also controls the release of cisplatin dependent on the tumour microenvironment. It is likely that the acidic pH at the tumour interstitium facilitates the release of cisplatin from CB[7] whereas cisplatin still remains encapsulated in the renal and hepatic tissues which are well vascularised and oxygenated. As discussed in the introduction chapter, the fundamental principle of macromolecular drug delivery is that these drug delivery systems enhance drug delivery through exploiting the principle of enhanced permeability and retention in tumours. However, although CB[7] is a macrocycle, the size of CB[7]cisplatin is approximately 1nm (nanometre) and this size is not large enough for CB[7]cisplatin to be trapped in the permeable vasculature of tumours. Hence it possible that the altered microenvironment in the tumour facilitates the release of cisplatin from CB[7]cisplatin but this phenomenon could not have happened in organs with normal vascularisation and perfusion.

4.9 Conclusion

The observations noted in this chapter confirm the validity of ICP-MS as a suitable bio-analytical assay to evaluate platinum levels in cell, plasma and tissue samples. To conclude, the experiments in chapter 3 and 4 have shown that CB[7]cisplatin could overcome cisplatin resistance and this is due the distinct pharmacokinetic properties of the encapsulated cisplatin which results in increased tissue exposure of platinum as measured by AUC. These

experiments are proof of principle that cucurbit[7]uril can be an effective drug delivery system for cisplatin. In addition, it could also be hypothesised that encapsulation of cisplatin hinders the degradation of cisplatin by the sulphur containing thiols, thereby resulting in enhanced cytotoxic activity. In the following chapters, the effect of cucurbit[7]uril cisplatin in a disseminated ovarian cancer model will be explored using bioluminescence imaging as a pharmacodynamic marker for response to treatment. In addition, the activity of subcutaneously administered CB[7]cisplatin will also be evaluated to ascertain the relationship between the route administration of the drug and its cytotoxic activity

5 Activity of Cucurbituril encapsulated cisplatin in disseminated model of ovarian cancer

5.1 Introduction

Epithelial ovarian cancer is the most lethal gynaecological cancer in part, due to advanced stage at presentation and in 2010 was the 4th most common cause of female cancer deaths in the UK (CancerResearchUK 2012; Konstantinopoulos Pa 2012). Advanced stage ovarian cancer presents with widespread peritoneal dissemination and ascites. Treatment primarily involves aggressive cytoreductive surgery, modern combination chemotherapy (platinum analogues and paclitaxel) and/or i.p. cisplatin based-chemotherapy (Armstrong, Bundy et al. 2006; Guarneri, Piacentini et al. 2010; Ledermann and Kristeleit 2010). Difficulty in early cancer detection due to vague non-specific symptoms and lack of reliable screening tests resulting in advanced stage presentation, and the rapid progression to chemo-resistance have prevented an appreciable improvement in the five year survival rate of patients with ovarian cancer (Hennessy, Coleman et al. 2009; Schorge, Modesitt et al. 2010; Buys, Partridge et al. 2011). Dissemination of single tumour cells into the peritoneal cavity is the major cause of tumour recurrence even after complete resection of the primary solid tumour (Scott, Holdsworth et al. 2000; Lim, Song et al. 2010). Despite the advent of targeted therapy, there is no effective treatment for peritoneal recurrence (Guarneri, Piacentini et al. 2010; Burger, Brady et al. 2011) and there is a clear need for the development of new therapies.

Animal models of cancer are essential in the preclinical evaluation of anti-cancer agents. Potential new drugs are usually identified from studies *in vitro*. These studies range from random screen of compounds for activity in cell lines (Shoemaker 2006) to more detailed studies involving drug design and target specificity. Whilst studies *in vitro* with cancer cell lines can answer a number of mechanistic questions they do not address selectivity for tumour compared to normal tissues and do not take account of the physiological and pharmacological properties of the compound. These properties are of critical importance to studies of drug delivery since they can be exploited to ensure tumour specific delivery. Human tumour xenograft models, produced by transplantation of

human cancer cell lines or tumour biopsies in to immunodeficient mice play a vital role in drug development (Morton and Houghton 2007). Ovarian cancer cell lines derived from ascites or primary ovarian tumours have been used extensively and can be very effective for studying the processes controlling growth regulation and chemosensitivity (Ingersoll, Yue et al. 2009). Many of these studies of human tumour growth *in vivo* are based on subcutaneous xenografts where growth is measured by changes in tumour volume which is estimated by calliper measurements. This works well for rapidly growing tumours such as those derived from the human ovarian cancer cell line A2780 and, where the aim is to demonstrate growth inhibition in response to drug treatment. However, calliper measurements do not give a true estimate of viable tumour mass and can underestimate the treatment efficacy(Rehemtulla, Stegman et al. 2000). Growth of subcutaneous xenografts depends on the blood supply derived from either the skin or the body wall. The vasculature tends to predominate round the periphery of the tumour with poor penetration in to the tumour mass such that the central region becomes necrotic. Furthermore, subcutaneous xenografts can be criticised as lacking an appropriate tumour microenvironment and the ability to spontaneously metastasise to clinically relevant sites. It should be stressed, however, that almost all the conventional chemotherapeutic agents that are now in clinical use have demonstrated notable preclinical activity in these models (Sharpless and DePinho 2006). However, as stressed above the ability to kill tumour cells is not the only requirement of a drug delivery system since the tumour microenvironment can have a major impact on the efficacy of delivery systems.

One approach to address these criticisms has been the development of orthotopic tumours, whereby tumour cells are injected into the tissue or organ of origin. Examples of these models are the injection of breast cancer cells in to the mammary pad of fat or of pancreatic cancer cells into the pancreas. These tumour models can reproduce the tumour micro-environment to a certain degree and have been used to monitor drug activity (Kim, Evans et al. 2009). Development of such models frequently requires surgical implantation and is technically challenging. Besides, tumour development is not easy to monitor without sacrifice of the animal. Other animal models of disseminated ovarian cancer include spontaneous ovarian carcinoma in experimental animals

(Vanderhyden, Shaw et al. 2003; Connolly and Hensley 2009) or genetically modified animals (Dinulescu, Ince et al. 2005; Hensley, Quinn et al. 2007). However, the generation of these models is time-consuming, involves large animal cohorts and tumour growth is difficult to monitor and they are thus not ideal for the evaluation of novel drugs.

5.2 Biophotonic imaging

The development of new tools that can non-invasively assess the molecular and cellular events leading to the generation and proliferation of transformed cells, and their response to anti-cancer agents, would overcome many of the drawbacks of the existing pre-clinical models used in developing anti-cancer therapies. Several advanced imaging strategies that utilise fluorescence imaging, magnetic resonance imaging (MRI) and positron emission tomography (PET) have been described for studying cancer (Tjuvajev, Finn et al. 1996; Chenevert, McKeever et al. 1997; Uehara, Miyagawa et al. 1997; Bogdanov Jr and Weissleder 1998; Ross, Zhao et al. 1998; Tjuvajev, Avril et al. 1998; Galons, Altbach et al. 1999; Gambhir, Barrio et al. 1999; Gambhir, Barrio et al. 1999; Jacobs, Dubrovin et al. 1999; Weissleder, Tung et al. 1999). However there are many biological processes that cannot be externally monitored with non-invasive scanning techniques such as computed tomography (CT), ultrasound and MRI because key molecules in these processes are not distinguishable even in the presence of contrast dyes or radioactive tracers, although methods for acquiring functional data and analysis of transgene expression have been developed with MRI (Weissleder, Moore et al. 2000). However, MRI requires long scan times and expensive instrumentation. PET imaging provides metabolic information and some reporter genes that contain radionuclides are available (Tjuvajev, Finn et al. 1996; Tjuvajev, Avril et al. 1998; Gambhir, Barrio et al. 1999; Gambhir, Barrio et al. 1999). PET is also limited by the requirement of radioactive tracers with relatively short half-lives.

Photoproteins such as luciferase from the firefly, *Photinus pyralis*, have been used as reporter genes in both *in vitro* and *ex vivo* assays (Wood 1995; Hastings 1996). This luciferase has been used to study gene expression in cancer cells in culture (Chen, Biel et al. 1997; Willard, Faught et al. 1997) and to tag tumour

cells for the purpose of monitoring growth and response to therapy in animal models of human disease (Zhang, Hellstrom et al. 1994; Takakuwa, Fujita et al. 1997). However, analysis of cell proliferation *in vivo* in these studies was performed using an *ex vivo* assay. Analysis of reporter gene expression following removal of tumour tissues is limited by the loss both of the contextual influences of intact organ systems, and most of the temporal information. The goal of real-time analysis of biological events in intact living animals has now been realised (Contag, Contag et al. 1995) by biophotonic imaging. Biological sources of light are sufficiently intense such that the light generated within a mammal can be detected externally and either endogenous or exogenous substrate can be made available to bioluminescent reporters in living mammals (Contag, Contag et al. 1995). Among the many strengths of bioluminescence as a reporter in living mammals is the inherent low background of bioluminescent markers as compared with fluorescent or colorimetric reporters. This makes luciferase a superior reporter *in vivo* compared to fluorescent reporters where autofluorescence of tissues results in significant background, and already poor signal-to-noise ratios can further be reduced by photobleaching. Furthermore the rate of luciferase enzyme turnover in the presence of substrate allows for real-time measurements as this reporter does not accumulate to the extent of other reporters in cells (Contag, Olomu et al. 1998).

Sensitive detection devices have been designed to visualise and quantify bioluminescent light by detecting photons that are transmitted through mammalian tissue from internal sources (Contag, Contag et al. 1995). Technology such as the IVIS™ imaging system from Perkin Elmer use a charge coupled device (CCD) camera (with liquid nitrogen cooling and micro-channel plate intensifier to reduce background and increase signal), a dark imaging chamber to reduce incident light, and software to quantify the results. The number of photons transmitted through mouse tissues is sufficient to detect 1 x 10^3 cells in the peritoneal cavity, 1 x 10^4 cells at subcutaneous sites, and 1 x 10^6 circulating cells immediately following injection of the substrate (luciferin) suggesting that this approach may be applicable in evaluating agents in minimal disease states (Edinger, Sweeney et al. 1999). A quantitative comparison of bioluminescence imaging with serial MRI measurements of orthotopic rat brain tumours treated with the alkylating agent, carmustine (BCNU) demonstrated an

excellent correlation between detected photons and tumour volume with statistically similar cell kill values for the two imaging modalities (Rehemtulla, Stegman et al. 2000).

5.3 Assessment of tumour growth *in vivo* by bioluminescence imaging

An IVIS50 imaging system (Parkin Elmer) was available in the department but there was only very limited experience of the application of this technology to evaluate tumour growth in mice. Previous studies by the research group aimed to validate the use of bioluminescence imaging by comparing the technique with calliper measurements to monitor the growth and response to cisplatin of the ovarian cancer cell line A2780. Attempts to transfect the ovarian cancer cell lines A2780 and A2780/cp70 with the luciferase gene linked to the CMV promoter resulted in heterogeneous expression of luciferase. Selection of clones with high expression of the reporter often resulted in poor tumour uptake in mice. It was also noted that intraperitoneal injection of luciferin did not always provide a signal and that frequent anaesthesia, even for the short time required for imaging was not ideal.

These problems are addressed in the initial studies described in this chapter. The manufacturers of the IVIS 50 were aware of the problems with transfection of tumour cell lines and had developed a panel of tumour cell lines expressing the luciferase gene. In order to increase the efficiency of gene transfer, they used a lentiviral system for infection and linked the gene to the human ubiquitin C promoter to ensure high expression. One of these lines, HCT116Luc, was compared with the A2780/cp70CMVLuc cells developed “in house” for the initial validation study.

The aim of the validation studies was to be able to develop a disseminated model of ovarian cancer and to use bioluminescence imaging to monitor tumour growth and response to treatment. This chapter also describes development of a disseminated model by a colleague (Dr Gomez-Roman) and a study, carried out in collaboration with Dr Gomez-Roman, of the activity of encapsulated cisplatin in this model.

5.4 Rab25 model of disseminated ovarian cancer

Many genes have been identified, both from cell lines and tumour samples, which are associated with enhanced tumour growth and invasiveness. Cheng and colleagues identified a region located on chromosome 1q22 which was amplified in 54% of ovarian cancer who failed to respond to chemotherapy (Cheng, Lahad et al. 2004). Subsequently Rab25, a member of the RAS oncoprotein superfamily, was identified as the oncogene associated with amplification of chromosome 1q22. Rab25 is a member of the Rab11 subfamily which control trafficking events from late endosomes to the plasma membrane (Peter, Nuoffer et al. 1994). Rab25 expression is up-regulated in around 80% of ovarian cancer samples compared to normal ovarian epithelium (Cheng, Lahad et al. 2004). Much of our understanding of the role of Rab25 in tumour growth and invasion has come from the work of Prof Jim Norman and colleagues in the Beatson Institute for Cancer Research, Glasgow. They showed that Rab25 contributes to tumour progression by enabling the tumour cells to invade the extracellular matrix by altering the trafficking of integrin (Caswell, Spence et al. 2007). Rab25 associates with the α5β1 integrin through the cytoplasmic tail of the β1 integrin (Caswell, Spence et al. 2007). α5β1 integrin is known to have a key role in tumour cell proliferation and metastasis (Sawada, Mitra et al. 2008; Mitra, Sawada et al. 2011). Rab25 driven invasiveness is due to Rab25 dependent localisation and recycling of α5β1 integrin vesicles at the pseudopodial tips of the cell and this invasiveness is strongly dependent on association of Rab25 with β1 integrin and ligation of fibronectin by α5β1 (Caswell, Spence et al. 2007).

Over-expression of Rab25 in the human ovarian cancer cell line A2780 has been shown to confer invasive properties both *in vitro* and *in vivo* (Cheng, Lahad et al. 2004). Furthermore expression of Rab25 in ovarian and breast cancer cell lines increased cell survival through reduced apoptosis after multiple stress conditions including UV radiation and paclitaxel. These results suggest that Rab25 expression might regulate resistance to chemotherapy. Since A2780 is well characterised as a subcutaneous xenograft this model of disseminated cancer was chosen for these studies. Before the advent of biophotonic imaging techniques, the *in vivo* assessment of the growth of disseminated ovarian cancer models was primarily done by monitoring the abdominal distension. Given that

peritoneal disease contains cells and ascitic fluid this was a crude assessment of tumour burden.

For routine clinical use cisplatin is given by an intravenous infusion. This route is not practical in mice and the intraperitoneal route is often used since the pharmacokinetics parameters are closer to an intravenous infusion than those obtained by a bolus intravenous dose. It could be argued that intraperitoneal administration of drug when the tumour is located in the peritoneal cavity (as in the case of disseminated ovarian cancer model) is inappropriate. In order to address this issue subcutaneous drug administration was also investigated.

5.5 Methods

5.5.1 Bioluminescence imaging of animals

The IVIS 50 imaging system was housed within a laminar flow work station in order to maintain sterility and was controlled and images analysed by Living Image 2.50.2 software (Perkin Elmer). The camera was initialised about 15 minutes before imaging commenced to allow the camera to cool. Mice were brought into the work station in filter top cages and all subsequent steps were carried out within the work station. Mice bearing human tumour xenografts (established as described in section 2.4.2, chapter 2) were injected either intraperitoneally or subcutaneously, just below the back of the neck, with 100μL of a sterile solution of D-luciferin (30mg/mL in PBS, Perkin Elmer). They were then placed in the chamber of the Xenogen GGI-8 gas anaesthesia system and anaesthetised according to the manufacturer's instructions. The system delivers oxygen and vapourised isoflurane gas (3% isoflurane and 1 litre/min oxygen) to the induction chamber and to the imaging chamber through a 3 port anaesthesia manifold. In addition, it also contains activated charcoal evacuation filters which absorb the waste isoflurane from the induction chamber, thereby protecting the handlers from the effects of anaesthesia. The stopcock controlling the supply of isoflurane to the nose cone in the imaging chamber was turned on, to maintain the anaesthesia for the mice when they were placed in the imaging chamber. After 2-3 minutes, once the mice were anaesthetised they were placed in the imaging chamber. The chamber contained a manifold with 3 nose cones allowing

three mice to be imaged together. Mice were placed with their noses in the cone to maintain anaesthesia throughout the imaging procedure. Initially a black and white image of the mice was captured. The bioluminescent image was then captured. The duration of image capture varied depending on the intensity of the signal with an average capture time of 1 to 2 minutes. The intensity is proportional to time such that the duration of capture is not critical for comparisons but it is important not to let the signal saturate which can happen if the signal is intense. On completion of the imaging, mice were placed back in the cage and monitored for recovery which occurred within 1-2 minutes.

5.5.2 Development of A2780-Rab25Luc

A2780 cells stably expressing Rab25 were produced by transfecting A2780 cells with plasmids pcDNA3-Rab25 using Lipofectamine 2000 as described in section 2.5.6, chapter 2. Geneticin (0.5mg/mL) was used as the selection agent. The cells were then evaluated for expression of Rab25 using Western blotting with a primary antibody developed "in house" by Prof Jim Norman's research group, (antibody dilution 1:4000). A2780Rab25 cell line expressing the firefly luciferase gene under the control of Ubiquitin C promoter was constructed using a commercially available lentiviral gene delivery system. The luciferase gene was amplified from Pgl4-CMVLuc vector obtained from Promega with the aid the primers outlined below: Forward-5' CACCATGGAAGACGCCAAA; Reverse-5' AAACACGGCGATCTTTCCG. Virapower promoterless lentiviral gateway kit (described in detail in chapter 6) was used to clone the luciferase product into pENTR gene. Plasmid containing Ubiquitin C promoter (UbCp) was supplied in the kit. Lentiviral constructs were produced by recombination of pENTR/UbC promoter, the cloned pENTR luciferase and pLenti6/R4R2/V5-DEST. The resultant plasmid was then used to transfect HEK293FT cells (supplied in the kit) as per the Lipofectamine 2000 protocol described in section 2.5.6, chapter 2. Supernatant medium containing virus was harvested 72 hours post-transfection into a 15mL sterile capped, conical tube. This was then centrifuged and filtered through 0.45μm PVDF filter (Millipore, Bedford, MA) and resuspended in fresh medium. Determination of lentiviral titre was performed using A2780 cells and the lentiviral stocks were stored at -80^{o}C.

Transduction of lentiviral constructs containing luciferase gene into A2780 and A2780Rab25cells was performed by plating the cells in a 6 well plate at a density of 5 x10^7 cells/well. After 24 hours, the supernatant medium was removed and 2mL of lentivirus in culture medium was added along with 2 µg/mL of hexadimethrine bromide (Polybrene®). The next day (day 2), virus was removed and fresh medium was added and on the following day (day 3), culture medium containing blasticidin (2.5 µg/mL, A2780 and A2780-Rab25Luc) and geneticin (0.5mg/mL, A2780-Rab25 only) as a selection agent was added for selecting cells stably expressing luciferase and Rab25. Expression of both genes was confirmed by Western blotting and bioluminescence imaging as above. These cells were labelled as A2780-Luc and A2780-Rab25Luc and their chemosensitivity to platinum based compounds was determined as described in section 2.2, chapter 2.

5.5.3 *Growth and drug sensitivity of A2780-Rab25Luc in vivo*

For i.p. xenografts (disseminated ovarian cancer model), about 5x10^7 cells of either A2780-Luc or A2780-Rab25Luc were injected into the peritoneal cavity of mice. Mice were imaged weekly until the appearance of bioluminescent signal and the signal was greater than 8x10^5photons/second (around three to four weeks). Mice were treated (day 1) with PBS, cisplatin (6mg/kg) or CB[7]cisplatin (34mg/kg) and both drugs were given either intraperitoneally or subcutaneously. They were then imaged on days 4, 7 and 14. Analysis of the bioluminescent images was performed by defining a set region of interest to be used in all animals and for the disseminated model the signal over the entire abdomen of the mouse was analysed.

5.6 Results

5.6.1 Route of administration of luciferin

Luciferin was administered as a bolus dose either intraperitoneally or subcutaneously to mice bearing HCT116Luc tumours and mice were imaged at intervals of 1 minute for 14 minutes (Figure 5.1). Initially the flux, which is the measure of bioluminescent signal emitted, increased with time. It reached a plateau after which the signal decreased. The shape of the curve was

independent of the size of the tumour (signal intensity) and of the route of administration. The plateau was achieved slightly earlier following subcutaneous administration but the duration of the plateau phase was similar for the two routes of administration.

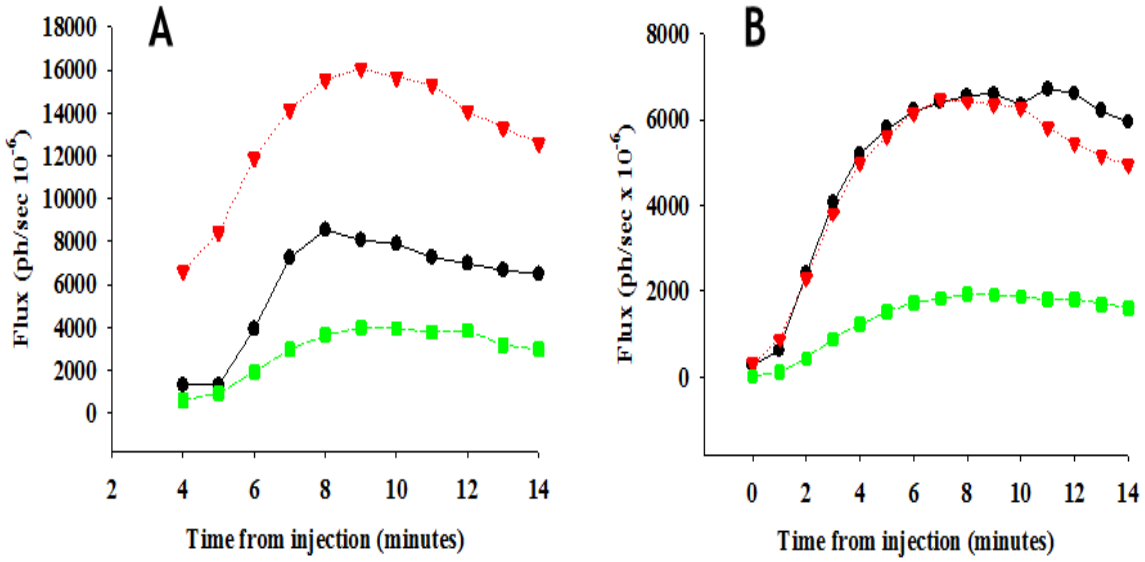

Figure 5.1: Bioluminescent signal (flux) obtained at various times after administration of D-luciferin to HCT116Luc tumour bearing mice. D-luciferin (3mg/mouse in 100µL PBS) was administered either intraperitoneally (A) or subcutaneously (B). The lines represent the signal from each of three mice used for each route of administration and maximum flux for each mouse is related to the size of the tumour.

5.6.2 Sensitivity of bioluminescence measurement in vivo

Mice were injected intravenously with cells at different concentration ranging from 10^4-10^6/mL, and bioluminescent imaging was done after 10 minutes as explained in section 5.5.1. The bioluminescent signal measured after about 10 minutes and a rectangular field was placed over the mice (after BLI) to measure the total flux from each of the mice (Figure 5.2 and Table 5.1). The cells used were either HCT116Luc or A2780/cp70 that had been transfected with a luciferase reporter (A2780/cp70CMVLuc). Cells were detected in the lungs of all mice although the signal was much greater for HCT116Luc cells than for A2780/cp70CMVLuc cells.

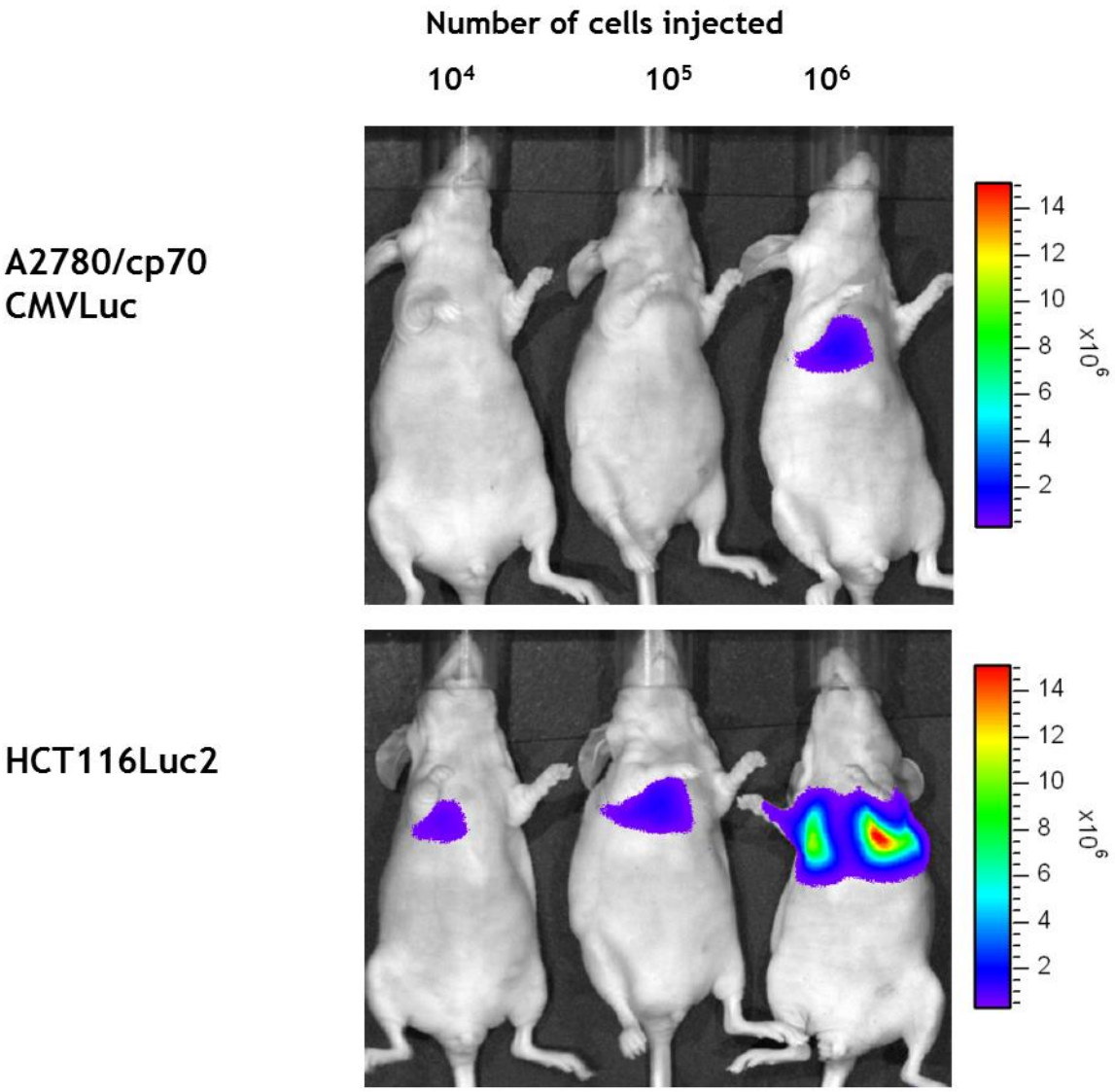

Figure 5.2: Bioluminescent signal measured 10 minutes after intravenous injection of cells at the densities shown. For comparison the colour bar has been set to the same range for the two images.

	Total Flux (photons x 10^{-6}/sec)		
Cell line / cell number	**10^4**	**10^5**	**10^6**
A2780/cp70CMVLuc	0.5	2.0	18.7
HCT116Luc	10.2	27.0	195.7

Table 5.1 Quantitation of the bioluminescent signal (total flux) for the mice shown in figure 5.2.

5.6.3 Effect of seeding density on tumour growth

HCT116Luc cells were injected subcutaneously into mice at a range of seeding densities ($2.5x10^5$ to $2x10^6$cells/injection) and the bioluminescent signal, measured at various times, is shown in figure 5.3. Tumours were visible by eye after 5 days in mice injected with $1x10^6$ and $2x10^6$ cells but were only detectable by bioluminescence at the lower densities. Only one mouse injected with $2.5x10^5$ cells had a visible tumour by day 15 and the bioluminescent signal showed only a very small increase by day 15 in the other mice in the group. At the higher densities (1 and $2x10^6$) the bioluminescent signal increased with time up to day 12 but there was no further increase at day 15 although the tumour size was smaller than could be measured by callipers (5mm). At a seeding density of $5x10^5$ all mice had visible tumours by day 15 and the bioluminescent signal showed a gradual increase with time.

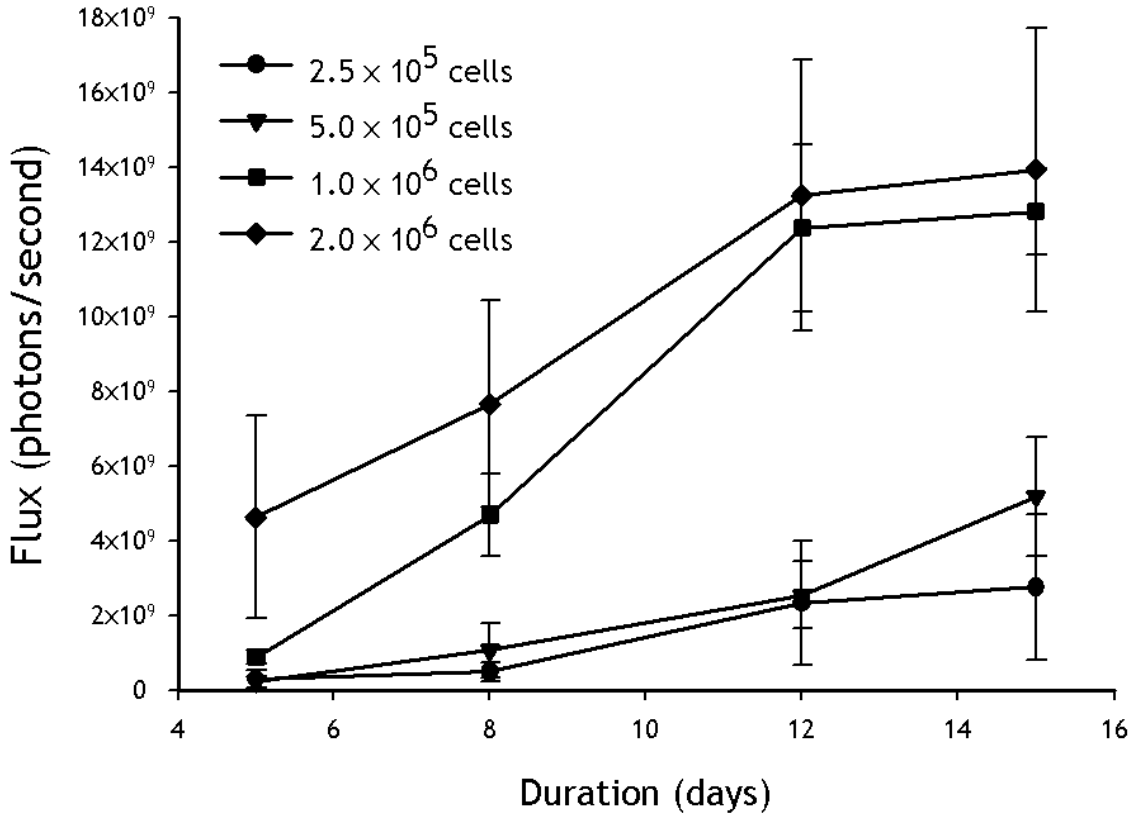

Figure 5.3: Bioluminescent signal (flux) measured in mice at various times following subcutaneous injection of HCT116Luc cells at a range of seeding densities. Results are the mean ± SEM of 6 mice.

5.6.4 Quantitation of tumour growth

A group of six mice was injected subcutaneously on Day 0 with HCT116Luc cells (5 x 10^5cells/mouse) and tumour growth for individual mice as measured by bioluminescence is shown in figure 5.4A. All mice developed tumours and an exponential increase in flux with time was observed. The size of the tumours, indicated by the total flux, differed markedly between mice. When the flux was related to the initial flux measured on Day 0, a consistent growth rate was observed as seen by the small error bars in the mean plot (Figure 5.4B).

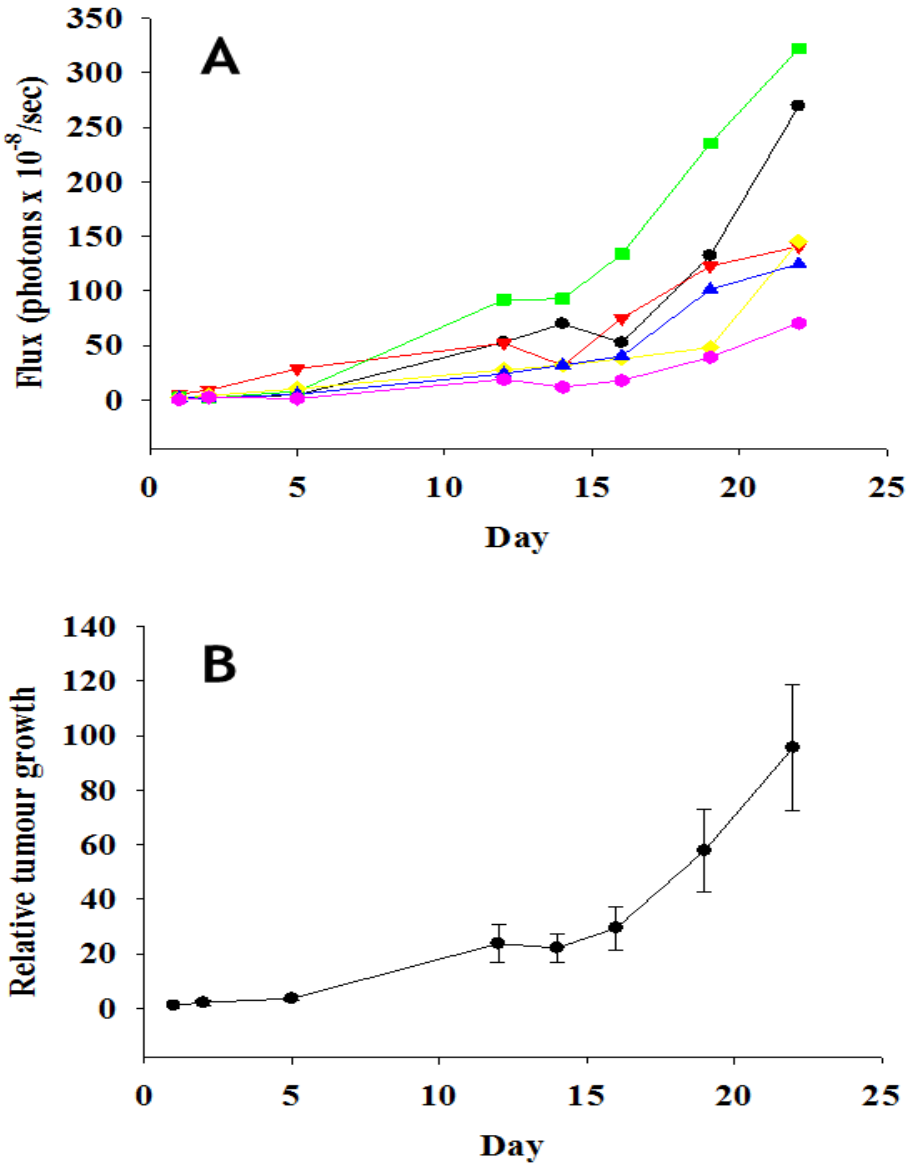

Figure 5.4: Tumour growth measured by bioluminescence following subcutaneous injection of HCT116Luc cells (5 x 10^5cells/mouse). The flux measurement for each mouse was standardised relative to that measured on Day 1 and the mean ± SEM of the relative flux (relative tumour growth) is shown in (B).

5.6.5 Effect of subcutaneous administration of cisplatin on tumour growth

Subcutaneous xenografts of A2780 are sensitive to cisplatin and the growth delay is not affected by the route of administration of the drug (Figure 5.5A). The subcutaneous route of administration is not toxic to the mice as seen by the maintenance of body weight (Figure 5.5B).

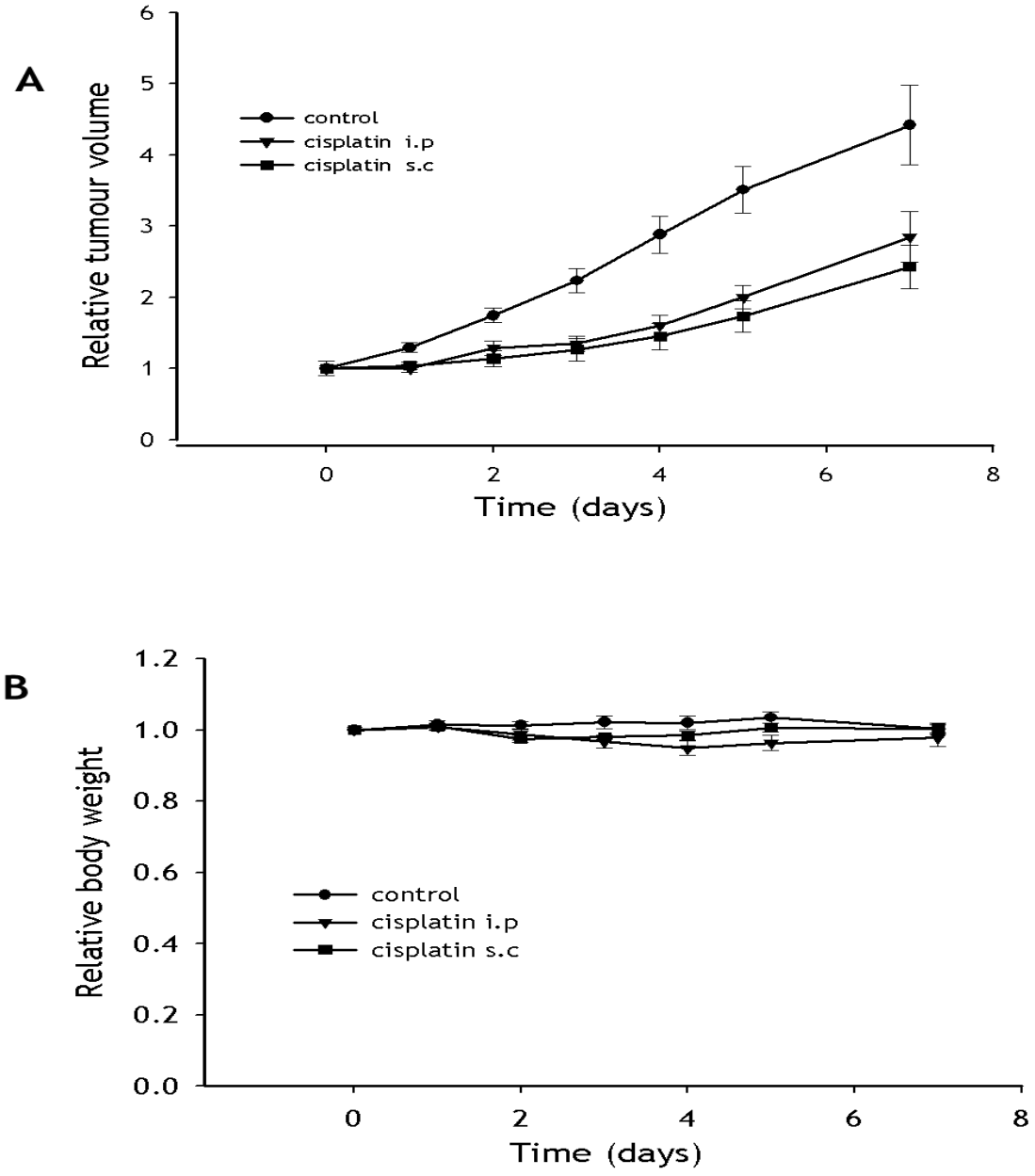

Figure 5.5: Growth of A2780 xenografts following treatment on Day 0 with PBS (●) or cisplatin (6mg/kg i.p.▲ or subcutaneous ■). Values are mean ± SEM of 6 mice in each cohort. Also shown is the body weight of the mice (B).

5.6.6 *Cisplatin sensitivity of A2780-Rab25Luc in vitro*

The cisplatin sensitivity of A2780, A2780-Luc and A2780-Rab25Luc is shown in Table 5.2. Infection of A2780 with the control plasmid containing just the luciferase gene (A2780-Luc) had no effect on the cisplatin sensitivity of the cells. However, infection with Rab25 resulted in a four-fold decrease in cisplatin sensitivity when compared with A2780-Luc cells ($P < 0.001$). Similar results were obtained when the encapsulated cisplatin (CB[7]cisplatin) was used.

Cell line	IC_{50} (μM)	
	Cisplatin	CB[7]cisplatin
A2780	0.13 ± 0.02	0.14 ± 0.03
A2780-Luc	0.12 ± 0.01	0.13 ± 0.008
A2780-Rab25Luc	0.46 ± 0.04	0.42 ± 0.02

Table 5.2: Sensitivity to cisplatin and CB[7]cisplatin of the parental ovarian cancer cell line A2780 and the two derivatives that express luciferase (A2780-Luc) and Rab25 and luciferase (A2780-Rab25Luc). Drug sensitivity was determined by the MTT based assay and cells were exposed to drug for 24 hours. Results are the mean ± SEM of three replicates within one experiment.

5.6.7 Growth of A2780-Rab25 in mice

A2780-Luc and A2780-Rab25Luc cells were injected intraperitoneally into mice and they were imaged weekly for 5 weeks and the results are shown in figure 5.6. After 1 week cells are present in all four A2780-Rab25Luc mice and in 3 out of 4 A2780Luc mice. By week 2 there is very little signal from the A2780-Luc mice and only one mouse shows evidence of viable tumour cells by week 5. All four A2780-Rab25Luc mice show a marked increase in the bioluminescent signal throughout the experiment. This difference is clear when the bioluminescent signal is quantified and plotted against time (Figure 5.6B). There was no apparent distension of the abdomen until week 5.

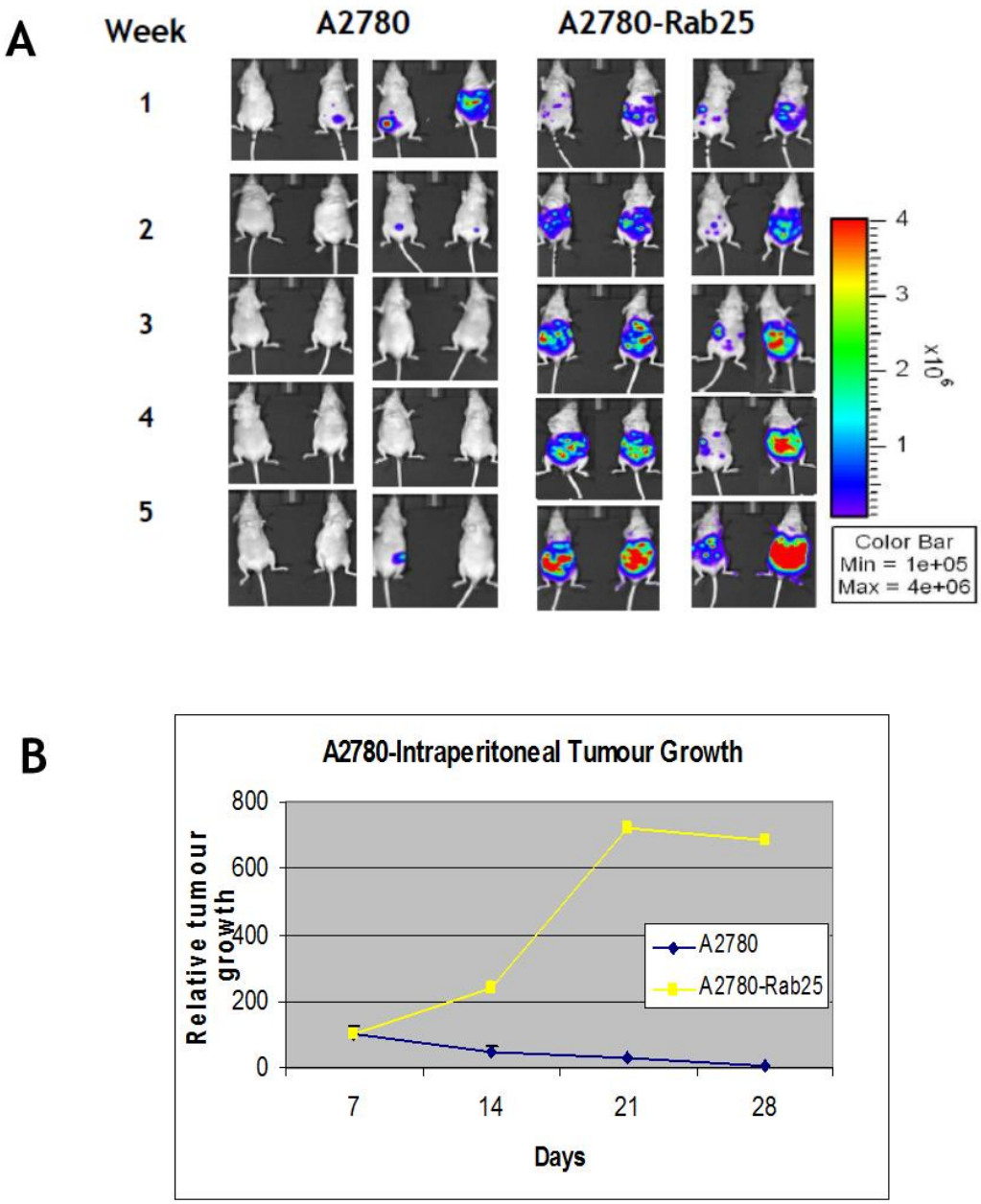

Figure 5.6: Growth of A2780-Luc and A2780-Rab25Luc in the peritoneal cavity of mice. Cells ($5x10^7$) were injected intraperitoneally and mice were imaged after 1 week and then weekly for 5 weeks. Mice were identified by ear tags and sequential bioluminescent overlay images are shown for 4 mice in each group (A). The bioluminescent signal was quantified with Living Image 2.50.2 software with the area of measurement defined by a rectangle, drawn to cover the entire abdomen, and the same area was used for all mice and all measurements. For each mouse the signal at week 1 was defined as 100 and all subsequent measurements were related to this initial signal. The change in signal with time is also shown (B).

5.6.8 Cisplatin sensitivity of A2780-Rab25Luc in vivo

Growth of A2780-Rab25Luc in the peritoneal cavity of mice following treatment with cisplatin and CB[7]cisplatin is shown in figure 5.7 and quantified in table 5.3. A2780-Rab25Luc is less sensitive to cisplatin but the growth delay is only just significant by Day 14. Growth delay is enhanced when mice are treated with the encapsulated form of cisplatin (CB[7]cisplatin) given either intraperitoneally ($P<0.001$) or subcutaneously ($P<0.002$). None of the treatments had a significant effect on the body weight of the mice (Figure 5.8).

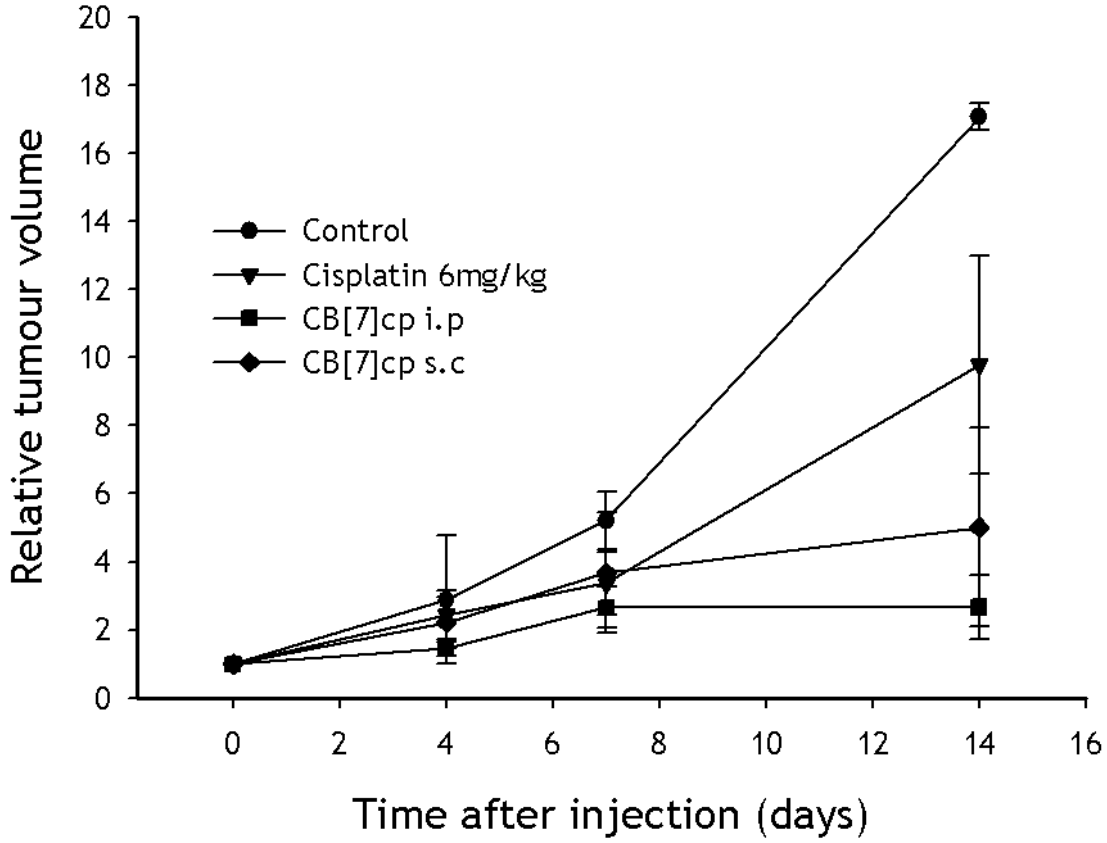

Figure 5.7: Growth of A2780-Rab25Luc as a disseminated tumour in mice following treatment on day 1 with PBS (i.p. ●), cisplatin (6 mg/kg ▼), CB[7]-cisplatin (34 mg/kg i.p ■, or subcutaneously◆). Values are mean ± SEM of 6 mice.

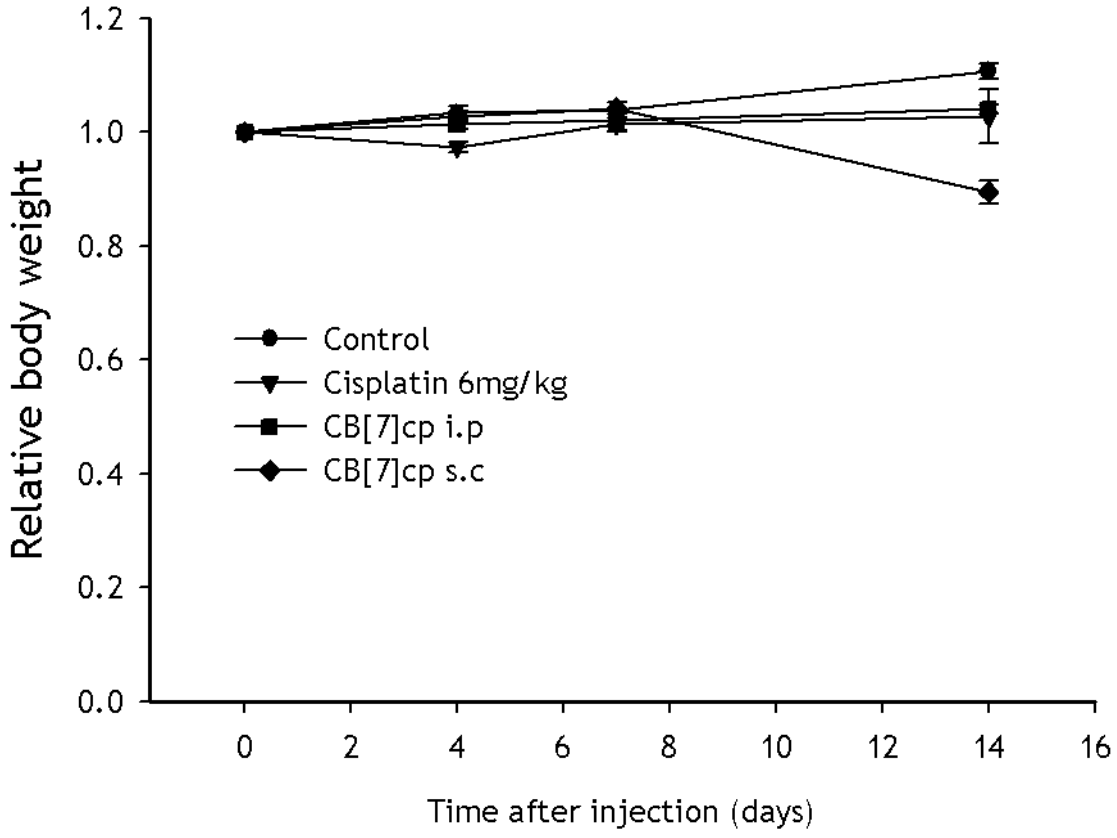

Figure 5.8: Body weight of mice bearing A2780-Rab25Luc disseminated tumours after treatment on day 1 with PBS (i.p. ●) cisplatin (i.p. 6 mg/kg ▼) or CB[7]cisplatin (34 mg/kg i.p ■ ,or subcutaneous ◆). Values are mean ± SEM of 6 mice.

Days	Control	Cisplatin (6m/kg)	CB[7]cisplatin (34mg/kg) i.p	CB[7]cisplatin (34mg/kg) s.c
1	1	1	1	1
4	2.88 ± 1.88	2.43 ± 0.70 NS	1.44 ± 0.22 P<0.05	2.22 ± 0.75 NS
7	5.21 ± 0.85	3.36 ± 0.93 NS	2.66 ± 0.61 P<0.05	3.67 ± 1.77 NS
14	17.1 ± 0.34	9.78 ± 3.19 P<0.05	2.66 ± 0.9 P<0.001	5.01 ± 2.92 P<0.002

Table 5.3: Increase in bioluminescent signal relative to that measured on day 1 (day of treatment) of A2780-Rab25Luc. Values are the mean ± SEM of 6 mice. Statistically significant differences when compared with the control untreated tumours are also shown. NS = not significant

5.7 Discussion

These results clearly show that bioluminescence can be used to measure tumour growth in mice *in vivo*. The bioluminescent signal relies on the presence of luciferin as a substrate for the light emitting reaction and the subcutaneous route of administration was shown to be more consistent than intraperitoneal administration. The level of luciferase expression by the tumour cells not only determines the sensitivity in terms of the number of cells that can be detected but also determines the total tumour burden that can be measured without saturation of the camera. Expression of luciferase in A2780-Rab25Luc cells allowed measurement of tumour growth in the peritoneal cavity of mice at an early stage when no visible distention of the abdomen was present. Treatment of A2780-rab25Luc tumour bearing mice with cisplatin resulted in small growth delay which was only just significant by Day14. This was consistent with the observation that A2780-Rab25Luc cells were 4 fold resistant to cisplatin *in vitro* when compared with parental A2780 cells. However, treatment with the encapsulated form of cisplatin (CB[7]cisplatin) resulted in a significant growth delay regardless of the route of administration of the drug.

5.7.1 Route of administration

For bioluminescence imaging luciferin can be injected intraperitoneally, subcutaneously or intravenously since luciferin permeates tissues including blood-brain and placental barrier easily. However, the kinetics of light emission varies significantly with the route of administration. On intraperitoneal administration of luciferin the peak bioluminescent signal was obtained at 6-8 minutes after injection following which the intensity of the signals plateau and eventually taper (Figure 5.1A). This gives a narrow window of time to capture the bioluminescent signal from the luciferase expressing cells. The intraperitoneal administration of luciferin is error prone due to risk of injecting into the bowel or bowel wall which results in suppression or loss of bioluminescent signal (Contero, Richer et al. 2009). Besides, i.p administration of luciferin in disseminated ovarian tumour models can result in overestimation of signals due to direct diffusion of D-luciferin, in addition to the systemic absorption (Inoue, Kiryu et al. 2009). For these reasons, the subcutaneous route of administration of luciferin was evaluated. The risk of injection failure is

virtually absent with subcutaneous administration as allows the direct visualisation of the injection which is evident by a transient swelling at the site of injection. As shown in figure 5.1B, with subcutaneous administration, the peak intensity of bioluminescent signal was attained relatively earlier but with similar plateau phase compared to i.p administration and this allows slightly broader window of time for imaging.

There is an apparent variability in the intensity of the bioluminescent signal emitted by each of the xenografts which is explained by the variable sizes of the xenografts. However, in the drug efficacy experiments the mice with xenografts of uniform sizes were chosen to minimise gross variability.

The primary aims of preclinical evaluation of drugs in animals, in addition to checking the anti-tumour activity, are to evaluate the pharmacokinetics and toxicities. The experiments described in chapter 3 and 4 demonstrated that CB[7]cisplatin administered intraperitoneally in mice bearing subcutaneous ovarian cancer xenografts exerted enhanced anti-tumour activity over that of cisplatin. This was due to the favourable pharmacokinetic properties of CB[7]cisplatin and established that drug delivery could overcome tumour drug-resistance. However, intraperitoneal administration of CB[7]cisplatin in the disseminated ovarian cancer model described in this chapter is questionable. This could be compared to tissue culture where the cultured cells are directly exposed to the drugs without the need for drug delivery mechanisms. Hence both subcutaneous and intraperitoneal route of drug administration was explored. CB[7] cisplatin exerted anti-tumour activity irrespective of the route of drug administration (Figure 5.7). Of note, cisplatin exerted similar growth reduction of subcutaneous A2780 xenografts either with subcutaneous or intraperitoneal route of administration (Figure 5.5A) without a significant change in body weight between the cohorts of mice (Figure 5.5B).

5.7.2 Sensitivity of bioluminescence imaging

Initial experiments to transfect A2780 and A2780/cp70 cell lines with luciferase expressing plasmids (pd2CMVLuc) were largely unsuccessful. The development of subcutaneous xenografts with transfected cells was unpredictable and the bioluminescent signal intensity was suboptimal. Hence bioluminescent

experiments were performed using HCT116Luc cell line that was obtained from Caliper Life sciences, which was shown to express high signal intensity. Mice were administered intravenous injection (through tail vein) of either HCT116Luc or A2780/cp70CMVLuc to compare the bioluminescence expression and the sensitivity. The injected cells were predominantly deposited in the lungs. As shown in figure 5.2, bioluminescent signal was not seen in mice injected with 10^4 and 10^5 A2780/cp70CMVLuc cells whereas strong bioluminescent signal was noted in mice injected with same number of HCT116Luc cells. There was at least a 10-fold difference in the bioluminescent signal between these two cell lines (Table 5.1). On the basis of this promising result, subcutaneous xenografts of HCT116Luc cells were developed with seeding density of 10^7 cells/mouse as described in section 2.4.2, chapter 2. The increased bioluminescent signal from HCT116Luc allowed earlier detection of the tumour compared to external measurements (with callipers). However, these signals reached the saturation limits of camera despite reducing the imaging time to 10 seconds (compared to conventional 1-2 minutes) and were not suitable for longitudinal studies of tumour growth. To strike a balance between signal saturation and optimum seeding density required for establishing the xenografts, experiment was performed to optimise the seeding density and imaging time (Figure 5.3). HCT116Luc cells at 5 x 10^5cells/mouse was chosen as the optimum seeding density as it allowed measurement of tumour growth (with callipers) and also using bioluminescence imaging over 22 days. In this experiment as illustrated in figure 5.4A, all the 6 mice exhibited tumour growth and the bioluminescent signal increased exponentially with time. Although the signals varied between each of the mice there was a consistent growth in tumour size with time (Figure 5.4B). This illustrates that the optimum seeding density that is required for meaningful bioluminescent experiment is lesser than that required for conventional measurement with callipers and with lower seeding density the issues with saturation of signal could be overcome.

5.7.3 Development of A2780-Rab25Luc model

A disseminated ovarian tumour model was developed with A2780-Rab25Luc cells to evaluate the efficacy of CB[7]cisplatin using bioluminescence imaging. A2780 is a well-established ovarian cancer cell line and its chemo-sensitivity has been well characterised by our research group both *in vitro* and *in vivo* (Strathdee,

MacKean et al. 1999; Plumb, Strathdee et al. 2000). Both A2780 and its cisplatin resistant derivative A2780/cp70 were sourced originally from Dr R Ozols (Fox Chase cancer centre, Pennsylvania, USA) who derived these cells from ovarian cancer patients. Although A2780-Rab25 cell lines were readily available from Prof Jim Norman's group, to avoid risking the variability between cell lines sourced from different laboratories and groups, transfection of A2780 with Rab25 was done *de novo*. A2780-Rab25 cell lines were successfully established by transfecting with pcDNA3-Rab25 vectors. However, the subsequent transfection of A2780-Rab25 with luciferase genes was difficult and the stable expression of luciferase in the A2780 cells already transfected with Rab25 was not achievable. A2780 cells were not able to retain both the luciferase and Rab25 genes and there was loss expression of either of the two genes. Hence gene transfer was done with lentiviral vectors given the promising bioluminescent signal with HCT116Luc cells which were transfected with lentiviral vectors. A2780 cells were transfected with pcDNA3-Rab25 vectors using Lipofectamine 2000 and then transduction of lentiviral constructs containing luciferase gene was done which resulted in the successful establishment of A2780-Rab25Luc cell line. The expression of Rab25 in this cell line was confirmed through Western blotting and the luciferase expression through bioluminescence imaging.

A2780-Rab25Luc cells were injected intraperitoneally into mice and their growth was compared with A2780-Luc by monitoring the intensity of bioluminescent signal. Mice injected with A2780-Rab25Luc cells had clear bioluminescent signal which increased with time indicating establishment and growth of peritoneal tumour deposits (Figure 5.6). A2780-Luc cells on the other hand did not have such increase in bioluminescent signal indicating lack of peritoneal tumours. This strengthens the case that the forced expression of Rab25 has resulted in an invasive phenotype. Consistent with published literature (Cheng, Lahad et al. 2004), tumour was evident in 100% of mice injected with A2780-Rab25Luc cells even before the clinical evidence of ascites (abdominal distension). The consistent uptake of tumour in all the mice injected with A2780-Rab25Luc and the associated emission of bioluminescent signal indicate that this disseminated ovarian cancer model of A2780-Rab25Luc is suitable to measure drug effects.

5.7.4 Cisplatin sensitivity of A2780-Rab25Luc

A2780-Rab25Luc cells exhibit 4-fold resistance to cisplatin compared with A2780Luc cells (IC_{50}: 0.13 ± 0.02 μM for A2780 versus 0.46 ± 0.04 μM for A2780-Rab25Luc, P<0.001) (Table 5.2). Expression of Rab25 in A2780 has resulted in the chemo-resistance to cisplatin which is consistent with published literature. Chang and colleagues reported that overexpression of Rab25 down-regulates the expression of pro-apoptotic Bcl2 family members and also increases proliferation through anchorage independent growth (Cheng, Lahad et al. 2004). These properties are likely to have contributed to cisplatin resistance *in vitro*. Mice with A2780-Rab25Luc xenografts are less sensitive to cisplatin and reduction in the bioluminescent signal just reached statistical significance on day 14 (Figure 5.7). This is the first evidence of Rab25 induced decreased sensitivity to cisplatin *in vivo*. These data further confirm the role of Rab25 in the aggressiveness of ovarian cancer and also that Rab25 could be a prognostic marker and therapeutic target.

5.7.5 Effect of CB[7]cisplatin on growth of A2780-Rab25 *in vivo*

Treatment with CB[7]cisplatin resulted in significant growth delay in A2780-Rab25Luc xenografts when compared with controls both by intraperitoneal or subcutaneous route of administration (Figure 5.7 & Table 5.3). Treatment with CB[7]cisplatin also resulted in tumour growth delay when compared with cisplatin at later stages of the experiment although this was not statistically significant. On day 14, the bioluminescent signal from CB[7]cisplatin treated mice was only 15.6± 5% of that in control mice compared with 57.2 ± 21% to that of control mice in the cisplatin treated cohort (Table 5.3).

This tumour growth delay in the Rab25 models produced by CB[7]cisplatin irrespective of the route of administration is likely due to the distinct pharmacokinetic profile of CB[7]cisplatin which results in prolonged tissue exposure of platinum. The experiments described in chapter 3 demonstrated that CB[7]cisplatin exerted anti-tumor activity even in the cisplatin resistant A2780/cp70 xenografts. Together, these observations suggest that drug delivery of cisplatin with CB[7] could be used to circumvent platinum resistance. However, it is debatable if the disseminated ovarian tumor model (with

Rab25Luc) is a suitable model to evaluate drug delivery of drugs that are administered intraperitoneally since the drug is physically delivered almost directly to the tumour. Parallel pharmacokinetic studies of intra-peritoneal administration of CB[7]cisplatin was not performed and this is a limitation of this section. Intraperitoneal delivery of chemotherapy in patients with peritoneal disease can result in increased diffusion of drug into the tumour compared with systemic delivery (Ceelen and Flessner 2010). Nevertheless it was a reasonable approach to evaluate the *in vivo* activity of CB[7]cisplatin in this model as CB[7]cisplatin exerts its enhanced anti-cancer activity due to its favourable pharmacokinetic profile rather than by exploiting the enhanced permeability and retention (EPR) effect. The disseminated ovarian tumor model described in this chapter could be used for evaluating drug delivery system which relies on tumour microenvironment and also for active targeting where the target may be better expressed by the intraperitoneal model.

5.8 Conclusion

The experiments described in this chapter illustrate the advantages of biophotonic imaging. Conventional measurement of tumour with external callipers is based on assumption that tumours have spherical configurations. This assumption, however, is not always true as tumours are of variable shapes. Besides, the calliper measurements are subject to error due to variability in thickness of skin and subcutaneous pad of fat. Observer subjectivity and differences in the compressibility of the tumour can easily lead to increased errors in measurements (Jensen, Jorgensen et al. 2008). In addition, since the vascular supply of the xenografts is primarily derived from the skin and tumour bed, the centre of the tumour could be hypo-perfused. It is well established that subcutaneous xenografts are known to develop necrotic centre, and this results in the underestimation of the value of drug effect (Black, Shetty et al. 2010). Bioluminescence imaging, although time consuming, overcomes most of the problems outlined above once the method is standardised. The key parameters of bioluminescence imaging include efficient administration of luciferin and establishing the precise time for imaging, both of which could be easily standardised. Bioluminescence imaging does not have high background (in contrast to fluorescence) and since viable cells are required for the generation of bioluminescent signal, it gives a reliable and reproducible estimate of the

functional/biological activity of the tumour. Of note, bioluminescence imaging is not subject to inter-observer and operator variability and the quantitation of the signal intensity could be re-analysed at any given time. Importantly bioluminescence imaging could also assist to probe the key molecular pathways in tumourigenesis and their response to drug treatment by acting as reporters and this will be described in the next chapter.

6 Development of a pharmacodynamic marker of drug activity

6.1 Introduction

The rational development of novel therapies based on our increased understanding of the molecular basis of cancer is likely to place greater emphasis on the biological effectiveness of the therapeutic strategy in addition to the conventional endpoints of toxicity and objective tumour responses (Caponigro and Sellers 2011). This, in turn, will have implications for designing the optimal animal models for pre-clinical evaluation *in vivo* and the mechanisms of evaluating biological endpoints in these models.

Several potential animal models exist for the pre-clinical evaluation of novel anti-cancer agents including xenograft mouse models, orthotopic models and gene-modified animals (e.g. transgenic oncomice) and the optimal model will depend on a number of factors including the putative mechanism of action of the agent undergoing evaluation. The advantages and disadvantages of each of these models have been extensively reviewed (Sausville and Burger 2006; Frese and Tuveson 2007; Kung 2007). However all of these potential models have the disadvantage of assaying endpoints which give limited information on the biological effects of the agent on specific processes within the tumour. The development of new tools that can non-invasively assess the molecular and cellular events involved in the response of tumour cells to anti-cancer agents, would overcome many of the drawbacks of the existing pre-clinical models used in developing anti-cancer therapies.

Development of pharmacodynamic biomarkers of drug activity is now an integral part of preclinical drug development. Thus the optimal dose and schedule of an active agent can be determined based on biological (i.e. pharmacodynamic) endpoints and any correlation of biological activity with pharmacokinetic parameters can be explored. This approach will also be useful in designing drug delivery systems since biological endpoints could be used to determine if and when the drug reaches the tumour even if not in sufficient amounts to cause tumour growth delay.

The studies described in the previous chapter clearly demonstrated the value of bioluminescence imaging in studies of tumour growth *in vivo*. The technique is sensitive and reproducible and can detect a signal originating from within the body cavity. For the tumour growth studies, cancer cells were manipulated such that the luciferase gene was expressed under the control of a constitutively active promoter. As a result the signal was proportional to the number of viable cells present within the tumour. Reporter assays, where cells are transiently transfected with the luciferase reporter gene linked to a promoter or transcription response element (TRE) of interest, are widely used in cell studies. These *in vitro* assays rely on the short half-life of the luciferase gene product (< 1 hour). The advent of the technology to enable bioluminescence imaging *in vivo* allows the transfer of this approach to animal studies (Kang and Chung 2008; Kimbrel, Davis et al. 2009; O'Neill, Lyons et al. 2010). Reporter assays are very sensitive since the product is an enzyme, luciferase, which results in amplification of the signal.

The aim of the studies described in this chapter was to develop a dynamic real-time marker of drug activity. Nearly all cytotoxic drugs including cisplatin and paclitaxel activate the transcription factor p53 (Vogelstein, Lane et al. 2000). A p53 luciferase reporter system was therefore chosen for this study. For this approach to work, it is important to ensure that the luciferase gene expression is regulated by p53 binding to the TRE and not due to non-specific effects. The codon optimised Luc2 luciferase gene (Promega) was used in the lentiviral vector system, described in the previous chapter, in order to obtain stable and specific expression of the vector in A2780 cells which have wild type p53. Initially, transfected cells were characterised for p53 response *in vitro* both by bioluminescence imaging and by Western blotting. Cells were then grown as xenografts *in vivo* and expression of p53 was determined by bioluminescence imaging. The results obtained from the application of bioluminescence imaging were compared with a more traditional technique, immunohistochemistry, for the detection of p53 expression *in vivo*.

6.2 Methods

6.2.1 Construction of the plasmid

Invitrogen Virapower™ promoterless Lentiviral Gateway kit® (Invitrogen, catalogue number: L5910-00) was used to clone p53 promoter and Luciferase (Luc2) gene into lentiviral vector (pLenti6/R4R2/V5-DEST) to be expressed in A2780 cell lines. The process involved three vital steps namely, cloning the promoter (p53) into the pENTR-TOPO vector (supplied in the kit) to produce the promoter entry clone, cloning the gene of interest (Luc2) into p-ENTR vector to produce the gene entry clones and finally constructing pLenti6p53Luc2 gene through the recombination reaction of the two entry clones with pLenti6/R4R2/V5-DEST vector. This pLenti6p53Luc2 gene was then used for transfecting A2780 and A2780-Rab25 cell lines. A schematic representation of this process is illustrated in figure 6.1.

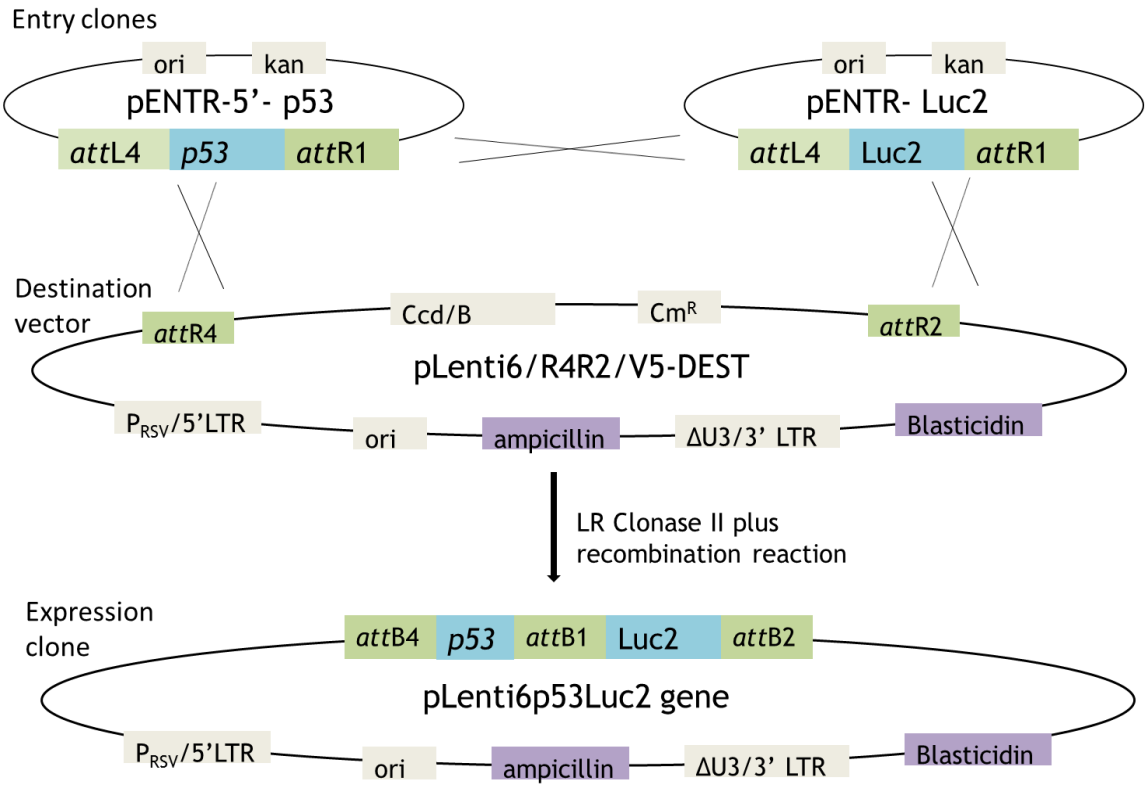

Figure 6.1: Schematic representation of development of bioluminescent reporter containing p53 reporter using lentiviral derived plasmid.

6.2.1.1 Development of entry clones with p53 gene

pENTR 5'-TOPO® cloning kit, supplied with the Invitrogen Virapower™ promoterless Lentiviral Gateway kit®, contained the pENTR 5'-TOPO® vector which was able to clone p53. Polymerase chain reaction (PCR) was performed using Taq polymerase to produce a PCR product containing p53 and also a negative control which contained minimal TATA element (without any active gene of interest). PCR was conducted as outlined in section 2.5.1, chapter 2 and with specific reference to this experiment, 100 nanograms of DNA of both p53 and control were used. Other calculations used were as follows:

Taq polymerase: 0.5mL
DNA(100ng/μL): 1μL
10μM dNTP: 1mL
50 μM $MgCl_2$: 1.5mL
Primer 1 (10μM): 5mL
Primer 2 (10μM): 5mL

The mixture was thoroughly mixed in vortex and was run using Bio-Rad tetrad Peltier thermal cycle. The following day, the PCR products were checked using DNA gel electrophoresis to confirm the presence of DNA. Subsequently the bands of gel containing the DNA (checked using UV transilluminator) were cut and weighed. DNA was extracted from the gel using QIAEX II gel extraction kit. In brief, 10μL of QIAEX II buffer was added to gel, vortexed for 30 seconds, left at 50ºC for 2 minutes and vortexed every 2 minutes till the solution turned yellow. The sample was then centrifuged at 12000g for 30 seconds at room temperature and the supernatant was aspirated. The DNA pellet was washed with 500μL of QIAEX buffer, vortexed and centrifuged for 30 seconds and the supernatant was aspirated. This step was repeated twice and the DNA was air-dried for 10 minutes. 20μL of distilled water was added to the air-dried pellet and incubated for 5 minutes at room temperature. Finally the supernatant containing the DNA was collected and stored in Eppendorf tubes at 4ºC in a refrigerator.

6.2.1.2 TOPO® cloning reaction

The final product of the PCR was cloned into pENTR 5'-TOPO® vector by ligase reaction. 2µL of PCR product, 1µL of salt solution (supplied with the kit), 1µL pENTR 5'-TOPO® vector and 2µL of sterile water was mixed and incubated at room temperature for 5 minutes. The resultant product was transformed into chemically competent E.coli supplied with the kit by bacterial transformation as per the method described in section 2.5.3, chapter 2. Kanamycin was used as the selection antibiotic. The extracted DNA was sequenced using the DNA sequencing services at the Beatson labs and the alignment was cross examined. The sequence of p53 gene used in the entry vector is given below: TACAGAACATGTCTAAGCATGCTGTGCCTTGCCTGGACTTGCCTGGCCTTGCCTTGGG.

Subsequently large samples of the entry clone containing p53 gene and negative control was prepared using maxi-prep of DNA and quantified as described in sections 2.5.4 & 2.5.5, chapter 2. This entry clone containing the gene of interest (p53) will be hereafter named as pENTR TOPOp53. Similarly entry clones containing Luc2 gene (hereafter referred to as pENTR TOPOLuc2) and negative control containing minimal TATA alone (hereafter referred as pENTR TOPO control) was also constructed and all the above analyses were conducted. The DNA content of all the entry clones and destination vector was the calculated (in ng) to facilitate the recombination reaction. The final concentrations of the plasmids were as given below:

pENTR TOPO p53:1660ng/µL
pENTR TOPO Luc2: 1166ng/µL
pENTR TOPO control: 973ng/µL
The concentration of the pLenti6/R4R2/V5-DESTvector was 1100ng/µL

6.2.1.3 LR Recombination Reaction

The two entry clones containing p53 gene and Luc2 reporter were added to final destination vector, pLenti6/R4R2/V5-DEST, by means of Multisite Gateway® LR recombination reaction. LR clonase II Plus enzyme used for the recombination reaction was supplied in the kit. The required amount of plasmid DNA was 10 femtomoles (fmoles) for both the entry clones and 20 fmoles for

pLenti6/R4R2/V5-DEST. The number of basepairs (bp) in the entry clone, pENTR TOPOp53 was 2808bp (2680bp for the pENTR 5'-TOPO® vector and 128bp for the p53reporter). Similarly the number of basepairs in the entry clones pENTR TOPO Luc2 and pENTR TOPO control was 4351bp and 2760bp respectively. Since the LR recombination reaction stipulated that the concentration of plasmid DNA to be in fmoles, the following formula (given in the manual) was used for the conversion from nanograms to femtomoles.

Nanograms (ng) = (x fmoles) (N) [660fg/fmoles] [1 ng /10^6 fg], where "x" is the number of fmoles and "N" is the size of the DNA in bp.

One µL each of pLenti6/R4R2/V5-DEST vector, pENTRTOPOp53 and pENTR TOPOLuc2 plasmid containing the required concentration of DNA (in fmoles) was mixed with 2µL of LR clonase II plus enzyme, made up to a final volume of 10µL with TE buffer and incubated overnight at 21ºC. Proteinase K solution (2µg/µL) was added to resultant product and incubated at 37ºC for 10 minutes. Following this step, 10µL of the resultant solution from the recombination reaction was used for the bacterial transformation reaction using One Shot® competent as per the method described in section 2.5.3, chapter 2. Ampicillin and blasticidin were the selection antibiotics used to streak the agar plates.

Colonies were isolated after 24 hours and DNA was extracted and quantified as described in section 2.5.4 and 2.5.5, chapter 2. The final construct containing the p53 response element (p53RE) promoter was named as pLenti6p53RELuc2 and the negative control containing TATA sequence alone was named as pLenti6TATALuc2. The sequencing of both these final constructs was done indirectly by confirming the sequence of the p53 and Luc2 gene. Prior to expression of the pLenti6p53RELuc2 plasmid, restriction digest was performed to check the correct alignment and length of the construct. Restriction digest was performed as described in section 2.5.2, chapter 2. ECor V enzyme was used for the digestion which resulted in two DNA fragments each of 6974bp and 1713bp which was verified using Hyperladder™ I (Bioline). The plasmids (pLenti6p53RELuc2 and pLentiTATALuc2) were then used to transfect A2780 cells.

6.2.2 Transfection

A2780 cells were transfected with the plasmids, pLenti6p53RELuc2 and pLentiTATALuc2 using Lipofectamine 2000 as described in section 2.5.6, chapter 2. In addition, the plasmid containing luciferase gene alone without the promoter, pLenti6TATALuc2 was also used to transfect cells which acted as a negative control. For this experiment A2780 cells were plated in 6 well plates and upon 90-95% confluence, the transfection was performed. 4µg of plasmid DNA was used to transfect the cells and the rest of the procedure was done as per section 2.5.6, chapter 2. The cells were sub-cultured into two separate flasks and allowed to grow for 24-48 hours. At 60-80% confluence, cells in each of the replicate flasks were checked for transgene expression by incubating with cisplatin (0.1µM) for 24 hours to induce p53. The transiently transfected cells were then checked for luciferase expression using bioluminescence imaging by adding D-Luciferin (30mg/ml). Once the gene expression was confirmed, stable cell lines were generated by propagating the cells in the presence of blasticidin (2.5mg/mL) as the selection antibiotic.

6.3 Cytotoxic drug treatment

6.3.1 Bioluminescence

A2780pLentip53RELuc2 cells were plated in 24 well Iwaki™ plates at a density of 300 cells/well and allowed to attach and grow in a humidified incubator at 37^{o}C equilibrated with 5% CO_2 for 24 hours. Upon 90% confluence, the cells were treated with a range of concentrations of cisplatin, doxorubicin or paclitaxel for 24 hours. These three drugs were chosen to cover a spectrum of chemotherapeutic agents with different mechanisms of action. The drug containing medium was replaced with fresh medium containing D-Luciferin (30mg/mL) and plates imaged immediately with the IVIS 50 imaging system. After imaging, the cells were trypsinised and counted.

6.3.2 Western blotting

A2780pLenti6p53RELuc2 and A2780 cells were plated at a density of 10^6cells/ml in 6 well plates and allowed to attach and grow in a humidified incubator at 37^0C equilibrated with 5% CO_2 for 24 hours. Cells were treated with a range of

concentrations of cisplatin, doxorubicin or paclitaxel for 24 hours. Protein was then extracted and quantified as described in section 2.1.5 and 2.1.6, chapter 2, respectively. Western blotting was performed as described in section 2.3, chapter 2. The primary antibody was anti-p53 (Novocastra clone D-01 from Leica Biosystems Ltd) at a dilution of 1:1000.

6.3.3 Human tumour xenografts

Monolayer cultures of A2780pLenti6p53RELuc2 cells were harvested with trypsin/EDTA and resuspended in PBS. About 10^7 cells were injected subcutaneously into both the left and right flank of athymic nude mice (CD1 *nu*/*nu* mice from Charles River). After 7 to 10 days when the mean tumour diameter was at ≥ 0.5 cm^3 the baseline bioluminescent signal was measured (see chapter 5). Mice were then allowed to recover from the anaesthetic for 4 hours following which they were treated with either PBS or cisplatin (6mg/kg i.p.). After 24 hours, p53 induced bioluminescence was measured.

6.3.4 Immunohistochemistry

Monolayer cultures of A2780 were harvested with trypsin/EDTA and resuspended in PBS. About 10^7 cells were injected subcutaneously into the right and left flank of athymic nude mice (CD1 *nu*/*nu* mice from Charles River). Once tumours had reached a mean diameter of about 1cm, mice were treated with either PBS, cisplatin (6mg/kg) or CB[7]cisplatin (34mg/kg, dose equivalent of cisplatin at 6mg/kg). After 24 hours, tumours were harvested and fixed in neutral buffered formalin. Samples were processed, sectioned and mounted on glass slides by Histology Services, Beatson Institute for Cancer Research.

Sections were dewaxed in xylene for 5 minutes. They were then hydrated by immersing the sections in 100% ethanol for one minute thrice, 70% ethanol for 1 minute and then immersed in tap water. Antigen retrieval was performed using heat induced epitope retrieval (HIER) technique. Sodium citrate buffer with pH 6.0 (Thermo scientific) was used for antigen retrieval which was preheated in a pressure cooker that was placed in a microwave. The slides were immersed in the pre-heated sodium citrate buffer, left in the pressure cooker which was sealed and heated to maximum pressure for 10 minutes. The pressure cooker

was allowed to cool under cold tap water. The slides were removed from the sodium citrate buffer and placed in wash buffer made of TBS-Tween 20 (TBS-Tween 20x, diluted 20 fold with distilled water). Besides the HIER using pressure cooker, pre-treatment (PT™) module (Thermo scientific) was also used for antigen retrieval. In PT module, PT module buffer (100x citrate buffer, pH:6 diluted with distilled water) was preheated in the PT module chamber for 90 minutes and slides were placed in the chamber and heated at 98^{o}C for 20 minutes. The final results were comparable for both these antigen retrieval techniques. Following antigen retrieval, the slides were washed twice for 5 minutes with TBS-Tween and the tissue margins were delineated with DAKO marker. 100µL of peroxidase blocking solution was added to the tissues mounted on the slide and incubated at room temperature in a humidified chamber.

The slides were then washed twice with TBS-Tween for 5 minutes each, after which 150µL of mouse anti-human p53 antibody (Leica microsystem, DO-6) (diluted 100 fold) was added and incubated for 45-60 minutes. The washing steps were repeated and the slides were incubated with secondary antibody, anti-rabbit p53 (DAKO) at room temperature for 45-60 minutes. The slides were washed with PBS-Tween and 150µL of DAB solution with its substrate was added to the tissue section. The sections were monitored for uptake of the stain after which point the reaction was terminated by adding water. The sections were stained with Mayers haematoxylin stain for 2 minutes, washed with Scotts tap water and distilled water for two alternate cycles. The sections were dehydrated by immersing in ethanol and xylene sequentially after which they were mounted.

6.4 Results

6.4.1 Confirmation of the construct sequence

The final construct containing the p53 response element (p53RE) promoter (pLenti6p53RELuc2) and the negative control containing TATA sequence alone (pLenti6TATALuc2) were digested with the ECor V enzyme to confirm the sequence of the p53 and Luc2 gene. The expected two digestion products of 6974bp and 1713bp were present for both constructs (Figure 6.2).

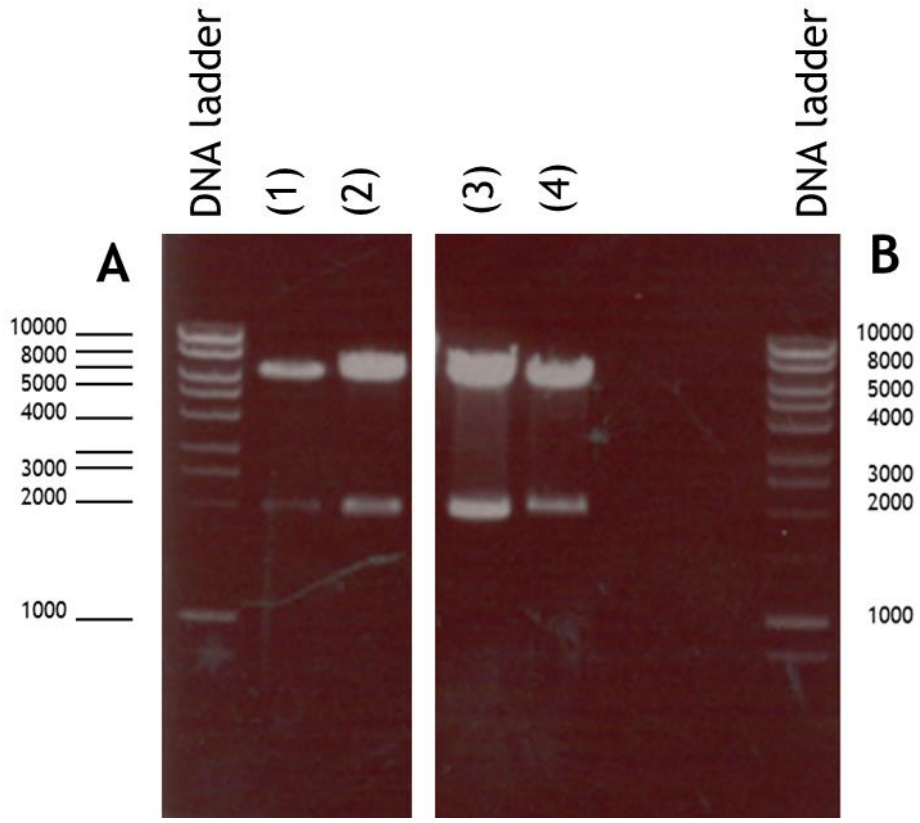

Figure 6.2: Restriction fragment of plasmid DNA using Ecor V. Left Panel (A) indicates two replicates (1) and (2) of pLentip53RELuc2 plasmid DNA and right panel (B) indicates two replicates (3) and (4) of pLenti6TATALuc2 plasmid DNA. The DNA ladder is shown on both sides.

6.4.2 Confirmation of transfection

A2780 cells transfected with pLenti6p53RELuc2 or pLenti6TATALuc2 and parental A2780 cells were treated with cisplatin (0.1μM) for 24 hours and the bioluminescence measured. The results are shown in figure 6.3 and table 6.1. The left column indicates the cells that were transfected with pLenti6p53RELuc2, the centre column indicates the cells transfected with pLenti6TATALuc2 and the right column indicates parental A2780 cells. The top row contains cells that were incubated with cisplatin (0.1μM) and the cells in bottom row were treated with DMSO(0.1μM) only. A2780 cells transfected with the control vector (pLenti6TATALuc2) and parental A2780 cells show background

bioluminescence only. A2780 cells transfected with the p53 reporter (A2780pLenti6p53RELuc2) show a small increase in bioluminescence when treated with DMSO as compared to those transfected with the control vector (A2780pLenti6TATALuc2). Only the cells transfected with p53 reporter show a significant increase in bioluminescence (7 fold) when treated with cisplatin in comparison with the cells transfected with control vector (Table 6.1 and Figure 6.3).

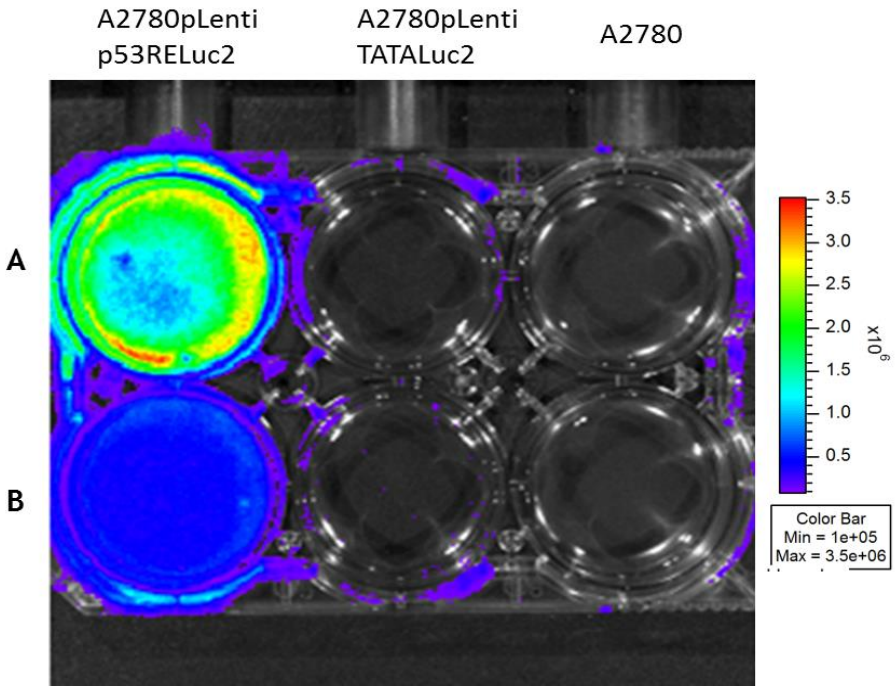

Figure 6.3: Bioluminescence imaging of cells parental A2780 cells (right column), A2780 cells transfected with pLentip53RELuc2 (left column) and pLentiTATALuc2(centre column). The cells on the top row (A) were treated with cisplatin (0.1µM) and bottom row (B) were treated with DMSO (0.1µM).

Cell line	Total Flux(photons/second)/well	
	Cisplatin	DMSO
A2780p53RELuc2	2.365×10^8	6.06×10^7
A2780TATALuc	3.351×10^6	5.48×10^6
A2780	5.54×10^5	4.56×10^5

Table 6.1: Bioluminescent signal (flux) emitted by the cells in each well upon treatment with cisplatin (0.1µM) or DMSO (0.1µM) for 24 hours.

6.4.3 Induction of p53 in vitro

A2780pLenti6p53RELuc2 cells were treated with cisplatin, doxorubicin or paclitaxel at a range of doses for 24 hours and the p53 expression was determined by bioluminescence and confirmed by Western blotting. Expression of p53 determined by Western blotting for the reporter cells and parental A2780 cells upon treatment by the three drugs is shown in figure 6.4. There is a clear induction of expression of p53 by all the three drugs (cisplatin, paclitaxel and doxorubicin).

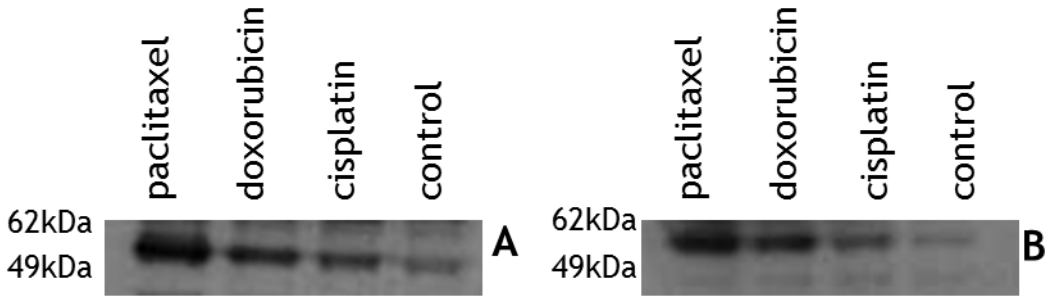

Figure 6.4: Induction of p53 in A2780pLenti6p53RELuc2 cells (left panel A) and A2780 cells (right panel B) upon treatment with paclitaxel (40nM), doxorubicin (400nM) and cisplatin (1μM). The molecular size markers are shown.

Induction of p53 as measured by bioluminescence imaging is shown in figure 6.5. In the absence of drug treatment, the bioluminescent signal is at background levels. However, treatment with the cytotoxic drugs at doses around the IC_{50} concentration shows a marked increase in the flux. The flux was measured, quantified and expressed relative to cell numbers and a clear dose response was seen for all three cytotoxic drugs (Figure 6.5).

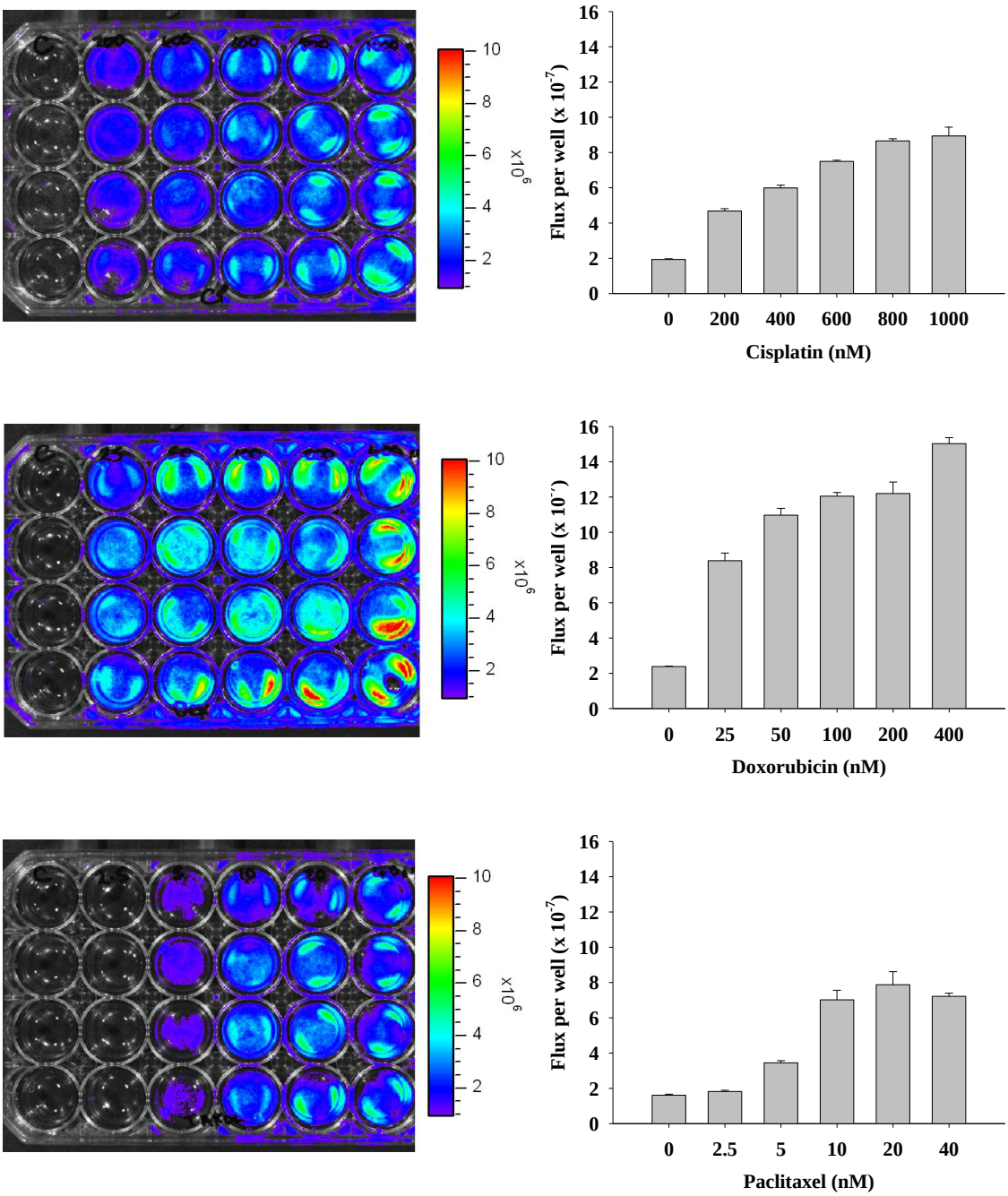

Figure 6.5: Bioluminescent images of the induction of luciferase gene expression in A2780pLenti6p53RELuc2 cells 24hours after treatment with increasing doses (from left to right) of cisplatin (top panel), doxorubicin (middle panel) and paclitaxel (bottom panel). The first column of each plate contains untreated cells. Luciferase gene expression measured in flux per million A2780pLenti6p53RELuc2 cells is also shown. Bioluminescence for each well was quantified and the results, expressed as flux per 10 million cells (mean ± SEM of 4 wells), are shown as a histogram on the right.

6.4.4 Induction of p53 in vivo

A2780pLenti6p53RELuc2 cells were grown as xenografts in nude mice and were imaged before and 24 hours after treatment with cisplatin. Results are shown as images and as the quantified flux in figure 6.6. Significant bioluminescent signal was obtained in the tumours before treatment (Figure 6.6A left panel & B). After 24 hours there was a small increase in the signal obtained from the control, PBS treated, mice (Figure 6.6A right panel & C). This increase in bioluminescent signal was not statistically significant ($P > 1$, t-test). However, when mice were treated with cisplatin (6mg/kg, i.p) there was a significant increase (2.8 fold, $P < 0.001$) in the bioluminescent signal when compared with the pre-treatment signal (Figure 6.6B right panel & C).

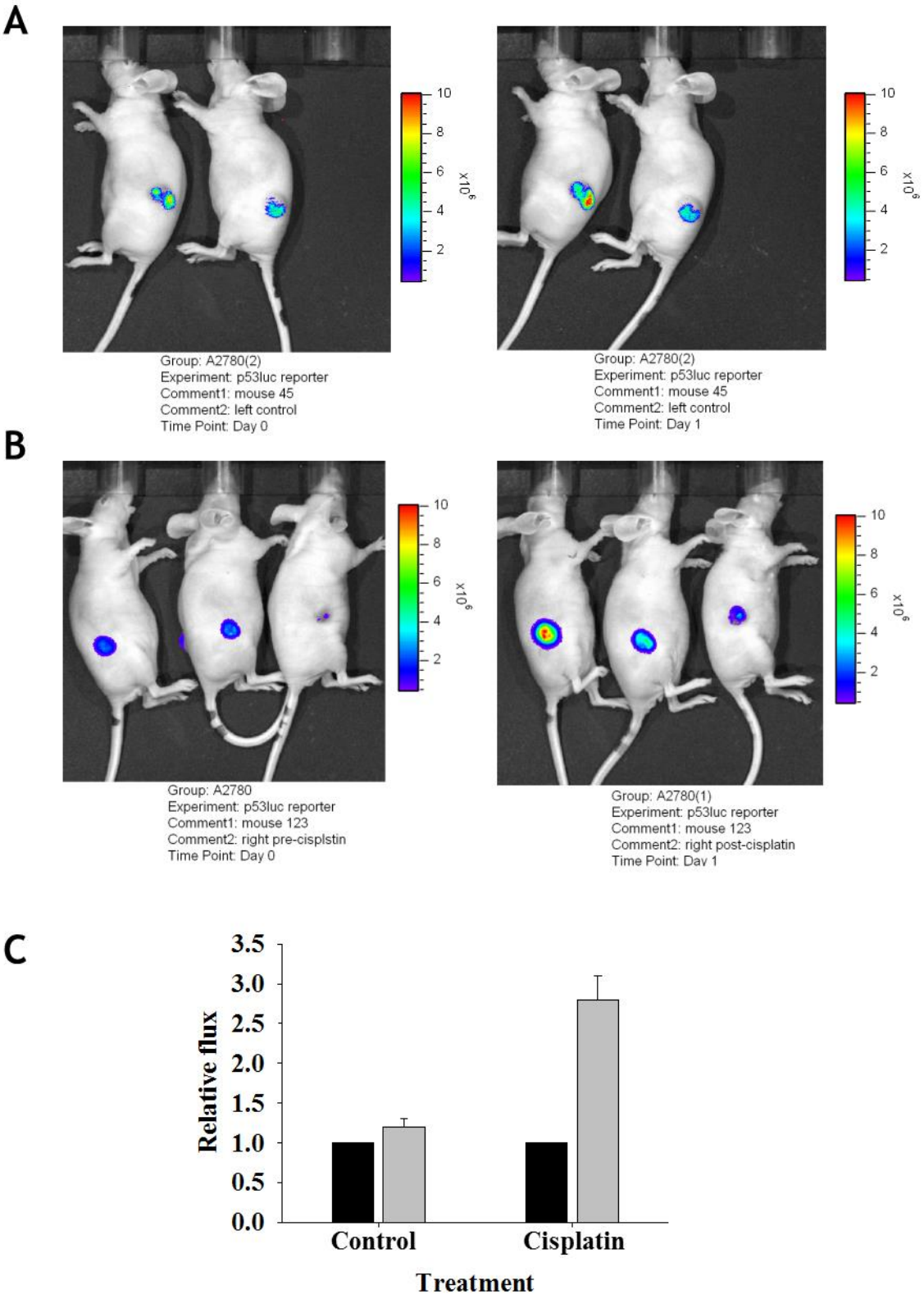

Figure 6.6: Induction of p53 *in vivo* in mice bearing A2780pLenti6p53RELuc2 tumours. Mice were imaged (left) and then treated with either PBS (A) or cisplatin (6mg/kg i.p., B) and imaged again after 24 hours (right). The bioluminescent signal was quantified and the post-treatment signals (grey bars) expressed relative to the pre-treatment signal are shown (black bars). Results are the mean ± SEM of 5 mice.

6.4.5 Detection of p53 expression by IHC

Expression of p53 determined by immunohistochemistry of A2780 tumours taken from mice 24 hours after treatment with a single intraperitoneal injection of PBS, cisplatin (6mg/kg) or CB[7]cisplatin (34mg/kg) are shown in figures 6.7, 6.8 and 6.9 respectively. There were four mice in each treatment group and each of the images corresponds to the representative section of each of the mice in the cohort. p53 protein is present at low levels in tumours taken from the control PBS treated mice (Figure 6.7). However, expression is much greater in tumours taken from mice that were treated with cisplatin (Figure 6.8) or CB[7]cisplatin (Figure 6.9).

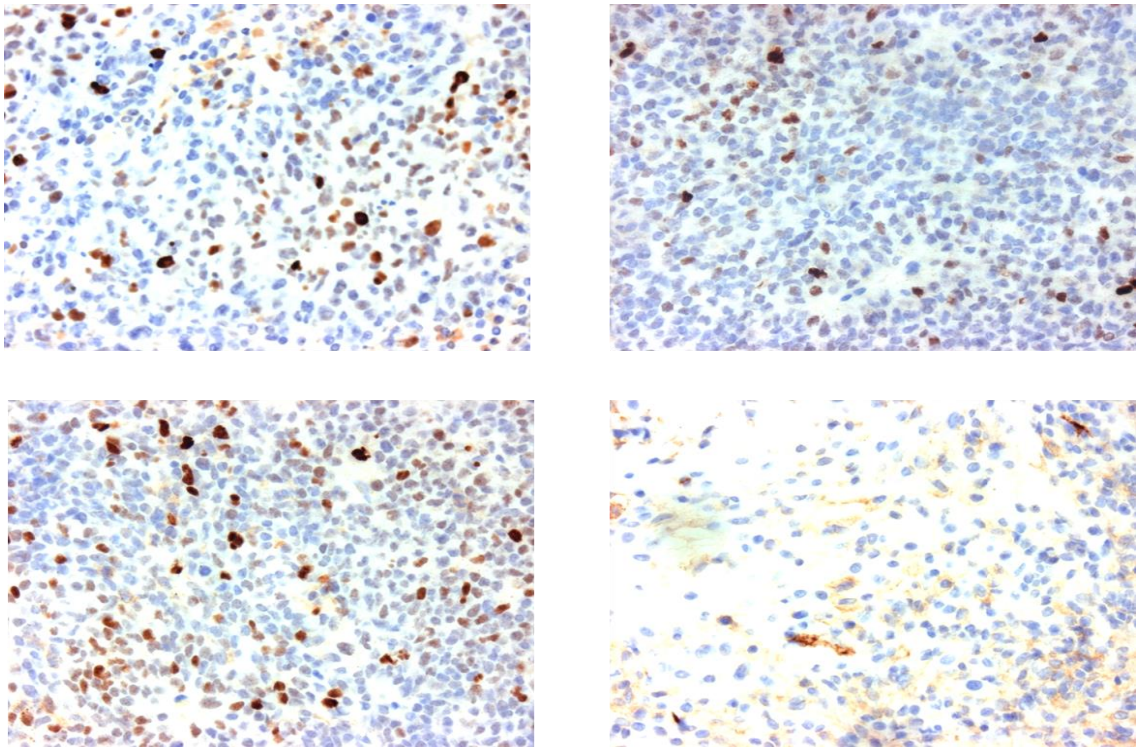

Figure 6.7: Expression of p53 determined by immunohistochemistry. Mice bearing A2780 tumours were treated with PBS and the tumours removed after 24 hours. They were then fixed and stained for p53 protein. Representative section from the cohort of 4 mice is shown.

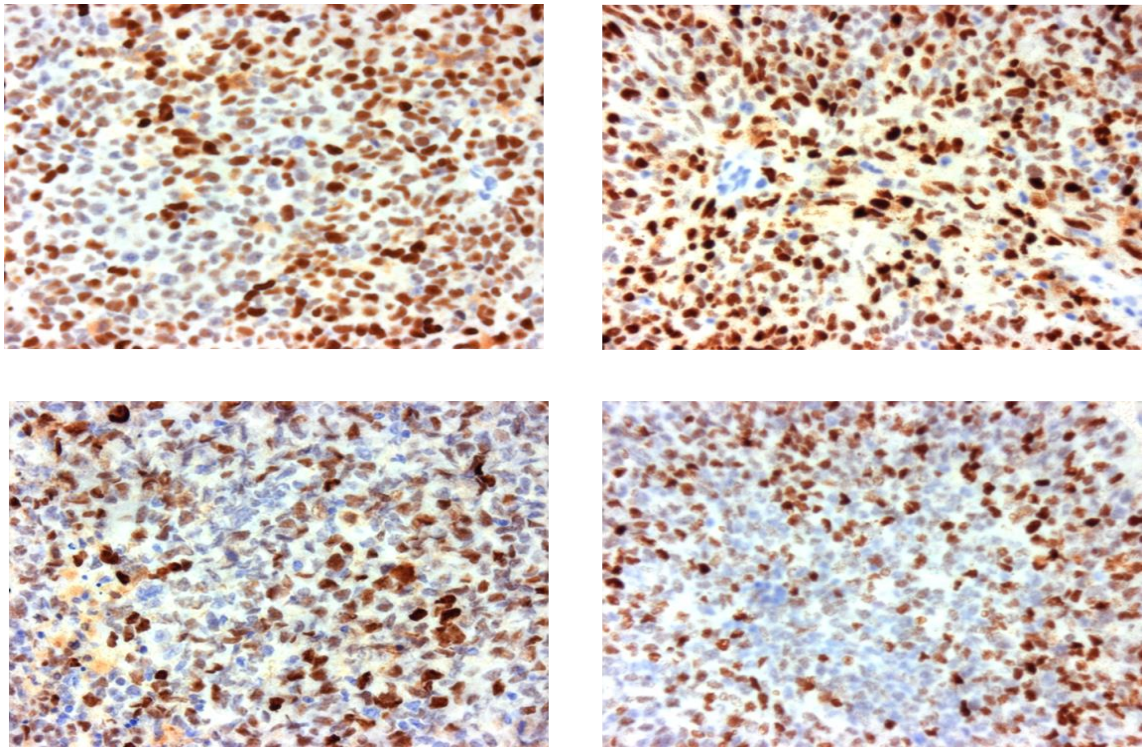

Figure 6.8: Expression of p53 determined by immunohistochemistry. Mice bearing A2780 tumours were treated with cisplatin (6mg/kg, i.p.) and the tumours removed after 24 hours. They were then fixed and stained for p53 protein. Representative section from the cohort of 4 mice is shown.

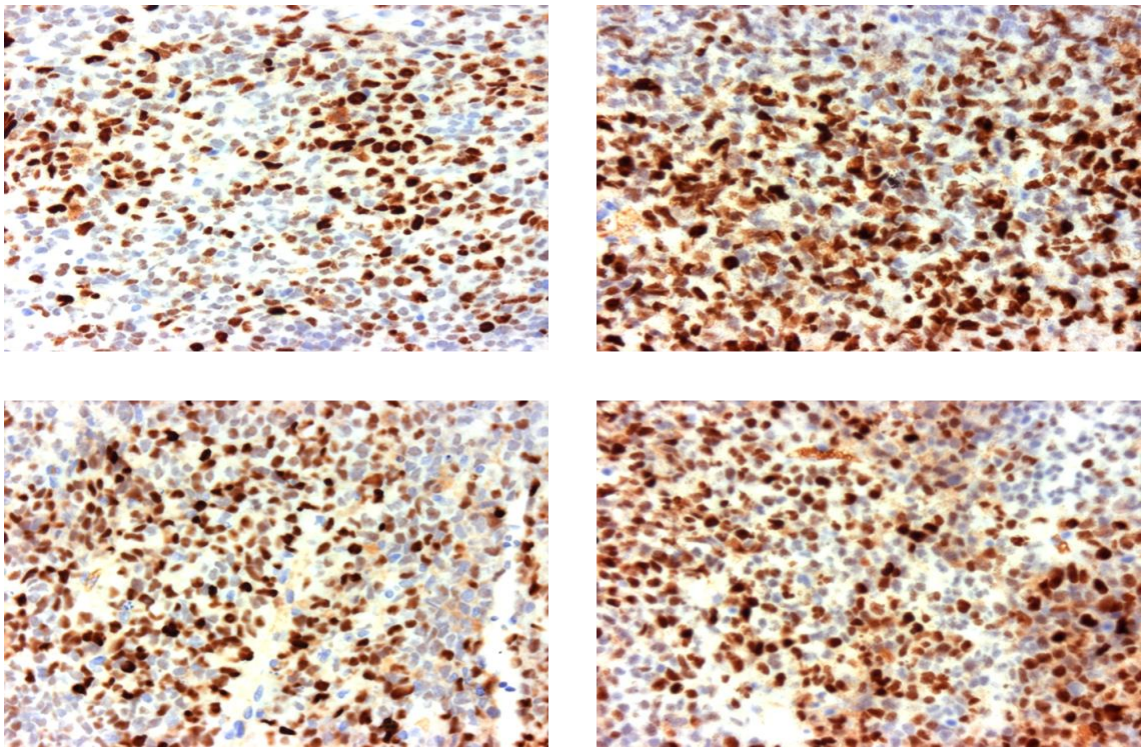

Figure 6.9: Expression of p53 determined by immunohistochemistry. Mice bearing A2780 tumours were treated with CB[7]cisplatin (34mg/kg, i.p) and the tumours removed after 24 hours. They were then fixed and stained for p53 protein. Representative section from the cohort of 4 mice is shown.

6.5 Discussion

A2780 cells were successfully transfected with a plasmid designed to link the TRE site of p53 responsive genes to the luciferase gene. This construct allowed the detection of p53 induction in both cells in culture and in the cells when grown as xenografts in mice. For cells in culture, the bioluminescent signal was clearly related to the dose of drug used to induce p53 expression, with higher concentrations of the cytotoxic drug inducing around an eight fold increase in the flux measurement. The expression of p53 as measured by bioluminescence was very low in the control untreated cells and this was confirmed by Western blotting. However, the baseline bioluminescent signal detected *in vivo* in control untreated tumours was relatively high and even at the maximum tolerated dose of cisplatin the increase in signal was only 2.8 fold compared to baseline. A significant expression of p53 was also detected in the control (PBS treated) tumours by immunohistochemistry. As with bioluminescence imaging, there was a demonstrable increase in p53 expression in tumours taken from cisplatin or CB[7]cisplatin treated mice on immunohistochemical analysis.

6.5.1 The plasmid

The reporter used in the experiments described in this chapter contains luciferase gene under the control of transcriptional response elements (TRE) induced by p53. p53 was chosen as the promoter of interest since p53 is ubiquitously induced by a variety of genotoxic stressors including chemotherapy and radiotherapy (Wang and El-Deiry 2003). In addition, induction of p53 is the the key mechanism through which cisplatin and other platinum compounds exert their cytotoxic action and induction of p53 culminates in apoptosis (Lowe and Lin 2000; Wang and Lippard 2005).

Lipid based transfection, although simple and quick, does not always result in stable transgene expression. As demonstrated in figure 5.2, chapter 5 the transgene expression of A2780/cp70CMVLuc cell lines which were generated by transfecting A2780/cp70 cell lines with pd2CMVLuc plasmid by Lipofectamine was not successful. Hence gene delivery was attempted using lentiviral vectors. Use of lentiviral vectors for gene delivery generates cell lines with stable and long term transgene expression, without affecting the normal function of the

host genome (Cockrell and Kafri 2007). Lentiviral vectors used in the experiments described in this chapter were easy to develop as per manufacturer's instructions. This lentiviral vector was also used for the development of disseminated ovarian cancer model described in chapter 5.

6.5.2 Characterisation of p53 reporter in vitro

Ovarian cancer cell line A2780 is one of the widely used cell lines to evaluate specific molecular pathways and chemosensitivity. A2780 cell line is characterised by the presence of wild type p53 (Brown, Clugston et al. 1993) and this is also shown in the Western blotting experiments in chapter 3 whereby treatment with cisplatin resulted in a clear dose response with incremental induction of p53 with increasing doses of the drug (Figure 3.4, chapter 3). Construction of a bioluminescent p53 reporter, wherein the expression of luciferase enzyme is controlled downstream of p53 response elements, enables to reliably monitor and quantify the induction of p53. In the *in vitro* bioluminescence imaging experiments with A2780 cells transfected with p53 reporter, up to an 8 fold increase in the bioluminescent signal was noted depending on the dose and type of cytotoxic drug used (Figure 6.5). The induction of p53 demonstrated by bioluminescent reporter cell lines was confirmed with Western blotting to check for p53 induction upon treatment with similar doses of the drugs (Figure 6.4). The background bioluminescent signal noted in untreated bioluminescent reporters was very low and there was no evidence of p53 induction in untreated cells when assessed by western blotting. Clearly this would indicate that the increase (up to 8 fold) in bioluminescent signal is specifically due to the induction of p53. An ideal reporter would also require negative control, i.e. treatment which would not result in p53 induction. However there is no clear negative control for p53 (Dr Diane Crighton, Personal communication).

The p53 reporter described in these experiments give readout of the p53 induction that has been brought on by a variety of cytotoxic drugs, thereby indicating that this reporter would serve a suitable tool-box for evaluating the efficacy of drugs and molecular pathways through which the drug exerts their cytotoxic activity. Paclitaxel which exerts its anti-tumour activity by disrupting the mitotic spindle can also induce p53 in a cell dependent manner and the

results of these experiments are in keeping with such observation (Giannakakou, Robey et al. 2001).

Bioluminescent reporters have facilitated the drug development process and evaluation of a specific molecular pathway in tumourigenesis and serve as a pharmacodynamic marker of target activity. Unlike conventional Western blotting, use of reporter cell lines is less time consuming and simple. In addition, serial measurements and observer-independent quantification of target activation is possible with the bioluminescent reporters. Ubiquitin luciferase reporters were used to assess the function of proteasomes in animals and have enabled the preclinical evaluation of proteasome inhibitor, bortezomib. Luker and colleagues developed ubiquitin reporter by fusing luciferase to ubiquitin, which emitted bioluminescent signal upon treatment with proteasome inhibitor, bortezomib (Luker, Pica et al. 2003). Here they demonstrated that bioluminescent activity was noticed in mouse tumour models within 30 minutes after treatment with bortezomib and returned to baseline at 46 hours indicating rapid inhibition of proteasome. Similarly, the transcriptional activity of hypoxia inducible factor response elements (HIF-RE) can be monitored using luciferase reporters (Kung, Zabludoff et al. 2004). These studies indicate that the drug activity could be reliably monitored with the help of a robustly established luciferase reporter. Clearly the lenti-viral vector used for gene delivery in our experiments has resulted in stable transgene expression. Results from study with cells indicate that the p53 reporter developed with lentiviral vectors is sensitive to drug dose and should be suitable for animal studies.

6.5.3 Characterisation of p53 reporter in vivo

Xenografts of A2780 cells with the luciferase reporters (A2780pLentip53RELuc2) and empty vectors (A2780pLentiTATALuc2) were developed to characterise the p53 luciferase reporter *in vivo*. In contrast to the *in vitro* experiments where the untreated cells did not exhibit notable bioluminescent signal, there was significant bioluminescent signal even from the untreated xenografts (Figure 6.6A, left panel). This relatively high background bioluminescence could be due to the sensitivity of the reporter. The defective vasculature in tumours results in hypo-perfused area where the cells are exposed to hypoxic stress. It is well established that hypoxia induces p53 (Vousden and Ryan 2009) and this

underlying induction of p53 accounts for the high background bioluminescent signal. In contrast, cultured cells grown *in vitro* are adequately fed and well oxygenated and hence not under hypoxic stress that could induce p53 and hence the background bioluminescence was not high (Figure 6.5). Despite the background bioluminescent signal, as shown in figure 6.6, there was a 2.8 fold increase in bioluminescent signal in cisplatin-treated p53 luciferase xenografts compared with controls (untreated xenografts). This 2.8 fold increase in signal in the xenografts is lesser than the 8 fold increase noticed *in vitro* questioning the sensitivity of the reporter. The p53 luciferase reporter, however, is sensitive to p53 induction since the dose of cisplatin required to induce p53 in the *in vitro* experiments were closer to IC_{50} doses (Figure 6.5). This is in contrast to the PARP cleavage (Figure 3.5, chapter 3) which showed that doses as high as 5μM-25μM were required to induce PARP cleavage that could be monitored using Western blotting. The differential fold response between *in vitro* and *in vivo* experiments could be due to the heterogeneity of transfected A2780 cells, which result in the inevitable selection of a subpopulation of cells with variable degree of transgene expression. This also explains the challenges with establishing xenografts with transfected cells (Zeamari, Rumping et al. 2004). Gene transfer through lentiviral infection and selection of clones could potentially overcome this handicap and this could be considered in future.

The induction of p53 in the xenografts was also correlated with conventional immunohistochemistry. As shown in figure 6.7, there was induction of p53 in the untreated xenografts which corresponds to the background bioluminescent signal noted in reporter assays (Figure 6.6). This indicates that the background bioluminescent signal noted in untreated control is genuine and not artefactual. There was a demonstrable increase in p53 staining in the A2780 tumours treated with cisplatin compared with control (Figure 6.8). However this increase in p53 induction did not significantly differ between cisplatin and CB[7]cisplatin treated xenografts and the intensity and distribution of p53 staining were not dissimilar between these two groups (Figure 6.8 and 6.9). Various semi-quantitative and automated methods have been described to standardise the immunohistochemistry reporting. This includes H-scores and Allred score which essentially measure the intensity and reactivity of the cells and the percentage of cells which are stained (Walker 2006). Despite the guidelines to standardise

the procedures involved in immunohistochemical analysis there are still significant issues with sensitivity and specificity of this valuable technique (Hammond, Hayes et al. 2010). On the other hand, the bioluminescent signal emitted *in vivo* could be easily quantified and is independent of observer bias. Bioluminescent luciferase reporters allow sequential and repetitive measurement of the drug activity which is particularly useful in *in vivo* experiments.

6.6 Conclusion

The results of *in vitro* and *in vivo* experiments demonstrate that the p53 luciferase reporter enables repetitive analysis of p53 activity and could be used to investigate target hit activity in drug development process. Bioluminescence is a good tool for studies with cell lines. The bioluminescent p53 reporter works *in vivo* but is not sensitive enough and there is scope to improve the sensitivity *in vivo*.

7 General Discussion

The aims of this thesis, on the whole, have been achieved. Although this is not the first study of a drug delivery system for cisplatin the results demonstrate clearly that encapsulation of cisplatin increases the plasma and tumour concentration of platinum without an associated increase in toxicity. The delivery system is non-toxic, has no inherent anti-tumour activity and shows promise for further development. The lack of suitable tumour models for studies of drug delivery *in vivo* was addressed and biophotonic imaging is shown to allow estimation of growth and drug sensitivity of a disseminated model of human ovarian cancer. The results also demonstrate that biophotonic imaging can be used to monitor induction of p53 in real time *in vivo*.

The results have been discussed in detail in each chapter and only the main points will be discussed in the final chapter.

7.1 Cucurbituril encapsulated cisplatin

Many drug delivery systems show promising preclinical activity but fail to reproduce this activity when tested in patients. There are many reasons for this but as for any preclinical drug discovery programme the choice of model system for evaluation of activity is critical. Cucurbituril encapsulated cisplatin was, therefore, evaluated in a well characterised model of human ovarian cancer. The parental A2780 cell line has wild type p53 and is relatively sensitive to cisplatin. By contrast, the drug resistant derivative, A2780/cp70 shows loss of regulation of p53 and has lost a functional DNA mismatch repair pathway which is known to be associated with cisplatin resistance (Plumb, Strathdee et al. 2000). Both mechanisms of resistance are known to be relevant to patient tumours and the demonstration that CB[7]cisplatin can inhibit growth of the drug resistant tumour when grown *in vivo* as a xenograft suggests that the delivery system has potential for use in the clinic. Cucurbiturils are relatively small delivery systems (~ 1μm) and thus would not be expected to be trapped in the tumour as a result of the enhance permeability and retention properties of tumours (Maeda, Wu et al. 2000). There are also no suitable surface groups that could be implicated in tumour specific binding. Since the delivery system did not alter the activity of cisplatin *in vitro* it was proposed that the enhanced activity

was due to a change in plasma pharmacokinetics. There is no suitable method for the detection of cisplatin and breakdown products in biological samples so the highly sensitive inductively coupled plasma mass spectroscopy method was established and validated to study the pharmacokinetics of cisplatin. The results supported the hypothesis that encapsulation altered the plasma pharmacokinetics of cisplatin. This study has now been published (Plumb, Venugopal et al. 2012). However, the assay only measured elemental platinum so it was not possible to determine whether encapsulation did, indeed, protect the cisplatin from thiol degradation. It also gave no information on whether the cisplatin in the circulation in the mice was retained within the cucurbituril or was present as free drug. This problem could be addressed in further studies in which both cisplatin and cucurbituril are labelled in some way. The most obvious method would be to use a radioactive label since this is least likely to alter the properties of the two molecules.

7.1.1 Further development of the delivery system

Cucurbituril encapsulated cisplatin needs to be characterised further before it could be used for clinical evaluation. However, there is a clear proof of principle that this drug delivery system can circumvent cisplatin resistance and, the promising activity already demonstrated could be enhanced in a number of ways. One of the apparent advantages is an increased delivery to tumours but this is non-specific. Many groups have exploited the characteristics of tumour to target drugs specifically to tumours. Cucurbiturils do not have suitable groups on the surface to allow attachment of a targeting moiety. However, it has been proposed that cucurbiturils could be incorporated into liposomes or nanosomes which can be conjugated to a targeting molecule. Other ideas include incorporation of cucurbiturils into a hydrogel which could be implanted into the body to allow a sustained release of drug.

7.2 Biophotonic imaging

Studies of drug sensitivity *in vivo* in mice have been limited due to the lack of techniques to measure tumour growth. Subcutaneous xenografts can be measured by callipers and provided that the tumour has a rapid growth rate this allows assessment of growth inhibition as a result of drug treatment. One of the

most rewarding aspects of this work was the demonstration that biophotonic imaging could be used to measure tumour growth *in vivo* in mice. Although it was known that the technique was very good at detecting light within the body of mice and could thus show the location of tumour cells it was not clear that the technique was sufficiently sensitive to allow accurate measurement of the viable tumour mass. However, these results show that provided the luciferin substrate is administered by the subcutaneous route and that measurements are taken within a fixed time period after injection it is possible to measure tumour burden. Interestingly, subcutaneous administration of luciferin is now the route recommended by the manufacturers of the IVIS bioluminescence equipment. One of the clear advantages of biophotonic imaging is that the bioluminescent signal is not affected by the person taking the measurement. Although there can be differences in the way the image is analysed the information is stored and can be re-analysed at any time.

7.3 A2780-Rab25 model of disseminated human ovarian cancer

Once it was clear that biophotonic imaging was suitable for measurement of tumour growth *in vivo* it was possible to evaluate the activity of encapsulated cisplatin in the A2780-Rab25 model of disseminated human ovarian cancer. This was an ideal model for these studies since it would extend the observations obtained with the subcutaneous xenografts. It was known that expression of Rab25 in A2780 reduced their sensitivity to induction of apoptosis under stress but these results were the first to demonstrate that Rab25 expression was associated with a reduced sensitivity to cisplatin. Although the resistance was only four fold this was sufficient to reduce the cisplatin sensitivity of A2780 when grown as a disseminated tumour in the peritoneal cavity of mice. It was therefore encouraging to observe that encapsulated cisplatin retained activity in the A2780-Rab25 model. The mechanism of resistance clearly differs from that of A2780/cp70 and the fact that activity is retained supports the proposed pharmacokinetic basis for the enhanced activity.

7.4 The p53 reporter

The ability to image drug activity *in vivo* is clearly an advantage in studies of drug development. This is now possible through techniques such as PET and MRI imaging but these techniques are highly specialised and not generally available. The introduction of biophotonic imaging *in vivo* raises the possibility that the reporter assays that are now widely used in studies with tumour cell lines *in vitro* could be translated to studies *in vivo*. Induction of p53 expression is an early response to cytotoxic drug activity and thus provides a suitable marker of drug activity. Expression in A2780 of a plasmid containing the p53 TRE linked to luciferase allowed the measurement of p53 induction by bioluminescence. Since the signal could be quantified by the simple addition of luciferin to the cells and capture of the image with the IVIS-50 the technique allowed assessment of multiple treatments within a single experiment. A clear advantage when compared with measurement by Western blotting. Preliminary studies showed that the response to p53 could also be detected *in vivo*. Time constraints did not allow further evaluation of the p53 reporter *in vivo*. However, in subsequent work a colleague has shown a clear dose response to cisplatin *in vivo* when the plasmid was expressed in the A2780-Rab25 cells (Dr Gomez-Roman personal communication).

7.5 Conclusion

These results have identified a novel drug delivery system that could form the basis of an effective system for improvement of the clinical activity of cisplatin. The results obtained for the use of biophotonic imaging clearly support the value of this technology to studies of cytotoxic drug activity *in vivo*. They also demonstrate the importance of such developments in technology since they allow the development of more complex mouse models for the study of drug activity *in vivo*.

Appendix 1 Buffers, solution and media

Tris Buffered Saline (TBS) 10X:

Tris Base	24.22g
NaCl	180g
Distilled water	1800mL

Stirred until dissolved, adjusted to pH 7.4 with HCl and made up to volume of 2 litres with ultrahigh pure deionised water

25% Tween-20:

Distilled water	75mL
Tween 20	25mL

Mix well and store in the dark room at room temperature

TBS-T:

Dilute 200mL TBS (10X) in ultrahigh pure deionised water to make up to 2 litres of 1X concentration and add 4mL of 20% Tween-20

3M Sodium Hydroxide:

Sodium hydroxide tablets	1g

Dissolve in 8.3mL distilled water

Phosphate Buffer Saline (pH 7.4):

NaCl	8g
KCl	0.2g
KH_2PO_4	0.2g
$Na_2HPO_4.2H_20$	1.44g
$MgCl_2.6H_2O$	2.03g

Made up to volume of 1 litre with ultrahigh pure deionised water

Cell Lysis Buffer:

MOPS (20mM)
EGTA (2mM)
EDTA (5mM)
Sodium fluoride (30mM)
Glycerophosphate (40 mM)
Sodium pyrophosphate (20mM)
Sodium orthovanadate (1mM)
Triton-X 100

Phenylmethyl sulfonyl fluoride (1mM)

Adjusted to pH 7.2 with 1N NaOH and made up in 100mL ultrapure water.
Add two tablets of Protease inhibitor (COMPLETE protein lysis kit)

EDTA 100mM:

EDTA	3.7g
NaOH	2.0g
Ultra-pure water	80mL

Adjust to pH 7.4 with HCl and make up to 100mLwith ultra-pure water

NaOH 1N:

NaOH	2g

Made up to volume of 100mL distilled water

Running Buffer:

50mL NuPAGE MOPS SDS running buffer (20x)
950mL of ultrahigh pure deionised water

Transfer Buffer:

NuPAGE transfer buffer (20x)	50mL
Methanol	200mL
Ultrahigh pure deionised water	750mL

Washing Buffer:

25% Tween-20	2mL
Tris Buffered Saline (10x)	100mL
Ultrahigh pure deionised water	900mL

Blocking buffer:

Marvel mild powder	5g
25% Tween-20	0.2mL
Tris Buffered Saline (10x)	10mL

Made up to 100mL with ultrahigh pure deionised water

Sorensen's Glycine Buffer:

Glycine (0.1M)	7.5g
NaCl (0.1M)	5.85g

Equilibrated to pH10.5 with 0.1M NaOH and made up to 1 litre with ultrahigh pure deionised water

RPMI 1640 Medium:

RPMI 1640	500ml
L-Glutamine	5ml
1M Sodium hydroxide	0.8mL
Penicillin/streptomycin 100mg/mL (optional)	2.5mL
G418 1g/mL (optional)	5mL
Blasticidin 5mg/mL (optional)	250µL

DMEM medium:

DMEM medium	500mL
L-Glutamine	5mL
1M Sodium hydroxide	0.8mL
Penicillin/streptomycin 100mg/mL (optional)	2.5mL

Trypsin solution:

Trypsin 2.5% solution	10mL
PBS	90mL
EDTA	1mM

MTT solution:

MTT	1gm
Sterile PBS	200mL

Filtered through a stericup vacuum derived pre-sterilised filtration system and stored at 4ºC in a dark room

1.5% Agarose gel

1 X TAE buffer	100mL
Agarose	1.5gm

Bring the solution to boil by heating in microwave for 1-2 minutes. Cool it to 50ºC and add two drops of ethidium bromide solution

Appendix 2 Suppliers

Amersham biosciences
Amersham place
Little Chalfont, HP79NA
United Kingdom
www.amersham.com

Becton Dickinson
Between Towns Road
Cambridge, CB4 9ZR
United Kingdom
www.bd.com

Bibby Sterlin
Barloworld Scientific Ltd
Beacon Road
Stone, ST15 0SA
United Kingdom
www.barloworld-scientific.com

Bio Rad Laboratories
Bio Rad House
Maryland Avenue
Hemel Hempstead, HP2 7DX
United Kingdom
www.bio-rad.com

Braun B Biotech
Thorncliffe Park
Sheffield, S35 2PW
United Kingdom
www.sartorius-bbi-systems.com

Charles River UK
Manston Road
Margate, CT9 4LT
United Kingdom
www.criver.com

Corning International
Quantum House, Maryland Avenue
Hemel Hempstead, HP2 7DF
United Kingdom
www.corning.com

Drummond Scientific
Alpha Laboratories
Eastleigh, SO5 4NU
United Kingdom
www.drummondsci.com

Elkay Laboratories Ltd
Unit E, Lutyens Industrial Centre
Bilton Road, Basingstoke, RG24 8LJ
United Kingdom
www.elkay-uk.co.uk

Eppendorf
Endurance House, Chivers Way
Oxford, OX4 3LY
United Kingdom
www.eppendorf.com

Fisher Scientific UK
Bishop Meadow Road
Loughborough, LE11 5RG
United Kingdom
www.fisher.co.uk

Fuji Photo Film Ltd
125, Finchley Road
London, NW3 6JH
United Kingdom
www.fujifilm.co.uk

Grant Instruments
29 Station Road
Royston, SG8 6PZ
United Kingdom
www.grant-scientific.com

Inorganic Ventures Ltd
300 Technology Drive
Christiansburg, VA 24073
USA
www.inorganicventures.com

Invitrogen
Inchinnan Business Park
Inchinnan, PA4 9RF
United Kingdom
www.invitrogen.com

Millipore
The Boulevard, Blackmoor Lane
Watford, WD1 8YW
United Kingdom
www.millipore.com

Molecular Devices
135, Wharfedale Road
Workingham, RG41 5RB
United Kingdom
www.moleculardevices.com

NanoDrop products
3411 Silverside Road
Wilmington, DE 19810
USA
www.nanodrop.com

Novocastra
Vision Biosytems, Benton Lane
Newcastle, NE12 8EW
United Kingdom
www.novocastra.co.uk

Parkin Elmer
Chalfont Road
Beaconsfield, HP9 2FX
United Kingdom
www.parkinelmer.com

Promega
Delta House, Enterprise Road
Southampton, SO1 7NS
United Kingdom
www.promega.com

Qiagen
Qiagen House, Fleming Way
Crawley, RH10 9NQ
United Kingdom
www.qiagen.com

Roche Diagnositics
Bell Lane
Lewes, BN71LG
United Kingdom
www.roche-diagnostics.com

Scharfe Systems
Kramerstrasse 22
Reutingen, D72764
Germany
www.casy-technology.com

Sigma
The Old Brickyard, New Road
Gillingham, SP8 4XT
United Kingdom
www.sigmaaldrich.com

Surgipath
Venture Park, Stirling Way
Peterborough, PE3 8YD
United Kingdom
www.surgipath.com

Thermo Electron
Stortford Hall Park
Bishops Stortford, CM23 5GZ
www.thermo.com

Thermo Life Sciences
Unit 5, The Ringway Centre
Basingstoke, RG21 6YH
United Kingdom
www.thermo.com

Vector Laboratories
Accent Park, Bakenwell Road
Peterborough, PE2 6XS
United Kingdom
www.vectorlabs.com

Whatman International
James Whatman Way
Maidstone, ME14 2LE
United Kingdom
www.whatman.com

Appendix 3 Antibodies and drugs

Antibody	Dilution	Supplier
Anti-actin	1/1000	BD Biosciences
Anti-p53	1/1000	Leica Microsystems
Anti-PARP	1/1000	BD Biosciences
Anti-MLH	1/5000	BD Biosciences
Peroxidase linked anti-mouse IgG	1/10,000	Amersham
Peroxidase linked anti-rabbit IgG	1/10,000	Amersham

Table A.1: Primary and secondary antibodies. The dilution used and suppliers are given.

Drug	Vehicle	Supplier
Cisplatin	DMSO	Sigma
Cisplatin (for *in vivo* use)	Normal saline	Donation from Beatson Pharmacy
Paclitaxel	Sterile water	Sigma
Doxorubicin	Sterile water	Sigma

Table A.2: Drugs and vehicle

List of References

Adam, R., D. A. Wicherts, et al. (2009). "Patients With Initially Unresectable Colorectal Liver Metastases: Is There a Possibility of Cure?" Journal of Clinical Oncology **27**(11): 1829-1835.

Andrews, P. A., S. Velury, et al. (1988). "cis-Diamminedichloroplatinum(II) accumulation in sensitive and resistant human ovarian carcinoma cells." Cancer Res **48**(1): 68-73.

Anthoney, D. A., A. J. McIlwrath, et al. (1996). "Microsatellite instability, apoptosis, and loss of p53 function in drug-resistant tumor cells." Cancer Res **56**(6): 1374-1381.

Ardizzoni, A., L. Boni, et al. (2007). "Cisplatin- versus carboplatin-based chemotherapy in first-line treatment of advanced non-small-cell lung cancer: an individual patient data meta-analysis." J Natl Cancer Inst **99**(11): 847-857.

Armstrong, D. K., B. Bundy, et al. (2006). "Intraperitoneal Cisplatin and Paclitaxel in Ovarian Cancer." New England Journal of Medicine **354**(1): 34-43.

Bali, M. S., D. P. Buck, et al. (2006). "Cucurbituril binding of trans-[{PtCl(NH3)2}2([small micro]-NH2(CH2)8NH2)]2+ and the effect on the reaction with cysteine." Dalton Transactions(45): 5337-5344.

Bangham, A. D., M. M. Standish, et al. (1965). "Diffusion of univalent ions across the lamellae of swollen phospholipids." Journal of Molecular Biology **13**(1): 238-IN227.

Batist, G., G. Ramakrishnan, et al. (2001). "Reduced Cardiotoxicity and Preserved Antitumor Efficacy of Liposome-Encapsulated Doxorubicin and Cyclophosphamide Compared With Conventional Doxorubicin and Cyclophosphamide in a Randomized, Multicenter Trial of Metastatic Breast Cancer." Journal of Clinical Oncology **19**(5): 1444-1454.

Black, P. C., A. Shetty, et al. (2010). "Validating bladder cancer xenograft bioluminescence with magnetic resonance imaging: the significance of hypoxia and necrosis." BJU Int **106**(11): 1799-1804.

Bogdanov Jr, A. and R. Weissleder (1998). "The development of in vivo imaging systems to study gene expression." Trends in Biotechnology **16**(1): 5-10.

Bonadonna, G., E. Brusamolino, et al. (1976). "Combination Chemotherapy as an Adjuvant Treatment in Operable Breast Cancer." New England Journal of Medicine **294**(8): 405-410.

Boulikas, T. (2004). "Low toxicity and anticancer activity of a novel liposomal cisplatin (Lipoplatin) in mouse xenografts." Oncol Rep **12**(1): 3-12.

Boulikas, T. (2009). "Clinical overview on Lipoplatin™: a successful liposomal formulation of cisplatin." Expert Opinion on Investigational Drugs **18**(8): 1197-1218.

Bradford, M. M. (1976). "A rapid and sensitive method for the quantitation of microgram quantities of protein utilizing the principle of protein-dye binding." Analytical Biochemistry **72**(1-2): 248-254.

Broeders, M., S. Moss, et al. (2012). "The impact of mammographic screening on breast cancer mortality in Europe: a review of observational studies." Journal of Medical Screening **19**(suppl 1): 14-25.

Brouwers, E. E. M., M. Tibben, et al. (2008). "The application of inductively coupled plasma mass spectrometry in clinical pharmacological oncology research." Mass Spectrometry Reviews **27**(2): 67-100.

Brown, R., C. Clugston, et al. (1993). "Increased accumulation of p53 protein in cisplatin-resistant ovarian cell lines." Int J Cancer **55**(4): 678-684.

Brown, R., G. L. Hirst, et al. (1997). "hMLH1 expression and cellular responses of ovarian tumour cells to treatment with cytotoxic anticancer agents." Oncogene **15**(1): 45-52.

Brown, S. D., P. Nativo, et al. (2010). "Gold Nanoparticles for the Improved Anticancer Drug Delivery of the Active Component of Oxaliplatin." Journal of the American Chemical Society **132**(13): 4678-4684.

Brozovic, A., A. Ambriović-Ristov, et al. (2010). "The relationship between cisplatin-induced reactive oxygen species, glutathione, and BCL-2 and resistance to cisplatin." Critical Reviews in Toxicology **40**(4): 347-359.

Burger, R. A., M. F. Brady, et al. (2011). "Incorporation of Bevacizumab in the Primary Treatment of Ovarian Cancer." New England Journal of Medicine **365**(26): 2473-2483.

Buys, S. S., E. Partridge, et al. (2011). "Effect of screening on ovarian cancer mortality: the Prostate, Lung, Colorectal and Ovarian (PLCO) Cancer Screening Randomized Controlled Trial." JAMA **305**(22): 2295-2303.

Calabro, F., P. Albers, et al. (2012). "The contemporary role of chemotherapy for advanced testis cancer: a systematic review of the literature." Eur Urol **61**(6): 1212-1221.

Calvert, A. H., D. R. Newell, et al. (1989). "Carboplatin dosage: prospective evaluation of a simple formula based on renal function." Journal of Clinical Oncology **7**(11): 1748-1756.

Campone, M., J. M. Rademaker-Lakhai, et al. (2007). "Phase I and pharmacokinetic trial of AP5346, a DACH-platinum-polymer conjugate, administered weekly for three out of every 4 weeks to advanced solid tumor patients." Cancer Chemother Pharmacol **60**(4): 523-533.

CancerResearchUK (2012). CancerResearchUK cancer statistics**:** Cancer Research UK/statistics.

Caponigro, G. and W. R. Sellers (2011). "Advances in the preclinical testing of cancer therapeutic hypotheses." Nat Rev Drug Discov **10**(3): 179-187.

Cassidy, J., R. Duncan, et al. (1989). "Activity of N-(2-hydroxypropyl)methacrylamide copolymers containing daunomycin against a rat tumour model." Biochemical Pharmacology **38**(6): 875-879.

Caswell, P. T., H. J. Spence, et al. (2007). "Rab25 associates with alpha5beta1 integrin to promote invasive migration in 3D microenvironments." Dev Cell **13**(4): 496-510.

Ceelen, W. P. and M. F. Flessner (2010). "Intraperitoneal therapy for peritoneal tumors: biophysics and clinical evidence." Nat Rev Clin Oncol **7**(2): 108-115.

Chabner, B. A. and T. G. Roberts (2005). "Chemotherapy and the war on cancer." Nat Rev Cancer **5**(1): 65-72.

Chen, H., M. A. Biel, et al. (1997). "Tissue-specific expression of human achaete-scute homologue-1 in neuroendocrine tumors: transcriptional regulation by dual inhibitory regions." Cell Growth Differ **8**(6): 677-686.

Chenevert, T. L., P. E. McKeever, et al. (1997). "Monitoring early response of experimental brain tumors to therapy using diffusion magnetic resonance imaging." Clin Cancer Res **3**(9): 1457-1466.

Cheng, K. W., J. P. Lahad, et al. (2004). "The RAB25 small GTPase determines aggressiveness of ovarian and breast cancers." Nat Med **10**(11): 1251-1256.

Cho, K., X. Wang, et al. (2008). "Therapeutic Nanoparticles for Drug Delivery in Cancer." Clinical Cancer Research **14**(5): 1310-1316.

Choi, H. S., W. Liu, et al. (2007). "Renal clearance of quantum dots." Nat Biotechnol **25**(10): 1165-1170.

Choy, H., C. Park, et al. (2008). "Current status and future prospects for satraplatin, an oral platinum analogue." Clin Cancer Res **14**(6): 1633-1638.

Cockrell, A. and T. Kafri (2007). "Gene delivery by lentivirus vectors." Molecular Biotechnology **36**(3): 184-204.

Coleman, M. P., M. Quaresma, et al. (2008). "Cancer survival in five continents: a worldwide population-based study (CONCORD)." The Lancet Oncology **9**(8): 730-756.

Connolly, D. C. and H. H. Hensley (2009). "Xenograft and Transgenic Mouse Models of Epithelial Ovarian Cancer and Non Invasive Imaging Modalities to Monitor Ovarian Tumor Growth In situ -Applications in Evaluating Novel Therapeutic Agents." Curr Protoc Pharmacol **45**: 14 12 11-14 12 26.

Contag, C. H., P. R. Contag, et al. (1995). "Photonic detection of bacterial pathogens in living hosts." Mol Microbiol **18**(4): 593-603.

Contag, P. R., I. N. Olomu, et al. (1998). "Bioluminescent indicators in living mammals." Nat Med **4**(2): 245-247.

Contero, A., E. Richer, et al. (2009). "High-throughput quantitative bioluminescence imaging for assessing tumor burden." Methods Mol Biol **574**: 37-45.

Cornelison, T. L. and E. Reed (1993). "Nephrotoxicity and Hydration Management for Cisplatin, Carboplatin, and Ormaplatin." Gynecologic Oncology **50**(2): 147-158.

Cunningham, D., W. H. Allum, et al. (2006). "Perioperative Chemotherapy versus Surgery Alone for Resectable Gastroesophageal Cancer." New England Journal of Medicine **355**(1): 11-20.

Danhier, F., O. Feron, et al. (2010). "To exploit the tumor microenvironment: Passive and active tumor targeting of nanocarriers for anti-cancer drug delivery." Journal of Controlled Release **148**(2): 135-146.

Day, A., A. P. Arnold, et al. (2001). "Controlling Factors in the Synthesis of Cucurbituril and Its Homologues." The Journal of Organic Chemistry **66**(24): 8094-8100.

DeConti, R. C., B. R. Toftness, et al. (1973). "Clinical and Pharmacological Studies with cis-Diamminedichloroplatinum(II)." Cancer Research **33**(6): 1310-1315.

DeVita, V. T. and E. Chu (2008). "A History of Cancer Chemotherapy." Cancer Research **68**(21): 8643-8653.

Devita, V. T., A. A. Serpick, et al. (1970). "Combination Chemotherapy in the Treatment of Advanced Hodgkin's Disease." Annals of Internal Medicine **73**(6): 881-895.

DiMasi, J. A. and H. G. Grabowski (2007). "Economics of New Oncology Drug Development." Journal of Clinical Oncology **25**(2): 209-216.

Dinulescu, D. M., T. A. Ince, et al. (2005). "Role of K-ras and Pten in the development of mouse models of endometriosis and endometrioid ovarian cancer." Nature Medicine **11**(1): 63-70.

Duncan, R. (2006). "Polymer conjugates as anticancer nanomedicines." Nat Rev Cancer **6**(9): 688-701.

E. E. M. Brouwers, M. M. T., H. Rosing, M. J. X. Hillebrand ,M. Joerger ,J. H. M. Schellens and J. H. Beijnen (2006). "Sensitive inductively coupled plasma mass spectrometry assay for the determination of platinum originating from cisplatin, carboplatin, and oxaliplatin in human plasma ultrafiltrate." Journal of Mass Spectrometry **41**(9): 1186-1194.

EBCTCG (2005). "Effects of chemotherapy and hormonal therapy for early breast cancer on recurrence and 15-year survival: an overview of the randomised trials." The Lancet **365**(9472): 1687-1717.

Edinger, M., T. J. Sweeney, et al. (1999). "Noninvasive assessment of tumor cell proliferation in animal models." Neoplasia **1**(4): 303-310.

Einhorn, L. H. (2002). "Curing metastatic testicular cancer." Proceedings of the National Academy of Sciences **99**(7): 4592-4595.

Engstrom, P. F., J. P. Arnoletti, et al. (2009). "Colon Cancer." Journal of the National Comprehensive Cancer Network **7**(8): 778-831.

Erdlenbruch, B., M. Nier, et al. (2001). "Pharmacokinetics of cisplatin and relation to nephrotoxicity in paediatric patients." Eur J Clin Pharmacol **57**(5): 393-402.

Farber, S., L. K. Diamond, et al. (1948). "Temporary Remissions in Acute Leukemia in Children Produced by Folic Acid Antagonist, 4-Aminopteroyl-Glutamic Acid (Aminopterin)." New England Journal of Medicine **238**(23): 787-793.

Ferlay, J., H.-R. Shin, et al. (2010). "Estimates of worldwide burden of cancer in 2008: GLOBOCAN 2008." International Journal of Cancer **127**(12): 2893-2917.

Freeman, W. A., W. L. Mock, et al. (1981). "Cucurbituril." Journal of the American Chemical Society **103**(24): 7367-7368.

Frese, K. K. and D. A. Tuveson (2007). "Maximizing mouse cancer models." Nat Rev Cancer **7**(9): 654-658.

Gabizon, A., H. Shmeeda, et al. (2003). "Pharmacokinetics of Pegylated Liposomal Doxorubicin: Review of Animal and Human Studies." Clinical Pharmacokinetics **42**(5): 419-436.

Galluzzi, L., L. Senovilla, et al. (2012). "Molecular mechanisms of cisplatin resistance." Oncogene **31**(15): 1869-1883.

Galons, J. P., M. I. Altbach, et al. (1999). "Early increases in breast tumor xenograft water mobility in response to paclitaxel therapy detected by non-invasive diffusion magnetic resonance imaging." Neoplasia **1**(2): 113-117.

Gambhir, S. S., J. R. Barrio, et al. (1999). "Imaging gene expression: principles and assays." J Nucl Cardiol **6**(2): 219-233.

Gambhir, S. S., J. R. Barrio, et al. (1999). "Imaging adenoviral-directed reporter gene expression in living animals with positron emission tomography." Proceedings of the National Academy of Sciences **96**(5): 2333-2338.

Gamelin, E., P. Allain, et al. (1995). "Long-term pharmacokinetic behavior of platinum after cisplatin administration." Cancer Chemotherapy and Pharmacology **37**(1): 97-102.

Ghezzi, A., M. Aceto, et al. (2004). "Uptake of antitumor platinum(II)-complexes by cancer cells, assayed by inductively coupled plasma mass spectrometry (ICP-MS)." Journal of Inorganic Biochemistry **98**(1): 73-78.

Gianasi, E., M. Wasil, et al. (1999). "HPMA copolymer platinates as novel antitumour agents: in vitro properties, pharmacokinetics and antitumour activity in vivo." European Journal of Cancer **35**(6): 994-1002.

Giannakakou, P., R. Robey, et al. (2001). "Low concentrations of paclitaxel induce cell type-dependent p53, p21 and G1/G2 arrest instead of mitotic arrest: molecular determinants of paclitaxel-induced cytotoxicity." Oncogene **20**(29): 3806-3813.

Gietema, J. A., M. T. Meinardi, et al. (2000). "Circulating plasma platinum more than 10 years after cisplatin treatment for testicular cancer." The Lancet **355**(9209): 1075-1076.

Gifford, G., J. Paul, et al. (2004). "The Acquisition of hMLH1 Methylation in Plasma DNA after Chemotherapy Predicts Poor Survival for Ovarian Cancer Patients." Clinical Cancer Research **10**(13): 4420-4426.

Gilman, A. and F. S. Philips (1946). "The Biological Actions and Therapeutic Applications of the B-Chloroethyl Amines and Sulfides." Science **103**(2675): 409-436.

Godwin, A. K., A. Meister, et al. (1992). "High resistance to cisplatin in human ovarian cancer cell lines is associated with marked increase of glutathione synthesis." Proceedings of the National Academy of Sciences **89**(7): 3070-3074.

Gordon, A. N., J. T. Fleagle, et al. (2001). "Recurrent Epithelial Ovarian Carcinoma: A Randomized Phase III Study of Pegylated Liposomal Doxorubicin Versus Topotecan." Journal of Clinical Oncology **19**(14): 3312-3322.

Gradishar, W. J., S. Tjulandin, et al. (2005). "Phase III Trial of Nanoparticle Albumin-Bound Paclitaxel Compared With Polyethylated Castor Oil–Based Paclitaxel in Women With Breast Cancer." Journal of Clinical Oncology **23**(31): 7794-7803.

Graham, M. A., G. F. Lockwood, et al. (2000). "Clinical Pharmacokinetics of Oxaliplatin: A Critical Review." Clinical Cancer Research **6**(4): 1205-1218.

Guarneri, V., F. Piacentini, et al. (2010). "Achievements and unmet needs in the management of advanced ovarian cancer." Gynecologic Oncology **117**(2): 152-158.

Hammond, M. E. H., D. F. Hayes, et al. (2010). "American Society of Clinical Oncology/College of American Pathologists Guideline Recommendations for Immunohistochemical Testing of Estrogen and Progesterone Receptors in Breast Cancer." Journal of Clinical Oncology **28**(16): 2784-2795.

Hanahan, D. and Robert A. Weinberg (2011). "Hallmarks of Cancer: The Next Generation." Cell **144**(5): 646-674.

Harrap, K. R. (1985). "Preclinical studies identifying carboplatin as a viable cisplatin alternative." Cancer Treatment Reviews **12, Supplement A**(0): 21-33.

Hartmann, J. T. and H.-P. Lipp (2003). "Toxicity of platinum compounds." Expert Opinion on Pharmacotherapy **4**(6): 889-901.

Hartmann, L. C., G. L. Keeney, et al. (2007). "Folate receptor overexpression is associated with poor outcome in breast cancer." International Journal of Cancer **121**(5): 938-942.

Hastings, J. W. (1996). "Chemistries and colors of bioluminescent reactions: a review." Gene **173**(1 Spec No): 5-11.

Hennessy, B. T., R. L. Coleman, et al. (2009). "Ovarian cancer." The Lancet **374**(9698): 1371-1382.

Hensley, H., B. A. Quinn, et al. (2007). "Magnetic resonance imaging for detection and determination of tumor volume in a genetically engineered mouse model of ovarian cancer." Cancer Biology & Therapy **6**(11): 1717-1725.

Hesketh, P. J., S. M. Grunberg, et al. (2003). "The Oral Neurokinin-1 Antagonist Aprepitant for the Prevention of Chemotherapy-Induced Nausea and Vomiting: A Multinational, Randomized, Double-Blind, Placebo-Controlled Trial in Patients Receiving High-Dose Cisplatin—The Aprepitant Protocol 052 Study Group." Journal of Clinical Oncology **21**(22): 4112-4119.

Hettiarachchi, G., D. Nguyen, et al. (2010). "Toxicology and Drug Delivery by Cucurbit[n]uril Type Molecular Containers." PLoS ONE **5**(5): e10514.

Hofheinz, R.-D., S. U. Gnad-Vogt, et al. (2005). "Liposomal encapsulated anti-cancer drugs." Anti-Cancer Drugs **16**(7): 691-707.

Holzer, A. K., G. H. Manorek, et al. (2006). "Contribution of the major copper influx transporter CTR1 to the cellular accumulation of cisplatin, carboplatin, and oxaliplatin." Mol Pharmacol **70**(4): 1390-1394.

Hotta, K., K. Matsuo, et al. (2004). "Meta-analysis of randomized clinical trials comparing Cisplatin to Carboplatin in patients with advanced non-small-cell lung cancer." J Clin Oncol **22**(19): 3852-3859.

Howard, M. D., M. Jay, et al. (2008). "PEGylation of Nanocarrier Drug Delivery Systems: State of the Art." Journal of Biomedical Nanotechnology **4**(2): 133-148.

Huang, J., X. Hu, et al. (2006). "The application of inductively coupled plasma mass spectrometry in pharmaceutical and biomedical analysis." Journal of Pharmaceutical and Biomedical Analysis **40**(2): 227-234.

Hurvitz, S. A., L. Dirix, et al. (2013). "Phase II Randomized Study of Trastuzumab Emtansine Versus Trastuzumab Plus Docetaxel in Patients With Human Epidermal Growth Factor Receptor 2-Positive Metastatic Breast Cancer." J Clin Oncol.

Ibrahim, A., S. Hirschfeld, et al. (2004). "FDA Drug Approval Summaries: Oxaliplatin." The Oncologist **9**(1): 8-12.

Ibrahim, N. K., N. Desai, et al. (2002). "Phase I and Pharmacokinetic Study of ABI-007, a Cremophor-free, Protein-stabilized, Nanoparticle Formulation of Paclitaxel." Clinical Cancer Research **8**(5): 1038-1044.

Ingersoll, S. B., P. Yue, et al. (2009). "Molecular characterization of highly tumorigenic cell lines used in a xenograph model to investigate cellular therapy for the treatment of refractory ovarian cancer." Journal of Clinical Oncology **27**(15): -.

Inoue, Y., S. Kiryu, et al. (2009). "Comparison of subcutaneous and intraperitoneal injection of d-luciferin for in vivo bioluminescence imaging." European Journal of Nuclear Medicine and Molecular Imaging **36**(5): 771-779.

Ishida, S., J. Lee, et al. (2002). "Uptake of the anticancer drug cisplatin mediated by the copper transporter Ctr1 in yeast and mammals." Proceedings of the National Academy of Sciences **99**(22): 14298-14302.

Jacobs, A., M. Dubrovin, et al. (1999). "Functional coexpression of HSV-1 thymidine kinase and green fluorescent protein: implications for noninvasive imaging of transgene expression." Neoplasia **1**(2): 154-161.

Jamieson, E. R. and S. J. Lippard (1999). "Structure, Recognition, and Processing of Cisplatin−DNA Adducts." Chemical Reviews **99**(9): 2467-2498.

Jandial, D. D., K. Messer, et al. (2009). "Tumor platinum concentration following intraperitoneal administration of cisplatin versus carboplatin in an ovarian cancer model." Gynecologic Oncology **115**(3): 362-366.

Jason, L., M. Pritam, et al. (2005). "The Cucurbit[n]uril Family." Angewandte Chemie International Edition **44**(31): 4844-4870.

Jehn, C. F., T. Boulikas, et al. (2007). "Pharmacokinetics of Liposomal Cisplatin (Lipoplatin) in Combination with 5-FU in Patients with Advanced Head and Neck Cancer: First Results of a Phase III Study." Anticancer Research **27**(1A): 471-475.

Jensen, M. M., J. T. Jorgensen, et al. (2008). "Tumor volume in subcutaneous mouse xenografts measured by microCT is more accurate and reproducible than determined by 18F-FDG-microPET or external caliper." BMC Med Imaging **8**: 16.

Jin Jeon, Y., S.-Y. Kim, et al. (2005). "Novel molecular drug carrier: encapsulation of oxaliplatin in cucurbit[7]uril and its effects on stability and reactivity of the drug." Organic & Biomolecular Chemistry **3**(11): 2122-2125.

Johnsson, A., C. Olsson, et al. (1995). "Pharmacokinetics and tissue distribution of cisplatin in nude mice: platinum levels and cisplatin-DNA adducts." Cancer Chemotherapy and Pharmacology **37**(1): 23-31.

Jones, R. H. and P. A. Vasey (2003). "Part I: Testicular cancer—management of early disease." The Lancet Oncology **4**(12): 730-737.

Kang, J. H. and J. K. Chung (2008). "Molecular-genetic imaging based on reporter gene expression." J Nucl Med **49 Suppl 2**: 164S-179S.

Kelland, L. (2007). "The resurgence of platinum-based cancer chemotherapy." Nat Rev Cancer **7**(8): 573-584.

Kemp, S., N. J. Wheate, et al. (2007). "The Host-Guest Chemistry of Proflavine with Cucurbit[6,7,8]urils." Supramolecular Chemistry **19**(7): 475-484.

Kemp, S., N. J. Wheate, et al. (2007). "Encapsulation of platinum(II)-based DNA intercalators within cucurbit[6,7,8]urils." J. Biol. Inorg. Chem. **12**: 969-979.

Kennedy, A. R., A. J. Florence, et al. (2009). "A chemical preformulation study of a host-guest complex of cucurbit[7]uril and a multinuclear platinum agent for enhanced anticancer drug delivery." Dalton Transactions(37): 7695-7700.

Kim, E. S., C. Lu, et al. (2001). "A phase II study of STEALTH cisplatin (SPI-77) in patients with advanced non-small cell lung cancer." Lung Cancer **34**(3): 427-432.

Kim, J., I.-S. Jung, et al. (2000). "New Cucurbituril Homologues: Syntheses, Isolation, Characterization, and X-ray Crystal Structures of Cucurbit[n]uril (n = 5, 7, and 8)." Journal of the American Chemical Society **122**(3): 540-541.

Kim, K., N. Selvapalam, et al. (2007). "Functionalized cucurbiturils and their applications." Chemical Society Reviews **36**(2): 267-279.

Kim, M. P., D. B. Evans, et al. (2009). "Generation of orthotopic and heterotopic human pancreatic cancer xenografts in immunodeficient mice." Nat. Protocols **4**(11): 1670-1680.

Kimbrel, E. A., T. N. Davis, et al. (2009). "In vivo pharmacodynamic imaging of proteasome inhibition." Mol Imaging **8**(3): 140-147.

Kirkpatrick, G. J., J. A. Plumb, et al. (2011). "Evaluation of anionic half generation 3.5–6.5 poly(amidoamine) dendrimers as delivery vehicles for the active component of the anticancer drug cisplatin." Journal of Inorganic Biochemistry **105**(9): 1115-1122.

Konstantinopoulos Pa, A. C. S. (2012). "Management of ovarian cancer: A 75-year-old woman who has completed treatment." JAMA: The Journal of the American Medical Association **307**(13): 1420-1429.

Krop, I. E., P. LoRusso, et al. (2012). "A phase II study of trastuzumab emtansine in patients with human epidermal growth factor receptor 2-positive metastatic breast cancer who were previously treated with trastuzumab, lapatinib, an anthracycline, a taxane, and capecitabine." J Clin Oncol **30**(26): 3234-3241.

Kung, A. L. (2007). "Practices and pitfalls of mouse cancer models in drug discovery." Adv Cancer Res **96**: 191-212.

Kung, A. L., S. D. Zabludoff, et al. (2004). "Small molecule blockade of transcriptional coactivation of the hypoxia-inducible factor pathway." Cancer Cell **6**(1): 33-43.

Ledermann, J. A. and R. S. Kristeleit (2010). "Optimal treatment for relapsing ovarian cancer." Ann Oncol **21 Suppl 7**: vii218-222.

Ledermann, J. A. and F. A. Raja (2011). "Clinical trials and decision-making strategies for optimal treatment of relapsed ovarian cancer." European Journal of Cancer **47, Supplement 3**(0): S104-S115.

Lee, J. W., S. Samal, et al. (2003). "Cucurbituril Homologues and Derivatives:â€‰ New Opportunities in Supramolecular Chemistry." Accounts of Chemical Research **36**(8): 621-630.

Lewis Phillips, G. D., G. Li, et al. (2008). "Targeting HER2-positive breast cancer with trastuzumab-DM1, an antibody-cytotoxic drug conjugate." Cancer Res **68**(22): 9280-9290.

Li, M. C., R. Hertz, et al. (1958). "Therapy of Choriocarcinoma and Related Trophoblastic Tumors with Folic Acid and Purine Antagonists." New England Journal of Medicine **259**(2): 66-74.

Lim, M. C., Y. J. Song, et al. (2010). "Residual Cancer Stem Cells after Interval Cytoreductive Surgery following Neoadjuvant Chemotherapy Could Result in Poor Treatment Outcomes for Ovarian Cancer." Onkologie **33**(6): 324-330.

Lin, X., Q. Zhang, et al. (2004). "Improved targeting of platinum chemotherapeutics: the antitumour activity of the HPMA copolymer platinum agent AP5280 in murine tumour models." European Journal of Cancer **40**(2): 291-297.

Low, P. S., W. A. Henne, et al. (2007). "Discovery and Development of Folic-Acid-Based Receptor Targeting for Imaging and Therapy of Cancer and Inflammatory Diseases." Accounts of Chemical Research **41**(1): 120-129.

Lowe, S. W. and A. W. Lin (2000). "Apoptosis in cancer." Carcinogenesis **21**(3): 485-495.

Luker, G. D., C. M. Pica, et al. (2003). "Imaging 26S proteasome activity and inhibition in living mice." Nat Med **9**(7): 969-973.

Maeda, H., G. Y. Bharate, et al. (2009). "Polymeric drugs for efficient tumor-targeted drug delivery based on EPR-effect." European Journal of Pharmaceutics and Biopharmaceutics **71**(3): 409-419.

Maeda, H., J. Wu, et al. (2000). "Tumor vascular permeability and the EPR effect in macromolecular therapeutics: a review." Journal of Controlled Release **65**(1-2): 271-284.

Markman, M., A. Kennedy, et al. (2000). "Paclitaxel-Associated Hypersensitivity Reactions: Experience of the Gynecologic Oncology Program of the Cleveland Clinic Cancer Center." Journal of Clinical Oncology **18**(1): 102.

Martin, L. P., T. C. Hamilton, et al. (2008). "Platinum Resistance: The Role of DNA Repair Pathways." Clinical Cancer Research **14**(5): 1291-1295.

Marty, M., P. Pouillart, et al. (1990). "Comparison of the 5-Hydroxytryptamine3 (Serotonin) Antagonist Ondansetron (Gr 38032F) with High-Dose Metoclopramide in the Control of Cisplatin-Induced Emesis." New England Journal of Medicine **322**(12): 816-821.

Matsumura, Y. and H. Maeda (1986). "A New Concept for Macromolecular Therapeutics in Cancer Chemotherapy: Mechanism of Tumoritropic Accumulation of Proteins and the Antitumor Agent Smancs." Cancer Research **46**(12 Part 1): 6387-6392.

Meerum Terwogt, J. M., G. Groenewegen, et al. (2002). "Phase I and pharmacokinetic study of SPI-77, a liposomal encapsulated dosage form of cisplatin." Cancer Chemother Pharmacol **49**(3): 201-210.

Miller, K. J., R. R. Bowsher, et al. (2001). "Workshop on Bioanalytical Methods Validation for Macromolecules: Summary Report." Pharmaceutical Research **18**(9): 1373-1383.

Minchinton, A. I. and I. F. Tannock (2006). "Drug penetration in solid tumours." Nat Rev Cancer **6**(8): 583-592.

Mitra, A. K., K. Sawada, et al. (2011). "Ligand-independent activation of c-Met by fibronectin and alpha(5)beta(1)-integrin regulates ovarian cancer invasion and metastasis." Oncogene **30**(13): 1566-1576.

Mock, W. L. and N. Y. Shih (2002). "Structure and selectivity in host-guest complexes of cucurbituril." The Journal of Organic Chemistry **51**(23): 4440-4446.

Montes-Navajas, P., M. Gonzalez-Bejar, et al. (2009). "Cucurbituril complexes cross the cell membrane." Photochemical & Photobiological Sciences **8**(12).

Moore, M. J., D. Goldstein, et al. (2007). "Erlotinib plus gemcitabine compared with gemcitabine alone in patients with advanced pancreatic cancer: a phase III trial of the National Cancer Institute of Canada Clinical Trials Group." J Clin Oncol **25**(15): 1960-1966.

Morrison, J. G., P. White, et al. (2000). "Validation of a highly sensitive ICP-MS method for the determination of platinum in biofluids: application to clinical pharmacokinetic studies with oxaliplatin." Journal of Pharmaceutical and Biomedical Analysis **24**(1): 1-10.

Morton, C. L. and P. J. Houghton (2007). "Establishment of human tumor xenografts in immunodeficient mice." Nat. Protocols **2**(2): 247-250.

Mylonakis, N., A. Athanasiou, et al. (2010). "Phase II study of liposomal cisplatin (Lipoplatin™) plus gemcitabine versus cisplatin plus gemcitabine as first line treatment in inoperable (stage IIIB/IV) non-small cell lung cancer." Lung Cancer **68**(2): 240-247.

Nagai, N., M. Kinoshita, et al. (1996). "Relationship between pharmacokinetics of unchanged cisplatin and nephrotoxicity after intravenous infusions of cisplatin to cancer patients." Cancer Chemother Pharmacol **39**(1-2): 131-137.

Newman, M. S., G. T. Colbern, et al. (1999). "Comparative pharmacokinetics, tissue distribution, and therapeutic effectiveness of cisplatin encapsulated in long-circulating, pegylated liposomes (SPI-077) in tumor-bearing mice." Cancer Chemotherapy and Pharmacology **43**(1): 1-7.

Nishiyama, N., S. Okazaki, et al. (2003). "Novel Cisplatin-Incorporated Polymeric Micelles Can Eradicate Solid Tumors in Mice." Cancer Research **63**(24): 8977-8983.

Nowotnik, D. P. and E. Cvitkovic (2009). "ProLindac™ (AP5346): A review of the development of an HPMA DACH platinum Polymer Therapeutic." Advanced Drug Delivery Reviews **61**(13): 1214-1219.

O'Neill, K., S. K. Lyons, et al. (2010). "Bioluminescent imaging: a critical tool in pre-clinical oncology research." The Journal of Pathology **220**(3): 317-327.

Olaussen, K. A., A. Dunant, et al. (2006). "DNA Repair by ERCC1 in Non–Small-Cell Lung Cancer and Cisplatin-Based Adjuvant Chemotherapy." New England Journal of Medicine **355**(10): 983-991.

Ozols, R. F. (2002). "Recurrent Ovarian Cancer: Evidence-Based Treatment." Journal of Clinical Oncology **20**(5): 1161-1163.

Peter, F., C. Nuoffer, et al. (1994). "Guanine nucleotide dissociation inhibitor is essential for Rab1 function in budding from the endoplasmic reticulum and transport through the Golgi stack." J Cell Biol **126**(6): 1393-1406.

Petros, R. A. and J. M. DeSimone (2010). "Strategies in the design of nanoparticles for therapeutic applications." Nat Rev Drug Discov **9**(8): 615-627.

Piccart, M. J., K. Bertelsen, et al. (2000). "Randomized intergroup trial of cisplatin-paclitaxel versus cisplatin-cyclophosphamide in women with advanced epithelial ovarian cancer: three-year results." J Natl Cancer Inst **92**(9): 699-708.

Pisani, M. J., Y. Zhao, et al. (2010). "Cucurbit[10]uril binding of dinuclear platinum(II) and ruthenium(II) complexes: association/dissociation rates from seconds to hours." Dalton Transactions **39**(8): 2078-2086.

Plumb, J. A., R. Milroy, et al. (1989). "Effects of the pH Dependence of 3-(4,5-Dimethylthiazol-2-yl)-2,5-diphenyltetrazolium Bromide-Formazan Absorption on Chemosensitivity Determined by a Novel Tetrazolium-based Assay." Cancer Research **49**(16): 4435-4440.

Plumb, J. A., G. Strathdee, et al. (2000). "Reversal of Drug Resistance in Human Tumor Xenografts by 2′-Deoxy-5-azacytidine-induced Demethylation of the hMLH1 Gene Promoter." Cancer Research **60**(21): 6039-6044.

Plumb, J. A., B. Venugopal, et al. (2012). "Cucurbit[7]uril encapsulated cisplatin overcomes cisplatin resistance via a pharmacokinetic effect." Metallomics **4**(6): 561-567.

Plummer, R., R. H. Wilson, et al. (2011). "A Phase I clinical study of cisplatin-incorporated polymeric micelles (NC-6004) in patients with solid tumours." Br J Cancer **104**(4): 593-598.

Prestayko, A. W., F. C. Luft, et al. (1978). "Cisplatin pharmacokinetics in a patient with renal dysfunction." Medical and Pediatric Oncology **5**(1): 183-188.

Rademaker-Lakhai, J. M., C. Terret, et al. (2004). "A Phase I and Pharmacological Study of the Platinum Polymer AP5280 Given as an Intravenous Infusion Once Every 3 Weeks in Patients with Solid Tumors." Clinical Cancer Research **10**(10): 3386-3395.

Raymond, E., S. G. Chaney, et al. (1998). "Oxaliplatin: A review of preclinical and clinical studies." Annals of Oncology **9**(10): 1053-1071.

Raymond, E., S. Faivre, et al. (2002). "Cellular and Molecular Pharmacology of Oxaliplatin1." Molecular Cancer Therapeutics **1**(3): 227-235.

Rehemtulla, A., L. D. Stegman, et al. (2000). "Rapid and quantitative assessment of cancer treatment response using in vivo bioluminescence imaging." Neoplasia **2**(6): 491-495.

Rice, J. R., J. L. Gerberich, et al. (2006). "Preclinical Efficacy and Pharmacokinetics of AP5346, A Novel Diaminocyclohexane-Platinum Tumor-Targeting Drug Delivery System." Clin Cancer Res **12**(7): 2248-2254.

Ringsdorf, H. (1975). "Structure and properties of pharmacologically active polymers." Journal of Polymer Science: Polymer Symposia **51**(1): 135-153.

Rixe, O., W. Ortuzar, et al. (1996). "Oxaliplatin, tetraplatin, cisplatin, and carboplatin: spectrum of activity in drug-resistant cell lines and in the cell lines of the National Cancer Institute's Anticancer Drug Screen panel." Biochem Pharmacol **52**(12): 1855-1865.

Rosenberg, B., L. Van Camp, et al. (1965). "Inhibition of Cell Division in Escherichia coli by Electrolysis Products from a Platinum Electrode." Nature **205**(4972): 698-699.

Rosenberg, B., L. Vancamp, et al. (1969). "Platinum Compounds: a New Class of Potent Antitumour Agents." Nature **222**(5191): 385-386.

Ross, B. D., Y.-J. Zhao, et al. (1998). "Contributions of cell kill and posttreatment tumor growth rates to the repopulation of intracerebral 9L

tumors after chemotherapy: An MRI study." Proceedings of the National Academy of Sciences **95**(12): 7012-7017.

Salazar, M. and M. Ratnam (2007). "The folate receptor: What does it promise in tissue-targeted therapeutics?" Cancer and Metastasis Reviews **26**(1): 141-152.

Samimi, G. and S. Howell (2006). "Modulation of the cellular pharmacology of JM118, the major metabolite of satraplatin, by copper influx and efflux transporters." Cancer Chemotherapy and Pharmacology **57**(6): 781-788.

Sausville, E. A. and A. M. Burger (2006). "Contributions of Human Tumor Xenografts to Anticancer Drug Development." Cancer Research **66**(7): 3351-3354.

Sawada, K., A. K. Mitra, et al. (2008). "Loss of E-cadherin promotes ovarian cancer metastasis via alpha 5-integrin, which is a therapeutic target." Cancer Res **68**(7): 2329-2339.

Schiller, J. H., D. Harrington, et al. (2002). "Comparison of Four Chemotherapy Regimens for Advanced Non–Small-Cell Lung Cancer." New England Journal of Medicine **346**(2): 92-98.

Schorge, J. O., S. C. Modesitt, et al. (2010). "SGO White Paper on Ovarian Cancer: Etiology, Screening and Surveillance." Gynecologic Oncology **119**(1): 7-17.

Scott, K. A., H. Holdsworth, et al. (2000). "Exploiting changes in the tumour microenvironment with sequential cytokine and matrix metalloprotease inhibitor treatment in a murine breast cancer model." British Journal of Cancer **83**(11): 1538-1543.

Shah, V., K. Midha, et al. (2000). "Bioanalytical Method Validation—A Revisit with a Decade of Progress." Pharmaceutical Research **17**(12): 1551-1557.

Sharpless, N. E. and R. A. DePinho (2006). "The mighty mouse: genetically engineered mouse models in cancer drug development." Nat Rev Drug Discov **5**(9): 741-754.

Shoemaker, R. H. (2006). "The NCI60 human tumour cell line anticancer drug screen." Nat Rev Cancer **6**(10): 813-823.

Siddik, Z. H. (2003). "Cisplatin: mode of cytotoxic action and molecular basis of resistance." Oncogene **22**(47): 7265-7279.

Sparreboom, A., C. D. Scripture, et al. (2005). "Comparative Preclinical and Clinical Pharmacokinetics of a Cremophor-Free, Nanoparticle Albumin-Bound Paclitaxel (ABI-007) and Paclitaxel Formulated in Cremophor (Taxol)." Clinical Cancer Research **11**(11): 4136-4143.

Sprauten, M., T. H. Darrah, et al. (2012). "Impact of long-term serum platinum concentrations on neuro- and ototoxicity in Cisplatin-treated survivors of testicular cancer." J Clin Oncol **30**(3): 300-307.

Stathopoulos, G. P. (2010). "Liposomal cisplatin: a new cisplatin formulation." Anti-Cancer Drugs **21**(8): 732-736

Stathopoulos, G. P., D. Antoniou, et al. (2010). "Liposomal cisplatin combined with paclitaxel versus cisplatin and paclitaxel in non-small-cell lung cancer: a randomized phase III multicenter trial." Annals of Oncology **21**(11): 2227-2232.

Stathopoulos, G. P., T. Boulikas, et al. (2005). "Pharmacokinetics and adverse reactions of a new liposomal cisplatin (Lipoplatin): phase I study." Oncol Rep **13**(4): 589-595.

Stathopoulos, G. P., S. K. Rigatos, et al. (2010). "Liposomal Cisplatin Dose Escalation for Determining the Maximum Tolerated Dose and Dose-limiting Toxicity: A Phase I Study." Anticancer Research **30**(4): 1317-1321.

Stone, R. L., A. K. Sood, et al. (2010). "Collateral damage: toxic effects of targeted antiangiogenic therapies in ovarian cancer." The Lancet Oncology **11**(5): 465-475.

Strathdee, G., M. J. MacKean, et al. (1999). "A role for methylation of the hMLH1 promoter in loss of hMLH1 expression and drug resistance in ovarian cancer." Oncogene **18**(14): 2335-2341.

Strebhardt, K. and A. Ullrich (2008). "Paul Ehrlich's magic bullet concept: 100 years of progress." Nat Rev Cancer **8**(6): 473-480.

Sugasawa, K., J. M. Y. Ng, et al. (1998). "Xeroderma Pigmentosum Group C Protein Complex Is the Initiator of Global Genome Nucleotide Excision Repair." Molecular Cell **2**(2): 223-232.

Takakuwa, K., K. Fujita, et al. (1997). "Direct intratumoral gene transfer of the herpes simplex virus thymidine kinase gene with DNA-liposome complexes: growth inhibition of tumors and lack of localization in normal tissues." Jpn J Cancer Res **88**(2): 166-175.

ten Tije, A. J., J. Verweij, et al. (2003). "Pharmacological effects of formulation vehicles : implications for cancer chemotherapy." Clin Pharmacokinet **42**(7): 665-685.

Tjuvajev, J. G., N. Avril, et al. (1998). "Imaging Herpes Virus Thymidine Kinase Gene Transfer and Expression by Positron Emission Tomography." Cancer Research **58**(19): 4333-4341.

Tjuvajev, J. G., R. Finn, et al. (1996). "Noninvasive Imaging of Herpes Virus Thymidine Kinase Gene Transfer and Expression: A Potential Method for Monitoring Clinical Gene Therapy." Cancer Res **56**(18): 4087-4095.

Tothill, P., L. M. Matheson, et al. (1990). "Inductively coupled plasma mass spectrometry for the determination of platinum in animal tissues and a comparison with atomic absorption spectrometry." Journal of Analytical Atomic Spectrometry **5**(7): 619-622.

Uchino, H., Y. Matsumura, et al. (2005). "Cisplatin-incorporating polymeric micelles (NC-6004) can reduce nephrotoxicity and neurotoxicity of cisplatin in rats." Br J Cancer **93**(6): 678-687.

Uehara, H., T. Miyagawa, et al. (1997). "Imaging experimental brain tumors with 1-aminocyclopentane carboxylic acid and alpha-aminoisobutyric acid: comparison to fluorodeoxyglucose and diethylenetriaminepentaacetic acid in morphologically defined tumor regions." J Cereb Blood Flow Metab **17**(11): 1239-1253.

Undevia, S. D., G. Gomez-Abuin, et al. (2005). "Pharmacokinetic variability of anticancer agents." Nat Rev Cancer **5**(6): 447-458.

Uzunova, V. D., C. Cullinane, et al. (2010). "Toxicity of cucurbit[7]uril and cucurbit[8]uril: an exploratory in vitro and in vivo study." Organic & Biomolecular Chemistry **8**(9): 2037-2042.

Vanderhyden, B. C., T. J. Shaw, et al. (2003). "Animal models of ovarian cancer." Reprod Biol Endocrinol **1**: 67.

Venugopal, B. and J. Cassidy (2009). "How to integrate biologicals in the continuum of care." European Journal of Cancer **45, Supplement 1**(0): 57-69.

Vogelstein, B., D. Lane, et al. (2000). "Surfing the p53 network." Nature **408**(6810): 307-310.

von der Maase, H., S. W. Hansen, et al. (2000). "Gemcitabine and Cisplatin Versus Methotrexate, Vinblastine, Doxorubicin, and Cisplatin in Advanced or Metastatic Bladder Cancer: Results of a Large, Randomized, Multinational, Multicenter, Phase III Study." Journal of Clinical Oncology **18**(17): 3068-3077.

Vousden, K. H. and K. M. Ryan (2009). "p53 and metabolism." Nat Rev Cancer **9**(10): 691-700.

Walker, R. A. (2006). "Quantification of immunohistochemistry--issues concerning methods, utility and semiquantitative assessment I." Histopathology **49**(4): 406-410.

Walker, S., R. Oun, et al. (2011). "The Potential of Cucurbit[n]urils in Drug Delivery." Israel Journal of Chemistry **51**(5-6): 616-624.

Wang, D. and S. J. Lippard (2005). "Cellular processing of platinum anticancer drugs." Nat Rev Drug Discov **4**(4): 307-320.

Wang, W. and W. S. El-Deiry (2003). "Bioluminescent molecular imaging of endogenous and exogenous p53-mediated transcription in vitro and in vivo using an HCT116 human colon carcinoma xenograft model." Cancer Biol Ther **2**(2): 196-202.

Watanabe, R., Y. Takiguchi, et al. (2003). "Feasibility of combination chemotherapy with cisplatin and etoposide for haemodialysis patients with lung cancer." Br J Cancer **88**(1): 25-30.

Weiss, R. B., R. C. Donehower, et al. (1990). "Hypersensitivity reactions from taxol." Journal of Clinical Oncology **8**(7): 1263-1268.

Weissleder, R., A. Moore, et al. (2000). "In vivo magnetic resonance imaging of transgene expression." Nat Med **6**(3): 351-355.

Weissleder, R., C. H. Tung, et al. (1999). "In vivo imaging of tumors with protease-activated near-infrared fluorescent probes." Nat Biotechnol **17**(4): 375-378.

Wheate, N. J. (2008). "Improving platinum(II)-based anticancer drug delivery using cucurbit[n]urils." Journal of Inorganic Biochemistry **102**(12): 2060-2066.

Wheate, N. J., R. I. Taleb, et al. (2007). "Novel platinum(II)-based anticancer complexes and molecular hosts as their drug delivery vehicles." Dalton Trans.: 5055-5064.

Wheate, N. J., S. Walker, et al. (2010). "The status of platinum anticancer drugs in the clinic and in clinical trials." Dalton Transactions **39**(35): 8113-8127.

Wheeler, J. M. D., N. E. Beck, et al. (1999). "Mechanisms of inactivation of mismatch repair genes in human colorectal cancer cell lines: The predominant role of hMLH1." Proceedings of the National Academy of Sciences **96**(18): 10296-10301.

White, S. C., P. Lorigan, et al. (2006). "Phase II study of SPI-77 (sterically stabilised liposomal cisplatin) in advanced non-small-cell lung cancer." Br J Cancer **95**(7): 822-828.

Willard, S. T., W. J. Faught, et al. (1997). "Real-time monitoring of estrogen-regulated gene expression in single, living breast cancer cells: a new paradigm for the study of molecular dynamics." Cancer Res **57**(20): 4447-4450.

Wisse, E., F. Braet, et al. (1996). "Structure and Function of Sinusoidal Lining Cells in the Liver." Toxicologic Pathology **24**(1): 100-111.

Wood, K. V. (1995). "Marker proteins for gene expression." Curr Opin Biotechnol **6**(1): 50-58.

Yamada, A., Y. Taniguchi, et al. (2008). "Design of Folate-Linked Liposomal Doxorubicin to its Antitumor Effect in Mice." Clinical Cancer Research **14**(24): 8161-8168.

Yamamoto, Y., I. Kawano, et al. (2011). "Nab-paclitaxel for the treatment of breast cancer: efficacy, safety, and approval." Onco Targets Ther **4**: 123-136.

Yan, X., G. L. Scherphof, et al. (2005). "Liposome Opsonization." Journal of Liposome Research **15**(1-2): 109-139.

Yoshida, M., A. R. Khokhar, et al. (1994). "Biochemical Pharmacology of Homologous Alicyclic Mixed Amine Platinum(II) Complexes in Sensitive and Resistant Tumor Cell Lines." Cancer Research **54**(13): 3468-3473.

Yuan, F., M. Dellian, et al. (1995). "Vascular Permeability in a Human Tumor Xenograft: Molecular Size Dependence and Cutoff Size." Cancer Research **55**(17): 3752-3756.

Zamboni, W., A. Gervais, et al. (2004). "Systemic and tumor disposition of platinum after administration of cisplatin or STEALTH liposomal-cisplatin formulations (SPI-077 and SPI-077 B103) in a preclinical tumor model of melanoma." Cancer Chemotherapy and Pharmacology **53**(4): 329-336.

Zeamari, S., G. Rumping, et al. (2004). "In vivo bioluminescence imaging of locally disseminated colon carcinoma in rats." Br J Cancer **90**(6): 1259-1264.

Zhang, L., K. E. Hellstrom, et al. (1994). "Luciferase activity as a marker of tumor burden and as an indicator of tumor response to antineoplastic therapy in vivo." Clin Exp Metastasis **12**(2): 87-92.

Published papers